

MATHEMATICAL THEORY AND NUMERICAL METHODS FOR BOSE-EINSTEIN CONDENSATION

WEIZHU BAO

Department of Mathematics and Center for Computational Science and Engineering
National University of Singapore, Singapore 119076

YONGYONG CAI

Department of Mathematics, National University of Singapore, Singapore 119076
and
Beijing Computational Science Research Center, Beijing 100084, P. R. China

ABSTRACT. In this paper, we mainly review recent results on mathematical theory and numerical methods for Bose-Einstein condensation (BEC), based on the Gross-Pitaevskii equation (GPE). Starting from the simplest case with one-component BEC of the weakly interacting bosons, we study the reduction of GPE to lower dimensions, the ground states of BEC including the existence and uniqueness as well as nonexistence results, and the dynamics of GPE including dynamical laws, well-posedness of the Cauchy problem as well as the finite time blow-up. To compute the ground state, the gradient flow with discrete normalization (or imaginary time) method is reviewed and various full discretization methods are presented and compared. To simulate the dynamics, both finite difference methods and time splitting spectral methods are reviewed, and their error estimates are briefly outlined. When the GPE has symmetric properties, we show how to simplify the numerical methods. Then we compare two widely used scalings, i.e. physical scaling (commonly used) and semiclassical scaling, for BEC in strong repulsive interaction regime (Thomas-Fermi regime), and discuss semiclassical limits of the GPE. Extensions of these results for one-component BEC are then carried out for rotating BEC by GPE with an angular momentum rotation, dipolar BEC by GPE with long range dipole-dipole interaction, and two-component BEC by coupled GPEs. Finally, as a perspective, we show briefly the mathematical models for spin-1 BEC, Bogoliubov excitation and BEC at finite temperature.

CONTENTS

1. Introduction	3
1.1. Background	3
1.2. Many body system and mean field approximation	4
1.3. The Gross-Pitaevskii equation	6
1.4. Outline of the review	11
2. Mathematical theory for the Gross-Pitaevskii equation	12
2.1. Ground states	12
2.2. Dynamics	20

2000 *Mathematics Subject Classification.* 34C29, 35Q55, 46E35, 65M70.

Key words and phrases. Bose-Einstein condensation, Gross-Pitaevskii equation, numerical method, ground state, quantized vortex, dynamics, error estimate.

2.3. Convergence of dimension reduction	25
3. Numerical methods for computing ground states	28
3.1. Gradient flow with discrete normalization	29
3.2. Backward Euler finite difference discretization	30
3.3. Backward Euler pseudospectral method	32
3.4. Simplified methods under symmetric potentials	34
3.5. Numerical results	37
3.6. Comments of different methods	40
4. Numerical methods for computing dynamics of GPE	41
4.1. Time splitting pseudospectral/finite difference method	42
4.2. Finite difference time domain method	44
4.3. Simplified methods for symmetric potential and initial data	45
4.4. Error estimates for SIFD and CNFD	47
4.5. Error estimates for TSSP	54
4.6. Numerical results	58
4.7. Extension to damped Gross-Pitaevskii equations	60
5. Theory for rotational BEC	61
5.1. GPE with an angular momentum rotation term	62
5.2. Theory for ground states	63
5.3. Critical speeds for quantized vortices	64
5.4. Well-posedness of Cauchy problem	66
5.5. Dynamical laws	67
6. Numerical methods for rotational BEC	69
6.1. Computing ground states	69
6.2. Central vortex states with polar/cylindrical symmetry	71
6.3. Numerical methods for dynamics	80
6.4. A generalized Laguerre-Fourier-Hermite pseudospectral method	85
6.5. Numerical results	90
7. Semiclassical scaling and limit	90
7.1. Semiclassical scaling in the whole space	93
7.2. Semiclassical scaling in bounded domain	94
7.3. Semiclassical limits and geometric optics	95
8. Mathematical theory and numerical methods for dipolar BEC	96
8.1. GPE with dipole-dipole interaction	97
8.2. Dimension reduction	98
8.3. Theory for ground states	99
8.4. Well-posedness for dynamics	101
8.5. Convergence rate of dimension reduction	103
8.6. Numerical methods for computing ground states	105
8.7. Time splitting scheme for dynamics	107
8.8. Numerical results	108
8.9. Extensions in lower dimensions	111
9. Mathematical theory and numerical methods for two component BEC	113
9.1. Coupled Gross-Pitaevskii equations	113
9.2. Ground states for the case without Josephson junction	114
9.3. Ground states for the case with Josephson junction	115
9.4. Dynamical properties	118
9.5. Numerical methods for computing ground states	118
9.6. Numerical methods for computing dynamics	121

9.7. Numerical results	121
10. Perspectives and challenges	122
10.1. Spin-1 BEC	122
10.2. Bogoliubov excitation	125
10.3. BEC at finite temperature	126
Acknowledgments	127
REFERENCES	127

1. Introduction. Quantum theory is one of the most important science discoveries in the last century. It asserts that all objects behave like waves in the micro length scale. However, quantum world remains a mystery as it is hard to observe quantum phenomena due to the extremely small wavelength. Now, it is possible to explore quantum world in experiments due to the remarkable discovery of a new state of matter, Bose-Einstein condensate (BEC). In the state of BEC, the temperature is very cold (near absolute zero). In such case, the wavelength of an object increases extremely, which leads to the incredible and observable BEC.

1.1. Background. The idea of BEC originated in 1924-1925, when A. Einstein generalized a work of S. N. Bose on the quantum statistics for photons [58] to a gas of non-interacting bosons [94, 95]. Based on the quantum statistics, Einstein predicted that, below a critical temperature, part of the bosons would occupy the same quantum state to form a condensate. Although Einstein's work was carried out for non-interacting bosons, the idea can be applied to interacting system of bosons. When temperature T is decreased, the de-Broglie wavelength λ_{dB} of the particle increases, where $\lambda_{dB} = \sqrt{2\pi\hbar^2/mk_B T}$, m is the mass of the particle, \hbar is the Planck constant and k_B is the Boltzmann constant. At a critical temperature T_c , the wavelength λ_{dB} becomes comparable to the inter-particle average spacing, and the de-Broglie waves overlap. In this situation, the particles behave coherently as a giant atom and a BEC is formed.

Einstein's prediction did not receive much attention until F. London suggested the superfluid ^4He as an evidence of BEC in 1938 [137]. London's idea had inspired extensive studies on the superfluid and interacting boson system. In 1947, by developing the idea of London, Bogliubov established the first microscopic theory of superfluid in a system consisting of interacting bosons [57]. Later, it was found in experiment that less than 10% of the superfluid ^4He is in the condensation due to the strong interaction between helium atoms. This fact motivated physicists to search for weakly interacting system of Bose gases with higher occupancy of BEC. The difficulty is that almost all substances become solid or liquid at temperature which the BEC phase transition occurs. In 1959, Hecht [116] pointed out that spin-polarized hydrogen atoms would remain gaseous even at 0K. Hence, H atoms become an attractive candidate for BEC. In 1980, spin-polarized hydrogen gases were realized by Silvera and Walraven [167]. In the following decade, extensive efforts had been devoted to the experimental realization of hydrogen BEC, resulting in the developments of magnetically trapping and evaporative cooling techniques. However, those attempts to observe BEC failed.

In 1980s, due to the developments of laser trapping and cooling, alkali atoms became suitable candidates for BEC experiments as they are well-suited to laser cooling and trapping. By combining the advanced laser cooling and the evaporative

cooling techniques together, the first BEC of dilute ^{87}Rb gases was achieved in 1995, by E. Cornell and C. Wieman's group in JILA [12]. In the same year, two successful experimental observations of BEC, with ^{23}Na by Ketterle's group [86] and ^7Li by Hulet's group [59], were announced. The experimental realization of BEC for alkali vapors has two stages: the laser pre-cooling and evaporative cooling. The alkali gas can be cooled down to several μK by laser cooling, and then be further cooled down to 50nK–100nK by evaporative cooling. As laser cooling can not be applied to hydrogen, it took atomic physicists much more time to achieve hydrogen BEC. In 1998, atomic condensate of hydrogen was finally realized [99]. For better understanding of the long history towards the Bose-Einstein condensation, we refer to the Nobel lectures [80, 126].

The experimental advances [12, 59, 86] have spurred great excitement in the atomic physics community and condensate physics community. Since 1995, numerous efforts have been devoted to the studies of ultracold atomic gases and various kinds of condensates of dilute gases have been produced for both bosonic particles and fermionic particles [11, 84, 97, 129, 144, 146, 151]. In this rapidly growing research area, numerical simulation has been playing an important role in understanding the theories and the experiments. Our aim is to review the numerical methods and mathematical theories for BEC that have been developed over these years.

1.2. Many body system and mean field approximation. We are interested in the ultracold dilute bosonic gases confined in an external trap, which is the case for most of the BEC experiments. In these cold dilute gases, only binary interaction is important. Hence, the many body Hamiltonian for N identical bosons held in a trap can be written as [129, 132]

$$H_N = \sum_{j=1}^N \left(-\frac{\hbar^2}{2m} \Delta_j + V(\mathbf{x}_j) \right) + \sum_{1 \leq j < k \leq N} V_{\text{int}}(\mathbf{x}_j - \mathbf{x}_k), \quad (1.1)$$

where $\mathbf{x}_j \in \mathbb{R}^3$ ($j = 1, \dots, N$) denote the positions of the particles, m is the mass of a boson, Δ_j is the Laplace operator with respect to \mathbf{x}_j , $V(\mathbf{x}_j)$ is the external trapping potential, and $V_{\text{int}}(\mathbf{x}_j - \mathbf{x}_k)$ denotes the inter-atomic two body interactions. The wave function $\Psi_N := \Psi_N(\mathbf{x}_1, \dots, \mathbf{x}_N, t) \in L^2(\mathbb{R}^{3N} \times \mathbb{R})$ is symmetric, with respect to any permutation of the positions \mathbf{x}_j . The evolution of the system is then described by the time-dependent Schrödinger equation

$$i\hbar\partial_t\Psi_N(\mathbf{x}_1, \dots, \mathbf{x}_N, t) = H_N\Psi_N(\mathbf{x}_1, \dots, \mathbf{x}_N, t). \quad (1.2)$$

Here i denotes the imaginary unit. In the sequel, we may omit time t when we write the N body wave function Ψ_N .

In principle, the above many body system can be solved, but the cost increases quadratically as N goes large, due to the binary interaction term. To simplify the interaction, mean-field potential is introduced to approximate the two-body interactions. In the ultracold dilute regime, the binary interaction V_{int} is well approximated by the effective interacting potential:

$$V_{\text{int}}(\mathbf{x}_j - \mathbf{x}_k) = g\delta(\mathbf{x}_j - \mathbf{x}_k), \quad (1.3)$$

where $\delta(\cdot)$ is the Dirac distribution and the constant $g = \frac{4\pi\hbar^2 a_s}{m}$. Here a_s is the s -wave scattering length of the bosons (positive for repulsive interaction and negative for attractive interaction), and it is related to the potential V_{int} [132]. The above

approximation (1.3) is valid for the dilute regime case, where the scattering length a_s is much smaller than the average distance between the particles.

For a BEC, all particles are in the same quantum state and we can formally take the Hartree ansatz for the many body wave function as

$$\Psi_N(\mathbf{x}_1, \dots, \mathbf{x}_N, t) = \prod_{j=1}^N \psi_H(\mathbf{x}_j, t), \quad (1.4)$$

with the normalization condition for the single-particle wave function ψ_H as

$$\int_{\mathbb{R}^3} |\psi_H(\mathbf{x}, t)|^2 d\mathbf{x} = 1. \quad (1.5)$$

Then the energy of the state (1.4) can be written as

$$E = N \int_{\mathbb{R}^3} \left[\frac{\hbar^2}{2m} |\nabla \psi_H(\mathbf{x}, t)|^2 + V(\mathbf{x}) |\psi_H(\mathbf{x}, t)|^2 + \frac{N-1}{2} g |\psi_H(\mathbf{x}, t)|^4 \right] d\mathbf{x}. \quad (1.6)$$

Let us introduce the wave function for the whole condensate

$$\psi(\mathbf{x}, t) = \sqrt{N} \psi_H(\mathbf{x}, t). \quad (1.7)$$

Neglecting terms of order $1/N$, we obtain the energy of the N body system as

$$E(\psi) = \int_{\mathbb{R}^3} \left[\frac{\hbar^2}{2m} |\nabla \psi(\mathbf{x}, t)|^2 + V(\mathbf{x}) |\psi(\mathbf{x}, t)|^2 + \frac{1}{2} g |\psi(\mathbf{x}, t)|^4 \right] d\mathbf{x}, \quad (1.8)$$

where the wave function is normalized according to the total number of the particles,

$$\int_{\mathbb{R}^3} |\psi(\mathbf{x}, t)|^2 d\mathbf{x} = N. \quad (1.9)$$

Eq. (1.8) is the well-known Gross-Pitaevskii energy functional. The equation governing the motion of the condensate can be derived by [150]

$$i\hbar \partial_t \psi(\mathbf{x}, t) = \frac{\delta E(\psi)}{\delta \bar{\psi}} = \left[-\frac{\hbar^2}{2m} \nabla^2 + V(\mathbf{x}) + g |\psi|^2 \right] \psi, \quad (1.10)$$

where $\bar{\psi}$ denotes the complex conjugate of $\psi := \psi(\mathbf{x}, t)$. Eq. (1.10) is a non-linear Schrödinger equation (NLSE) with cubic nonlinearity, known as the Gross-Pitaevskii equation (GPE).

In the derivation, we have used both the dilute property of the gases and the Hartree ansatz (1.4). Eq. (1.4) requires that the BEC system is at extremely low temperature such that almost all particles are in the same states. Thus, mean field approximation (1.8) and (1.10) are only valid for dilute boson gases (or usually called weakly interacting boson gases) at temperature T much smaller than the critical temperature T_c .

The Gross-Pitaevskii (GP) theory (1.10) was developed by Pitaevskii [149] and Gross [109] independently in 1960s. For a long time, the validity of this mean field approximation lacks of rigorous mathematical justification. Since the first experimental observation of BEC in 1995, much attention has been paid to the GP theory. In 2000, Lieb et al. proved that the energy (1.8) describes the ground state energy of the many body system correctly in the mean field regime [132, 133]. Later H. T. Yau and his collaborators studied the validity of GPE (1.10) as an approximation for (1.2) to describe the dynamics of BEC [96], without the trapping potential $V(\mathbf{x})$.

GP theory, or mean field theory, has been proven to predict many properties of BEC quite well. It has become the fundamental mathematical model to understand BEC. In this review article, we will concentrate on the GP theory.

1.3. The Gross-Pitaevskii equation. As shown in section 1.2, at temperature $T \ll T_c$, the dynamics of a BEC is well described by the Gross-Pitaevskii equation (GPE) in three dimensions (3D)

$$i\hbar\partial_t\psi(\mathbf{x}, t) = \left[-\frac{\hbar^2}{2m}\nabla^2 + V(\mathbf{x}) + Ng|\psi(\mathbf{x}, t)|^2 \right] \psi(\mathbf{x}, t), \quad \mathbf{x} \in \mathbb{R}^3, t > 0, \quad (1.11)$$

where $\mathbf{x} = (x, y, z)^T \in \mathbb{R}^3$ is the Cartesian coordinates, ∇ is the gradient operator and $\nabla^2 := \nabla \cdot \nabla = \Delta$ is the Laplace operator. In fact, the above GPE (1.11) is obtained from the GPE (1.10) by a rescaling $\psi \rightarrow \sqrt{N}\psi$, noticing (1.9), the wave function ψ in (1.11) is normalized by

$$\|\psi(\cdot, t)\|_2^2 = \int_{\mathbb{R}^3} |\psi(\mathbf{x}, t)|^2 dx = 1. \quad (1.12)$$

1.3.1. Different external trapping potentials. In the early BEC experiments, a single harmonic oscillator well was used to trap the atoms in the condensate [60, 84]. Recently more advanced and complicated traps are applied in studying BEC in laboratory [61, 72, 143, 150]. Here we present several typical trapping potentials which are widely used in current experiments.

I. Three-dimensional (3D) harmonic oscillator potential [150]:

$$V_{\text{ho}}(\mathbf{x}) = V_{\text{ho}}(x) + V_{\text{ho}}(y) + V_{\text{ho}}(z), \quad V_{\text{ho}}(\alpha) = \frac{m}{2}\omega_\alpha^2\alpha^2, \quad \alpha = x, y, z, \quad (1.13)$$

where ω_x , ω_y and ω_z are the trap frequencies in x -, y - and z -direction, respectively. Without loss of generality, we assume that $\omega_x \leq \omega_y \leq \omega_z$ throughout the paper.

II. 2D harmonic oscillator + 1D double-well potential (Type I) [143]:

$$V_{\text{dw}}^{(1)}(\mathbf{x}) = V_{\text{dw}}^{(1)}(x) + V_{\text{ho}}(y) + V_{\text{ho}}(z), \quad V_{\text{dw}}^{(1)}(x) = \frac{m}{2}\nu_x^4(x^2 - \hat{a}^2)^2, \quad (1.14)$$

where $\pm\hat{a}$ are the double-well centers in x -axis, ν_x is a given constant with physical dimension $1/[\text{s m}]^{1/2}$.

III. 2D harmonic oscillator + 1D double-well potential (Type II) [67, 118]:

$$V_{\text{dw}}^{(2)}(\mathbf{x}) = V_{\text{dw}}^{(2)}(x) + V_{\text{ho}}(y) + V_{\text{ho}}(z), \quad V_{\text{dw}}^{(2)}(x) = \frac{m}{2}\omega_x^2(|x| - \hat{a})^2. \quad (1.15)$$

IV. 3D harmonic oscillator + optical lattice potential [3, 79, 150]:

$$V_{\text{hop}}(\mathbf{x}) = V_{\text{ho}}(\mathbf{x}) + V_{\text{opt}}(x) + V_{\text{opt}}(y) + V_{\text{opt}}(z), \quad V_{\text{opt}}(\alpha) = I_\alpha E_\alpha \sin^2(\hat{q}_\alpha \alpha), \quad (1.16)$$

where $\hat{q}_\alpha = 2\pi/\lambda_\alpha$ is fixed by the wavelength λ_α of the laser light creating the stationary 1D lattice wave, $E_\alpha = \hbar^2\hat{q}_\alpha^2/2m$ is the so-called recoil energy, and I_α is a dimensionless parameter providing the intensity of the laser beam. The optical lattice potential has periodicity $T_\alpha = \pi/\hat{q}_\alpha = \lambda_\alpha/2$ along α -axis ($\alpha = x, y, z$).

V. 3D box potential [150]:

$$V_{\text{box}}(\mathbf{x}) = \begin{cases} 0, & 0 < x, y, z < L, \\ \infty, & \text{otherwise.} \end{cases} \quad (1.17)$$

where L is the length of the box in the x -, y -, z -direction.

For more types of external trapping potential, we refer to [148, 150]. When a harmonic potential is considered, a typical set of parameters used in experiments with ^{87}Rb is given by

$m = 1.44 \times 10^{-25} [\text{kg}]$, $\omega_x = \omega_y = \omega_z = 20\pi [\text{rad/s}]$, $a = 5.1 \times 10^{-9} [\text{m}]$, $N : 10^2 \sim 10^7$ and the Planck constant has the value

$$\hbar = 1.05 \times 10^{-34} [\text{Js}].$$

1.3.2. *Nondimensionalization.* In order to nondimensionalize Eq. (1.11) under the normalization (1.12), we introduce

$$\tilde{t} = \frac{t}{t_s}, \quad \tilde{\mathbf{x}} = \frac{\mathbf{x}}{x_s}, \quad \tilde{\psi}(\tilde{\mathbf{x}}, \tilde{t}) = x_s^{3/2} \psi(\mathbf{x}, t), \quad \tilde{E}(\tilde{\psi}) = \frac{E(\psi)}{E_s}, \quad (1.18)$$

where t_s , x_s and E_s are the scaling parameters of dimensionless time, length and energy units, respectively. Plugging (1.18) into (1.11), multiplying by $t_s^2/mx_s^{1/2}$, and then removing all $\tilde{\cdot}$, we obtain the following dimensionless GPE under the normalization (1.12) in 3D:

$$i\partial_t \psi(\mathbf{x}, t) = -\frac{1}{2} \nabla^2 \psi(\mathbf{x}, t) + V(\mathbf{x})\psi(\mathbf{x}, t) + \kappa |\psi(\mathbf{x}, t)|^2 \psi(\mathbf{x}, t), \quad (1.19)$$

where the dimensionless energy functional $E(\psi)$ is defined as

$$E(\psi) = \int_{\mathbb{R}^3} \left[\frac{1}{2} |\nabla \psi|^2 + V(\mathbf{x})|\psi|^2 + \frac{\kappa}{2} |\psi|^4 \right] d\mathbf{x}, \quad (1.20)$$

and the choices for the scaling parameters t_s and x_s , the dimensionless potential $V(\mathbf{x})$ with $\gamma_y = t_s \omega_y$ and $\gamma_z = t_s \omega_z$, the energy unit $E_s = \hbar/t_s = \hbar^2/mx_s^2$, and the interaction parameter $\kappa = 4\pi a_s N/x_s$ for different external trapping potentials are given below [135]:

I. 3D harmonic oscillator potential:

$$t_s = \frac{1}{\omega_x}, \quad x_s = \sqrt{\frac{\hbar}{m\omega_x}}, \quad V(\mathbf{x}) = \frac{1}{2} (x^2 + \gamma_y^2 y^2 + \gamma_z^2 z^2).$$

II. 2D harmonic oscillator + 1D double-well potential (type I):

$$t_s = \left(\frac{m}{\hbar\nu_x^4} \right)^{1/3}, \quad x_s = \left(\frac{\hbar}{m\nu_x^2} \right)^{1/3}, \quad a = \frac{\hat{a}}{x_s}, \quad V(\mathbf{x}) = \frac{1}{2} \left[(x^2 - a^2)^2 + \gamma_y^2 y^2 + \gamma_z^2 z^2 \right].$$

III. 2D harmonic oscillator + 1D double-well potential (type II):

$$t_s = \frac{1}{\omega_x}, \quad x_s = \sqrt{\frac{\hbar}{m\omega_x}}, \quad a = \frac{\hat{a}}{x_s}, \quad V(\mathbf{x}) = \frac{1}{2} \left[(|x| - a)^2 + \gamma_y^2 y^2 + \gamma_z^2 z^2 \right].$$

IV. 3D harmonic oscillator + optical lattice potentials:

$$t_s = \frac{1}{\omega_x}, \quad x_s = \sqrt{\frac{\hbar}{m\omega_x}}, \quad k_\tau = \frac{2\pi^2 x_s^2 I_\tau}{\lambda_\tau^2}, \quad q_\tau = \frac{2\pi x_s}{\lambda_\tau}, \quad \tau = x, y, z,$$

$$V(\mathbf{x}) = \frac{1}{2} (x^2 + \gamma_y^2 y^2 + \gamma_z^2 z^2) + k_x \sin^2(q_x x) + k_y \sin^2(q_y y) + k_z \sin^2(q_z z).$$

V. 3D Box potential:

$$t_s = \frac{mL^2}{\hbar}, \quad x_s = L, \quad V(\mathbf{x}) = \begin{cases} 0, & 0 < x, y, z < 1, \\ \infty, & \text{otherwise.} \end{cases}$$

1.3.3. *Dimension reduction.* Under the external potentials I–IV, when $\omega_y \approx 1/t_s = \omega_x$ and $\omega_z \gg 1/t_s = \omega_x$ ($\Leftrightarrow \gamma_y \approx 1$ and $\gamma_z \gg 1$), i.e. a disk-shape condensate, the 3D GPE can be reduced to a two dimensional (2D) GPE. In the following discussion, we take potential I, i.e. the harmonic potential as an example.

For a disk-shaped condensate with small height in z -direction, i.e.

$$\omega_x \approx \omega_y, \quad \omega_z \gg \omega_x, \quad \Leftrightarrow \quad \gamma_y \approx 1, \quad \gamma_z \gg 1, \quad (1.21)$$

the 3D GPE (1.19) can be reduced to a 2D GPE by assuming that the time evolution does not cause excitations along the z -axis since these excitations have larger energies at the order of $\hbar\omega_z$ compared to excitations along the x and y -axis with energies at the order of $\hbar\omega_x$.

To understand this [31], consider the total condensate energy $E(\psi(t))$ with $\psi(t) := \psi(\mathbf{x}, t)$:

$$\begin{aligned} E(\psi(t)) &= \frac{1}{2} \int_{\mathbb{R}^3} |\nabla \psi(t)|^2 d\mathbf{x} + \frac{1}{2} \int_{\mathbb{R}^3} (x^2 + \gamma_y^2 y^2) |\psi(t)|^2 d\mathbf{x} \\ &\quad + \frac{\gamma_z^2}{2} \int_{\mathbb{R}^3} z^2 |\psi(t)|^2 d\mathbf{x} + \frac{\kappa}{2} \int_{\mathbb{R}^3} |\psi(t)|^4 d\mathbf{x}. \end{aligned} \quad (1.22)$$

Multiplying (1.19) by $\overline{\psi}_t$ and integrating by parts show the energy conservation

$$E(\psi(t)) = E(\psi_I), \quad t \geq 0, \quad (1.23)$$

where $\psi_I = \psi(t=0)$ is the initial function which may depend on all parameters γ_y , γ_z and κ . Now assume that ψ_I satisfies

$$\frac{E(\psi_I)}{\gamma_z^2} \rightarrow 0, \quad \text{as } \gamma_z \rightarrow \infty. \quad (1.24)$$

Take a sequence $\gamma_z \rightarrow \infty$ (and keep all other parameters fixed). Since $\int_{\mathbb{R}^3} |\psi(t)|^2 d\mathbf{x} = 1$, we conclude from weak compactness that there is a positive measure $n^0(t)$ such that

$$|\psi(t)|^2 \rightharpoonup n^0(t) \quad \text{weakly as } \gamma_z \rightarrow \infty.$$

Energy conservation implies

$$\int_{\mathbb{R}^3} z^2 |\psi(t)|^2 d\mathbf{x} \rightarrow 0, \quad \text{as } \gamma_z \rightarrow \infty,$$

and thus we conclude concentration of the condensate in the plane $z=0$:

$$n^0(x, y, z, t) = n_2^0(x, y, t) \delta(z),$$

where $n_2^0(t) := n_2^0(x, y, t)$ is a positive measure on \mathbb{R}^2 .

Now let $\psi_3 = \psi_3(z)$ be a wave function with

$$\int_{\mathbb{R}} |\psi_3(z)|^2 dz = 1,$$

depending on γ_z such that

$$|\psi_3(z)|^2 \rightharpoonup \delta(z), \quad \text{as } \gamma_z \rightarrow \infty. \quad (1.25)$$

Denote by S_{fac} the subspace

$$S_{\text{fac}} = \{\psi = \psi_2(x, y) \psi_3(z) \mid \psi_2 \in L^2(\mathbb{R}^2)\} \quad (1.26)$$

and let

$$\Pi : L^2(\mathbb{R}^3) \rightarrow S_{\text{fac}} \subseteq L^2(\mathbb{R}^3) \quad (1.27)$$

be the projection on S_{fac} :

$$(\Pi\psi)(x, y, z) = \psi_3(z) \int_{\mathbb{R}} \overline{\psi_3(z')} \psi(x, y, z') dz'. \quad (1.28)$$

Now write the equation (1.19) in the form

$$i\partial_t\psi = \mathcal{A}\psi + \mathcal{F}(\psi), \quad (1.29)$$

where $\mathcal{A}\psi$ stands for the linear part and $\mathcal{F}(\psi)$ for the nonlinearity. Applying Π to the GPE gives

$$\begin{aligned} i\partial_t(\Pi\psi) &= \Pi\mathcal{A}\psi + \Pi\mathcal{F}(\psi) \\ &= \Pi\mathcal{A}(\Pi\psi) + \Pi\mathcal{F}(\Pi\psi) + \Pi((\Pi\mathcal{A} - \mathcal{A}\Pi)\psi + (\Pi\mathcal{F}(\psi) - \mathcal{F}(\Pi\psi))). \end{aligned} \quad (1.30)$$

The projection approximation of (1.19) is now obtained by dropping the commutator terms and it reads

$$i\partial_t(\Pi\sigma) = \Pi\mathcal{A}(\Pi\sigma) + \Pi\mathcal{F}(\Pi\sigma), \quad (1.31)$$

$$(\Pi\sigma)(t=0) = \Pi\psi_I, \quad (1.32)$$

or explicitly, with

$$(\Pi\sigma)(x, y, z, t) =: \psi_2(x, y, t)\psi_3(z), \quad (1.33)$$

we find

$$i\partial_t\psi_2 = -\frac{1}{2}\nabla^2\psi_2 + \frac{1}{2}(x^2 + \gamma_y^2 y^2 + C)\psi_2 + \left(\kappa \int_{-\infty}^{\infty} \psi_3^4(z) dz\right) |\psi_2|^2\psi_2, \quad (1.34)$$

where

$$C = \gamma_z^2 \int_{-\infty}^{\infty} z^2 |\psi_3(z)|^2 dz + \int_{-\infty}^{\infty} \left| \frac{d\psi_3}{dz} \right|^2 dz.$$

Since this GPE is time-transverse invariant, we can replace $\psi_2 \rightarrow \psi e^{-iC/2}$ and drop the constant C in the trap potential. The observables are not affected by this. For the same reason, we will always assume that $V(\mathbf{x}) \geq 0$ in (1.11).

The ‘effective’ GPE (1.34) is well known in the physical literature, where the projection method is often referred to as ‘integrating out the z -coordinate’. However, an analysis of the limit process $\gamma_z \rightarrow \infty$ has to be based on the derivation as presented above, in particular on studying the commutators $\Pi\mathcal{A} - \mathcal{A}\Pi$, $\Pi\mathcal{F} - \mathcal{F}\Pi$. In the case of small interaction $\beta = o(1)$ [53], a good choice for $\psi_3(z)$ is the ground state of the harmonic oscillator in z -dimension:

$$\psi_3(z) = \left(\frac{\gamma_z}{\pi}\right)^{1/4} e^{-\gamma_z z^2/2}. \quad (1.35)$$

For condensates with interaction other than small interaction the choice of ψ_3 is much less obvious. Often one assumes that the condensate density along the z -axis is well described by the (x, y) -trace of the ground state position density $|\phi_g|^2$

$$|\psi(x, y, z, t)|^2 \approx |\psi_2(x, y, t)|^2 \int_{\mathbb{R}^2} |\phi_g(x_1, y_1, z)|^2 dx_1 dy_1 \quad (1.36)$$

and (taking a pure-state-approximation)

$$\psi_3(z) = \left(\int_{\mathbb{R}^2} |\phi_g(x, y, z)|^2 dx dy \right)^{1/2}. \quad (1.37)$$

Similarly, when $\omega_y \gg 1/t_s = \omega_x$ and $\omega_z \gg 1/t_s = \omega_x$ ($\Leftrightarrow \gamma_y \gg 1$ and $\gamma_z \gg 1$), i.e. a cigar-shaped condensate, the 3D GPE can be reduced to a 1D GPE. For a cigar-shaped condensate [31, 148, 150]

$$\omega_y \gg \omega_x, \quad \omega_z \gg \omega_x, \quad \Leftrightarrow \quad \gamma_y \gg 1, \quad \gamma_z \gg 1, \quad (1.38)$$

the 3D GPE (1.11) can be reduced to a 1D GPE by proceeding analogously.

Then the 3D GPE (1.11), 2D and 1D GPEs can be written in a unified way

$$i\partial_t \psi(\mathbf{x}, t) = -\frac{1}{2} \nabla^2 \psi(\mathbf{x}, t) + V(\mathbf{x}) \psi(\mathbf{x}, t) + \beta |\psi(\mathbf{x}, t)|^2 \psi(\mathbf{x}, t), \quad \mathbf{x} \in \mathbb{R}^d, \quad (1.39)$$

where

$$\beta = \kappa \begin{cases} \int_{\mathbb{R}^2} \psi_{23}^4(y, z) dy dz, & d = 1, \\ \int_{\mathbb{R}} \psi_3^4(z) dz, & d = 2, \\ 1, & d = 3; \end{cases} \quad V(\mathbf{x}) = \begin{cases} \frac{1}{2} \gamma_x^2 x^2, & d = 1, \\ \frac{1}{2} (\gamma_x^2 x^2 + \gamma_y^2 y^2), & d = 2, \\ \frac{1}{2} (\gamma_x^2 x^2 + \gamma_y^2 y^2 + \gamma_z^2 z^2), & d = 3; \end{cases} \quad (1.40)$$

where $\gamma_x \geq 1$ is a constant and $\psi_{23}(y, z) \in L^2(\mathbb{R}^2)$ is often chosen to be the x -trace of the ground state $\phi_g(x, y, z)$ in 3D as $\psi_{23}(y, z) = (\int_{\mathbb{R}} |\phi_g(x, y, z)|^2 dx)^{1/2}$ which is usually approximated by the ground state of the corresponding 2D harmonic oscillator [31, 148, 150]. The normalization condition for (1.39) is

$$\int_{\mathbb{R}^d} |\psi(\mathbf{x}, t)|^2 d\mathbf{x} = 1, \quad (1.41)$$

and the energy of (1.39) is given by

$$E(\psi(\cdot, t)) := \int_{\mathbb{R}^d} \left[\frac{1}{2} |\nabla \psi(\mathbf{x}, t)|^2 + V(\mathbf{x}) |\psi(\mathbf{x}, t)|^2 + \frac{\beta}{2} |\psi(\mathbf{x}, t)|^4 \right] d\mathbf{x}. \quad (1.42)$$

For a weakly interacting condensate, choosing ψ_{23} and ψ_3 as the ground states of the corresponding 2D and 1D harmonic oscillator [31, 148, 150], respectively, we derive,

$$\beta := \kappa \begin{cases} \frac{(\gamma_y \gamma_z)^{1/2}}{\sqrt{\frac{2\pi}{\gamma_z}}}, & d = 1, \\ \sqrt{\frac{\gamma_z}{2\pi}}, & d = 2, \\ 1, & d = 3. \end{cases} \quad (1.43)$$

1.3.4. *BEC on a ring.* BEC on a ring has been realized by choosing Toroidal potential (3D harmonic oscillator +2D Gaussian potential) [158]:

$$V_{\text{tor}}(\mathbf{x}) = V_{\text{ho}}(\mathbf{x}) + V_{\text{gau}}(x, y), \quad V_{\text{gau}}(x, y) = V_0 e^{-2 \frac{x^2 + y^2}{w_0^2}}, \quad (1.44)$$

where V_{gau} is produced by a laser beam, w_0 is the beam waist, and V_0 is related to the power of the plug-beam.

In the quasi-1D regime [158], $\omega_x = \omega_y = \omega_r$, the toroidal potential can be written in cylindrical coordinate (r, θ, z) as

$$V_{\text{tor}}(r, \theta, z) = \frac{m}{2} \omega_r^2 r^2 + \frac{m}{2} \omega_z^2 z^2 + V_0 e^{-2 \frac{r^2}{w_0^2}}. \quad (1.45)$$

When $\omega_r, \omega_z \gg 1$, the dynamics of BEC in the ring trap (1.44) would be confined in $r = R$ and $z = 0$, where $\frac{m}{2} \omega_r^2 r^2 + V_0 e^{-2 \frac{r^2}{w_0^2}}$ attains the minimum at R . Then similar to the above dimension reduction process and nondimensionlization, we can obtain the dimensionless 1D GPE for BEC on a ring as [110]:

$$i\partial_t \psi(\theta, t) = -\frac{1}{2} \partial_{\theta\theta} \psi(\theta, t) + \beta |\psi|^2 \psi(\theta, t), \quad \theta \in [0, 2\pi], \quad t > 0, \quad (1.46)$$

with periodic boundary condition, where $\psi := \psi(\theta, t)$ is the wave function and β is a dimensionless parameter.

1.4. Outline of the review. Concerning the GPE (1.39), there are two basic issues, the ground state and the dynamics. Mathematically speaking, the dynamics include the time dependent behavior of GPE, such as the well-posedness of the Cauchy problem, finite time blow-up, stability of traveling waves, etc. The ground state is usually defined as the minimizer of the energy functional (1.42) under the normalization constraint (1.41). In the remaining part of the paper, we will review the mathematical theories and numerical methods for ground states and dynamics of BECs.

In section 2, we review the theories of GPE for single-component BEC. Existence and uniqueness, as well as other properties for the ground states are presented. Well-posedness of the Cauchy problem for GPE is also reviewed. The rigorous analysis on the convergence rates for the dimension reduction is introduced in section 2.3. After an overview on the mathematical results for GPE, we list the numerical methods to find the ground states and compute the dynamics for GPE in sections 3 and 4, respectively. The most popular way for computing the ground states of BEC is the gradient flow with discrete normalization (or imaginary time) method. Section 3 provides a solid mathematical background on the method and details on the full discretizations. For computing the dynamics of GPE, the traditional finite difference methods and the popular time splitting methods are taken into consideration in section 4, with rigorous error analysis.

In section 5, we investigate the rotating BEC with quantized vortices. There exist critical rotating speeds for the vortex configuration. In order to compute the ground states and dynamics of rotating BEC in the presence of the multi-scale vortex structure, we report the efficient and accurate numerical methods in section 6. For fast rotating BEC, the semiclassical scaling is usually adopted other than the physical scaling used in the introduction. We demonstrate these two different scalings in section 7, for the whole space case (harmonic trap) and the bounded domain case (box potential). In fact, the semiclassical scaling is very useful in the case of Thomas-Fermi regime.

Section 8 is devoted to the mathematical theory and numerical methods for dipolar BEC. There are both isotropic contact interactions (short range) and anisotropic dipole-dipole interactions (long range) in a dipolar BEC, and the dipolar GPE involves a highly singular kernel representing the dipole-dipole interaction. We overcome the difficulty caused by the singular kernel via a reformulation of the dipolar GPE, and carry out accurate and efficient numerical methods for dipolar BECs. In section 9, we consider a two component BEC, which is the simplest multi component BEC system. Ground state properties as well as dynamical properties are described. Efficient numerical methods are proposed by generalizing the existing methods for single component BEC. Finally, we briefly introduce some other important topics that are not covered in the current review in section 10, such as spinor BEC, Bogoliubov excitations and BEC at finite temperature.

Throughout the paper, we adopt the standard Sobolev spaces and write the $\|\cdot\|_p$ for standard $L^p(\mathbb{R}^d)$ norm when there is no confusion on the spatial variables. The notations are consistent in each section, and the meaning of notation remains the same if not specified.

2. Mathematical theory for the Gross-Pitaevskii equation. In this section, we consider the dimensionless GPE in d ($d = 1, 2, 3$) dimensions (1.39),

$$i\partial_t \psi(\mathbf{x}, t) = -\frac{1}{2}\nabla^2 \psi(\mathbf{x}, t) + V(\mathbf{x})\psi(\mathbf{x}, t) + \beta |\psi(\mathbf{x}, t)|^2 \psi(\mathbf{x}, t), \quad \mathbf{x} \in \mathbb{R}^d, \quad (2.1)$$

where $V(\mathbf{x}) \geq 0$ is a real-valued potential and $\beta \in \mathbb{R}$ is treated as an arbitrary dimensionless parameter. The GPE (2.1) can be generalized to any dimensions and many results presented here are valid in higher dimensions, but we focus on the most relevant cases $d = 1, 2, 3$ for BEC.

There are two important invariants, i.e., the normalization (mass),

$$N(\psi(\cdot, t)) = \int_{\mathbb{R}^d} |\psi(\mathbf{x}, t)|^2 d\mathbf{x} \equiv N(\psi_0) = \int_{\mathbb{R}^d} |\psi(\mathbf{x}, 0)|^2 d\mathbf{x} = 1, \quad t \geq 0, \quad (2.2)$$

and the energy per particle

$$E(\psi(\cdot, t)) = \int_{\mathbb{R}^d} \left[\frac{1}{2} |\nabla \psi|^2 + V(\mathbf{x})|\psi|^2 + \frac{\beta}{2} |\psi|^4 \right] d\mathbf{x} \equiv E(\psi(\cdot, 0)), \quad t \geq 0. \quad (2.3)$$

In fact, the energy functional $E(\psi)$ can be split into three parts, i.e. kinetic energy $E_{\text{kin}}(\psi)$, potential energy $E_{\text{pot}}(\psi)$ and interaction energy $E_{\text{int}}(\psi)$, which are defined as

$$E_{\text{int}}(\psi) = \int_{\mathbb{R}^d} \frac{\beta}{2} |\psi(\mathbf{x}, t)|^4 d\mathbf{x}, \quad E_{\text{pot}}(\psi) = \int_{\mathbb{R}^d} V(\mathbf{x}) |\psi(\mathbf{x}, t)|^2 d\mathbf{x}, \quad (2.4)$$

$$E_{\text{kin}}(\psi) = \int_{\mathbb{R}^d} \frac{1}{2} |\nabla \psi(\mathbf{x}, t)|^2 d\mathbf{x}, \quad E(\psi) = E_{\text{kin}}(\psi) + E_{\text{pot}}(\psi) + E_{\text{int}}(\psi). \quad (2.5)$$

For convenience, we introduce the following function spaces:

$$L_V(\mathbb{R}^d) = \left\{ \phi \mid \int_{\mathbb{R}^d} V(\mathbf{x}) |\phi(\mathbf{x})|^2 d\mathbf{x} < \infty \right\}, \quad X := X(\mathbb{R}^d) = H^1(\mathbb{R}^d) \cap L_V(\mathbb{R}^d). \quad (2.6)$$

2.1. Ground states. To find the stationary solution of (2.1), we write

$$\psi(\mathbf{x}, t) = \phi(\mathbf{x}) e^{-i\mu t}, \quad (2.7)$$

where μ is the chemical potential of the condensate and $\phi(\mathbf{x})$ is a function independent of time. Substituting (2.7) into (2.1) gives the following equation for $(\mu, \phi(\mathbf{x}))$:

$$\mu \phi(\mathbf{x}) = -\frac{1}{2}\Delta \phi(\mathbf{x}) + V(\mathbf{x})\phi(\mathbf{x}) + \beta |\phi(\mathbf{x})|^2 \phi(\mathbf{x}), \quad \mathbf{x} \in \mathbb{R}^d, \quad (2.8)$$

under the normalization condition

$$\|\phi\|_2^2 := \int_{\mathbb{R}^d} |\phi(\mathbf{x})|^2 d\mathbf{x} = 1. \quad (2.9)$$

This is a nonlinear eigenvalue problem with a constraint and any eigenvalue μ can be computed from its corresponding eigenfunction $\phi(\mathbf{x})$ by

$$\begin{aligned} \mu &= \mu(\phi) = \int_{\mathbb{R}^d} \left[\frac{1}{2} |\nabla \phi(\mathbf{x})|^2 + V(\mathbf{x})|\phi(\mathbf{x})|^2 + \beta |\phi(\mathbf{x})|^4 \right] d\mathbf{x} \\ &= E(\phi) + \int_{\mathbb{R}^d} \frac{\beta}{2} |\phi(\mathbf{x})|^4 d\mathbf{x} = E(\phi) + E_{\text{int}}(\phi). \end{aligned} \quad (2.10)$$

The ground state of a BEC is usually defined as the minimizer of the following minimization problem:

Find $\phi_g \in S$ such that

$$E_g := E(\phi_g) = \min_{\phi \in S} E(\phi), \quad (2.11)$$

where $S = \{\phi \mid \|\phi\|_2 = 1, E(\phi) < \infty\}$ is the unit sphere.

It is easy to show that the ground state ϕ_g is an eigenfunction of the nonlinear eigenvalue problem. Any eigenfunction of (2.8) whose energy is larger than that of the ground state is usually called as excited states in the physics literatures.

2.1.1. *Existence.* In this section, we discuss the existence and uniqueness of the ground state (2.11). Denote the best Sobolev constant C_b in 2D as

$$C_b = \inf_{0 \neq f \in H^1(\mathbb{R}^2)} \frac{\|\nabla f\|_{L^2(\mathbb{R}^2)}^2 \|f\|_{L^2(\mathbb{R}^2)}^2}{\|f\|_{L^4(\mathbb{R}^2)}^4}. \quad (2.12)$$

The best constant C_b can be attained at some H^1 function [184] and it is crucial in considering the existence of ground states in 2D.

For existence and uniqueness of the ground state, we have the following results.

Theorem 2.1. (*Existence and uniqueness*) Suppose $V(\mathbf{x}) \geq 0$ ($\mathbf{x} \in \mathbb{R}^d$) satisfies the confining condition

$$\lim_{|\mathbf{x}| \rightarrow \infty} V(\mathbf{x}) = \infty, \quad (2.13)$$

there exists a ground state $\phi_g \in S$ for (2.11) if one of the following holds

- (i) $d = 3$, $\beta \geq 0$;
- (ii) $d = 2$, $\beta > -C_b$;
- (iii) $d = 1$, for all $\beta \in \mathbb{R}$.

Moreover, the ground state can be chosen as nonnegative $|\phi_g|$, and $\phi_g = e^{i\theta} |\phi_g|$ for some constant $\theta \in \mathbb{R}$. For $\beta \geq 0$, the nonnegative ground state $|\phi_g|$ is unique. If potential $V(\mathbf{x}) \in L^2_{\text{loc}}$, the nonnegative ground state is strictly positive.

In contrast, there exists no ground state, if one of the following holds:

- (i') $d = 3$, $\beta < 0$;
- (ii') $d = 2$, $\beta \leq -C_b$.

To prove the theorem, we present the following lemmas.

Lemma 2.1. Suppose that $V(\mathbf{x}) \geq 0$ ($\mathbf{x} \in \mathbb{R}^d$) satisfies $\lim_{|\mathbf{x}| \rightarrow \infty} V(\mathbf{x}) = \infty$, the embedding $X \hookrightarrow L^p(\mathbb{R}^d)$ is compact, where $p \in [2, \infty]$ for $d = 1$, $p \in [2, \infty)$ for $d = 2$, and $p \in [2, 6)$ for $d = 3$.

Proof. It suffices to prove the case for $p = 2$ and the other cases can be obtained by interpolation in view of the Sobolev inequalities. Since X is a Hilbert space, we need show that any weakly convergent sequence in X has a strong convergent subsequence in $L^2(\mathbb{R}^d)$. Taking a bounded sequence $\{\phi^n\}_{n=1}^\infty \subset X$ such that

$$\phi^n \rightharpoonup \phi \text{ in } X, \quad (2.14)$$

in order to prove the strong $L^2(\mathbb{R}^d)$ convergence of the sequence, we need only prove that

$$\|\phi^n\|_{L^2(\mathbb{R}^d)} \rightarrow \|\phi\|_{L^2(\mathbb{R}^d)}. \quad (2.15)$$

Using the weak convergence, there exists $C > 0$ such that $\int_{\mathbb{R}^d} V(\mathbf{x}) |\phi^n|^2 d\mathbf{x} \leq C$. For any $\varepsilon > 0$, from $\lim_{|\mathbf{x}| \rightarrow \infty} V(\mathbf{x}) = \infty$, there exists $R > 0$ such that $V(\mathbf{x}) \geq \frac{C}{\varepsilon}$ for

$|\mathbf{x}| \geq R$, which implies that

$$\int_{|\mathbf{x}| \geq R} |\phi^n|^2 \leq \varepsilon. \quad (2.16)$$

For $|\mathbf{x}| \geq R$, applying Sobolev embedding theorem, we obtain

$$\int_{|\mathbf{x}| \leq R} |\phi|^2 d\mathbf{x} = \lim_{n \rightarrow \infty} \int_{|\mathbf{x}| \leq R} |\phi^n|^2 d\mathbf{x}. \quad (2.17)$$

Combining (2.16) and (2.17) together as well as the lower semi-continuity of the $L^2(\mathbb{R}^d)$ norm, we have

$$\limsup_{n \rightarrow \infty} \|\phi^n\|_{L^2(\mathbb{R}^d)}^2 - \varepsilon \leq \|\phi\|_{L^2(\mathbb{R}^d)}^2 \leq \liminf_{n \rightarrow \infty} \|\phi^n\|_{L^2(\mathbb{R}^d)}^2. \quad (2.18)$$

Hence we get $\|\phi^n\|_{L^2(\mathbb{R}^d)} \rightarrow \|\phi\|_{L^2(\mathbb{R}^d)}$ and the strong convergence in $L^2(\mathbb{R}^d)$ holds true. The conclusion then follows. \square

The following lemma ensures that the ground state must be nonnegative.

Lemma 2.2. *For any $\phi \in X(\mathbb{R}^d)$ and energy $E(\cdot)$ (2.3), we have*

$$E(\phi) \geq E(|\phi|), \quad (2.19)$$

and the equality holds iff $\phi = e^{i\theta}|\phi|$ for some constant $\theta \in \mathbb{R}$.

Proof. Noticing the inequality for $\phi \in H^1(\mathbb{R}^d)$ ($d \in \mathbb{N}$) [130],

$$\|\nabla|\phi|\|_{L^2(\mathbb{R}^d)} \leq \|\nabla\phi\|_{L^2(\mathbb{R}^d)}, \quad (2.20)$$

where the equality holds iff $\phi = e^{i\theta}|\phi|$ for some constant $\theta \in \mathbb{R}$, a direct application implies the conclusion. \square

The minimization problem (2.11) is nonconvex, but it can be transformed to a convex minimization problem through the following lemma when $\beta \geq 0$.

Lemma 2.3. (*[133]*) *Considering the density $\rho(\mathbf{x}) = |\phi(\mathbf{x})|^2 \geq 0$, for $\sqrt{\rho} \in S$, the energy $E(\sqrt{\rho})$ (2.3) is strictly convex in ρ if $\beta \geq 0$.*

Proof. The potential energy (2.4) is linear in ρ and the interaction energy (2.4) is quadratic in ρ . Hence, $E_{\text{pot}} + E_{\text{int}}$ is convex in ρ . For $\phi_1(\mathbf{x}) = \sqrt{\rho_1(\mathbf{x})}$, $\phi_2(\mathbf{x}) = \sqrt{\rho_2(\mathbf{x})} \in S$ ($\rho_1, \rho_2 \geq 0$), we have $\phi_\theta(\mathbf{x}) = \sqrt{\theta\rho_1(\mathbf{x}) + (1-\theta)\rho_2(\mathbf{x})} \in S$ for any $\theta \in (0, 1)$. Using Cauchy inequality, we get

$$\begin{aligned} |\nabla\phi_\theta(\mathbf{x})|^2 &= \frac{\left| \sqrt{\theta\rho_1(\mathbf{x})}\sqrt{\theta}\nabla\phi_1(\mathbf{x}) + \sqrt{(1-\theta)\rho_2(\mathbf{x})}\sqrt{1-\theta}\nabla\phi_2(\mathbf{x}) \right|^2}{\theta\rho_1(\mathbf{x}) + (1-\theta)\rho_2(\mathbf{x})} \\ &\leq \frac{(\theta\rho_1(\mathbf{x}) + (1-\theta)\rho_2(\mathbf{x})) (\theta|\nabla\phi_1(\mathbf{x})|^2 + (1-\theta)|\nabla\phi_2(\mathbf{x})|^2)}{\theta\rho_1(\mathbf{x}) + (1-\theta)\rho_2(\mathbf{x})} \\ &= \theta|\nabla\phi_1(\mathbf{x})|^2 + (1-\theta)|\nabla\phi_2(\mathbf{x})|^2, \end{aligned}$$

which implies the convexity of the kinetic energy E_{kin} (2.5) (with possible approximation procedure). The conclusion then follows. \square

Proof of Theorem 2.1: We separate the proof into the existence and nonexistence parts.

(1) Existence. First, we claim that the energy E (2.3) is bounded below under the assumptions. Case (i) is clear. For case (ii), using the constraint $\|\phi\|_2^2 = 1$ and Gagliardo-Nirenberg inequality, we have

$$\beta\|\phi\|_4^4 \geq -\|\phi\|_2^2 \cdot \|\nabla\phi\|_2^2 = -\|\nabla\phi\|_2^2.$$

For case (iii), using Cauchy inequality and Sobolev inequality, for any $\varepsilon > 0$, there exists $C_\varepsilon > 0$ such that

$$\|\phi\|_4^4 \leq \|\phi\|_\infty^2 \|\phi\|_2^2 \leq \|\phi\|_\infty^2 \leq \|\nabla\phi\|_2 \|\phi\|_2 \leq \varepsilon \|\nabla\phi\|_2^2 + C_\varepsilon,$$

which yields the claim. Hence, in all cases, we can take a sequence $\{\phi^n\}_{n=1}^\infty$ minimizing the energy E in S , and the sequence is uniformly bounded in X . Taking a weakly convergent subsequence (denoted as the original sequence for simplicity) in X , we have

$$\phi^n \rightharpoonup \phi^\infty, \quad \text{weakly in } X. \quad (2.21)$$

Lemma 2.1 ensures that $\{\phi^n\}_{n=1}^\infty$ converges to ϕ^∞ in L^p where p is given in Lemma 2.1. Combining the lower-semi-continuity of the H^1 and L_V norms, we conclude that $\phi^\infty \in S$ is a ground state [133]. Lemma 2.2 ensures that the ground state can be chosen as the nonnegative one. Actually, the nonnegative ground state is strictly positive [133]. The uniqueness comes from the strict convexity of the energy in Lemma 2.3.

(2) Nonexistence. Firstly, we consider the case $d = 3$, i.e. case (i'). If $\beta < 0$, let $\phi(\mathbf{x}) = \pi^{-\frac{3}{4}} e^{-|\mathbf{x}|^2/2} \in S$ and denote

$$\phi^\varepsilon(\mathbf{x}) = \varepsilon^{-3/2} \phi(\mathbf{x}/\varepsilon) \in S, \quad \varepsilon > 0, \quad (2.22)$$

we find

$$E(\phi^\varepsilon) = \frac{C_1}{\varepsilon^2} + \frac{\beta C_2}{\varepsilon^3} + C_3 + O(1), \quad C_1, C_2 > 0. \quad (2.23)$$

Hence $E(\phi^\varepsilon) \rightarrow -\infty$ as $\varepsilon \rightarrow 0^+$ which shows that there exists no ground state.

Secondly, we consider the case $d = 2$. Let $\phi_b(\mathbf{x})$ ($\mathbf{x} \in \mathbb{R}^2$) be the smooth, radial symmetric (decreasing) function such that the best constant C_b is attained in (2.12). If $\beta < -C_b$, let $\phi_b^\varepsilon(\mathbf{x}) = \varepsilon^{-1} \phi_b(\mathbf{x}/\varepsilon)$ ($\varepsilon > 0$), and we have

$$E(\phi_b^\varepsilon) = \frac{\beta + C_b}{2\varepsilon^2} + C_4 + O(1) \text{ as } \varepsilon \rightarrow 0^+. \quad (2.24)$$

As $\varepsilon \rightarrow 0^+$, $E(\phi_b^\varepsilon) \rightarrow -\infty$, which shows that there exists no ground state. For $\beta = -C_b$, as $\varepsilon \rightarrow 0^+$, ϕ_b^ε will converge to the Dirac distribution and the infimum of the energy E will be the minimal of $V(\mathbf{x})$ (suppose $V(\mathbf{x})$ take minimal at origin), given by the sequence ϕ_b^ε . Thus, there exists no ground state for $\beta = -C_b$. The proof is complete. \square

Remark 2.1. The conclusions in Theorem 2.1 hold for potentials satisfying the confining condition, including the box potential as in (1.17). Since box potentials are not in L_{loc}^2 , there exists zeros in the ground state at the points where $V(\mathbf{x}) = +\infty$. Results for the 3D case were first obtained by Lieb et al. [133].

2.1.2. *Properties of ground states.* In this section, when we refer to the ground state, the conditions guaranteeing the existence in Theorem 2.1 are always assumed and potentials are locally bounded.

For the ground state $\phi_g \in S$, we have the following Virial theorem when $V(\mathbf{x})$ is homogenous.

Theorem 2.2. (*Virial identity*) Suppose $V(\mathbf{x})$ ($\mathbf{x} \in \mathbb{R}^d$, $d = 1, 2, 3$) is homogenous of order $s > 0$, i.e. $V(\lambda\mathbf{x}) = \lambda^s V(\mathbf{x})$ for all $\lambda \in \mathbb{R}$, then the ground state solution $\phi_g \in S$ for (2.11) satisfies

$$2E_{\text{kin}}(\phi_g) - s E_{\text{pot}}(\phi_g) + d E_{\text{int}}(\phi_g) = 0. \quad (2.25)$$

Proof. Consider $\phi^\varepsilon(\mathbf{x}) = \varepsilon^{-d/2} \phi_g(\mathbf{x}/\varepsilon) \in S$ ($\varepsilon > 0$), and use the stationary condition of the energy $E(\phi^\varepsilon)$ at $\varepsilon = 1$, then we get $\left. \frac{dE(\phi^\varepsilon)}{d\varepsilon} \right|_{\varepsilon=1} = 0$, which yields the Virial identity (2.25). \square

Many properties of the ground state are determined by the potential $V(\mathbf{x})$.

Theorem 2.3. [133] (*Symmetry*) Suppose $V(\mathbf{x})$ is spherically symmetry and monotone increasing, then the positive ground state solution $\phi_g \in S$ for (2.11) must be spherically symmetric and monotonically decreasing.

Proof. This fact comes from the symmetric rearrangements. \square

To learn more on the ground state, we study the Euler-Lagrange equation (2.8).

Theorem 2.4. The ground state of (2.11) satisfies the Euler-Lagrange equation (2.8). Suppose $V(\mathbf{x}) \in L_{\text{loc}}^\infty$, the ground state $\phi_g \in S$ of (2.11) is H_{loc}^2 . In addition, if $V \in C^\infty$, the ground state is also C^∞ .

Proof. It is easy to show the ground state satisfies the nonlinear eigenvalue problem (2.8). The regularity follows from the elliptic theory. \square

For confining potentials, we can show that ground states decay exponentially fast when $|\mathbf{x}| \rightarrow \infty$.

Theorem 2.5. Suppose that $0 \leq V(\mathbf{x}) \in L_{\text{loc}}^2$ satisfies (2.13) and $\phi_g \in S$ is a ground state of (2.11). When $\beta \geq 0$, for any $\nu > 0$, there exists a constant $C_\nu > 0$ such that

$$|\phi_g(\mathbf{x})| \leq C_\nu e^{-\nu|\mathbf{x}|}, \quad \mathbf{x} \in \mathbb{R}^d, \quad d = 1, 2, 3. \quad (2.26)$$

Proof. The proof for $d = 3$ is given in [133] and the cases for $d = 1, 2$ are the same. For any $\nu > 0$, rewrite the Euler-Lagrange equation (2.8) for ϕ_g as

$$\left(-\frac{1}{2}\nabla^2 + \frac{\nu^2}{2} \right) \phi_g = \left(\mu + \frac{\nu^2}{2} - V - \beta|\phi_g|^2 \right) \phi_g. \quad (2.27)$$

Making use of the d -dimensional Yukawa potential $Y_d^\nu(\mathbf{x})$ ($d = 1, 2, 3$) [130] associated with $-\frac{1}{2}\nabla^2 + \frac{\nu^2}{2}$, ϕ_g can be expressed as

$$\phi_g(\mathbf{x}) = \int_{\mathbb{R}^d} Y_d^\nu(\mathbf{x} - \mathbf{y}) \left[\mu + \frac{\nu^2}{2} - V(\mathbf{y}) - \beta|\phi_g(\mathbf{y})|^2 \right] d\mathbf{y}. \quad (2.28)$$

Noticing that ϕ_g and the Yukawa potential are positive and V is confining potential, we see that for sufficiently large $R > 0$, $\mu + \frac{\nu^2}{2} - V(\mathbf{x}) - \beta|\phi_g(\mathbf{x})|^2 \leq 0$ for $|\mathbf{x}| \geq R$. Thus, we get

$$\phi_g(\mathbf{x}) \leq \int_{|\mathbf{y}| < R} Y_d^\nu(\mathbf{x} - \mathbf{y}) \left[\mu + \frac{\nu^2}{2} - V(\mathbf{y}) - \beta|\phi_g(\mathbf{y})|^2 \right] d\mathbf{y}. \quad (2.29)$$

Noticing that $Y_d^\nu \in L_{\text{loc}}^2$ ($d = 1, 2, 3$) and $|Y_d^\nu(\mathbf{x})| \leq Ce^{-\nu|\mathbf{x}|}$ for sufficiently large $|\mathbf{x}|$, we find

$$C_\nu = \sup_{\mathbf{x}} \int_{|\mathbf{y}| < R} e^{\nu|\mathbf{x}|} Y_d^\nu(\mathbf{x} - \mathbf{y}) \left[\mu + \frac{\nu^2}{2} - V(\mathbf{y}) - \beta|\phi_g(\mathbf{y})|^2 \right] d\mathbf{y} < \infty, \quad (2.30)$$

and the conclusion (2.26) holds. \square

Remark 2.2. Results (2.26) can be generalized to 1D case for arbitrary β , where $\|\phi_g\|_\infty$ is bounded by Sobolev inequality. The proof is the same.

For convex potentials, the ground states are shown to be log concave.

Theorem 2.6. *Suppose $V(\mathbf{x})$ ($\mathbf{x} \in \mathbb{R}^d$, $d = 1, 2, 3$) is convex, then the positive ground state ϕ_g of (2.11) is log concave, i.e. $\ln(\phi_g(\mathbf{x}))$ is concave,*

$$\ln(\phi_g(\lambda\mathbf{x} + (1-\lambda)\mathbf{y})) \geq \lambda \ln(\phi_g(\mathbf{x})) + (1-\lambda) \ln(\phi_g(\mathbf{y})), \quad \mathbf{x}, \mathbf{y} \in \mathbb{R}^d, \lambda \in [0, 1].$$

Proof. See [133]. \square

When $\beta > 0$, we can actually estimate the L^∞ bound for the ground state.

Theorem 2.7. *Suppose that $0 \leq V(\mathbf{x}) \in C_{\text{loc}}^\alpha$ ($\alpha > 0$) satisfies (2.13) and $\beta > 0$. Let ϕ_g be the unique positive ground state of (2.11), we have*

$$\|\phi_g\|_\infty \leq \sqrt{\frac{\mu_g}{\beta}}, \quad \mu_g = E(\phi_g) + \frac{\beta}{2} \|\phi_g\|_4^4. \quad (2.31)$$

The chemical potential $\mu_g \leq 2E(\phi_g)$ and hence can be bounded by choosing arbitrary testing function.

Proof. Applying elliptic theory to the Euler-Lagrange equation,

$$\mu_g \phi_g = \left(-\frac{1}{2} \nabla^2 + V + \beta|\phi_g|^2 \right) \phi_g, \quad (2.32)$$

we get $\phi_g \in C_{\text{loc}}^{2,\alpha}$. From Theorem 2.5, ϕ_g is bounded in L^∞ . Consider the point \mathbf{x}_0 where ϕ_g takes its maximal, we can obtain

$$\begin{aligned} \mu_g \phi_g(\mathbf{x}_0) &= \left(-\frac{1}{2} \nabla^2 \phi_g + V + \beta|\phi_g|^2 \right) \Big|_{\mathbf{x}_0} \phi_g(\mathbf{x}_0) \\ &\geq [V(\mathbf{x}_0) + \beta|\phi_g(\mathbf{x}_0)|^2] \phi_g(\mathbf{x}_0) \geq \beta|\phi_g(\mathbf{x}_0)|^2 \phi_g(\mathbf{x}_0), \end{aligned}$$

and so

$$\|\phi_g\|_\infty^2 = |\phi_g(\mathbf{x}_0)|^2 \leq \frac{\mu_g}{\beta}. \quad (2.33)$$

\square

Remark 2.3. In 2D and 3D, for small $\beta > 0$ or $\beta < 0$, the L^∞ estimate above can be improved by employing the $W^{2,p}$ estimates for (2.32) and the embedding $H^2(\mathbb{R}^d) \hookrightarrow L^\infty(\mathbb{R}^d)$ ($d = 2, 3$). In 1D, L^∞ bound can be simply obtained by $H^1(\mathbb{R}) \hookrightarrow L^\infty(\mathbb{R})$, while the H^1 norm can be estimated by the energy.

2.1.3. *Approximations of ground states.* For a few external potentials, we can find approximations of ground states in the weakly interaction regime, i.e. $|\beta| = o(1)$, and strongly repulsive interaction regime, i.e. $\beta \gg 1$ [33, 37]. These approximations show the leading order behavior of the ground states and they can be used as initial data for computing ground states numerically.

Under a box potential, i.e. we take

$$V(\mathbf{x}) = \begin{cases} 0, & \mathbf{x} = (x_1, \dots, x_d)^T \in U = (0, 1)^d, \\ +\infty, & \text{otherwise,} \end{cases} \quad (2.34)$$

in (2.8). When $\beta = 0$, i.e. linear case, (2.8) collapses to

$$\mu\phi = -\frac{1}{2}\nabla^2\phi, \quad \phi|_{\partial U} = 0, \quad \|\phi\|_2^2 = \int_U |\phi(\mathbf{x})|^2 d\mathbf{x} = 1. \quad (2.35)$$

For this linear eigenvalue problem, it is easy to find an orthonormal set of eigenfunctions as [31, 148, 150]

$$\phi_{\mathbf{J}}(\mathbf{x}) = \prod_{m=1}^d \phi_{j_m}(x_m), \quad \phi_l(x) = \sqrt{2} \sin(l\pi x), \quad l \in \mathbb{N}, \quad \mathbf{J} = (j_1, \dots, j_d) \in \mathbb{N}^d, \quad (2.36)$$

with the corresponding eigenvalues as

$$\mu_{\mathbf{J}} = \sum_{m=1}^d \mu_{j_m}, \quad \mu_l = \frac{1}{2}l^2\pi^2, \quad l \in \mathbb{N}. \quad (2.37)$$

Thus, for linear case, we can find the exact ground state as $\phi_g(\mathbf{x}) = \phi_{(1, \dots, 1)}(\mathbf{x})$. In addition, when $|\beta| = o(1)$, we can approximate the ground state as $\phi_g(\mathbf{x}) \approx \phi_{(1, \dots, 1)}(\mathbf{x})$. The corresponding energy and chemical potential can be found as

$$\begin{aligned} E_g &= E(\phi_g) \approx E(\phi_{(1, \dots, 1)}(\mathbf{x})) = d\pi^2/2 + O(\beta), \\ \mu_g &= \mu(\phi_g) \approx \mu(\phi_{(1, \dots, 1)}(\mathbf{x})) = d\pi^2/2 + O(\beta). \end{aligned}$$

On the other hand, when $\beta \gg 1$, by dropping the diffusion term (i.e. the first term on the right hand side of (2.8)) – Thomas-Fermi (TF) approximation – [11, 130], we obtain

$$\mu_g^{\text{TF}} \phi_g^{\text{TF}}(\mathbf{x}) = \beta |\phi_g^{\text{TF}}(\mathbf{x})|^2 \phi_g^{\text{TF}}(\mathbf{x}), \quad \mathbf{x} \in U. \quad (2.38)$$

From (2.38), we obtain

$$\phi_g^{\text{TF}}(\mathbf{x}) = \sqrt{\frac{\mu_g^{\text{TF}}}{\beta}}, \quad \mathbf{x} \in U. \quad (2.39)$$

Plugging (2.39) into the normalization condition, we obtain

$$1 = \int_U |\phi_g^{\text{TF}}(\mathbf{x})|^2 d\mathbf{x} = \int_U \frac{\mu_g^{\text{TF}}}{\beta} d\mathbf{x} = \frac{\mu_g^{\text{TF}}}{\beta} \Rightarrow \mu_g^{\text{TF}} = \beta. \quad (2.40)$$

The TF energy E_g^{TF} is obtained via (2.10),

$$E_g^{\text{TF}} = \mu_g^{\text{TF}} - \frac{\beta}{2} \int_U |\phi_g^{\text{TF}}|^4 d\mathbf{x} = \frac{\mu_g^{\text{TF}}}{2} = \frac{\beta}{2}. \quad (2.41)$$

Therefore, we get the TF approximation for the ground state, the energy and the chemical potential when $\beta \gg 1$:

$$\phi_g(\mathbf{x}) \approx \phi_g^{\text{TF}}(\mathbf{x}) = 1, \quad \mathbf{x} \in U, \quad (2.42)$$

$$E_g \approx E_g^{\text{TF}} = \frac{\beta}{2}, \quad \mu_g \approx \mu_g^{\text{TF}} = \beta. \quad (2.43)$$

It is easy to see that the TF approximation for the ground state does not satisfy the boundary condition $\phi|_{\partial U} = 0$. This is due to removing the diffusion term in (2.8) and it suggests that a boundary layer will appear in the ground state when $\beta \gg 1$. Due to the existence of the boundary layer, the kinetic energy does not go to zero when $\beta \rightarrow \infty$ and thus it cannot be neglected. Better approximation with matched asymptotic expansion can be found in [37].

Under a harmonic potential, i.e. we take $V(\mathbf{x})$ as (1.40). When $\beta = 0$, the exact ground state can be found as [31, 148, 150]

$$\mu_g^0 = \begin{cases} \frac{\gamma_x}{2}, \\ \frac{\gamma_x + \gamma_y}{2}, \\ \frac{\gamma_x + \gamma_y + \gamma_z}{2}, \end{cases} \quad \phi_g^0(\mathbf{x}) = \begin{cases} \frac{(\gamma_x)^{1/4}}{(\pi)^{1/4}} e^{-(\gamma_x x^2)/2}, & d = 1, \\ \frac{(\gamma_x \gamma_y)^{1/4}}{(\pi)^{1/2}} e^{-(\gamma_x x^2 + \gamma_y y^2)/2}, & d = 2, \\ \frac{(\gamma_x \gamma_y \gamma_z)^{1/4}}{(\pi)^{3/4}} e^{-(\gamma_x x^2 + \gamma_y y^2 + \gamma_z z^2)/2}, & d = 3. \end{cases}$$

Thus when $|\beta| = o(1)$, the ground state ϕ_g can be approximated by ϕ_g^0 , i.e.

$$\phi_g(\mathbf{x}) \approx \phi_g^0(\mathbf{x}), \quad \mathbf{x} \in \mathbb{R}^d.$$

Again, when $\beta \gg 1$, by dropping the diffusion term (i.e. the first term on the right hand side of (2.8)) – Thomas-Fermi (TF) approximation – [11, 130], we obtain

$$\mu_g^{\text{TF}} \phi_g^{\text{TF}}(\mathbf{x}) = V(\mathbf{x}) \phi_g^{\text{TF}}(\mathbf{x}) + \beta |\phi_g^{\text{TF}}(\mathbf{x})|^2 \phi_g^{\text{TF}}(\mathbf{x}), \quad \mathbf{x} \in \mathbb{R}^d. \quad (2.44)$$

Solving the above equation, we get

$$\phi_g(\mathbf{x}) \approx \phi_g^{\text{TF}}(\mathbf{x}) = \begin{cases} \sqrt{(\mu_g^{\text{TF}} - V(\mathbf{x})) / \beta}, & V(\mathbf{x}) < \mu_g^{\text{TF}}, \\ 0, & \text{otherwise,} \end{cases} \quad (2.45)$$

where μ_g^{TF} is chosen to satisfy the normalization $\|\phi_g^{\text{TF}}\|_2 = 1$. After some tedious computations [33, 37], we get

$$\mu_g^{\text{TF}} = \begin{cases} \frac{1}{2} \left(\frac{3\beta\gamma_x}{2} \right)^{2/3}, \\ \left(\frac{\beta\gamma_x\gamma_y}{\pi} \right)^{1/2}, \\ \frac{1}{2} \left(\frac{15\beta\gamma_x\gamma_y\gamma_z}{4\pi} \right)^{2/5}, \end{cases} \quad E_g^{\text{TF}} = \begin{cases} \frac{3}{10} \left(\frac{3\beta\gamma_x}{2} \right)^{2/3}, & d = 1, \\ \frac{2}{3} \left(\frac{\beta\gamma_x\gamma_y}{\pi} \right)^{1/2}, & d = 2, \\ \frac{5}{14} \left(\frac{15\beta\gamma_x\gamma_y\gamma_z}{4\pi} \right)^{2/5}, & d = 3. \end{cases}$$

It is easy to verify that the Thomas-Fermi approximation (2.45) does not have limit as $\beta \rightarrow \infty$.

Remark 2.4. For the harmonic potential (1.40), the energy of the Thomas-Fermi approximation is unbounded, i.e.

$$E(\phi_g^{\text{TF}}) = +\infty. \quad (2.46)$$

This is due to the low regularity of ϕ_g^{TF} at the free boundary $V(\mathbf{x}) = \mu_g^{\text{TF}}$. More precisely, ϕ_g^{TF} is locally $C^{1/2}$ at the interface. This is a typical behavior for solutions of free boundary value problems, which indicates that an interface layer correction has to be constructed in order to improve the approximation quality.

2.2. Dynamics. Many properties of dynamics for BEC can be reported by solving GPE (2.1). In this section, we will consider the well-posedness for Cauchy problem of GPE (2.1). For BEC, energy (2.3) is an important physical quantity and thus it is natural to study the well-posedness in the energy space $X(\mathbb{R}^d)$ ($d = 1, 2, 3$) (2.6).

2.2.1. Well-posedness. To investigate the Cauchy problem of (2.3), dispersive estimates (Strichartz estimates) have played very important roles. For smooth potentials $V(\mathbf{x})$ with at most quadratic growth in far field, i.e.,

$$V(\mathbf{x}) \in C^\infty(\mathbb{R}^d) \text{ and } D^{\mathbf{k}}V(\mathbf{x}) \in L^\infty(\mathbb{R}^d), \quad \text{for all } \mathbf{k} \in \mathbb{N}_0^d \text{ with } |\mathbf{k}| \geq 2, \quad (2.47)$$

where $\mathbb{N}_0 = \{0\} \cup \mathbb{N}$, Strichartz estimates are well established [73, 172].

Definition 2.1. In d dimensions ($d = 1, 2, 3$), let q' and r' be the conjugate index of q and r ($1 \leq q, r \leq \infty$), respectively, i.e. $1 = 1/q' + 1/q = 1/r' + 1/r$, we call the pair (q, r) admissible and (q', r') conjugate admissible if

$$\frac{2}{q} = d \left(\frac{1}{2} - \frac{1}{r} \right), \quad (2.48)$$

and

$$2 \leq r < \frac{2d}{d-2}, \quad (2 \leq r \leq \infty \text{ if } d = 1; 2 \leq r < \infty \text{ if } d = 2). \quad (2.49)$$

Consider the unitary group $e^{it\mathbf{H}_\mathbf{x}^V}$ generated by $\mathbf{H}_\mathbf{x}^V = -\frac{1}{2}\nabla^2 + V(\mathbf{x})$, for $V(\mathbf{x})$ satisfying (2.47), then the following estimates are available.

Lemma 2.4. (Strichartz's estimates) Let (q, r) be an admissible pair and (γ, ϱ) be a conjugate admissible pair, $I \subset \mathbb{R}$ be a bounded interval satisfying $0 \in I$, then we have

(i) There exists a constant C depending on I and q such that

$$\left\| e^{-it\mathbf{H}_\mathbf{x}^V} \varphi \right\|_{L^q(I, L^r(\mathbb{R}^d))} \leq C(I, q) \|\varphi\|_{L^2(\mathbb{R}^d)}. \quad (2.50)$$

(ii) If $f \in L^\gamma(I, L^\varrho(\mathbb{R}^d))$, there exists a constant C depending on I , q and ϱ , such that

$$\left\| \int_{I \cap s \leq t} e^{-i(t-s)\mathbf{H}_\mathbf{x}^V} f(s) ds \right\|_{L^q(I, L^r(\mathbb{R}^d))} \leq C(I, q, \varrho) \|f\|_{L^\gamma(I, L^\varrho(\mathbb{R}^d))}. \quad (2.51)$$

Using the above lemma, we can get the following results [73, 173].

Theorem 2.8. (Well-posedness of Cauchy problem) Suppose the real-valued trap potential satisfies $V(\mathbf{x}) \geq 0$ ($\mathbf{x} \in \mathbb{R}^d$, $d = 1, 2, 3$) and the condition (2.47), then we have

(i) For any initial data $\psi(\mathbf{x}, t = 0) = \psi_0(\mathbf{x}) \in X(\mathbb{R}^d)$, there exists a $T_{\max} \in (0, +\infty]$ such that the Cauchy problem of (2.1) has a unique maximal solution $\psi \in C([0, T_{\max}), X)$. It is maximal in the sense that if $T_{\max} < \infty$, then $\|\psi(\cdot, t)\|_X \rightarrow \infty$ when $t \rightarrow T_{\max}^-$.

(ii) As long as the solution $\psi(\mathbf{x}, t)$ remains in the energy space X , the L^2 -norm $\|\psi(\cdot, t)\|_2$ and energy $E(\psi(\cdot, t))$ in (2.3) are conserved for $t \in [0, T_{\max})$.

(iii) The solution of the Cauchy problem for (2.1) is global in time, i.e., $T_{\max} = \infty$, if $d = 1$ or $d = 2$ with $\beta > C_b/\|\psi_0\|_2^2$ or $d = 3$ with $\beta \geq 0$.

2.2.2. *Dynamical properties.* From Theorem 2.8, the GPE (2.1) conserves the energy (2.3) and the mass (L^2 -norm) (2.2). There are other important quantities that measure the dynamical properties of BEC. Consider the momentum defined as

$$\mathbf{P}(t) = \int_{\mathbb{R}^d} \text{Im}(\bar{\psi}(\mathbf{x}, t) \nabla \psi(\mathbf{x}, t)) \, d\mathbf{x}, \quad t \geq 0, \quad (2.52)$$

where $\text{Im}(c)$ denotes the imaginary part of c . Then we can get the following result.

Lemma 2.5. *Suppose $\psi(\mathbf{x}, t)$ is the solution of the problem (2.1) and $|\nabla V(\mathbf{x})| \leq C(V(\mathbf{x}) + 1)$ ($V(\mathbf{x}) \geq 0$) for some constant C , then we have*

$$\dot{\mathbf{P}}(t) = - \int_{\mathbb{R}^d} |\psi(\mathbf{x}, t)|^2 \nabla V(\mathbf{x}) \, d\mathbf{x}. \quad (2.53)$$

In particular, for $V(\mathbf{x}) \equiv 0$, the momentum is conserved.

Proof. Differentiating (2.52) with respect to t , noticing (2.1), integrating by parts and taking into account that ψ decreases to 0 exponentially when $|\mathbf{x}| \rightarrow \infty$ (see also [73]), we have

$$\begin{aligned} \dot{\mathbf{P}}(t) &= -i \int_{\mathbb{R}^d} [\bar{\psi}_t \nabla \psi - \nabla \bar{\psi} \psi_t] \, d\mathbf{x} = \int_{\mathbb{R}^d} [(-i\bar{\psi}_t) \nabla \psi + i\psi_t \nabla \bar{\psi}] \, d\mathbf{x} \\ &= \int_{\mathbb{R}^d} \left[\left(-\frac{1}{2} \nabla^2 \bar{\psi} + V \bar{\psi} + \beta |\psi|^2 \bar{\psi} \right) \nabla \psi + \left(-\frac{1}{2} \nabla^2 \psi + V \psi + \beta |\psi|^2 \psi \right) \nabla \bar{\psi} \right] \, d\mathbf{x} \\ &= \int_{\mathbb{R}^d} \left[\frac{1}{2} \nabla |\nabla \psi|^2 + V(\mathbf{x}) \nabla |\psi|^2 + \frac{\beta}{2} \nabla |\psi|^4 \right] \, d\mathbf{x} \\ &= - \int_{\mathbb{R}^d} |\psi|^2 \nabla V(\mathbf{x}) \, d\mathbf{x}, \quad t \geq 0. \end{aligned}$$

The proof is complete. \square

Another quantity characterizing the dynamics of BEC is the condensate width defined as

$$\sigma_\alpha(t) = \sqrt{\delta_\alpha(t)}, \quad \text{where } \delta_\alpha(t) = \int_{\mathbb{R}^d} \alpha^2 |\psi(\mathbf{x}, t)|^2 \, d\mathbf{x}, \quad (2.54)$$

for $t \geq 0$ and α being either x, y or z , with $\mathbf{x} = x$ in 1D, $\mathbf{x} = (x, y)^T$ in 2D and $\mathbf{x} = (x, y, z)^T$ in 3D. For the dynamics of condensate widths, we have the following lemmas:

Lemma 2.6. *Suppose $\psi(\mathbf{x}, t)$ is the solution of (2.1) in \mathbb{R}^d ($d = 1, 2, 3$) with initial data $\psi(\mathbf{x}, 0) = \psi_0(\mathbf{x})$, then we have*

$$\ddot{\delta}_\alpha(t) = \int_{\mathbb{R}^d} [2|\partial_\alpha \psi|^2 + \beta |\psi|^4 - 2\alpha |\psi|^2 \partial_\alpha V(\mathbf{x})] \, d\mathbf{x}, \quad t \geq 0, \quad (2.55)$$

$$\delta_\alpha(0) = \delta_\alpha^{(0)} = \int_{\mathbb{R}^d} \alpha^2 |\psi_0(\mathbf{x})|^2 \, d\mathbf{x}, \quad \alpha = x, y, z, \quad (2.56)$$

$$\dot{\delta}_\alpha(0) = \delta_\alpha^{(1)} = 2 \int_{\mathbb{R}^d} \alpha \text{Im}(\bar{\psi}_0 \partial_\alpha \psi_0) \, d\mathbf{x}. \quad (2.57)$$

Proof. Differentiating (2.54) with respect to t , applying (2.1), and integrating by parts, we obtain

$$\dot{\delta}_\alpha(t) = -i \int_{\mathbb{R}^d} [\alpha \bar{\psi}(\mathbf{x}, t) \partial_\alpha \psi(\mathbf{x}, t) - \alpha \psi(\mathbf{x}, t) \partial_\alpha \bar{\psi}(\mathbf{x}, t)] \, d\mathbf{x}, \quad t \geq 0. \quad (2.58)$$

Similarly, we have

$$\ddot{\delta}_\alpha(t) = \int_{\mathbb{R}^d} [2|\partial_\alpha \psi|^2 + \beta|\psi|^4 - 2\alpha|\psi|^2 \partial_\alpha V(\mathbf{x})] d\mathbf{x}, \quad (2.59)$$

and the conclusion follows. \square

Based on the above Lemma, when $V(\mathbf{x})$ is taken as the harmonic potential (1.40), it is easy to show that the condensate width is a periodic function whose frequency is doubling the trapping frequency in a few special cases [47].

Lemma 2.7. (i) In 1D without interaction, i.e. $d = 1$ and $\beta = 0$ in (2.1), for any initial data $\psi(x, 0) = \psi_0 = \psi_0(x)$, we have

$$\delta_x(t) = \frac{E(\psi_0)}{\gamma_x^2} + \left(\delta_x^{(0)} - \frac{E(\psi_0)}{\gamma_x^2} \right) \cos(2\gamma_x t) + \frac{\delta_x^{(1)}}{2\gamma_x} \sin(2\gamma_x t), \quad t \geq 0. \quad (2.60)$$

(ii) In 2D with a radially symmetric trap, i.e. $d = 2$ and $\gamma_x = \gamma_y := \gamma_r$ in (1.40) and (2.1), for any initial data $\psi(x, y, 0) = \psi_0 = \psi_0(x, y)$, we have

$$\delta_r(t) = \frac{E(\psi_0)}{\gamma_r^2} + \left(\delta_r^{(0)} - \frac{E(\psi_0)}{\gamma_r^2} \right) \cos(2\gamma_r t) + \frac{\delta_r^{(1)}}{2\gamma_r} \sin(2\gamma_r t), \quad t \geq 0, \quad (2.61)$$

where $\delta_r(t) = \delta_x(t) + \delta_y(t)$, $\delta_r^{(0)} := \delta_x(0) + \delta_y(0)$, and $\delta_r^{(1)} := \dot{\delta}_x(0) + \dot{\delta}_y(0)$. Furthermore, when the initial condition $\psi_0(x, y)$ satisfies

$$\psi_0(x, y) = f(r)e^{im\theta} \quad \text{with } m \in \mathbb{Z} \quad \text{and} \quad f(0) = 0 \quad \text{when } m \neq 0, \quad (2.62)$$

we have, for any $t \geq 0$,

$$\begin{aligned} \delta_x(t) = \delta_y(t) &= \frac{1}{2} \delta_r(t) \\ &= \frac{E(\psi_0)}{2\gamma_x^2} + \left(\delta_x^{(0)} - \frac{E(\psi_0)}{2\gamma_x^2} \right) \cos(2\gamma_x t) + \frac{\delta_x^{(1)}}{2\gamma_x} \sin(2\gamma_x t), \quad t \geq 0. \end{aligned} \quad (2.63)$$

For the dynamics of BEC, the center of mass is also important, which is given by

$$\mathbf{x}_c(t) = \int_{\mathbb{R}^d} \mathbf{x} |\psi(\mathbf{x}, t)|^2 d\mathbf{x}, \quad t \geq 0. \quad (2.64)$$

Following the proofs for Lemmas 2.5 and 2.6, we can get the equation governing the motion of \mathbf{x}_c .

Lemma 2.8. Suppose $\psi(\mathbf{x}, t)$ is the solution of (2.1) in \mathbb{R}^d ($d = 1, 2, 3$) with initial data $\psi(\mathbf{x}, 0) = \psi_0(\mathbf{x})$, then we have

$$\dot{\mathbf{x}}_c(t) = \mathbf{P}(t), \quad \ddot{\mathbf{x}}_c(t) = - \int_{\mathbb{R}^d} |\psi(\mathbf{x}, t)|^2 \nabla V(\mathbf{x}) d\mathbf{x}, \quad t \geq 0, \quad (2.65)$$

$$\mathbf{x}_c(0) = \mathbf{x}_c^{(0)} = \int_{\mathbb{R}^d} \mathbf{x} |\psi_0(\mathbf{x})|^2 d\mathbf{x}, \quad (2.66)$$

$$\dot{\mathbf{x}}_c(0) = \mathbf{x}_c^{(1)} = \mathbf{P}(0) = \int_{\mathbb{R}^d} \text{Im}(\bar{\psi}_0 \nabla \psi_0) d\mathbf{x}. \quad (2.67)$$

Proof. Analogous calculation to Lemma 2.5 shows that

$$\dot{\mathbf{x}}_c(t) = \frac{i}{2} \int_{\mathbb{R}^d} (\psi \nabla \bar{\psi} - \bar{\psi} \nabla \psi) d\mathbf{x} = \mathbf{P}(t), \quad t \geq 0. \quad (2.68)$$

Hence, Lemma 2.5 leads to the expression for $\ddot{\mathbf{x}}_c(t)$. \square

Remark 2.5. When $V(\mathbf{x})$ is the harmonic potential (1.40), Eq. (2.65) can be rewritten as

$$\ddot{\mathbf{x}}_c(t) + A\mathbf{x}_c(t) = 0, \quad t \geq 0, \quad (2.69)$$

where A is a $d \times d$ diagonal matrix as $A = (\gamma_x^2)$ when $d = 1$, $A = \text{diag}(\gamma_x^2, \gamma_y^2)$ when $d = 2$ and $A = \text{diag}(\gamma_x^2, \gamma_y^2, \gamma_z^2)$ when $d = 3$. This immediately implies that each component of \mathbf{x}_c is a periodic function whose frequency is the same as the trapping frequency in that component.

For the harmonic potential (1.40), Remark 2.5 provides a way to construct the exact solution of the GPE (2.1) with a stationary state as initial data. Let $\phi_e(\mathbf{x})$ be a stationary state of the GPE (2.1) with a chemical potential μ_e [43, 46], i.e. (μ_e, ϕ_e) satisfying

$$\mu_e \phi_e(\mathbf{x}) = -\frac{1}{2} \nabla^2 \phi_e + V(\mathbf{x}) \phi_e + \beta |\phi_e|^2 \phi_e, \quad \|\phi_e\|_2^2 = 1. \quad (2.70)$$

If the initial data $\psi_0(\mathbf{x})$ for the Cauchy problem of (2.1) is chosen as a stationary state with a shift in its center, one can construct an exact solution of the GPE (2.1) with a harmonic oscillator potential (1.40) [55, 101]. This kind of analytical construction can be used, in particular, in the benchmark and validation of numerical algorithms for GPE.

Lemma 2.9. Suppose $V(\mathbf{x})$ is given by (1.40), if the initial data $\psi_0(\mathbf{x})$ for the Cauchy problem of (2.1) is chosen as

$$\psi_0(\mathbf{x}) = \phi_e(\mathbf{x} - \mathbf{x}_0), \quad \mathbf{x} \in \mathbb{R}^d, \quad (2.71)$$

where \mathbf{x}_0 is a given point in \mathbb{R}^d , then the exact solution of (2.1) satisfies:

$$\psi(\mathbf{x}, t) = \phi_e(\mathbf{x} - \mathbf{x}_c(t)) e^{-i\mu_e t} e^{iw(\mathbf{x}, t)}, \quad \mathbf{x} \in \mathbb{R}^d, \quad t \geq 0, \quad (2.72)$$

where for any time $t \geq 0$, $w(\mathbf{x}, t)$ is linear for \mathbf{x} , i.e.

$$w(\mathbf{x}, t) = \mathbf{c}(t) \cdot \mathbf{x} + g(t), \quad \mathbf{c}(t) = (c_1(t), \dots, c_d(t))^T, \quad \mathbf{x} \in \mathbb{R}^d, \quad t \geq 0, \quad (2.73)$$

and $\mathbf{x}_c(t)$ satisfies the second-order ODE system (2.69) with initial condition

$$\mathbf{x}_c(0) = \mathbf{x}_0, \quad \dot{\mathbf{x}}_c(0) = \mathbf{0}. \quad (2.74)$$

Proof. See detailed proof in [28]. \square

2.2.3. *Finite time blow-up and damping.* According to Theorem 2.8, there is a maximal time T_{\max} for the existence of the solution in energy space. If $T_{\max} < \infty$, there exists finite time blow up.

Theorem 2.9. (Finite time blow-up) In 2D and 3D, assume $V(\mathbf{x})$ satisfies (2.47) and $dV(\mathbf{x}) + \mathbf{x} \cdot \nabla V(\mathbf{x}) \geq 0$ for $\mathbf{x} \in \mathbb{R}^d$ ($d = 2, 3$). When $\beta < 0$, for any initial data $\psi(\mathbf{x}, t = 0) = \psi_0(\mathbf{x}) \in X$ with finite variance $\int_{\mathbb{R}^d} |\mathbf{x}|^2 |\psi_0|^2 d\mathbf{x} < \infty$ to the Cauchy problem of (2.1), there exists finite time blow-up, i.e., $T_{\max} < \infty$, if one of the following holds:

- (i) $E(\psi_0) < 0$;
- (ii) $E(\psi_0) = 0$ and $\text{Im} \left(\int_{\mathbb{R}^d} \bar{\psi}_0(\mathbf{x}) (\mathbf{x} \cdot \nabla \psi_0(\mathbf{x})) d\mathbf{x} \right) < 0$;
- (iii) $E(\psi_0) > 0$ and $\text{Im} \left(\int_{\mathbb{R}^d} \bar{\psi}_0(\mathbf{x}) (\mathbf{x} \cdot \nabla \psi_0(\mathbf{x})) d\mathbf{x} \right) < -\sqrt{d E(\psi_0)} \|\mathbf{x} \psi_0\|_{L^2}$.

Proof. Define the variance

$$\delta_v(t) = \int_{\mathbb{R}^d} |\mathbf{x}|^2 |\psi(\mathbf{x}, t)|^2 d\mathbf{x}. \quad (2.75)$$

Lemma 2.6 indicates that $\delta'_v(t) = 2 \operatorname{Im} \left(\int_{\mathbb{R}^d} \bar{\psi}(\mathbf{x}, t) (\mathbf{x} \cdot \nabla \psi(\mathbf{x}, t)) d\mathbf{x} \right)$ and

$$\begin{aligned} \ddot{\delta}_v(t) &= 2d \int_{\mathbb{R}^d} \left(\frac{1}{d} |\nabla \psi|^2 + \frac{\beta}{2} |\psi|^4 - \frac{1}{d} |\psi|^2 \mathbf{x} \cdot \nabla V(\mathbf{x}) \right) d\mathbf{x} \\ &= 2d E(\psi) - (d-2) \int_{\mathbb{R}^d} |\nabla \psi|^2 d\mathbf{x} - 2 \int_{\mathbb{R}^d} |\psi(\mathbf{x}, t)|^2 (dV(\mathbf{x}) + \mathbf{x} \cdot \nabla V(\mathbf{x})) d\mathbf{x} \\ &\leq 2d E(\psi) = 2d E(\psi_0), \quad d = 2, 3. \end{aligned}$$

Thus,

$$\delta_v(t) \leq d E(\psi_0) t^2 + \delta'_v(0) t + \delta_v(0). \quad (2.76)$$

When one of the conditions (i), (ii) and (iii) holds, there exists a finite time $t^* > 0$ such that $\delta_v(t^*) \leq 0$, which means that there is a singularity at or before $t = t^*$. \square

Theorem 2.9 shows that the solution of the GPE (2.1) may blow up for negative β (attractive interaction) in 2D and 3D. However, the physical quantities modeled by ψ do not become infinite which implies that the validity of (2.1) breaks down near the singularity. Additional physical mechanisms, which were initially small, become important near the singular point and prevent the formation of the singularity. In BEC, the particle density $|\psi|^2$ becomes large close to the critical point and inelastic collisions between particles which are negligible for small densities become important. Therefore a small damping (absorption) term is introduced into the NLSE (2.1) which describes inelastic processes. We are interested in the cases where these damping mechanisms are important and, therefore, restrict ourselves to the case of focusing nonlinearity, i.e. $\beta < 0$, where β may also be time dependent. We consider the following damped nonlinear Schrödinger equation:

$$i \partial_t \psi = -\frac{1}{2} \nabla^2 \psi + V(\mathbf{x}) \psi + \beta |\psi|^{2\sigma} \psi - i f(|\psi|^2) \psi, \quad t > 0, \quad \mathbf{x} \in \mathbb{R}^d, \quad (2.77)$$

$$\psi(\mathbf{x}, t = 0) = \psi_0(\mathbf{x}), \quad \mathbf{x} \in \mathbb{R}^d, \quad (2.78)$$

where $f(\rho) \geq 0$ for $\rho = |\psi|^2 \geq 0$ is a real-valued monotonically increasing function.

The general form of (2.77) covers many damped NLSE arising in various different applications. In BEC, for example, when $f(\rho) \equiv 0$, (2.77) reduces to the usual GPE (2.1); a linear damping term $f(\rho) \equiv \delta$ with $\delta > 0$ describes inelastic collisions with the background gas; cubic damping $f(\rho) = \delta_1 |\beta| \rho$ with $\delta_1 > 0$ corresponds to two-body loss [152, 159]; and a quintic damping term of the form $f(\rho) = \delta_2 \beta^2 \rho^2$ with $\delta_2 > 0$ adds three-body loss to the GPE (2.1) [152, 159]. It is easy to see that the decay of the normalization according to (2.77) due to damping is given by

$$\dot{N}(t) = \frac{d}{dt} \int_{\mathbb{R}^d} |\psi(\mathbf{x}, t)|^2 d\mathbf{x} = -2 \int_{\mathbb{R}^d} f(|\psi(\mathbf{x}, t)|^2) |\psi(\mathbf{x}, t)|^2 d\mathbf{x} \leq 0, \quad t > 0. \quad (2.79)$$

Particularly, if $f(\rho) \equiv \delta$ with $\delta > 0$, the normalization is given by

$$N(t) = \int_{\mathbb{R}^d} |\psi(\mathbf{x}, t)|^2 d\mathbf{x} = e^{-2\delta t} N(0) = e^{-2\delta t} \int_{\mathbb{R}^d} |\psi_0(\mathbf{x})|^2 d\mathbf{x}, \quad t \geq 0. \quad (2.80)$$

For more discussions, we refer to [30].

2.3. Convergence of dimension reduction. In an experimental setup with harmonic potential (1.40), the trapping frequencies in different directions can be very different. Especially, disk-shaped and cigar-shaped condensate were observed in experiments. In section 1.3.3, the 3D GPE is formally reduced to 2D GPE in disk-shaped condensate and to 1D GPE in cigar-shaped condensate. Mathematical and numerical justification for the dimension reduction of 3D GPE is only available in the weakly interaction regime, i.e. $\beta = o(1)$ [38, 52, 53]. Unfortunately, in the intermediate ($\beta = O(1)$) or strong repulsive interaction regime ($\beta \gg 1$), no mathematical results are available and numerical studies can be found in [29].

For weak interaction regime, the dimension reduction is verified by energy type method with projection discussed in section 1.3.3 [38, 53]. Later, Ben Abdallah et al. developed an averaging technique and proved the more general forms of the lower dimensional GPE [52] without using the projection method. A more refined model in lower dimensions is developed in [51]. Here, we introduce this general approach. We refer to [52] and references therein for more discussions.

Consider the 3D GPE for $(\mathbf{x}, \mathbf{z}) \in \mathbb{R}^d \times \mathbb{R}^n$ with $d + n = 3$ ($d = 1$ or $d = 2$)

$$i\partial_t \psi(\mathbf{x}, \mathbf{z}, t) = \left[-\frac{1}{2} (\Delta_{\mathbf{x}} + \Delta_{\mathbf{z}}) + V^\varepsilon(\mathbf{x}, \mathbf{z}) + \beta |\psi|^2 \right] \psi(\mathbf{x}, \mathbf{z}, t), \quad (2.81)$$

$$\psi(\mathbf{x}, \mathbf{z}, 0) = \Psi^{\text{init}}(\mathbf{x}, \mathbf{z}), \quad V^\varepsilon(\mathbf{x}, \mathbf{z}) = \frac{|\mathbf{x}|^2}{2} + \frac{|\mathbf{z}|^2}{2\varepsilon^2}, \quad \mathbf{x} \in \mathbb{R}^d, \quad \mathbf{z} \in \mathbb{R}^n,$$

where $\Delta_{\mathbf{x}}$ and $\Delta_{\mathbf{z}}$ are the Laplace operators in $\mathbf{x} \in \mathbb{R}^d$ and $\mathbf{z} \in \mathbb{R}^n$, respectively. The wave function is normalized as $\|\Psi^{\text{init}}\|_{L^2(\mathbb{R}^3)}^2 = 1$. Compared with the situation in section 1.3.3 (1.39), we have $0 < \varepsilon = 1/\gamma_z \ll 1$ ($d = 2$) with $\gamma_y = 1$ in disk-shaped BEC (2D) and $0 < \varepsilon = 1/\gamma \ll 1$ ($d = 1$) with $\gamma_y = \gamma_z = \gamma$ in cigar-shaped BEC (1D). Our purpose is to describe the limiting dynamics of (2.81) for $0 < \varepsilon \ll 1$.

First, we introduce the rescaling $\mathbf{z} \rightarrow \varepsilon^{1/2} \mathbf{z}$ and rescale $\psi \rightarrow e^{-itn/2\varepsilon} \varepsilon^{-n/4} \psi^\varepsilon(\mathbf{x}, \mathbf{z}, t)$ to keep the normalization. Then Eq. (2.81) becomes

$$i\partial_t \psi^\varepsilon(\mathbf{x}, \mathbf{z}, t) = \mathbf{H}_{\mathbf{x}} \psi^\varepsilon + \frac{1}{\varepsilon} \mathbf{H}_{\mathbf{z}} \psi^\varepsilon + \frac{\beta}{\varepsilon^{n/2}} |\psi^\varepsilon|^2 \psi^\varepsilon, \quad (\mathbf{x}, \mathbf{z}) \in \mathbb{R}^d \times \mathbb{R}^n, \quad (2.82)$$

with initial data

$$\psi^\varepsilon(t = 0) = \Psi^{\text{init}} \in L^2(\mathbb{R}^d \times \mathbb{R}^n), \quad (2.83)$$

where

$$\mathbf{H}_{\mathbf{x}} = \frac{1}{2} (-\Delta_{\mathbf{x}} + |\mathbf{x}|^2), \quad \mathbf{H}_{\mathbf{z}} = \frac{1}{2} (-\Delta_{\mathbf{z}} + |\mathbf{z}|^2 - n), \quad \frac{\beta}{\varepsilon^{n/2}} := \delta \in \mathbb{R}. \quad (2.84)$$

Here $\beta = \delta \varepsilon^{n/2}$ with a constant $\delta \in \mathbb{R}$ means that we are working in the weak interaction regime, i.e., $\beta = O(\varepsilon^{1/2})$ in 2D disk-shaped BEC and $\beta = O(\varepsilon)$ in 1D cigar-shaped BEC. Notice that the singularly perturbed Hamiltonian $\mathbf{H}_{\mathbf{z}}$ is a harmonic oscillator (conveniently shifted here such that it admits integer eigenvalues).

By introducing the filtered unknown

$$\Psi^\varepsilon = e^{it\mathbf{H}_{\mathbf{z}}/\varepsilon} \psi^\varepsilon, \quad (2.85)$$

we get the equation

$$i\partial_t \Psi^\varepsilon(\mathbf{x}, \mathbf{z}, t) = \mathbf{H}_{\mathbf{x}} \Psi^\varepsilon(\mathbf{x}, \mathbf{z}, t) + F\left(\frac{t}{\varepsilon}, \Psi^\varepsilon\right), \quad \Psi^\varepsilon(t = 0) = \Psi^{\text{init}}, \quad (2.86)$$

where F is equal to

$$F(s, \Psi) = \delta e^{is\mathbf{H}_{\mathbf{z}}} \left(|e^{-is\mathbf{H}_{\mathbf{z}}} \Psi|^2 e^{-is\mathbf{H}_{\mathbf{z}}} \Psi \right). \quad (2.87)$$

When ε is small, (2.82) (or, equivalently, (2.86)) couples the high oscillations in time generated by the strong confinement operator with a nonlinear dynamics in the \mathbf{x} plane, which is the only phenomenon that we want to describe.

In [52], Ben Abdallah et al. have developed an averaging technique and proved that, for general confining potentials in the z direction, the limiting model as ε goes to zero is

$$i\partial_t \Psi = \mathbf{H}_{\mathbf{x}} \Psi + F_{\text{av}}(\Psi), \quad \Psi(t=0) = \Psi^{\text{init}}, \quad (2.88)$$

where the long time average of F is defined by

$$F_{\text{av}}(\Psi) = \lim_{T \rightarrow +\infty} \frac{1}{T} \int_0^T F(s, \Psi) ds. \quad (2.89)$$

For general confining operator $\mathbf{H}_{\mathbf{z}}$, the convergence is proved using the fact that $F(s, \Psi)$ is almost periodic [52], but the convergence rates are generally unclear. In the specific case of a harmonic confinement operator, like here, this convergence result can be quantified. The important point is that $\mathbf{H}_{\mathbf{z}}$ admits only integer eigenvalues and the function F is 2π -periodic with respect to the s variable. Therefore, the expression of F_{av} is not a limit but a simple integral, and we have in fact

$$F_{\text{av}}(\Psi) = \frac{1}{2\pi} \int_0^{2\pi} F(s, \Psi) ds. \quad (2.90)$$

On top of that, one can characterize the rate of convergence and prove that Ψ is a first order approximation of Ψ^ε in ε .

Rigourously, in order to state the convergence, we introduce the convenient scale of functional spaces. For all $\ell \in \mathbb{R}^+$, we set

$$\mathcal{B}_\ell := \left\{ \psi \in H^\ell(\mathbb{R}^3) \mid (|\mathbf{x}|^2 + |\mathbf{z}|^2)^{\ell/2} \psi \in L^2(\mathbb{R}^3) \right\}$$

endowed with one of the two following equivalent norms:

$$\|u\|_{\mathcal{B}_\ell}^2 := \|u\|_{L^2(\mathbb{R}^3)}^2 + \|\mathbf{H}_{\mathbf{x}}^{\ell/2} u\|_{L^2(\mathbb{R}^3)}^2 + \|\mathbf{H}_{\mathbf{z}}^{\ell/2} u\|_{L^2(\mathbb{R}^3)}^2 \quad (2.91)$$

or

$$\|u\|_{\mathcal{B}_\ell}^2 := \|u\|_{H^\ell(\mathbb{R}^3)}^2 + \|(|\mathbf{x}|^2 + |\mathbf{z}|^2)^{\ell/2} u\|_{L^2(\mathbb{R}^3)}^2. \quad (2.92)$$

For the equivalence, see e.g. Theorem 2.1 in [52].

We have the convergence as the following.

Theorem 2.10. *For some real number $m > 3/2$, assume that the initial datum Ψ^{init} belongs to \mathcal{B}_{m+4} . Let $\Psi^\varepsilon(\mathbf{x}, \mathbf{z}, t) = e^{it\mathbf{H}_{\mathbf{z}}/\varepsilon} \psi^\varepsilon$ be the solution of the filtered equation*

$$i\partial_t \Psi^\varepsilon(\mathbf{x}, \mathbf{z}, t) = \mathbf{H}_{\mathbf{x}} \Psi^\varepsilon(t, \mathbf{x}, \mathbf{z}) + F\left(\frac{t}{\varepsilon}, \Psi^\varepsilon\right), \quad \Psi^\varepsilon(t=0) = \Psi^{\text{init}}, \quad (2.93)$$

where

$$F(s, \Psi) = \delta e^{is\mathbf{H}_{\mathbf{z}}} |e^{-is\mathbf{H}_{\mathbf{z}}} \Psi|^2 e^{-is\mathbf{H}_{\mathbf{z}}} \Psi. \quad (2.94)$$

Define also $\tilde{\Psi}$ as the solution of the averaged problem

$$i\partial_t \tilde{\Psi} = \mathbf{H}_{\mathbf{x}} \tilde{\Psi} + F_{\text{av}}(\tilde{\Psi}), \quad \tilde{\Psi}(t=0) = \Psi^{\text{init}}, \quad (2.95)$$

where F_{av} is defined by (2.90). Then, we have the following conclusions.

- (i) There exists $T_0 > 0$, depending only on $\|\Psi^{\text{init}}\|_{\mathcal{B}_{m+4}}$, such that Ψ^ε and $\tilde{\Psi}$ are uniquely defined and are uniformly bounded in the space $C([0, T_0]; \mathcal{B}_{m+4})$, independently of $\varepsilon \in (0, 1]$.

(ii) The function $\tilde{\Psi}$ is a first order approximation of the solution Ψ^ε in $C([0, T_0]; \mathcal{B}_m)$, i.e., for some $C > 0$, we have

$$\|\Psi^\varepsilon(t) - \tilde{\Psi}(t)\|_{\mathcal{B}_m} \leq C\varepsilon, \quad \forall t \in [0, T_0]. \quad (2.96)$$

The readers are referred to [51, 52] for a detailed proof of Theorem 2.10.

Remark 2.6. The key property here is the periodicity of $F(s, \Psi)$, and the result can be generalized to other dimensions $\mathbb{R}^p = \mathbb{R}^d \times \mathbb{R}^{p-d}$, more general nonlinearities $f(|\psi|^2)\psi$ in (2.82) and other operators \mathbf{H}_z such that $F(s, \Psi)$ defined by (2.87) is periodic.

Theorem 2.10 implies results of lower dimensional GPE (1.39). Let us take disk-shaped BEC as an example, i.e., $n = 1$ and $d = 2$. Thus, the eigenvalues of \mathbf{H}_z are the nonnegative integers. Let $\chi_p(\mathbf{z})$ be the normalized eigenfunction associated to the eigenvalue $p \in \mathbb{N}_0$:

$$\mathbf{H}_z \chi_p = p \chi_p, \quad \int \chi_p^2 d\mathbf{z} = 1. \quad (2.97)$$

In particular,

$$\chi_0(\mathbf{z}) = e^{-z^2/2}/\pi^{1/4}, \quad \mathbf{z} \in \mathbb{R}. \quad (2.98)$$

Consider a function $\Psi \in \mathcal{B}_m$ expanded on this basis as

$$\Psi(\mathbf{x}, z) = \sum_{p=0}^{+\infty} \varphi_p(\mathbf{x}) \chi_p(\mathbf{z}). \quad (2.99)$$

Then we have

$$F(s, \Psi) = \delta \sum_{p_1, p_2, p_3, p_4} a_{p_1 p_2 p_3 p_4} e^{is\Omega_{p_1 p_2 p_3 p_4}} \varphi_{p_2}(\mathbf{x}) \varphi_{p_3}(\mathbf{x}) \overline{\varphi_{p_4}(\mathbf{x})} \chi_{p_1}(\mathbf{z}), \quad (2.100)$$

where we define the coefficients

$$\Omega_{pqrs} = p + s - q - r, \quad a_{pqrs} = \langle \chi_p \chi_q \chi_r \chi_s \rangle.$$

Here and in the sequel, $\langle \cdot \rangle$ denotes the integration over the \mathbf{z} variable. We write the expansion (2.100) shortly as

$$F(s, \Psi) = \delta \sum_{p_1, p_2, p_3, p_4} a_{1234} e^{is\Omega_{1234}} \varphi_{p_2} \varphi_{p_3} \overline{\varphi_{p_4}} \otimes \chi_{p_1}. \quad (2.101)$$

In the above sums, and in the sequel, a_{1234} and Ω_{1234} stand for $a_{p_1 p_2 p_3 p_4}$ and $\Omega_{p_1 p_2 p_3 p_4}$, respectively.

The expansion of F_{av} (2.90) is obtained by averaging $F(s, \Psi)$ over time s . Noticing that the average of $e^{is\Omega_{1234}}$ vanishes if $\Omega_{1234} \neq 0$, let us define the following index set, whose information is preserved after averaging $F(s, \Psi)$ given by (2.101), for any $p \in \mathbb{N}$,

$$\Lambda(p) = \{(q, r, s), \text{ such that } p + s = q + r\}. \quad (2.102)$$

Then we have

$$F_{\text{av}}(\Phi) = \delta \sum_{p_1=0}^{\infty} \sum_{(p_2, p_3, p_4) \in \Lambda(p_1)} a_{1234} \varphi_{p_2} \varphi_{p_3} \overline{\varphi_{p_4}} \otimes \chi_{p_1}. \quad (2.103)$$

The solution of (2.93) is written as $\Psi^\varepsilon(\mathbf{x}, \mathbf{z}, t) = \sum_{p=0}^{\infty} \varphi_p^\varepsilon(\mathbf{x}, t) \chi_p(\mathbf{z})$ and the solution of (2.95) is written as $\Psi(\mathbf{x}, \mathbf{z}, t) = \sum_{p=0}^{\infty} \varphi_p(\mathbf{x}, t) \chi_p(\mathbf{z})$. If the initial data is polarized on the ground mode of the confinement Hamiltonian, i.e., we have

$$\forall p \in \mathbb{N} \setminus \{0\}, \quad \varphi_p^\varepsilon(t=0) = 0 \quad \text{and} \quad \varphi_0^\varepsilon(t=0) = \varphi^{\text{init}}.$$

In this case, the averaged system (2.95) reads

$$\begin{aligned} i\partial_t \varphi_{p_1} &= \mathbf{H}_{\mathbf{x}} \varphi_{p_1} + \delta \sum_{(p_2, p_3, p_4) \in \Lambda(p_1)} a_{1234} \varphi_{p_2} \varphi_{p_3} \overline{\varphi_{p_4}}, \\ \varphi_{p_1}(t=0) &= \delta_{0p_1} \varphi^{\text{init}}, \end{aligned}$$

where δ_{0p_1} is the Kronecker delta. It is readily seen from this expression that $\varphi_p(t) = 0$ for all t as soon as $p \neq 0$. Hence the averaged system (2.95) reduces to the single equation for φ_0 as

$$i\partial_t \varphi_0 = \mathbf{H}_{\mathbf{x}} \varphi_0 + \delta a_{0000} |\varphi_0|^2 \varphi_0, \quad (2.104)$$

where $a_{0000} = \frac{1}{\sqrt{2\pi}}$. This is exactly the 2D GPE (1.39) with the choice (1.43) (notice that we adopt a rescaling here).

Similarly, for a cigar-shaped BEC, i.e. $n = 2$, when initial data is polarized on the ground mode of the confinement Hamiltonian, we recover the 1D GPE (1.39).

This averaging technique has solved the dimension reduction of 3D GPE in the weak interaction regime $\beta = o(1)$ (2.81). However, there seems no progress for the intermediate interaction regime $\beta = O(1)$ (2.81) yet.

3. Numerical methods for computing ground states. In this section, we review different numerical methods for computing the ground states of BEC (2.11). Due to the presence of the confining potential, the ground state decays exponentially fast when $|\mathbf{x}| \rightarrow \infty$ and thus it is natural to truncate the whole space problem (2.1) to a bounded domain $U \subset \mathbb{R}^d$ with homogeneous Dirichlet boundary conditions. Thus, we consider the GPE (2.1) in U as

$$i \psi_t = -\frac{1}{2} \nabla^2 \psi + V(\mathbf{x}) \psi + \beta |\psi|^2 \psi, \quad t > 0, \quad \mathbf{x} \in U \subset \mathbb{R}^d, \quad (3.1)$$

$$\psi(\mathbf{x}, t) = 0, \quad \mathbf{x} \in \Gamma = \partial U, \quad t \geq 0. \quad (3.2)$$

The normalization (2.2) and energy (2.3) then become

$$N(\psi) = \|\psi(\cdot, t)\|_2^2 := \int_U |\psi(\mathbf{x}, t)|^2 d\mathbf{x} = 1, \quad t \geq 0, \quad (3.3)$$

and

$$E(\psi) = \int_U \left[\frac{1}{2} |\nabla \psi(\mathbf{x}, t)|^2 + V(\mathbf{x}) |\psi(\mathbf{x}, t)|^2 + \frac{\beta}{2} |\psi(\mathbf{x}, t)|^4 \right] d\mathbf{x}, \quad t \geq 0. \quad (3.4)$$

Replacing \mathbb{R}^d with U , many results presented in section 2 can be directly generalized to bounded domain case. Similarly, finding the ground state ϕ_g of (3.1), i.e. minimizing energy $E(\phi)$ (3.4) under normalization constraint $N(\phi) = 1$ (3.3), is equivalent to solving the nonlinear eigenvalue problem (2.8) with boundary condition (3.2). According to Theorem 2.1, ground state ϕ_g can be chosen as nonnegative, and we will restrict ourselves in real-valued wave function ϕ throughout this section.

3.1. Gradient flow with discrete normalization. One of the most popular techniques for dealing with the normalization constraint (3.3) is through the following construction: choose a time sequence $0 = t_0 < t_1 < t_2 < \dots < t_n < \dots$ with $\tau_n := \Delta t_n = t_{n+1} - t_n > 0$ and $\tau = \max_{n \geq 0} \tau_n$. To adapt an algorithm for the solution of the usual gradient flow to the minimization problem under a constraint, it is natural to consider the following gradient flow with discrete normalization (GFDN) which is widely used in physical literatures for computing the ground state solution of BEC [15, 27]:

$$\phi_t = -\frac{1}{2} \frac{\delta E(\phi)}{\delta \phi} = \frac{1}{2} \nabla^2 \phi - V(\mathbf{x})\phi - \beta |\phi|^2 \phi, \quad \mathbf{x} \in U, \quad t_n < t < t_{n+1}, \quad n \geq 0, \quad (3.5)$$

$$\phi(\mathbf{x}, t_{n+1}) \triangleq \phi(\mathbf{x}, t_{n+1}^+) = \frac{\phi(\mathbf{x}, t_{n+1}^-)}{\|\phi(\cdot, t_{n+1}^-)\|_2}, \quad \mathbf{x} \in U, \quad n \geq 0, \quad (3.6)$$

$$\phi(\mathbf{x}, t) = 0, \quad \mathbf{x} \in \Gamma, \quad \phi(\mathbf{x}, 0) = \phi_0(\mathbf{x}), \quad \mathbf{x} \in U, \quad (3.7)$$

where $\phi(\mathbf{x}, t_n^\pm) = \lim_{t \rightarrow t_n^\pm} \phi(\mathbf{x}, t)$ and $\|\phi_0\|_2 = 1$. In fact, the gradient flow (3.5) can be viewed as applying the steepest decent method to the energy functional $E(\phi)$ without constraint and (3.6) then projecting the solution back to the unit sphere in order to satisfy the constraint (3.3). From the numerical point of view, the gradient flow (3.5) can be solved via traditional techniques and the normalization of the gradient flow is simply achieved by a projection at the end of each time step. In fact, Eq. (3.5) can be obtained from the GPE (3.1) by $t \rightarrow it$. Thus GFDN is also known as the imaginary time method in physics literatures.

The GFDN (3.5)-(3.7) possesses the following properties [27].

Lemma 3.1. *Suppose $V(\mathbf{x}) \geq 0$ for all $\mathbf{x} \in U$, $\beta \geq 0$ and $\|\phi_0\|_2 = 1$, then*

- (i) $\|\phi(\cdot, t)\|_2 \leq \|\phi(\cdot, t_n)\|_2 = 1$ for $t_n \leq t \leq t_{n+1}$, $n \geq 0$.
- (ii) For any $\beta \geq 0$,

$$E(\phi(\cdot, t)) \leq E(\phi(\cdot, t')), \quad t_n \leq t' < t \leq t_{n+1}, \quad n \geq 0. \quad (3.8)$$

- (iii) For $\beta = 0$,

$$E\left(\frac{\phi(\cdot, t)}{\|\phi(\cdot, t)\|_2}\right) \leq E\left(\frac{\phi(\cdot, t_n)}{\|\phi(\cdot, t_n)\|_2}\right), \quad t_n \leq t \leq t_{n+1}, \quad n \geq 0. \quad (3.9)$$

The property (3.8) is often referred as the energy diminishing property of the gradient flow. It is interesting to note that (3.9) implies that the energy diminishing property is preserved even with the normalization of the solution of the gradient flow for $\beta = 0$, that is, for linear evolutionary equations.

Theorem 3.1. *Suppose $V(\mathbf{x}) \geq 0$ for all $\mathbf{x} \in U$ and $\|\phi_0\|_2 = 1$. For $\beta = 0$, the GFDN (3.5)-(3.7) is energy diminishing for any time step τ and initial data ϕ_0 , i.e.*

$$E(\phi(\cdot, t_{n+1})) \leq E(\phi(\cdot, t_n)) \leq \dots \leq E(\phi(\cdot, 0)) = E(\phi_0), \quad n = 0, 1, 2, \dots \quad (3.10)$$

For $\beta > 0$, the GFDN (3.5)-(3.7) does not preserve the diminishing property for the normalization of the solution (3.9) in general.

In fact, the normalized step (3.6) is equivalent to solving the following ODE exactly

$$\phi_t(\mathbf{x}, t) = \mu_\phi(t, \tau)\phi(\mathbf{x}, t), \quad \mathbf{x} \in U, \quad t_n < t < t_{n+1}, \quad n \geq 0, \quad (3.11)$$

$$\phi(\mathbf{x}, t_n^+) = \phi(\mathbf{x}, t_{n+1}^-), \quad \mathbf{x} \in U; \quad (3.12)$$

where

$$\mu_\phi(t, \tau) \equiv \mu_\phi(t_{n+1}, \tau_n) = -\frac{1}{2\tau_n} \ln \|\phi(\cdot, t_{n+1}^-)\|_2^2, \quad t_n \leq t \leq t_{n+1}. \quad (3.13)$$

Thus the GFDN (3.5)-(3.7) can be viewed as a first-order splitting method for the gradient flow with discontinuous coefficients [27]:

$$\phi_t = \frac{1}{2}\nabla^2\phi - V(\mathbf{x})\phi - \beta|\phi|^2\phi + \mu_\phi(t, \tau)\phi, \quad \mathbf{x} \in U, \quad t > 0, \quad (3.14)$$

$$\phi(\mathbf{x}, t) = 0, \quad \mathbf{x} \in \Gamma, \quad \phi(\mathbf{x}, 0) = \phi_0(\mathbf{x}), \quad \mathbf{x} \in U. \quad (3.15)$$

Let $\tau \rightarrow 0$, we see that

$$\lim_{\tau \rightarrow 0^+} \mu_\phi(t, \tau) = \mu_\phi(t) = \frac{1}{\|\phi(\cdot, t)\|_2^2} \int_U \left[\frac{1}{2}|\nabla\phi(\mathbf{x}, t)|^2 + V(\mathbf{x})\phi^2(\mathbf{x}, t) + \beta\phi^4(\mathbf{x}, t) \right] d\mathbf{x}.$$

This suggests us to consider the following continuous normalized gradient flow (CNGF) [27]:

$$\phi_t = \frac{1}{2}\nabla^2\phi - V(\mathbf{x})\phi - \beta|\phi|^2\phi + \mu_\phi(t)\phi, \quad \mathbf{x} \in U, \quad t \geq 0, \quad (3.16)$$

$$\phi(\mathbf{x}, t) = 0, \quad \mathbf{x} \in \Gamma, \quad \phi(\mathbf{x}, 0) = \phi_0(\mathbf{x}), \quad \mathbf{x} \in U. \quad (3.17)$$

In fact, the right hand side of (3.16) is the same as (2.10) if we view $\mu_\phi(t)$ as a Lagrange multiplier for the constraint (3.3).

Furthermore, for the above CNGF, as observed in [5, 27, 91], the solution of (3.16) also satisfies the following theorem:

Theorem 3.2. *Suppose $V(\mathbf{x}) \geq 0$ for all $\mathbf{x} \in U$, $\beta \geq 0$ and $\|\phi_0\|_2 = 1$. Then the CNGF (3.16)-(3.17) is normalization conservative and energy diminishing, i.e.*

$$\|\phi(\cdot, t)\|_2^2 = \int_U \phi^2(\mathbf{x}, t) d\mathbf{x} = \|\phi_0\|_2^2 = 1, \quad t \geq 0, \quad (3.18)$$

$$\frac{d}{dt}E(\phi) = -2\|\phi_t(\cdot, t)\|_2^2 \leq 0, \quad t \geq 0, \quad (3.19)$$

which in turn implies

$$E(\phi(\cdot, t_1)) \geq E(\phi(\cdot, t_2)), \quad 0 \leq t_1 \leq t_2 < \infty.$$

3.2. Backward Euler finite difference discretization. In this section, we will present a backward Euler finite difference method to discretize the GFDN (3.5)-(3.7) (or a full discretization of the CNGF (3.16)-(3.17)). For simplicity of notation, we introduce the method for the case of one spatial dimension $d = 1$ with homogeneous Dirichlet boundary conditions. Generalizations to higher dimension with a rectangle $U = [a, b] \times [c, d] \subset \mathbb{R}^2$ and a box $U = [a, b] \times [c, d] \times [e, f] \subset \mathbb{R}^3$ are straightforward for tensor product grids and the results remain valid without modifications. For

$d = 1$, we have [27]

$$\phi_t = \frac{1}{2}\phi_{xx} - V(x)\phi - \beta|\phi|^2\phi, \quad x \in U = (a, b), \quad t_n < t < t_{n+1}, \quad n \geq 0, \quad (3.20)$$

$$\phi(x, t_{n+1}) \triangleq \phi(x, t_{n+1}^+) = \frac{\phi(x, t_{n+1}^-)}{\|\phi(\cdot, t_{n+1}^-)\|_2}, \quad a \leq x \leq b, \quad n \geq 0, \quad (3.21)$$

$$\phi(x, 0) = \phi_0(x), \quad a \leq x \leq b, \quad \phi(a, t) = \phi(b, t) = 0, \quad t \geq 0; \quad (3.22)$$

with $\|\phi_0\|_2^2 = \int_a^b \phi_0^2(x) dx = 1$.

We choose the spatial mesh size $h = \Delta x > 0$ with $\Delta x = (b - a)/M$, choose the time step $\tau = \Delta t > 0$ and define the index sets

$$\mathcal{T}_M = \{j \mid j = 1, 2, \dots, M-1\}, \quad \mathcal{T}_M^0 = \{j \mid j = 0, 1, 2, \dots, M\}. \quad (3.23)$$

We denote grid points and time steps by

$$x_j := a + jh, \quad j \in \mathcal{T}_M^0; \quad t_n := n\tau, \quad n = 0, 1, 2, \dots. \quad (3.24)$$

Let ϕ_j^n be the numerical approximation of $\phi(x_j, t_n)$ and ϕ^n the solution vector at time $t = t_n = n\tau$ with components ϕ_j^n . Introduce the following finite difference operators:

$$\begin{aligned} \delta_x^+ \phi_j^n &= \frac{1}{h}(\phi_{j+1}^n - \phi_j^n), \quad \delta_x^- \phi_j^n = \frac{1}{h}(\phi_j^n - \phi_{j-1}^n), \quad \delta_x \phi_j^n = \frac{\phi_{j+1}^n - \phi_{j-1}^n}{2h}, \\ \delta_t^+ \phi_j^n &= \frac{1}{\tau}(\phi_j^{n+1} - \phi_j^n), \quad \delta_t^- \phi_j^n = \frac{1}{\tau}(\phi_j^n - \phi_j^{n-1}), \quad \delta_t \phi_j^n = \frac{\phi_j^{n+1} - \phi_j^{n-1}}{2\tau}, \\ \delta_x^2 \phi_j^n &= \frac{\phi_{j+1}^n - 2\phi_j^n + \phi_{j-1}^n}{h^2}, \quad \delta_t^2 \phi_j^n = \frac{\phi_j^{n+1} - 2\phi_j^n + \phi_j^{n-1}}{\tau^2}. \end{aligned} \quad (3.25)$$

We denote

$$X_M = \left\{v = (v_j)_{j \in \mathcal{T}_M^0} \mid v_0 = v_M = 0\right\} \subset \mathbb{C}^{M+1}, \quad (3.26)$$

and define the discrete l^p , semi- H^1 and l^∞ norms over X_M as

$$\begin{aligned} \|v\|_p^p &= h \sum_{j=0}^{M-1} |v_j|^p, \quad \|\delta_x^+ v\|_2^2 = h \sum_{j=0}^{M-1} |\delta_x^+ v_j|^2, \quad \|v\|_\infty = \sup_{j \in \mathcal{T}_M^0} |v_j|, \\ (u, v) &= \sum_{j=0}^{M-1} u_j \bar{v}_j, \quad \langle u, v \rangle = \sum_{j=1}^{M-1} u_j \bar{v}_j, \quad \forall u, v \in X_M. \end{aligned} \quad (3.27)$$

The **Backward Euler finite difference (BEFD)** method is to use backward Euler for time discretization and second-order centered finite difference for spatial derivatives. The detailed scheme is [27]:

$$\begin{aligned} \frac{\phi_j^{(1)} - \phi_j^n}{\tau} &= \frac{1}{2}\delta_x^2 \phi_j^{(1)} - V(x_j)\phi_j^{(1)} - \beta(\phi_j^n)^2 \phi_j^{(1)}, \quad j \in \mathcal{T}_M, \\ \phi_0^{(1)} = \phi_M^{(1)} &= 0, \quad \phi_j^0 = \phi_0(x_j), \quad \phi_j^{n+1} = \frac{\phi_j^{(1)}}{\|\phi^{(1)}\|_2}, \quad j \in \mathcal{T}_M^0, \quad n = 0, 1, \dots. \end{aligned} \quad (3.28)$$

The above BEFD method is implicit and unconditionally stable. The discretized system can be solved by Thomas' algorithm. The memory cost is $O(M)$ and computational cost per time step is $O(M)$. In higher dimensions (such as 2D or 3D), the associated discretized system can be solved by iterative methods, for example the Gauss-Seidel or conjugate gradient (CG) or multigrid (MG) iterative

method [15, 27, 45]. With the approximation ϕ^n of ϕ by BEFD, the energy and chemical potential can be computed as

$$E(\phi(\cdot, t_n)) \approx E^n = h \sum_{j=0}^{M-1} \left[\frac{1}{2} |\delta_x^+ \phi_j^n|^2 + V(x_j) |\phi_j^n|^2 + \frac{\beta}{2} |\phi_j^n|^4 \right],$$

$$\mu(\phi(\cdot, t_n)) \approx \mu^n = E^n + h \sum_{j=0}^{M-1} \frac{\beta}{2} |\phi_j^n|^4, \quad n \geq 0.$$

For $\beta = 0$, i.e., linear case, the BEFD discretization (3.28) is energy diminishing and monotone for any $\tau > 0$ (see [27]).

3.3. Backward Euler pseudospectral method. Spectral method enjoys high accuracy for smooth problems such as the ground state problems in BEC. Thus, it is favorable to use spectral method in numerical computation of ground states. For simplicity, we shall introduce the method in 1D (3.20)-(3.22), i.e. $d = 1$. Generalization to $d > 1$ is straightforward for tensor product grids and the results remain valid without modifications. We adopt the same mesh strategy and notations as those in section 3.2.

For any function $\psi(x) \in L^2(U)$ ($U = (a, b)$), $\phi(x) \in C_0(\bar{U})$, and vector $\phi = (\phi_0, \phi_1, \dots, \phi_M)^T \in X_M$ with M an even positive integer, denote finite dimensional spaces

$$Y_M = \text{span} \left\{ \Phi_l(x) = \sin(\mu_l(x - a)), \quad \mu_l = \frac{\pi l}{b - a}, \quad x \in U, l \in \mathcal{T}_M \right\}. \quad (3.29)$$

Let $P_M : L^2(U) \rightarrow Y_M$ be the standard L^2 projection onto Y_M and $I_M : C_0(\bar{U}) \rightarrow Y_M$ and $I_M : X_M \rightarrow Y_M$ be the standard sine interpolation operator as

$$(P_M \psi)(x) = \sum_{l=1}^{M-1} \hat{\psi}_l \sin(\mu_l(x - a)), \quad (I_M \phi)(x) = \sum_{l=1}^{M-1} \tilde{\phi}_l \sin(\mu_l(x - a)), \quad (3.30)$$

and the coefficients are given by

$$\hat{\psi}_l = \frac{2}{b - a} \int_a^b \psi(x) \sin(\mu_l(x - a)) dx, \quad \tilde{\phi}_l = \frac{2}{M} \sum_{j=1}^{M-1} \phi_j \sin\left(\frac{j l \pi}{M}\right), \quad l \in \mathcal{T}_M, \quad (3.31)$$

where $\phi_j = \phi(x_j)$ when ϕ is a function instead of a vector.

The backward Euler sine spectral discretization for (3.5)-(3.7) reads [25]: Find $\phi^{n+1}(x) \in Y_M$ (i.e. $\phi^+(x) \in Y_M$) such that

$$\frac{\phi^+(x) - \phi^n(x)}{\tau} = \frac{1}{2} \nabla^2 \phi^+(x) - P_M [(V(x) + \beta |\phi^n(x)|^2) \phi^+(x)], \quad x \in U, \quad (3.32)$$

$$\phi^{n+1}(x) = \frac{\phi^+(x)}{\|\phi^+(x)\|_2}, \quad x \in U, \quad n = 0, 1, \dots; \quad \phi^0(x) = P_M(\phi_0(x)). \quad (3.33)$$

The above discretization can be solved in phase space and it is not suitable in practice due to the difficulty of computing the integrals in (3.31). We now present an efficient implementation by choosing $\phi^0(x)$ as the interpolation of $\phi_0(x)$ on the grid points $\{x_j, j \in \mathcal{T}_M^0\}$, i.e. $\phi^0(x_j) = \phi_0(x_j)$ for $j \in \mathcal{T}_M^0$, and approximating the integrals in (3.31) by a quadrature rule on the grid points. Let ϕ_j^n be the

approximations of $\phi(x_j, t_n)$, which is the solution of (3.5)-(3.7). Backward Euler sine pseudospectral (BESP) method for discretizing (3.5)-(3.7) reads [25]:

$$\frac{\phi_j^{(1)} - \phi_j^n}{\tau} = \frac{1}{2} D_{xx}^s \phi^{(1)} \Big|_{x=x_j} - V(x_j) \phi_j^{(1)} - \beta |\phi_j^n|^2 \phi_j^{(1)}, \quad j \in \mathcal{T}_M, \quad (3.34)$$

$$\phi_0^{(1)} = \phi_M^{(1)} = 0, \quad \phi_j^0 = \phi_0(x_j), \quad \phi_j^{n+1} = \frac{\phi_j^{(1)}}{\|\phi^{(1)}\|_2}, \quad j \in \mathcal{T}_M^0, \quad n = 0, 1, \dots \quad (3.35)$$

Here D_{xx}^s , a pseudospectral differential operator approximation of ∂_{xx} , is defined as

$$D_{xx}^s u|_{x=x_j} = - \sum_{l=1}^{M-1} \mu_l^2 \tilde{u}_l \sin(\mu_l(x_j - a)). \quad j \in \mathcal{T}_M. \quad (3.36)$$

In the discretization (3.34), at every time step, a nonlinear system has to be solved. Here we present an efficient way to solve it iteratively by introducing a stabilization term with constant coefficient and using discrete sine transform (DST):

$$\frac{\phi_j^{(1),m+1} - \phi_j^n}{\tau} = \frac{1}{2} D_{xx}^s \phi^{(1),m+1} \Big|_{x=x_j} - \alpha \phi_j^{(1),m+1} + (\alpha - V(x_j) - \beta |\phi_j^n|^2) \phi_j^{(1),m}, \quad (3.37)$$

where $m \geq 0$, $\phi_j^{(1),0} = \phi_j^n$ and $j \in \mathcal{T}_M^0$. Here $\alpha \geq 0$ is called as a stabilization parameter to be determined. Taking discrete sine transform at both sides of (3.37), we obtain

$$\frac{(\widetilde{\phi^{(1),m+1}})_l - (\widetilde{\phi^n})_l}{\tau} = - \left(\alpha + \frac{1}{2} \mu_l^2 \right) (\widetilde{\phi^{(1),m+1}})_l + (\widetilde{G^m})_l, \quad l \in \mathcal{T}_M, \quad (3.38)$$

where $(\widetilde{G^m})_l$ are the sine transform coefficients of the vector $G^m = (G_0^m, \dots, G_M^m)^T$ defined as

$$G_j^m = (\alpha - V(x_j) - \beta |\phi_j^n|^2) \phi_j^{(1),m}, \quad j \in \mathcal{T}_M^0. \quad (3.39)$$

Solving (3.38), we get

$$(\widetilde{\phi^{(1),m+1}})_l = \frac{2}{2 + \tau(2\alpha + \mu_l^2)} \left[(\widetilde{\phi^n})_l + \tau (\widetilde{G^m})_l \right], \quad l \in \mathcal{T}_M. \quad (3.40)$$

Taking inverse discrete sine transform for (3.40), we get the solution for (3.37) immediately.

In order to make the iterative method (3.37) for solving (3.34) converges as fast as possible, the ‘optimal’ stabilization parameter α in (3.37) is suggested as [36]:

$$\alpha_{\text{opt}} = \frac{1}{2} (b_{\max} + b_{\min}), \quad (3.41)$$

where

$$b_{\max} = \max_{1 \leq j \leq M-1} (V(x_j) + \beta |\phi_j^n|^2), \quad b_{\min} = \min_{1 \leq j \leq M-1} (V(x_j) + \beta |\phi_j^n|^2). \quad (3.42)$$

Similarly, with the approximation ϕ^n of ϕ by BESP, the energy and chemical potential can be computed as

$$E(\phi(\cdot, t_n)) \approx E^n = \frac{b-a}{4} \sum_{l=1}^{M-1} \mu_l^2 |(\widetilde{\phi^n})_l|^2 + h \sum_{j=0}^{M-1} \left[V(x_j) |\phi_j^n|^2 + \frac{\beta}{2} |\phi_j^n|^4 \right],$$

$$\mu(\phi(\cdot, t_n)) \approx \mu^n = E^n + h \sum_{j=0}^{M-1} \frac{\beta}{2} |\phi_j^n|^4, \quad n \geq 0.$$

Remark 3.1. In practice, Fourier pseudospectral method or cosine pseudospectral method can also be applied to spatial discretization for discretizing (3.20)-(3.22) when the homogeneous Dirichlet boundary condition in (3.22) is replaced by periodic boundary condition or homogeneous Neumann boundary condition, respectively.

3.4. Simplified methods under symmetric potentials. The ground state ϕ_g of (2.11) shares the same symmetric properties with $V(\mathbf{x})$ ($\mathbf{x} \in \mathbb{R}^d$) ($d = 1, 2, 3$). In such cases, simplified numerical methods, especially with less memory requirement, for computing the ground states are available.

Radial symmetry in 1D, 2D and 3D. When the potential $V(\mathbf{x})$ is radially symmetric in $d = 1, 2$ and spherically symmetric in $d = 3$, the problem is reduced to 1D. Due to the symmetry, the GPE (2.1) essentially collapses to a 1D problem with $r = |\mathbf{x}| \in [0, +\infty)$ for $\psi := \psi(r, t)$ ($d = 1, 2, 3$):

$$i\partial_t \psi(r, t) = \frac{-1}{2r^{d-1}} \frac{\partial}{\partial r} \left(r^{d-1} \frac{\partial}{\partial r} \psi \right) + (V(r) + \beta|\psi|^2) \psi, \quad r \in (0, +\infty), \quad (3.43)$$

$$\frac{\partial \psi(0, t)}{\partial r} = 0, \quad \psi(r, t) \rightarrow 0, \quad \text{as } r \rightarrow \infty. \quad (3.44)$$

The normalization condition (2.2) becomes

$$N_r(\psi) = \omega(d) \int_0^\infty |\psi(r, t)|^2 r^{d-1} dr = 1. \quad (3.45)$$

Here $\omega(d)$ is the area of unit sphere in d dimensions, where $\omega(1) = 2$, $\omega(2) = 2\pi$ and $\omega(3) = 4\pi$. The energy (2.3) can be rewritten for radial wave function as

$$E_r(\psi) = \omega(d) \int_0^\infty \left(\frac{1}{2} |\partial_r \psi(r, t)|^2 + V(r) |\psi(r, t)|^2 + \frac{\beta}{2} |\psi(r, t)|^4 \right) r^{d-1} dr. \quad (3.46)$$

Then, the minimization problem (2.11) collapses to :

Find $\varphi_g \in S_r$ such that

$$E_g := E_r(\varphi_g) = \min_{\varphi \in S_r} E_r(\varphi), \quad (3.47)$$

where $S_r = \{\varphi \mid \omega(d) \int_0^\infty |\varphi(r)|^2 r^{d-1} dr = 1, E_r(\varphi) < \infty\}$.

The nonlinear eigenvalue problem (2.8) collapses to

$$\mu \varphi(r) = -\frac{1}{2r^{d-1}} \frac{d}{dr} \left(r^{d-1} \frac{d}{dr} \varphi(r) \right) + V(r) \varphi(r) + \beta |\varphi(r)|^2 \varphi(r), \quad r \in (0, +\infty), \quad (3.48)$$

with boundary conditions

$$\varphi'(0) = 0, \quad \varphi(r) \rightarrow 0, \quad \text{when } r \rightarrow \infty, \quad (3.49)$$

under the normalization constraint (3.45) with $\psi = \varphi$.

The eigenvalue problem (3.48)-(3.49) is defined in a semi-infinite interval $(0, +\infty)$. In practical computation, this is approximated by a problem defined on a finite interval. Since the full wave function vanishes exponentially fast as $r \rightarrow \infty$, choosing $R > 0$ sufficiently large, then the eigenvalue problem (3.48)-(3.49) can be approximated by

$$\mu \varphi(r) = -\frac{1}{2r^{d-1}} \frac{d}{dr} \left(r^{d-1} \frac{d}{dr} \varphi(r) \right) + [V(r) + \beta|\varphi|^2] \varphi(r), \quad 0 < r < R, \quad (3.50)$$

with boundary conditions

$$\varphi'(0) = 0, \quad \varphi(R) = 0, \quad (3.51)$$

under the normalization

$$\omega(d) \int_0^R |\varphi(r)|^2 r^{d-1} dr = 1. \quad (3.52)$$

To compute the ground state φ_g , a method based on GFDN (3.5)-(3.7) can be simplified. Here, we only present full discretization using a simplified BEFD method.

Choose time steps as (3.24), mesh size $\Delta r = 2R/(2M + 1)$ with positive integer M and grid points as

$$r_j = j\Delta r, \quad r_{j+\frac{1}{2}} = \left(j + \frac{1}{2}\right) \Delta r, \quad j \in \mathcal{T}_M^0. \quad (3.53)$$

We adopt the same notation for finite difference operator as (3.25). Let $\varphi_{j+\frac{1}{2}}^n$ be the numerical approximation of $\varphi(r_{j+\frac{1}{2}}, t_n)$ and φ^n be the solution vector at time $t = t_n$ with components $\varphi_{j+\frac{1}{2}}^n$. Then a simplified BEFD method for computing the ground state of (3.47) by GFDN with an initial guess $\varphi_0(r)$ is given as [27]

$$\frac{\varphi_{j+\frac{1}{2}}^{(1)} - \varphi_{j+\frac{1}{2}}^n}{\tau} = \left[\frac{1}{2} \delta_{r,d}^2 - V(r_{j+\frac{1}{2}}) - \beta \left(\varphi_{j+\frac{1}{2}}^n \right)^2 \right] \varphi_{j+\frac{1}{2}}^{(1)}, \quad j \in \mathcal{T}_M \cup \{0\}, \quad (3.54)$$

$$\varphi_{-\frac{1}{2}}^{(1)} = \varphi_{\frac{1}{2}}^{(1)}, \quad \varphi_{M+\frac{1}{2}}^{(1)} = 0, \quad \varphi_{j+\frac{1}{2}}^0 = \varphi_0(r_{j+\frac{1}{2}}), \quad j \in \mathcal{T}_M^0,$$

$$\varphi_{j+\frac{1}{2}}^{n+1} = \frac{\varphi_{j+\frac{1}{2}}^{(1)}}{\|\varphi^{(1)}\|_r}, \quad j \in \mathcal{T}_M^0, \quad n = 0, 1, \dots, \quad (3.55)$$

where

$$\delta_{r,d}^2 \varphi_{j+\frac{1}{2}}^{(1)} = \frac{1}{(\Delta r)^2 r_{j+\frac{1}{2}}^{d-1}} \left[r_{j+1}^{d-1} \varphi_{j+\frac{3}{2}}^{(1)} - (r_{j+1}^{d-1} + r_j^{d-1}) \varphi_{j+\frac{1}{2}}^{(1)} + r_j^{d-1} \varphi_{j-\frac{1}{2}}^{(1)} \right],$$

and the norm is defined as

$$\|\varphi^{(1)}\|_r^2 = \omega(d) \Delta r \sum_{j=0}^{M-1} |\varphi_{j+\frac{1}{2}}^{(1)}|^2 (r_{j+\frac{1}{2}})^{d-1}. \quad (3.56)$$

Here, we have introduced a ghost point $r_{-\frac{1}{2}}$ so that the Neumann boundary condition $\varphi'(0) = 0$ is approximated with second order accuracy. The linear system (3.54) can be solved very efficiently by the Thomas' algorithm, where the computational cost is $O(M)$ per time step, for all dimensions $d = 1, 2, 3$. The memory cost is $O(M)$. This tremendously reduces memory and computation complexity in higher dimensions ($d = 2, 3$) from $O(M^d)$ to $O(M)$ compared with the proposed BEFD (3.28) with Cartesian coordinates.

Cylindrical symmetry in 3D. For $\mathbf{x} = (x, y, z)^T \in \mathbb{R}^3$, when V is cylindrically symmetric, i.e., V is of the form $V(r, z)$ ($r = \sqrt{x^2 + y^2}$), the problem is reduced to 2D. Due to the symmetry, the GPE (2.1) essentially collapses to a 2D problem with $r \in (0, +\infty)$ and $z \in \mathbb{R}$ for $\psi := \psi(r, z, t)$:

$$i\partial_t \psi(r, z, t) = -\frac{1}{2} \left[\frac{1}{r} \frac{\partial}{\partial r} \left(r \frac{\partial \psi}{\partial r} \right) + \frac{\partial^2 \psi}{\partial z^2} \right] + (V(r, z) + \beta |\psi|^2) \psi, \quad (3.57)$$

$$\frac{\partial \psi(0, z, t)}{\partial r} = 0, \quad z \in \mathbb{R}, \quad \psi(r, z, t) \rightarrow 0, \quad \text{when } r + |z| \rightarrow \infty. \quad (3.58)$$

The normalization condition (2.2) becomes

$$N_c(\psi) = 2\pi \int_{\mathbb{R}^+} \int_{\mathbb{R}} |\psi(r, z, t)|^2 r dz dr = 1. \quad (3.59)$$

Then, the minimization problem (2.11) collapses to :
Find $\varphi_g \in S_c$ such that

$$E_g := E_c(\varphi_g) = \min_{\varphi \in S_c} E_c(\varphi), \quad (3.60)$$

where

$$E_c(\varphi) = \pi \int_{\mathbb{R}^+} \int_{\mathbb{R}} (|\varphi_r(r, z)|^2 + |\varphi_z(r, z)|^2 + 2V(r, z)|\varphi|^2 + \beta|\varphi|^4) r dz dr, \quad (3.61)$$

and $S_c = \{\varphi \mid 2\pi \int_{\mathbb{R}^+} \int_{\mathbb{R}} |\varphi(r, z)|^2 r dz dr = 1, E_c(\varphi) < \infty\}$.

The nonlinear eigenvalue problem (2.8) collapses to

$$\mu\varphi(r, z) = -\frac{1}{2} \left[\frac{1}{r} \frac{\partial}{\partial r} \left(r \frac{\partial \varphi}{\partial r} \right) + \frac{\partial^2 \varphi}{\partial z^2} \right] + (V(r, z) + \beta|\varphi|^2) \varphi, \quad r > 0, z \in \mathbb{R}, \quad (3.62)$$

with boundary conditions

$$\frac{\partial \varphi(0, z, t)}{\partial r} = 0, \quad z \in \mathbb{R}, \quad \varphi(r, z, t) \rightarrow 0, \quad \text{when } r + |z| \rightarrow \infty, \quad (3.63)$$

under the normalization constraint (3.59) with $\psi = \varphi$.

The eigenvalue problem (3.48)-(3.49) is defined in the r - z plane. In practical computation, this is approximated by a problem defined on a bounded domain. Since the full wave function vanishes exponentially fast as $r + |z| \rightarrow \infty$, choosing $R > 0$ and $Z_1 < Z_2$ with $|Z_1|, |Z_2|$ and R sufficiently large, then the eigenvalue problem (3.62)-(3.63) can be approximated for $(r, z) \in (0, R) \times (Z_1, Z_2)$,

$$\mu \varphi(r, z) = -\frac{1}{2} \left[\frac{1}{r} \frac{\partial}{\partial r} \left(r \frac{\partial \varphi}{\partial r} \right) + \frac{\partial^2 \varphi}{\partial z^2} \right] + (V(r, z) + \beta|\varphi|^2) \varphi, \quad (3.64)$$

with boundary conditions

$$\frac{\partial \varphi(0, z)}{\partial r} = 0, \quad \varphi(R, z) = \varphi(r, Z_1) = \varphi(r, Z_2) = 0, \quad z \in [Z_1, Z_2], r \in [0, R], \quad (3.65)$$

under the normalization

$$2\pi \int_0^R \int_{Z_1}^{Z_2} |\varphi(r, z)|^2 r dz dr = 1. \quad (3.66)$$

To compute the ground state, the GFDN (3.5)-(3.7) collapses to a 2D problem. We present a full finite difference discretization. Choose time steps as (3.24) and r -grid points (3.53) for positive integer $M > 0$. For integer $N > 0$, choose mesh size $\Delta z = (Z_2 - Z_1)/N$ and define z -grid points $z_k = Z_1 + k\Delta z$ for $k \in \mathcal{T}_N^0 = \{k \mid k = 0, 1, \dots, N\}$.

Let $\varphi_{j+\frac{1}{2}k}^n$ be the numerical approximation of $\varphi(r_{j+\frac{1}{2}}, z_k, t_n)$ and φ^n be the solution vector at time $t = t_n$ with components $\varphi_{j+\frac{1}{2}k}^n$. Then a simplified BEFD method for computing the ground state of (3.61) by GFDN with an initial guess

$\varphi_0(r, z)$ is given below [27]:

$$\begin{aligned} \frac{\varphi_{j+\frac{1}{2}k}^{(1)} - \varphi_{j+\frac{1}{2}k}^n}{\tau} &= \left[\frac{1}{2}(\delta_r^2 + \delta_z^2) - V(r_{j+\frac{1}{2}}, z_k) - \beta \left(\varphi_{j+\frac{1}{2}k}^n \right)^2 \right] \varphi_{j+\frac{1}{2}k}^{(1)}, \quad (j, k) \in \mathcal{T}_{MN}^*, \\ \varphi_{-\frac{1}{2}k}^{(1)} &= \varphi_{\frac{1}{2}k}^{(1)}, \quad \varphi_{M+\frac{1}{2}k}^{(1)} = \varphi_{j+\frac{1}{2}0}^{(1)} = \varphi_{j+\frac{1}{2}N}^{(1)} = 0, \quad (j, k) \in \mathcal{T}_{MN}^0, \\ \varphi_{j+\frac{1}{2}k}^0 &= \varphi_0(r_{j+\frac{1}{2}}, z_k), \quad \varphi_{j+\frac{1}{2}k}^{n+1} = \frac{\varphi_{j+\frac{1}{2}k}^{(1)}}{\|\varphi^{(1)}\|_c}, \quad (j, k) \in \mathcal{T}_{MN}^0, \quad n \geq 0, \end{aligned} \quad (3.67)$$

where $\mathcal{T}_{MN}^* = \{(j, k) \mid 0 \leq j \leq M-1, 1 \leq k \leq N-1\}$, $\mathcal{T}_{MN}^0 = \{(j, k) \mid 0 \leq j \leq M, 0 \leq k \leq N\}$ and

$$\begin{aligned} \delta_r^2 \varphi_{j+\frac{1}{2}k}^{(1)} &= \frac{1}{(\Delta r)^2 r_{j+\frac{1}{2}}} \left[r_{j+1} \varphi_{j+\frac{3}{2}k}^{(1)} - (r_{j+1} + r_j) \varphi_{j+\frac{1}{2}k}^{(1)} + r_j \varphi_{j-\frac{1}{2}k}^{(1)} \right], \\ \delta_z^2 \varphi_{j+\frac{1}{2}k}^{(1)} &= \frac{1}{(\Delta z)^2} [\varphi_{j+\frac{1}{2}k+1}^{(1)} - 2\varphi_{j+\frac{1}{2}k}^{(1)} + \varphi_{j+\frac{1}{2}k-1}^{(1)}], \quad (j, k) \in \mathcal{T}_{MN}^*, \end{aligned}$$

and the norm is defined by

$$\|\varphi^{(1)}\|_c^2 = 2\pi \Delta r \Delta z \sum_{j=0}^{M-1} \sum_{k=0}^{N-1} |\varphi_{j+\frac{1}{2}k}^{(1)}|^2 r_{j+\frac{1}{2}}. \quad (3.68)$$

Here, we use ghost points to approximate the Neumann boundary conditions, which is the same as the radially symmetric potential case.

Remark 3.2. When the potential $V(\mathbf{x})$ is an even function, BEFD (3.28) and BSP (3.34)-(3.35) can be used to compute the first excited states by choosing proper initial guess (see [27, 36]).

3.5. Numerical results. In this section, we report numerical results on the ground state by the proposed BEFD and BSP methods.

Example 3.1. Ground and first excited states (Remark 3.2) in 1D, i.e., we take $d = 1$ in (2.1) and study two kinds of trapping potentials

Case I. A harmonic oscillator potential $V(x) = \frac{x^2}{2}$ and $\beta = 400$;

Case II. An optical lattice potential $V(x) = \frac{x^2}{2} + 25 \sin^2\left(\frac{\pi x}{4}\right)$ and $\beta = 250$.

The initial data (3.7) is chosen as $\phi_0(x) = e^{-x^2/2}/\pi^{1/4}$ for computing the ground state, and resp., $\phi_0(x) = \frac{\sqrt{2}x}{\pi^{1/4}} e^{-x^2/2}$ for computing the first excited state. We solve the problem with BSP (3.34)-(3.35) on $[-16, 16]$, i.e. $a = -16$ and $b = 16$, and take time step $\tau = 0.05$ for computing the ground state, and resp., $\tau = 0.001$ for computing the first excited state. The steady state solution in our computation is reached when $\max_{1 \leq j \leq M-1} |\phi_j^{n+1} - \phi_j^n| < 10^{-12}$. Let ϕ_g and ϕ_1 be the ‘exact’ ground state and first excited state, respectively, which are obtained numerically by using BSP with a very fine mesh $h = \frac{1}{32}$ and $h = \frac{1}{128}$, respectively. We denote their energy and chemical potential as $E_g := E(\phi_g)$, $E_1 := E(\phi_1)$, and $\mu_g := \mu(\phi_g)$, $\mu_1 := \mu(\phi_1)$. Let $\phi_{g,h}^{\text{SP}}$ and $\phi_{1,h}^{\text{SP}}$ be the numerical ground state and first excited state obtained by using BSP with mesh size h , respectively. Similarly, $\phi_{g,h}^{\text{FD}}$ and $\phi_{1,h}^{\text{FD}}$ are obtained by using BEFD in a similar way. Tabs. 3.1 and 3.2 list the errors for Case I, and Tabs. 3.3 and 3.4 show the errors for Case II. Furthermore, we compute the energy and chemical potential for the ground state and first excited state based on our ‘exact’ solution ϕ_g and ϕ_1 . For Case I, we have $E_g := E(\phi_g) = 21.3601$ and $\mu_g := \mu(\phi_g) = 35.5775$ for ground state, and $E_1 := E(\phi_1) = 22.0777$ and

$\mu_1 := \mu(\phi_1) = 36.2881$ for the first excited state. Similarly, for Case II, we have $E_g = 26.0838$, $\mu_g = 38.0692$, $E_1 = 27.3408$ and $\mu_1 = 38.9195$. Fig. 3.1 plots ϕ_g and ϕ_1 as well as their corresponding trapping potentials for Cases I&II. Fig. 3.2a shows the excited states ϕ_1 for potential in Case I with different β .

mesh size	$h = 1$	$h = 1/2$	$h = 1/4$	$h = 1/8$
$\max \phi_g - \phi_{g,h}^{\text{SP}} $	1.310E-3	7.037E-5	1.954E-8	<E-12
$\ \phi_g - \phi_{g,h}^{\text{SP}}\ $	1.975E-3	7.425E-5	2.325E-8	<E-12
$ E_g - E(\phi_{g,h}^{\text{SP}}) $	5.688E-5	2.642E-6	9E-12	<E-12
$ \mu_g - \mu(\phi_{g,h}^{\text{SP}}) $	1.661E-2	8.705E-5	9.44E-10	4E-12
$\max \phi_g - \phi_{g,h}^{\text{FD}} $	2.063E-3	1.241E-3	2.890E-4	7.542E-5
$\ \phi_g - \phi_{g,h}^{\text{FD}}\ $	3.825E-3	1.439E-3	3.130E-4	7.705E-5
$ E_g - E(\phi_{g,h}^{\text{FD}}) $	2.726E-3	9.650E-4	2.540E-4	6.439E-5
$ \mu_g - \mu(\phi_{g,h}^{\text{FD}}) $	2.395E-2	6.040E-4	2.240E-4	5.694E-5

TABLE 3.1. Spatial resolution of BESP and BEFD for ground state of Case I in Example 3.1.

Mesh size	$h = 1/4$	$h = 1/8$	$h = 1/16$	$h = 1/32$
$\max \phi_1 - \phi_{1,h}^{\text{SP}} $	2.064E-1	6.190E-4	2.099E-7	<E-12
$\ \phi_1 - \phi_{1,h}^{\text{SP}}\ $	1.093E-1	3.200E-4	1.403E-7	<E-12
$ E_1 - E(\phi_{1,h}^{\text{SP}}) $	5.259E-2	3.510E-4	5.550E-9	<E-12
$ \mu_1 - \mu(\phi_{1,h}^{\text{SP}}) $	1.216E-1	1.509E-3	4.762E-8	<E-12
$\max \phi_1 - \phi_{1,h}^{\text{FD}} $	2.348E-1	8.432E-3	2.267E-3	6.040E-4
$\ \phi_1 - \phi_{1,h}^{\text{FD}}\ $	1.197E-1	4.298E-3	1.215E-3	2.950E-4
$ E_1 - E(\phi_{1,h}^{\text{FD}}) $	3.154E-1	5.212E-2	1.382E-2	3.449E-3
$ \mu_1 - \mu(\phi_{1,h}^{\text{FD}}) $	4.216E-1	5.884E-2	1.609E-2	3.999E-3

TABLE 3.2. Spatial resolution of BESP and BEFD for the first excited state of Case I in Example 3.1.

Mesh size	$h = 1$	$h = 1/2$	$h = 1/4$	$h = 1/8$
$\max \phi_g - \phi_{g,h}^{\text{SP}} $	7.982E-3	1.212E-3	2.219E-6	1.9E-11
$\ \phi_g - \phi_{g,h}^{\text{SP}}\ $	1.304E-2	1.313E-3	2.431E-6	2.8E-11
$ E_g - E(\phi_{g,h}^{\text{SP}}) $	4.222E-4	1.957E-4	4.994E-8	<E-12
$ \mu_g - \mu(\phi_{g,h}^{\text{SP}}) $	9.761E-2	4.114E-3	5.605E-7	<E-12
$\max \phi_g - \phi_{g,h}^{\text{FD}} $	1.019E-2	5.815E-3	1.001E-3	2.541E-4
$\ \phi_g - \phi_{g,h}^{\text{FD}}\ $	1.967E-2	7.051E-3	1.390E-3	3.387E-4
$ E_g - E(\phi_{g,h}^{\text{FD}}) $	7.852E-2	2.961E-2	7.940E-3	2.027E-3
$ \mu_g - \mu(\phi_{g,h}^{\text{FD}}) $	1.786E-1	1.716E-2	6.730E-3	1.728E-3

TABLE 3.3. Spatial resolution of BESP and BEFD for ground state of Case II in Example 3.1.

Mesh size	$h = 1/4$	$h = 1/8$	$h = 1/16$	$h = 1/32$
$\max \phi_1 - \phi_{1,h}^{\text{SP}} $	2.793E-1	1.010E-3	4.240E-7	2E-12
$\ \phi_1 - \phi_{1,h}^{\text{SP}}\ $	1.477E-1	5.241E-4	2.784E-7	2E-12
$ E_1 - E(\phi_{1,h}^{\text{SP}}) $	1.145E-1	8.337E-4	1.943E-8	<E-12
$ \mu_1 - \mu(\phi_{1,h}^{\text{SP}}) $	1.593E-1	2.357E-3	1.097E-7	5E-12
$\max \phi_1 - \phi_{1,h}^{\text{FD}} $	3.134E-1	1.124E-2	3.231E-3	8.450E-4
$\ \phi_1 - \phi_{1,h}^{\text{FD}}\ $	1.599E-1	5.779E-3	1.701E-3	4.122E-4
$ E_1 - E(\phi_{1,h}^{\text{FD}}) $	6.011E-1	1.002E-1	2.688E-2	6.707E-3
$ \mu_1 - \mu(\phi_{1,h}^{\text{FD}}) $	6.315E-1	9.887E-2	2.742E-2	6.827E-3

TABLE 3.4. Spatial resolution of BESP and BEFD for the first excited state of Case II in Example 3.1.

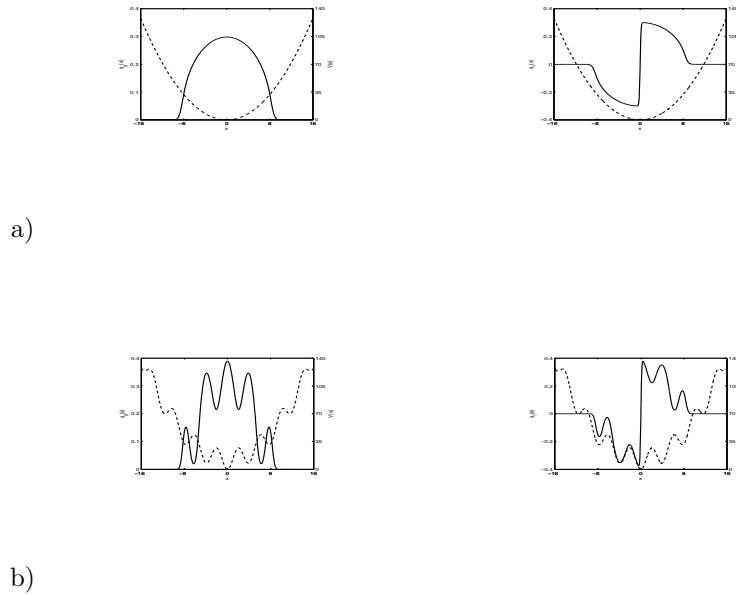


FIGURE 3.1. Ground state ϕ_g (left column, solid lines) and first excited state ϕ_1 (right column, solid lines) as well as trapping potentials (dashed lines) in Example 3.1. a): For Case I; b): For Case II.

From Tabs. 3.1-3.4, Figs. 3.1 and 3.2a, we can draw the following conclusions. For BESP, it is spectrally accurate in spatial discretization; where for BEFD, it is only second-order accurate. The error in the ground and first excited states is only due to the spatial discretization. Thus when high accuracy is required or the solution has multiscale structure [37], BESP is much better than BEFD in terms that it needs much less grid points. Therefore BESP can save a lot of memory and computational time, especially in 2D & 3D.

Example 3.2. Ground states in 2D with radial symmetric trap, i.e. we take $d = 2$ in (2.1) and

$$V(x, y) = V(r) = \frac{1}{2}r^2, \quad (x, y) \in \mathbb{R}^2, \quad r = \sqrt{x^2 + y^2} \geq 0. \quad (3.69)$$

The GFDN (3.5)-(3.7) is solved in polar coordinate with $R = 8 + 1/128$ under mesh size $\Delta r = \frac{1}{64}$ and time step $\tau = 0.1$ by using the simplified BEFD (3.54)-(3.55) with initial data $\phi_0(x, y) = \phi_0(r) = \frac{1}{\sqrt{\pi}} e^{-r^2/2}$. Fig. 3.2b shows the ground state solution $\phi_g(r)$ with different β . Tab. 3.5 displays the values of $\phi_g(0)$, radius mean square $r_{\text{rms}} = \sqrt{2\pi \int_0^\infty r^2 |\phi_g(r)|^2 r dr}$, energy $E(\phi_g)$ and chemical potential μ_g for different β .

β	$\phi_g(0)$	r_{rms}	$E(\phi_g)$	$\mu_g = \mu(\phi_g)$
0	0.5642	1.0000	1.0000	1.0000
10	0.4104	1.2619	1.5923	2.0637
50	0.2832	1.7018	2.8960	4.1430
100	0.2381	1.9864	3.9459	5.7597
250	0.1892	2.4655	6.0789	9.0031
500	0.1590	2.9175	8.5118	12.6783

TABLE 3.5. Numerical results for radial symmetric ground states in Example 3.2.

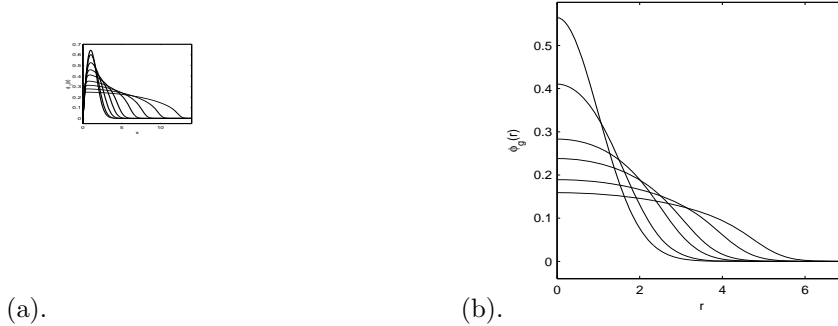


FIGURE 3.2. (a). First excited state solution $\phi_1(x)$ (an odd function) in Example 3.1 with potential in Case I for different $\beta = 0, 3.1371, 12.5484, 31.371, 62.742, 156.855, 313.71, 627.42, 1254.8$ (with decreasing peak); and (b). 2D ground states $\phi_g(r)$ in Example 3.2 for $\beta = 0, 10, 50, 100, 250, 500$ (with decreasing peak).

3.6. Comments of different methods. In literatures, different numerical methods have been introduced to compute ground states of BEC. In [157], Ruprecht et al. used Crank-Nicolson finite difference method to compute the ground states of BEC based on the Euler-Lagrange equation (2.8). Later, Edwards et al. proposed a Runge-Kutta method to find the ground states in 1D and 3D with spherical symmetry. Dodd [90] gave an analytical expansion of the energy $E(\phi)$ using the

Hermite polynomials when the trap V is harmonic. By minimizing the energy in terms of the expansion, approximated ground state results were reported in [90]. In [78], Succi et al. used an imaginary time method (equivalent to GFDN) to compute the ground states with centered finite-difference discretization in space and explicit forward discretization in time. Lin et al. designed an iterative method in [77]. After discretization in space, they transformed the problem to a minimization problem in finite dimensional vector space. Gauss-Seidel iteration methods were proposed to solve the corresponding problem. Bao and Tang proposed a finite element method to find the ground state by directly minimizing the energy functional in [43]. In [27, 36], Bao et al. developed the GFDN method to calculate the ground state, which contains a gradient flow and a projection at each step. Different discretizations have been discussed, including the finite difference discretization or spectral discretization in space, explicit (forward Euler) discretization or implicit (backward Euler, Crank-Nicolson) discretization in time.

In the current studies of BEC, the most popular method for computing the ground state is the GFDN method. In fact, imaginary time method [78] is the same as the GFDN method, while imaginary time is preferred in the physics community. There are many different discretizations for GFDN (3.5)-(3.7) [27, 36], including backward Euler, Crank-Nicolson, forward Euler, backward Euler for linear part and forward Euler for nonlinear part, time-splitting for the time discretization and centered finite difference or spectral method for spatial discretization. From our experience, among these discretizations, BEFD and BESP are very easy to use, robust, very efficient and accurate in practical computation. Furthermore, energy diminishing is observed in linear case under any time step $\tau > 0$ and nonlinear case when time step τ is not too big [27]. If high accuracy is crucial in computing ground states in BEC, e.g. under an optical lattice potential or in a rotational frame, BESP is recommended.

4. Numerical methods for computing dynamics of GPE. In this section, we review different numerical methods to discretize the Cauchy problem of the GPE (2.1) for computing the dynamics of BEC. In fact, many efficient and accurate numerical methods have been proposed for discretizing the above GPE, or the nonlinear Schrödinger equation (NLSE) in general, such as time-splitting sine pseudospectral method [31, 33, 34, 47], time-splitting finite difference method [42, 180], time-splitting Laguerre-Hermite pseudospectral method [40], conservative Crank-Nicolson finite difference method [20, 21, 76], semi-implicit finite difference method [20, 21], etc. Each method has its own advantages and disadvantages. Here we present the detailed algorithms for some of these methods.

In practice, we truncate the problem on a bounded domain $U \subset \mathbb{R}^d$ ($d = 1, 2, 3$) as Eq. (3.1), with either homogeneous Dirichlet boundary conditions (3.2) or periodic boundary conditions when U is an interval (1D), a rectangle (2D) or a box (3D). For simplicity of notation, we shall introduce the method in one space dimension ($d = 1$). Generalizations to $d > 1$ are straightforward for tensor product grids and the results remain valid without modifications. In 1D, the equation (3.1) becomes

$$i \frac{\partial \psi(x, t)}{\partial t} = -\frac{1}{2} \psi_{xx}(x, t) + V(x) \psi(x, t) + \beta |\psi|^2 \psi(x, t), \quad a < x < b, \quad t > 0, \quad (4.1)$$

$$\psi(x, t = 0) = \psi_0(x), \quad a \leq x \leq b, \quad (4.2)$$

with the homogenous Dirichlet boundary condition

$$\psi(a, t) = \psi(b, t) = 0, \quad t > 0. \quad (4.3)$$

The following periodic boundary condition

$$\psi(a, t) = \psi(b, t), \quad \partial_x \psi(a, t) = \partial_x \psi(b, t), \quad t > 0, \quad (4.4)$$

or homogeneous Neumann boundary condition

$$\partial_x \psi(a, t) = \partial_x \psi(b, t) = 0, \quad t > 0, \quad (4.5)$$

is also widely used in the literature.

To discretize Eq. (4.1), we use uniform grid points. Choose the spatial mesh size $h = \Delta x > 0$ with $\Delta x = (b - a)/M$ (M an even positive integer), the time step τ , the grid points and the time step as in (3.24). Let ψ_j^n be the approximation of $\psi(x_j, t_n)$ and ψ^n be the solution vector with components ψ_j^n .

In the following, we will introduce two widely used schemes: the time-splitting methods and the finite difference time domain (FDTD) methods.

4.1. Time splitting pseudospectral/finite difference method. The time splitting procedure was presented for differential equations in [171] and applied to Schrödinger equations in [114, 175]. For the simplest two-step case, consider an abstract initial value problem for $u : [0, T] \rightarrow \mathcal{B}$ (\mathcal{B} Banach space),

$$\frac{d}{dt}u(t) = (A + B)u(t), \quad u(0) \in \mathcal{B}, \quad (4.6)$$

where A and B are two operators, the solution can be written in the abstract form as $u(t) = e^{t(A+B)}u(0)$. For a given time step $\tau > 0$, let $t_n = n\tau$, $n = 0, 1, \dots$, and u^n be the approximation of $u(t_n)$. The time-splitting approximation, or operator splitting (split-step) is usually given as [171, 189]

$$u^{n+1} = e^{\tau A} e^{\tau B} u^n, \quad \text{Lie-Trotter splitting}, \quad (4.7)$$

or

$$u^{n+1} \approx e^{\tau A/2} e^{\tau B} e^{\tau A/2} u^n, \quad \text{Strang splitting}. \quad (4.8)$$

Formally, from Taylor expansion, it is easy to see that the approximation error of Lie-Trotter splitting is of first order $O(\tau)$, and the error of Strang splitting is of second order $O(\tau^2)$. In principle, splitting approximations of higher order accuracy can be constructed as [189]

$$u^{n+1} \approx e^{a_1 \tau A} e^{b_1 \tau B} e^{a_2 \tau A} e^{b_2 \tau B} \dots e^{a_m \tau A} e^{b_m \tau B} u^n, \quad m \geq 1, \quad (4.9)$$

where coefficients a_j and b_j ($j = 1, \dots, m$) are chosen properly. One of the most frequently used higher order splitting scheme is the fourth-order symplectic time integrator (cf. [40, 189]) for (4.6) as:

$$\begin{aligned} u^{(1)} &= e^{\theta \tau A} u^n, & u^{(2)} &= e^{2\theta \tau B} u^{(1)}, & u^{(3)} &= e^{(0.5-\theta)\tau A} u^{(2)}, \\ u^{(4)} &= e^{(1-4\theta)\tau B} u^{(3)}, & u^{(5)} &= e^{(0.5-\theta)\tau A} u^{(4)}, & u^{(6)} &= e^{2\theta \tau B} u^{(5)}, \\ u^{n+1} &= e^{\theta \tau A} u^{(6)}, \end{aligned} \quad (4.10)$$

where the coefficient θ can be calculated as

$$\theta = \frac{1}{6} \left(2 + 2^{1/3} + 2^{-1/3} \right) \approx 0.67560359597982881702. \quad (4.11)$$

4.1.1. *Time splitting sine pseudospectral method.* In this section we present a time-splitting sine pseudospectral method, to numerically solve the GPE (4.1) with homogenous Dirichlet boundary condition (4.3). The merit of this method is that it is unconditionally stable, time reversible, time-transverse invariant, and that it conserves the total particle number.

Time-splitting sine pseudospectral (TSSP) method. From time $t = t_n$ to $t = t_{n+1}$, the GPE (4.1) is solved in two splitting steps. One solves first

$$i\psi_t = -\frac{1}{2}\psi_{xx}, \quad (4.12)$$

for the time step of length τ , followed by solving

$$i\frac{\partial\psi(x,t)}{\partial t} = V(x)\psi(x,t) + \beta|\psi(x,t)|^2\psi(x,t), \quad (4.13)$$

for the same time step. Eq. (4.12) will be discretized in space by the sine spectral method and integrated in time *exactly*. For $t \in [t_n, t_{n+1}]$, the ODE (4.13) leaves $|\psi|$ invariant in t [31, 33] and therefore becomes

$$i\frac{\partial\psi(x,t)}{\partial t} = V(x)\psi(x,t) + \beta|\psi(x,t_n)|^2\psi(x,t) \quad (4.14)$$

and thus can be integrated *exactly*. This is equivalent to choosing operators A, B in (4.6) as

$$A\psi = \frac{i}{2}\partial_{xx}\psi, \quad B\psi = -i(V(x) + \beta|\psi|^2)\psi. \quad (4.15)$$

From time $t = t_n$ to $t = t_{n+1}$, we combine the splitting steps via the standard Strang splitting [31, 33, 47]:

$$\begin{aligned} \psi_j^{(1)} &= \frac{2}{M} \sum_{l=1}^{M-1} e^{-i\tau\mu_l^2/4} \widetilde{(\psi^n)}_l \sin(\mu_l(x_j - a)), \\ \psi_j^{(2)} &= e^{-i(V(x_j) + \beta|\psi_j^{(1)}|^2)\tau} \psi_j^{(1)}, \quad j \in \mathcal{T}_M, \\ \psi_j^{n+1} &= \frac{2}{M} \sum_{l=1}^{M-1} e^{-i\tau\mu_l^2/4} \widetilde{(\psi^{(2)})}_l \sin(\mu_l(x_j - a)), \quad \psi_0^{n+1} = \psi_M^{n+1} = 0, \end{aligned} \quad (4.16)$$

where $\mu_l = l\pi/(b-a)$ for $l \in \mathcal{T}_M$ and $\widetilde{(\psi^n)}_l$ and $\widetilde{(\psi^{(2)})}_l$ are the discrete sine transform coefficients of ψ^n and $\psi^{(2)}$, respectively, which are defined in (3.31). One can also exchange the order of the steps (4.13) and (4.14) in TSSP (4.16), and the numerical results are almost the same.

Remark 4.1. For the GPE (4.1) truncated in a bounded domain with periodic boundary condition (4.4) or homogenous Neumann boundary condition (4.5), a time splitting Fourier or cosine pseudospectral method similar to TSSP (4.16) is straightforward [31, 33, 44], i.e., solve the linear part (4.12) by Fourier or cosine spectral discretization instead of sine spectral discretization.

4.1.2. *Time splitting finite difference method.* In section 4.1.1, a sine pseudospectral method (or a Fourier pseudospectral method) is used to solve Eq. (4.12). Spectral method is favorable in view of its high accuracy if the solution of continuous problem (2.1) is smooth. For non-smooth potentials $V(x)$ (random potential), the regularity of the solution of the GPE (2.1) would be low. In such case, finite difference method is suggested instead of spectral method.

Time-splitting finite difference (TSFD) method From time $t = t_n$ to $t = t_{n+1}$, the GPE (4.1) with homogenous Dirichlet boundary condition (4.3) is solved in two splitting steps, (4.12) and (4.14). As indicated in section 4.1.1, Eq. (4.14) can be integrated exactly. For the linear part (4.12), we use Crank-Nicolson finite difference method. From time $t = t_n$ to $t = t_{n+1}$, we combine the splitting steps via the standard Strang splitting [42]:

$$\begin{aligned} \psi_j^{(1)} &= e^{-i\tau(V(x_j)+\beta|\psi_j^n|^2)/2} \psi_j^n, & j \in \mathcal{T}_M^0, \\ i\frac{\psi_j^{(2)} - \psi_j^{(1)}}{\tau} &= -\frac{1}{4}(\delta_x^2 \psi_j^{(2)} + \delta_x^2 \psi_j^{(1)}), & j \in \mathcal{T}_M, & \psi_0^{(2)} = \psi_M^{(2)} = 0, \\ \psi_j^{n+1} &= e^{-i\tau(V(x_j)+\beta|\psi_j^{(2)}|^2)/2} \psi_j^{(2)}, & j \in \mathcal{T}_M^0. \end{aligned} \quad (4.17)$$

This method is also unconditionally stable, time reversible, time-transverse invariant, and it conserves the total particle number. The linear part of TSFD (4.17) can be solved by the Thomas' algorithm in 1D and discrete sine transform (DST) in 2D and 3D. Thus, the computational costs of TSFD and TSSP are the same in 2D and 3D, while the cost of TSFD is cheaper in 1D due to the Thomas' algorithm.

4.2. Finite difference time domain method. Finite difference time domain (FDTD) methods for NLSE have been extensively studied in the literature [9, 76] and are widely used. In this section, we present the most popular finite difference discretizations for the GPE (4.1) with homogenous Dirichlet boundary condition (4.3).

4.2.1. Crank-Nicolson finite difference method. The conservative Crank-Nicolson finite difference (CNFD) discretization of GPE (4.1) reads [20, 21, 34, 76, 106]

$$i\delta_t^+ \psi_j^n = \left[-\frac{1}{2}\delta_x^2 + V_j + \frac{\beta}{2}(|\psi_j^{n+1}|^2 + |\psi_j^n|^2) \right] \psi_j^{n+1/2}, \quad j \in \mathcal{T}_M, \quad n \geq 0, \quad (4.18)$$

where

$$V_j = V(x_j), \quad \psi_j^{n+1/2} = \frac{1}{2}(\psi_j^{n+1} + \psi_j^n), \quad j \in \mathcal{T}_M^0, \quad n = 0, 1, 2, \dots$$

The boundary condition (4.3) is discretized as

$$\psi_0^{n+1} = \psi_M^{n+1} = 0, \quad n = 0, 1, \dots, \quad (4.19)$$

and the initial condition (4.2) is discretized as

$$\psi_j^0 = \psi_0(x_j), \quad j \in \mathcal{T}_M^0. \quad (4.20)$$

The above CNFD method conserves the mass and energy in the discretized level. However, it is a fully implicit method, i.e., at each time step, a fully nonlinear system must be solved, which may be very expensive, especially in 2D and 3D. In fact, if the fully nonlinear system is not solved numerically to extremely high accuracy, e.g., at machine accuracy, then the mass and energy of the numerical solution obtained in practical computation are no longer conserved [21]. This motivates us also consider the following semi-implicit discretization for the GPE.

4.2.2. *Semi-implicit finite difference method.* The *semi-implicit finite difference* (SIFD) discretization of the GPE (4.1), is to use Crank-Nicolson/leap-frog schemes for discretizing linear/nonlinear terms, respectively, as [20, 21]

$$i\delta_t\psi_j^n = \left[-\frac{1}{2}\delta_x^2 + V_j\right] \frac{\psi_j^{n+1} + \psi_j^{n-1}}{2} + \beta|\psi_j^n|^2\psi_j^n, \quad j \in \mathcal{T}_M, \quad n \geq 1. \quad (4.21)$$

Again, the boundary condition (4.3) and initial condition (4.2) are discretized in (4.19) and (4.20), respectively. In addition, the first step can be computed by any explicit second or higher order time integrator, e.g., the second-order modified Euler method, as

$$\begin{aligned} \psi_j^1 &= \psi_j^0 - i\tau \left[\left(-\frac{1}{2}\delta_x^2 + V_j\right) \psi_j^{(1)} + \beta|\psi_j^{(1)}|^2\psi_j^{(1)} \right], \quad j \in \mathcal{T}_M, \quad (4.22) \\ \psi_j^{(1)} &= \psi_j^0 - i\frac{\tau}{2} \left[\left(-\frac{1}{2}\delta_x^2 + V_j\right) \psi_j^0 + \beta|\psi_j^0|^2\psi_j^0 \right]. \end{aligned}$$

For this SIFD method, at each time step, only a linear system is to be solved, which is much more cheaper than that of the CNFD method in practical computation.

4.3. **Simplified methods for symmetric potential and initial data.** Similar to section 3.4, when the potential $V(\mathbf{x})$ ($\mathbf{x} \in \mathbb{R}^d$, $d = 1, 2, 3$) and the initial data ψ_0 are symmetric, then the solution of the GPE (2.1) is symmetric. In such cases, simplified numerical methods, especially with less memory requirement, are available for computing the dynamics of GPE.

4.3.1. *Radial symmetry in 1D, 2D and 3D.* When potential $V(\mathbf{x})$ and initial data $\psi(\mathbf{x}, 0) = \psi_0(\mathbf{x})$ are radially symmetric for $d = 1, 2$ and spherically symmetric for $d = 3$, the problem is reduced to 1D. In such case, the GPE (2.1) collapse to the 1D equation (3.43) for $\psi := \psi(r, t)$ with $r = |\mathbf{x}| \geq 0$.

In practical computation, the equation (3.43) is approximated on a finite interval. Since the wave function vanishes as $r \rightarrow \infty$, choosing $R > 0$ sufficiently large, equation (3.43) can be approximated by

$$i\partial_t\psi(r, t) = -\frac{1}{2r^{d-1}}\frac{\partial}{\partial r}\left(r^{d-1}\frac{\partial}{\partial r}\psi\right) + V(r)\psi + \beta|\psi|^2\psi, \quad 0 < r < R, \quad (4.23)$$

with boundary conditions

$$\partial_r\psi(0, t) = 0, \quad \psi(R, t) = 0, \quad t \geq 0, \quad (4.24)$$

and initial condition

$$\psi(r, 0) = \psi_0(r), \quad 0 \leq r \leq R. \quad (4.25)$$

For this 1D problem, an efficient and accurate method is the time-splitting finite difference (TSFD) method. Choose time steps as (3.24) and mesh size $\Delta r = 2R/(2M + 1)$ for some integer $M > 0$. We use the same notations for the grid points as (3.53), and let $\psi_{j+\frac{1}{2}}^n$ be the numerical approximation of $\psi(r_{j+\frac{1}{2}}, t_n)$ and ψ^n be the solution vector at time $t = t_n$ with components $\psi_{j+\frac{1}{2}}^n$. The time-splitting

finite difference (TSFD) discretization for (4.23) reads

$$\begin{aligned}
\psi_{j+\frac{1}{2}}^{(1)} &= e^{-i\tau\beta|\psi_{j+\frac{1}{2}}^n|^2/2} \psi_{j+\frac{1}{2}}^n, & j \in \mathcal{T}_M^0, \\
i\frac{\psi_{j+\frac{1}{2}}^{(2)} - \psi_{j+\frac{1}{2}}^{(1)}}{\tau} &= \left[-\frac{1}{2}\delta_{r,d}^2 + V(r_{j+\frac{1}{2}}) \right] \frac{\psi_{j+\frac{1}{2}}^{(2)} + \psi_{j+\frac{1}{2}}^{(1)}}{2}, & 0 \leq j \leq M-1, \\
\psi_{-\frac{1}{2}}^{(2)} &= \psi_{\frac{1}{2}}^{(2)}, & \psi_{M+\frac{1}{2}}^{(2)} = 0, & \psi_{j+\frac{1}{2}}^0 = \psi_0(r_{j+\frac{1}{2}}), & j \in \mathcal{T}_M^0, \\
\psi_{j+\frac{1}{2}}^{n+1} &= e^{-i\tau\beta|\psi_{j+\frac{1}{2}}^{(2)}|^2/2} \psi_{j+\frac{1}{2}}^{(2)}, & j \in \mathcal{T}_M^0, & n \geq 0.
\end{aligned} \tag{4.26}$$

This method is second-order accurate in space and time, unconditionally stable and it conserves the normalization in the discretized level. The memory cost is $O(M)$ and computational cost is $O(M)$ per time step, which save significantly from $O(M^d)$ and $O(M^d \ln M)$, respectively, in 2D and 3D when the Cartesian coordinates is used by TSSP.

4.3.2. Cylindrical symmetry in 3D. For $\mathbf{x} = (x, y, z)^T \in \mathbb{R}^3$, when V and ψ_0 are cylindrically symmetric, i.e., V and ψ_0 are of the form $V(r, z)$ and $\psi_0(r, z)$ ($r = \sqrt{x^2 + y^2}$), respectively, the Cauchy problem of the GPE (2.1) is reduced to 2D. Due to the symmetry, the GPE (2.1) essentially collapses to the 2D problem (3.57) with $r \in (0, +\infty)$ and $z \in \mathbb{R}$ for $\psi := \psi(r, z, t)$.

In practice, the GPE (3.57) is truncated on a bounded domain. Choosing $R > 0$ and $Z_1 < Z_2$ with $|Z_1|, |Z_2|$ and R sufficiently large, then Eq. (3.57) can be approximated for $(r, z) \in (0, R) \times (Z_1, Z_2)$ as,

$$i\partial_t \psi(r, z, t) = -\frac{1}{2} \left[\frac{1}{r} \frac{\partial}{\partial r} \left(r \frac{\partial \psi}{\partial r} \right) + \frac{\partial^2 \psi}{\partial z^2} \right] + (V(r, z) + \beta|\psi|^2) \psi, \tag{4.27}$$

with boundary condition

$$\frac{\partial \psi(0, z, t)}{\partial r} = 0, \quad \psi(R, z, t) = \psi(r, Z_1, t) = \psi(r, Z_2, t) = 0, \quad z \in [Z_1, Z_2], \quad r \in [0, R], \tag{4.28}$$

and initial condition

$$\psi(r, z, 0) = \psi_0(r, z), \quad z \in [Z_1, Z_2], \quad r \in [0, R]. \tag{4.29}$$

Similar to section 3.4, choose time steps as (3.24) and r - grid points (3.53) for positive integer $M > 0$. For integer $N > 0$, choose mesh size $\Delta z = (Z_2 - Z_1)/N$ and define z - grid points $z_k = Z_1 + k\Delta z$ for $k \in \mathcal{T}_N^0$. Let $\psi_{j+\frac{1}{2}k}^n$ be the numerical approximation of $\psi(r_{j+\frac{1}{2}}, z_k, t_n)$ and ψ^n be the solution vector at time $t = t_n$ with components $\psi_{j+\frac{1}{2}k}^n$. Then the time-splitting finite difference (TSFD) discretization for (4.27) reads

$$\begin{aligned}
\psi_{j+\frac{1}{2}k}^{(1)} &= e^{-i\tau[V(r_{j+\frac{1}{2}}, z_k) + \beta|\psi_{j+\frac{1}{2}k}^n|^2]/2} \psi_{j+\frac{1}{2}k}^n, & (j, k) \in \mathcal{T}_{MN}^0, \\
i\frac{\psi_{j+\frac{1}{2}k}^{(2)} - \psi_{j+\frac{1}{2}k}^{(1)}}{\tau} &= -\frac{1}{4}(\delta_r^2 + \delta_z^2) \left(\psi_{j+\frac{1}{2}k}^{(2)} + \psi_{j+\frac{1}{2}k}^{(1)} \right), & (j, k) \in \mathcal{T}_{MN}^*, \\
\psi_{-\frac{1}{2}k}^{(2)} &= \psi_{\frac{1}{2}k}^{(2)}, & \psi_{M+\frac{1}{2}k}^{(2)} = \psi_{j+\frac{1}{2}0}^{(2)} = \psi_{j+\frac{1}{2}N}^{(2)} = 0, & (j, k) \in \mathcal{T}_{MN}^0, \\
\psi_{j+\frac{1}{2}k}^{n+1} &= e^{-i\tau[V(r_{j+\frac{1}{2}}, z_k) + \beta|\psi_{j+\frac{1}{2}k}^{(2)}|^2]/2} \psi_{j+\frac{1}{2}k}^{(2)}, & (j, k) \in \mathcal{T}_{MN}^0,
\end{aligned} \tag{4.30}$$

with $\psi_{j+\frac{1}{2}k}^0 = \psi_0(r_{j+\frac{1}{2}}, z_k)$ for $(j, k) \in \mathcal{T}_{MN}^0$. This method is second-order accurate in space and time, unconditionally stable and it conserves the normalization in the discretized level. The memory cost is $O(MN)$ and computational cost is $O(MN \ln M)$ per time step, which save significantly from $O(M^2N)$ and $O(M^2N \ln M)$, respectively, when the Cartesian coordinates is used by TSSP.

4.4. Error estimates for SIFD and CNFD. In this section, we present the error estimates for CNFD (4.18) and SIFD (4.21). The notations for finite difference operators, related finite dimensional vector space and norms are given in section 3.2. Specially, for real valued nonnegative potential $V(x)$, we define the corresponding discrete weighted l^2 norm for $u = (u_0, u_1, \dots, u_M)^T \in X_M$ as:

$$\|u\|_V^2 = h \sum_{j=0}^{M-1} V_j |u_j|^2. \quad (4.31)$$

In the remaining part of this section, we use the notation $p \lesssim q$ to represent that there exists a generic constant C which is independent of time step τ and mesh size h such that $|p| \leq Cq$.

To state the error bounds, we define the ‘error’ function $e^n \in X_M$ as

$$e_j^n = \psi(x_j, t_n) - \psi_j^n, \quad j \in \mathcal{T}_M^0, \quad n \geq 0, \quad (4.32)$$

where $\psi := \psi(x, t)$ is the exact solution of the GPE (4.1) and ψ_j^n is the numerical solution. We make the following assumption on the exact solution ψ , i.e., let $0 < T < T_{\max}$ with T_{\max} the maximal existing time of the solution [73, 173]:

$$\psi \in C^3([0, T]; W^{1,\infty}) \cap C^2([0, T]; W^{3,\infty}) \cap C^0([0, T]; W^{5,\infty} \cap H_0^1), \quad (4.33)$$

where the spatial norms are taken in the interval $U = (a, b)$.

For the SIFD method, we have [20, 21]

Theorem 4.1. *Assuming that (4.33) holds and that $V(x) \in C^1(\bar{U})$, there exist $h_0 > 0$ and $0 < \tau_0 \leq \frac{1}{4}$ sufficiently small, when $0 < h \leq h_0$ and $0 < \tau \leq \tau_0 \leq \frac{1}{4}$, we have the following error estimates for the SIFD method (4.21) with (4.19), (4.20) and (4.22)*

$$\|e^n\|_2 \lesssim h^2 + \tau^2, \quad \|\delta_x^+ e^n\|_2 \lesssim h^{3/2} + \tau^{3/2}, \quad \|\psi^n\|_\infty \leq 1 + M_1, \quad 0 \leq n \leq \frac{T}{\tau}, \quad (4.34)$$

where $M_1 = \max_{0 \leq t \leq T} \|\psi(\cdot, t)\|_{L^\infty(U)}$. In addition, if either $\partial_n V(x)|_\Gamma = 0$ ($\Gamma = \partial U$, ∂_n is the outer normal derivative) or $\psi \in C^0([0, T]; H_0^2(U))$, we have the optimal error estimates

$$\|e^n\|_2 + \|\delta_x^+ e^n\|_2 \lesssim h^2 + \tau^2, \quad \|\psi^n\|_\infty \leq 1 + M_1, \quad 0 \leq n \leq \frac{T}{\tau}. \quad (4.35)$$

Similarly, for the CNFD method, we have [20, 21]

Theorem 4.2. *Assuming that (4.33) holds and that $V(x) \in C^1(\bar{U})$, there exists $h_0 > 0$ and $\tau_0 > 0$ sufficiently small, when $0 < h \leq h_0$ and $0 < \tau \leq \tau_0$, the CNFD discretization (4.18) with (4.19) and (4.20) admits a unique solution ψ^n ($0 \leq n \leq \frac{T}{\tau}$) such that the following error estimates hold,*

$$\|e^n\|_2 \lesssim h^2 + \tau^2, \quad \|\delta_x^+ e^n\|_2 \lesssim h^{3/2} + \tau^{3/2}, \quad \|\psi^n\|_\infty \leq 1 + M_1, \quad 0 \leq n \leq \frac{T}{\tau}. \quad (4.36)$$

In addition, if either $\partial_n V(x)|_\Gamma = 0$ or $\psi \in C^0([0, T]; H_0^2(U))$, we have the optimal error estimates

$$\|e^n\|_2 + \|\delta_x^+ e^n\|_2 \lesssim h^2 + \tau^2, \quad \|\psi^n\|_\infty \leq 1 + M_1, \quad 0 \leq n \leq \frac{T}{\tau}. \quad (4.37)$$

Error bounds of conservative CNFD method for NLSE in 1D (without potential $V(x)$) was established in [76, 106]. In fact, their proofs for CNFD rely strongly on the conservative property of the method and the discrete version of the Sobolev inequality in 1D

$$\|f\|_{L^\infty}^2 \leq \|\nabla f\|_{L^2} \cdot \|f\|_{L^2}, \quad \forall f \in H^1(U) \text{ with } U \subset \mathbb{R}, \quad (4.38)$$

which immediately implies *a priori* uniform bound for $\|f\|_{L^\infty}$. However, the extension of the discrete version of the above Sobolev inequality is no longer valid in 2D and 3D. Thus the techniques used in [76, 106] for obtaining error bounds of CNFD for NLSE only work for conservative schemes in 1D and they cannot be extended to either high dimensions or non-conservative finite difference scheme like SIFD.

Here, we are going to use different techniques to establish optimal error bounds of CNFD and SIFD for the GPE (2.1) in 1D which can be directly generalized to 2D and 3D. In the analysis, besides the standard techniques of the energy method, for SIFD, we adopt the mathematical induction; for CNFD, we cut off the nonlinearity.

4.4.1. *Convergence rate for SIFD.* Firstly, SIFD (4.21) is uniquely solvable [20].

Lemma 4.1. (*Solvability of the difference equations*) Under the assumption (4.33), for any given initial data $\psi^0 \in X_M$, there exists a unique solution $\psi^n \in X_M$ of (4.22) for $n = 1$ and (4.21) for $n > 1$.

Define the local truncation error $\eta^n \in X_M$ of the SIFD method (4.21) with (4.19), (4.20) and (4.22) for $n \geq 1$ and $j \in \mathcal{T}_M$ as

$$\eta_j^n := (i\delta_t - \beta|\psi(x_j, t_n)|^2) \psi(x_j, t_n) + \left[\frac{\delta_x^2}{2} - V_j \right] \frac{\psi(x_j, t_{n-1}) + \psi(x_j, t_{n+1})}{2}, \quad (4.39)$$

and by noticing (4.20) for $n = 0$ as

$$\begin{aligned} \eta_j^0 &:= i\delta_t^+ \psi(x_j, 0) - \left(-\frac{1}{2}\delta_x^2 + V_j \right) \psi_j^{(1)} - \beta|\psi_j^{(1)}|^2 \psi_j^{(1)}, \quad j \in \mathcal{T}_M, \quad (4.40) \\ \psi_j^{(1)} &= \psi_0(x_j) - i\frac{\tau}{2} \left[\left(-\frac{1}{2}\delta_x^2 + V_j \right) \psi_0(x_j) + \beta|\psi_0(x_j)|^2 \psi_0(x_j) \right]. \end{aligned}$$

Then we have

Lemma 4.2. (*Local truncation error*) Assuming $V(\mathbf{x}) \in C(\bar{U})$, under the assumption (4.33), we have

$$\|\eta^n\|_\infty \lesssim \tau^2 + h^2, \quad 0 \leq n \leq \frac{T}{\tau} - 1, \quad \text{and} \quad \|\delta_x^+ \eta^0\|_\infty \lesssim \tau + h. \quad (4.41)$$

In addition, assuming $V(\mathbf{x}) \in C^1(\bar{U})$, we have for $1 \leq n \leq \frac{T}{\tau} - 1$

$$|\delta_x^+ \eta_j^n| \lesssim \begin{cases} \tau^2 + h^2, & 1 \leq j \leq M - 2, \\ \tau + h, & j = 0, M - 1. \end{cases} \quad (4.42)$$

Furthermore, assuming either $\partial_n V(x)|_\Gamma = 0$ or $u \in C([0, T]; H_0^2(U))$, we have

$$\|\delta_x^+ \eta^n\|_\infty \lesssim \tau^2 + h^2, \quad 1 \leq n \leq \frac{T}{\tau} - 1. \quad (4.43)$$

Proof. First, we prove (4.41) and (4.42) when $n = 0$. Rewriting $\psi_j^{(1)}$ and then using Taylor's expansion at $(x_j, 0)$, noticing (4.1) and (4.2), we get

$$\begin{aligned}\psi_j^{(1)} &= \psi\left(x_j, \frac{\tau}{2}\right) + i\frac{\tau}{2} \left[\left(\frac{\delta_x^2}{2} - V_j - \beta|\psi_0(x_j)|^2 \right) \psi_0(x_j) + i \frac{\psi\left(x_j, \frac{\tau}{2}\right) - \psi_0(x_j)}{\tau/2} \right] \\ &= \psi\left(x_j, \frac{\tau}{2}\right) + i\frac{\tau}{2} \left[\frac{h^2}{2} \int_0^1 \int_0^{s_1} \int_0^{s_2} \int_{-s_3}^{s_3} \partial_{xxxx} \psi_0(x_j + sh) ds ds_3 ds_2 ds_1 \right. \\ &\quad \left. + i\frac{\tau}{2} \int_0^1 \int_0^\theta \partial_{tt} \psi(x_j, s\tau/2) ds d\theta \right] = \psi\left(x_j, \frac{\tau}{2}\right) + O(\tau^2 + \tau h^2), \quad j \in \mathcal{T}_M.\end{aligned}$$

Then, using Taylor expansion at $(x_j, \tau/2)$ in (4.40), noticing (4.1), in view of triangle inequality and the assumption (4.33), we have

$$\begin{aligned}|\eta_j^0| &\lesssim \tau^2 \|\psi_{ttt}\|_{L^\infty} + h\tau \|\psi_{xxxx}\|_{L^\infty} + \tau^2 \|\psi_{tttx}\|_{L^\infty} + \tau(h^2 \|\psi_{xxxx}\|_{L^\infty} + \tau \|\psi_{tt}\|_{L^\infty}) \\ &\quad \cdot (\|\psi\|_{L^\infty} + \tau h^2 \|\psi_{xxxx}\|_{L^\infty} + \tau^2 \|\psi_{tt}\|_{L^\infty})^2 \\ &\lesssim \tau^2 + h^2, \quad j \in \mathcal{T}_M,\end{aligned}$$

where the L^∞ -norm means $\|\psi\|_{L^\infty} := \sup_{0 \leq t \leq T} \sup_{x \in U} |\psi(x, t)|$. This immediately implies (4.41) when $n = 0$. Similarly, we can get

$$\begin{aligned}|\delta_x^+ \eta_j^0| &\lesssim \tau \|\psi_{xxxx}\|_{L^\infty} + \tau^2 \|\psi_{tttx}\|_{L^\infty} + \tau h \|\psi_{xxxx}\|_{L^\infty} (\|\psi\|_{W^{4,\infty}} + \|\psi_{tt}\|_{L^\infty})^2 \\ &\quad + \tau^2 \|\psi_{tttx}\|_{L^\infty} (\|\psi\|_{W^{4,\infty}} + \|\psi_{tt}\|_{L^\infty})^2 \\ &\lesssim \tau + h, \quad j \in \mathcal{T}_M,\end{aligned}$$

where for $j = 0$, we use equation (4.3) to deduce that $\psi_{tt}(a, t) = \psi_{ttt}(a, t) = 0$.

Now we prove (4.41), (4.42) and (4.43) when $n \geq 1$. Using Taylor's expansion at (x_j, t_n) in (4.39), noticing (4.1), using triangle inequality and assumption (4.33), we have for $1 \leq n \leq \frac{T}{\tau} - 1$,

$$|\eta_j^n| \lesssim h^2 \|\psi_{xxxx}\|_{L^\infty} + \tau^2 (\|\psi_{ttt}\|_{L^\infty} + \|\psi_{tttx}\|_{L^\infty}) \lesssim \tau^2 + h^2, \quad j \in \mathcal{T}_M.$$

Thus, (4.41) is true. For $j = 1, \dots, M-2$, we know

$$|\delta_x^+ \eta_j^n| \lesssim h^2 \|\psi_{xxxx}\|_{L^\infty} + \tau^2 (\|\psi_{ttt}\|_{L^\infty} + \|\psi_{tttx}\|_{L^\infty}) \lesssim \tau^2 + h^2, \quad 1 \leq n \leq \frac{T}{\tau} - 1. \quad (4.44)$$

However, for $j = 0, M-1$, we derive that ψ_{tt} , ψ_{xx} and ψ_{tttx} are all zero on the boundary Γ , and it follows that for $1 \leq n \leq \frac{T}{\tau} - 1$ and $j = 0, M-1$,

$$|\delta_x^+ \eta_j^n| \lesssim h \|\psi_{xxxx}\|_{L^\infty} + \tau^2 (\|\psi_{ttt}\|_{L^\infty} + \|\psi_{tttx}\|_{L^\infty}) \lesssim \tau + h. \quad (4.45)$$

(4.44) and (4.45) prove (4.42).

In the case of $\partial_n V(x)|_\Gamma = 0$ or $u \in C([0, T]; H_0^2(U))$, by differentiating (4.1), we can show that $\psi_{xx}|_\Gamma = \psi_{xxxx}|_\Gamma = \psi_{tttx}|_\Gamma = \psi_{tt}|_\Gamma = 0$. Then (4.44) holds for boundary case and (4.43) is correct. The proof is complete. \square

Now, we are going to establish the estimates in Theorem 4.1 by mathematical induction [20].

Proof of Theorem 4.1. We first prove the optimal discrete semi- H^1 norm convergence rate in the case of either $\partial_n V(x)|_\Gamma = 0$ or $\psi \in C^0([0, T]; H_0^2(U))$. Since $e^0 = \mathbf{0}$,

(4.35) is true. For $n = 1$, using Lemma 4.2 and noticing $e_j^1 = \psi(x_j, \tau) - \psi_j^1 = -i\tau\eta_j^0$ ($j \in \mathcal{T}_M^0$), we find that

$$\|e^1\|_2 + \|\delta_x^+ e^1\|_2 \lesssim h^2 + \tau^2. \quad (4.46)$$

Recalling discrete Sobolev inequality which implies that $\|e^1\|_\infty \leq C_1 \|\delta_x^+ e^1\|_2$, for sufficiently small h and τ , we derive

$$\|\psi^1\|_\infty \leq \|e^1\|_\infty + \|\psi\|_{L^\infty} \leq M_1 + 1. \quad (4.47)$$

Now we assume that (4.35) is valid for all $0 \leq n \leq m-1 \leq \frac{T}{\tau} - 1$, then we need to show that it is still valid when $n = m$. In order to do so, subtracting (4.39) from (4.21), noticing (4.4) and (4.19), we obtain the following equation for the ‘‘error’’ function $e^n \in X_M$:

$$i\delta_t e_j^n = \left[-\frac{1}{2}\delta_x^2 + V_j \right] \frac{e_j^{n+1} + e_j^{n-1}}{2} + \xi_j^n + \eta_j^n, \quad j \in \mathcal{T}_M, \quad n \geq 1, \quad (4.48)$$

where $\xi^n \in X_M$ ($n \geq 1$) is defined as

$$\xi_j^n = \beta |\psi(x_j, t_n)|^2 \psi(x_j, t_n) - \beta |\psi_j^n|^2 \psi_j^n, \quad j \in \mathcal{T}_M. \quad (4.49)$$

By the assumption of mathematical induction, we have [20]

$$\|\xi^n\|_2^2 \leq C_2 \|e^n\|_2^2, \quad \|\delta_x^+ \xi^n\|_2^2 \leq C_3 \|\delta_x^+ e^n\|_2^2 + \|e^n\|_2^2, \quad 1 \leq n \leq m-1, \quad (4.50)$$

where C_2 and C_3 are constants only depending on M_1 and β .

Multiplying both sides of (4.48) by $\overline{e_j^{n+1} + e_j^{n-1}}$ and summing all together for $j \in \mathcal{T}_M$, taking imaginary parts, using the triangular and Cauchy inequalities, noticing (4.41) and (4.50), we have for $1 \leq n \leq m-1$

$$\begin{aligned} \|e^{n+1}\|_2^2 - \|e^{n-1}\|_2^2 &= 2\tau \operatorname{Im} (\xi^n + \eta^n, e^{n+1} + e^{n-1}) \\ &\leq 2\tau [\|e^{n+1}\|_2^2 + \|e^{n-1}\|_2^2 + \|\eta^n\|_2^2 + \|\xi^n\|_2^2] \\ &\leq C_4 \tau (h^2 + \tau^2)^2 + 2\tau (\|e^{n+1}\|_2^2 + \|e^{n-1}\|_2^2) + 2\tau C_2 \|e^n\|_2^2. \end{aligned}$$

Summing above inequality for $n = 1, 2, \dots, m-1$, for $\tau \leq \frac{1}{4}$, we get

$$\|e^m\|_2^2 + \|e^{m-1}\|_2^2 \leq C_4 T (h^2 + \tau^2)^2 + C_5 \tau \sum_{l=1}^{m-1} \|e^l\|_2^2, \quad 1 \leq m \leq \frac{T}{\tau}, \quad (4.51)$$

with positive constants $C_4 > 0$ and $C_5 > 0$ independent of τ and h . In view of the discrete Gronwall inequality [20, 76, 106] and noticing $\|e^0\|_2 = 0$ and $\|e^1\|_2 \lesssim h^2 + \tau^2$, we immediately obtain $\|e^n\|_2 \lesssim h^2 + \tau^2$ for $n = m$.

For the semi- H^1 norm, define the discrete linear energy for $e^n \in X_M$ as

$$\mathcal{E}(e^n) = \frac{1}{2} \|\delta_x^+ e^n\|_2^2 + \|e^n\|_V^2. \quad (4.52)$$

Multiplying both sides of (4.48) by $\overline{e_j^{n+1} - e_j^{n-1}}$, summing over index $j \in \mathcal{T}_M$ and performing summation by parts, taking real part, we have

$$\mathcal{E}(e^{n+1}) - \mathcal{E}(e^{n-1}) = -2 \operatorname{Re} \langle \xi^n + \eta^n, e^{n+1} - e^{n-1} \rangle, \quad 1 \leq n \leq m-1. \quad (4.53)$$

Rewriting (4.48) as

$$e_j^{n+1} - e_j^{n-1} = -2i\tau [\xi_j^n + \eta_j^n + \chi_j^n], \quad j \in \mathcal{T}_M, \quad (4.54)$$

where $\chi^n \in X_M$ is defined as

$$\chi_j^n = \left[-\frac{1}{2}\delta_x^2 + V_j \right] \frac{e_j^{n+1} + e_j^{n-1}}{2}, \quad j \in \mathcal{T}_M, \quad (4.55)$$

then plugging (4.54) into (4.53), we obtain

$$\begin{aligned}\mathcal{E}(e^{n+1}) - \mathcal{E}(e^{n-1}) &= -4\tau \operatorname{Im} \langle \xi^n + \eta^n, \xi^n + \eta^n + \chi^n \rangle \\ &= -4\tau \operatorname{Im} \langle \xi^n + \eta^n, \chi^n \rangle, \quad 1 \leq n \leq m-1.\end{aligned}\quad (4.56)$$

From (4.55), (4.49) and summation by parts, we have

$$\begin{aligned}|\langle \xi^n, \chi^n \rangle| &= \frac{1}{2} \left| \left\langle \xi^n, \left(-\frac{1}{2} \delta_x^2 + V \right) (e^{n+1} + e^{n-1}) \right\rangle \right| \\ &\lesssim \left| \langle \delta_x^+ \xi^n, \delta_x^+ (e^{n+1} + e^{n-1}) \rangle \right| + \left| \langle \xi^n, V (e^{n+1} + e^{n-1}) \rangle \right| \\ &\lesssim \|\delta_x^+ e^{n+1}\|_2^2 + \|\delta_x^+ e^n\|_2^2 + \|\delta_x^+ e^{n-1}\|_2^2 + \|e^{n+1}\|_2^2 + \|e^n\|_2^2 + \|e^{n-1}\|_2^2 \\ &\quad + \|\delta_x^+ \xi^n\|_2^2 + \|\xi^n\|_2^2 \\ &\lesssim \|\delta_x^+ e^{n+1}\|_2^2 + \|\delta_x^+ e^n\|_2^2 + \|\delta_x^+ e^{n-1}\|_2^2, \quad 1 \leq n \leq m.\end{aligned}\quad (4.57)$$

Similarly, noticing (4.50), (4.41) and (4.43), we have

$$\begin{aligned}|\langle \eta^n, \chi^n \rangle| &= \frac{1}{2} \left| \left\langle \eta^n, \left(-\frac{1}{2} \delta_x^2 + V \right) (e^{n+1} + e^{n-1}) \right\rangle \right| \\ &\lesssim \left| \langle \delta_x^+ \eta^n, \delta_x^+ (e^{n+1} + e^{n-1}) \rangle \right| + \left| \langle \eta^n, V (e^{n+1} + e^{n-1}) \rangle \right| \\ &\lesssim \|\delta_x^+ e^{n+1}\|_2^2 + \|\delta_x^+ e^n\|_2^2 + \|\delta_x^+ e^{n-1}\|_2^2 + \|e^{n+1}\|_2^2 + \|e^n\|_2^2 + \|e^{n-1}\|_2^2 \\ &\quad + \|\delta_x^+ \eta^n\|_2^2 + \|\eta^n\|_2^2 \\ &\lesssim \|\delta_x^+ e^{n+1}\|_2^2 + \|\delta_x^+ e^n\|_2^2 + \|\delta_x^+ e^{n-1}\|_2^2 + (\tau^2 + h^2)^2, \quad 1 \leq n \leq m.\end{aligned}\quad (4.58)$$

Plugging (4.57) and (4.58) into (4.56), we get

$$\begin{aligned}\mathcal{E}(e^{n+1}) - \mathcal{E}(e^{n-1}) &\lesssim \tau(\tau^2 + h^2)^2 + \tau \left[\|\delta_x^+ e^{n+1}\|_2^2 + \|\delta_x^+ e^n\|_2^2 + \|\delta_x^+ e^{n-1}\|_2^2 \right] \\ &\lesssim \tau(\tau^2 + h^2)^2 + \tau \left[\mathcal{E}(e^{n+1}) + \mathcal{E}(e^n) + \mathcal{E}(e^{n-1}) \right], \quad 1 \leq n \leq m.\end{aligned}$$

Summing above inequality for $1 \leq n \leq m-1$, we get

$$\mathcal{E}(e^{n+1}) + \mathcal{E}(e^n) \lesssim T(\tau^2 + h^2)^2 + \mathcal{E}(e^1) + \mathcal{E}(e^0) + \tau \sum_{l=1}^{n+1} \mathcal{E}(e^l), \quad 1 \leq n \leq m-1.$$

Using the discrete Gronwall inequality [20, 76], we have

$$\mathcal{E}(e^{n+1}) + \mathcal{E}(e^n) \lesssim (\tau^2 + h^2)^2 + \mathcal{E}(e^1) + \mathcal{E}(e^0) \lesssim (\tau^2 + h^2)^2, \quad 1 \leq n \leq m-1. \quad (4.59)$$

Thus $\mathcal{E}(e^m) \lesssim (\tau^2 + h^2)^2$ and

$$\|\delta_x^+ e^m\|_2^2 \leq \mathcal{E}(e^m) + \|V\|_{L^\infty(U)} \|e^m\|_2^2 \lesssim (\tau^2 + h^2)^2. \quad (4.60)$$

In view of the discrete Sobolev inequality, we get

$$\|e^m\|_\infty \lesssim \|\delta_x^+ e^m\|_2 \lesssim \tau^2 + h^2. \quad (4.61)$$

Noticing that in all the above inequalities, the appearing constants are independent of h and τ . Hence, for sufficiently small τ and h , we conclude that

$$\|\psi^m\|_\infty \leq \|\psi(\cdot, t_m)\|_{L^\infty(U)} + \|e^m\|_\infty \leq M_1 + 1. \quad (4.62)$$

This completes the proof of (4.35) at $n = m$. Therefore the result is proved by mathematical induction.

For the case of assumption (4.33) and $V \in C^1$ without further assumptions, we will lose half order convergence rate in the semi- H^1 norm because of the boundary (4.42). Notice that the reminder term is $O(h^2 + \tau^2)^{3/2}$ instead of $O(h^2 + \tau^2)$ in (4.58), and that the remaining proof is the same. Hence, we will have the 3/2 order

convergence rate for discrete semi- H^1 norm. The proof is complete. \square

Remark 4.2. Here we emphasize that the above approach can be extended to the higher dimensions, e.g. 2D and 3D, directly. The key point is the discrete Sobolev inequality in 2D and 3D as

$$\|u_h\|_\infty \leq C |\ln h| \|u_h\|_{H_s^1}, \quad \|v_h\|_\infty \leq Ch^{-1/2} \|v_h\|_{H_s^1}, \quad (4.63)$$

where u_h and v_h are 2D and 3D mesh functions with zero at the boundary, respectively, and the discrete semi- H^1 norm $\|\cdot\|_{H_s^1}$ and l^∞ norm $\|\cdot\|_\infty$ can be defined similarly as the discrete semi- H^1 norm and the l^∞ norm in (3.27). The same proof works in 2D and 3D, with the above Sobolev inequalities and the additional technical assumption $\tau = o(1/|\ln h|)$ in 2D and $\tau = o(h^{1/3})$ in 3D.

4.4.2. *Convergence rate for CNFD.* Let $\psi^n \in X_M$ be the numerical solution of the CNFD (4.18) and $e^n \in X_M$ be the error function.

Lemma 4.3. (*Conservation of mass and energy*) For the CNFD scheme (4.18) with (4.19) and (4.20), for any mesh size $h > 0$, time step $\tau > 0$ and initial data ψ_0 , it conserves the mass and energy in the discretized level, i.e.

$$\|\psi^n\|_2^2 \equiv \|\psi^0\|_2^2, \quad E_h(\psi^n) \equiv E_h(\psi^0), \quad n = 0, 1, 2, \dots, \quad (4.64)$$

where the discrete energy is given by

$$E_h(\psi^n) = \frac{1}{2} \|\delta_x^+ \psi^n\|_2^2 + \|\psi^n\|_V^2 + \frac{\beta}{2} \|\psi^n\|_4^4. \quad (4.65)$$

Proof. Follow the analogous arguments of the CNFD method for the NLSE [77, 106] and we omit the details here for brevity. \square

For the solvability, we have

Lemma 4.4. (*Solvability of the difference equations*) For any given ψ^n , there exists a unique solution ψ^{n+1} of the CNFD discretization (4.18) with (4.19).

Proof. The proof is standard [10, 20]. In higher dimensions (2D and 3D), additional assumption is needed for uniqueness, i.e., time step τ is sufficiently small compared with mesh size. \square

Denote the local truncation error $\tilde{\eta}^n \in X_M$ ($n \geq 0$) of the CNFD scheme (4.18) with (4.19) and (4.20) as

$$\begin{aligned} \tilde{\eta}_j^n : &= i\delta_t^+ \psi(x_j, t_n) - \left[-\frac{1}{2} \delta_x^2 + V_j + \frac{\beta}{2} (|\psi(x_j, t_{n+1})|^2 + |\psi(x_j, t_n)|^2) \right] \\ &\quad \times \frac{\psi(x_j, t_n) + \psi(x_j, t_{n+1})}{2}, \quad j \in \mathcal{T}_M. \end{aligned} \quad (4.66)$$

Similar to Lemma 4.2, we have

Lemma 4.5. (*Local truncation error*) Assume $V(\mathbf{x}) \in C(\bar{U})$ and under assumption (4.33), we have

$$\|\tilde{\eta}^n\|_\infty \lesssim \tau^2 + h^2, \quad 0 \leq n \leq \frac{T}{\tau} - 1. \quad (4.67)$$

In addition, assuming $V(\mathbf{x}) \in C^1(\bar{U})$, we have for $1 \leq n \leq \frac{T}{\tau} - 1$

$$|\delta_x^+ \tilde{\eta}_j^n| \lesssim \begin{cases} \tau^2 + h^2, & 1 \leq j \leq M-2, \\ \tau + h, & j = 0, M-1. \end{cases} \quad (4.68)$$

In addition, if either $\partial_n V(x)|_\Gamma = 0$ or $\psi \in C^0([0, T]; H_0^2(U))$, we have

$$\|\delta_x^+ \tilde{\eta}^n\|_\infty \lesssim \tau^2 + h^2, \quad 1 \leq n \leq \frac{T}{\tau} - 1. \quad (4.69)$$

One main difficulty in deriving error bounds for CNFD in high dimensions is the l^∞ bounds for the finite difference solutions. In [10, 20, 177], this difficulty was overcome by truncating the nonlinearity to a global Lipschitz function with compact support in d -dimensions ($d = 1, 2, 3$). This cutoff would not change $\psi(x, t)$ and ψ^n if the continuous solution $\psi(x, t)$ is bounded and the numerical solution ψ^n is close to the continuous solution, i.e., if (4.36) or (4.37) holds.

Proof of Theorem 4.2. As in the proof of Theorem 4.1, we only prove the optimal convergence under assumptions (4.33) with either $\partial_n V(x)|_\Gamma = 0$ or $\psi \in C^0([0, T]; H_0^2(U))$. Choose a smooth function $\rho(s) \in C^\infty(\mathbb{R})$ such that

$$\rho(s) = \begin{cases} 1, & 0 \leq |s| \leq 1, \\ \in [0, 1], & 1 \leq |s| \leq 2, \\ 0, & |s| \geq 2. \end{cases} \quad (4.70)$$

Let us denote $B = (M_1 + 1)^2$ and denote

$$f_B(s) = \rho(s/B)s, \quad s \in \mathbb{R}, \quad (4.71)$$

then $f_B \in C_0^\infty(\mathbb{R})$. Choose $\phi^0 = \psi^0 \in X_M$ and define $\phi^n \in X_M$ ($n \geq 1$) as

$$i\delta_t^+ \phi_j^n = \left[-\frac{1}{2}\delta_x^2 + V_j + \frac{\beta}{2} (f_B(|\phi_j^{n+1}|^2) + f_B(|\phi_j^n|^2)) \right] \phi_j^{n+1/2}, \quad j \in \mathcal{T}_M, \quad (4.72)$$

where

$$\phi_j^{n+1/2} = \frac{1}{2}(\phi_j^{n+1} + \phi_j^n), \quad j \in \mathcal{T}_M^0, \quad n \geq 0. \quad (4.73)$$

In fact, ϕ^n can be viewed as another approximation of $\psi(x, t_n)$. Define the ‘error’ function $\hat{e}^n \in X_M$ ($n \geq 0$) with components $\hat{e}_j^n = \psi(x_j, t_n) - \phi_j^n$ for $j \in \mathcal{T}_M^0$ and denote the local truncation error $\hat{\eta}^n \in X_M$ as

$$\begin{aligned} \hat{\eta}_j^n &:= i\delta_t^+ \psi(x_j, t_n) - \left[-\frac{1}{2}\delta_x^2 + V_j + \frac{\beta}{2} (f_B(|\psi(x_j, t_{n+1})|^2) + f_B(|\psi(x_j, t_n)|^2)) \right] \\ &\quad \times \frac{\psi(x_j, t_n) + \psi(x_j, t_{n+1})}{2}, \quad j \in \mathcal{T}_M, \quad n \geq 0. \end{aligned} \quad (4.74)$$

Similar as Lemma 4.5, we can prove

$$\|\hat{\eta}^n\|_\infty + \|\delta_x^+ \hat{\eta}^n\|_\infty \lesssim \tau^2 + h^2, \quad 0 \leq n \leq \frac{T}{\tau} - 1. \quad (4.75)$$

Subtracting (4.74) from (4.72), we obtain

$$i\delta_t^+ \hat{e}_j^n = \left[-\frac{1}{2}\delta_x^2 + V_j \right] \hat{e}_j^{n+1/2} + \hat{\xi}_j^n + \hat{\eta}_j^n, \quad j \in \mathcal{T}_M, \quad n \geq 0, \quad (4.76)$$

where $\hat{\xi}^n \in X_M$ defined as

$$\hat{\xi}_j^n = \frac{\beta}{2} (|\psi(x_j, t_{n+1})|^2 + |\psi(x_j, t_n)|^2) \frac{\psi(x_j, t_{n+1}) + \psi(x_j, t_n)}{2} \quad (4.77)$$

$$- \frac{\beta}{2} (f_B(|\phi_j^{n+1}|^2) + f_B(|\phi_j^n|^2)) \phi_j^{n+1/2}, \quad j \in \mathcal{T}_M^0. \quad (4.78)$$

Recalling that $f_B \in C_0^\infty$, for $0 \leq n \leq \frac{T}{\tau} - 1$, we can show that [20]

$$\|\hat{\xi}^n\|_2 \lesssim \sum_{k=n, n+1} \|\hat{e}^k\|_2, \quad \|\delta_x^+ \hat{\xi}^n\|_2 \lesssim \sum_{k=n, n+1} (\|\hat{e}^k\|_2 + \|\delta_x^+ \hat{e}^k\|_2). \quad (4.79)$$

This property is similar to that of the SIFD case (4.50). The same proof for Theorem 4.1 works. However, there is no need to use mathematical induction here, as C_0^∞ property of f_B guarantees (4.79). For simplicity, we omit the details here. Finally, we derive the following for sufficiently small h and τ ,

$$\|\hat{e}^n\|_2 + \|\delta_x^+ \hat{e}^n\|_2 \lesssim h^2 + \tau^2, \quad \|\phi^n\|_\infty \leq M_1 + 1, \quad 0 \leq n \leq \frac{T}{\tau}. \quad (4.80)$$

From (4.80), we know that (4.72) collapses to CNFD (4.18), i.e., $\psi^n = \phi^n$. Thus, we prove error estimates (4.37) for CNFD (4.18).

Again, for the case of assumption (4.33) and $V \in C^1$ without further assumptions, we will lose half order convergence rate in the semi- H^1 norm. \square

Remark 4.3. If the cubic nonlinear term $\beta|\psi|^2\psi$ in (4.1) is replaced by a general nonlinearity $f(|\psi|^2)\psi$, the numerical discretization CNFD and its error estimates in l^2 -norm, l^∞ -norm and discrete H^1 -norm are still valid provided that the nonlinear real-valued function $f(\rho) \in C^3([0, \infty))$. The higher dimensional case (2D or 3D) is the same as Remark 4.2.

4.5. Error estimates for TSSP. From now on, we investigate the error bounds for time-splitting method. In the last decade, there have been many studies on the analysis of the splitting error for Schrödinger equations [54, 88, 139, 145, 176]. For NLSE, Besse et al. obtained order estimates for the Strang splitting error [54]. Later, Lubich introduced formal Lie derivatives to estimate the Strang splitting error [139]. The formal Lie calculus enables a systematical approach for studying splitting schemes.

In our consideration of the TSSP (4.16) for solving the GPE (4.1), we will restrict ourselves to certain subspaces of $H_0^1(U)$. Let $\phi(x) \in H^m(U) \cap H_0^1(U)$ be represented in sine series as

$$\phi(x) = \sum_{l=1}^{+\infty} \hat{\phi}_l \sin(\mu_l(x-a)), \quad x \in U = (a, b), \quad (4.81)$$

with $\hat{\phi}_l$ given in (3.36), define the subspace $H_{\sin}^m(U) \subset H^m \cap H_0^1$ equipped with the norm

$$\|\phi\|_{H_{\sin}^m(U)} = \left(\sum_{l=1}^{\infty} \mu_l^{2m} |\hat{\phi}_l|^2 \right)^{\frac{1}{2}}, \quad (4.82)$$

which is equivalent to the H^m norm in this subspace. We notice that $H_{\sin}^m(U) = \{\phi \in H^m(U) | \partial_x^{2k} \phi(a) = \partial_x^{2k} \phi(b) = 0, \quad 0 \leq 2k < m, k \in \mathbb{Z}\}$. It is easy to see that $e^{it\Delta}$ will preserve the H_{\sin}^m norm.

The TSSP (4.16) can be thought as the full discretization of the following semi-discretization scheme. Let $\psi^{[n]}(x)$ be the numerical approximation of $\psi(x, t_n)$. From time $t = t_n$ to $t = t_{n+1}$, we use the standard Strang splitting:

$$\begin{aligned}\psi^{\{1\}}(x) &= e^{i\tau\Delta/4}\psi^{[n]}(x), & \psi^{\{2\}}(x) &= e^{-i(V(x)+\beta|\psi^{\{1\}}(x)|^2)\tau}\psi^{\{1\}}(x), \\ \psi^{[n+1]}(x) &= e^{i\tau\Delta/4}\psi^{\{2\}}(x), & x &\in U.\end{aligned}\quad (4.83)$$

In order to guarantee that $e^{-i\tau(V+\beta|\phi|^2)}\phi$ is a flow in H_{sin}^m , we make the following assumptions on the potential $V(x)$

$$V(x) \in H^m(U) \quad \text{and} \quad \partial_x V(x) \in H_{\text{sin}}^{m-1}(U), \quad m \geq 1. \quad (4.84)$$

To derive the optimal error bounds, we make the following assumption on the exact solution ψ , i.e., let $0 < T < T_{\text{max}}$ with T_{max} the maximal existing time of the solution [73, 173]:

$$\psi \in C([0, T]; H^m(U) \cap H_0^1(U)). \quad (4.85)$$

It is easy to get that ψ is actually in H_{sin}^m under assumptions (4.84) and (4.85), by showing that $\partial_x^{2k}\psi|_{\Gamma} = 0$ ($0 \leq 2k < m$) from the GPE (4.1).

Now, we could state the error estimates for the TSSP (4.16).

Theorem 4.3. *Let $\psi^n \in X_M$ be the numerical approximation obtained by the TSSP (4.16). Under assumptions (4.84) and (4.85), there exist constants $0 < \tau_0, h_0 \leq 1$, such that if $0 < h \leq h_0$, $0 < \tau \leq \tau_0$ and $m \geq 5$, we have*

$$\begin{aligned}\|\psi(x, t_n) - I_M(\psi^n)(x)\|_{L^2(U)} &\lesssim h^m + \tau^2, & \|\psi^n\|_{\infty} &\leq M_1 + 1, \\ \|\nabla(\psi(x, t_n) - I_M(\psi^n)(x))\|_{L^2(U)} &\lesssim h^{m-1} + \tau^2, & 0 \leq n \leq \frac{T}{\tau},\end{aligned}\quad (4.86)$$

where the interpolation operator I_M is given in (3.30) and $M_1 = \max_{t \in [0, T]} \|\psi(\cdot, t)\|_{L^\infty}$.

By Parseval's identity, we can easily get the following.

Lemma 4.6. *(Conservation of mass) The TSSP (4.16) conserves the total mass, i.e.,*

$$\|\psi^n\|_2^2 = \|\psi^0\|_2^2, \quad n \geq 1. \quad (4.87)$$

The proof of Theorem 4.3 is separated into two steps. The first step is to establish the error estimates for semi-discretization (4.83). Then we analyze the error between the semi-discretization (4.83) and the full discretization TSSP (4.16).

The H^1 error bound for the semi-discretization (4.83) is the following.

Theorem 4.4. *Let $\psi^{[n]}(x)$ be the solution given by the splitting scheme (4.83). Under assumption (4.84) and (4.85) with $m \geq 5$, we have $\psi^{[n]}(x) \in H_{\text{sin}}^m$ and*

$$\|\psi^{[n]}(x) - \psi(x, t_n)\|_{L^2} + \|\nabla(\psi^{[n]}(x) - \psi(x, t_n))\|_{L^2} \lesssim \tau^2, \quad 0 \leq n \leq \frac{T}{\tau}. \quad (4.88)$$

The semi-discretization (4.83) can be simplified as

$$\psi^{[n+1]}(x) = S_\tau(\psi^{[n]}(x)). \quad (4.89)$$

Using the fact $L^\infty(U) \subset H^1(U)$ and following [139], we would easily obtain the H_0^1 stability of the splitting (4.83).

Lemma 4.7. (H_0^1 -conditional L^2 - and H_0^1 stability). If $\psi, \phi \in H_0^1(U)$ with

$$\|\psi\|_{H_0^1} \leq M_2, \quad \|\phi\|_{H_0^1} \leq M_2, \quad (4.90)$$

then we have

$$\begin{aligned} \|S_\tau(\psi) - S_\tau(\phi)\|_{L^2} &\leq e^{c_0\tau} \|\psi - \phi\|_{L^2}, \\ \|S_\tau(\psi) - S_\tau(\phi)\|_{H_0^1} &\leq e^{c_1\tau} \|\psi - \phi\|_{H_0^1}, \end{aligned} \quad (4.91)$$

where c_0 and c_1 depend on M_2 , $V(x)$ and β .

To prove Theorem 4.4, we need the local error, which is the key point in analyzing time-splitting methods.

Lemma 4.8. If $\psi_0 \in H_{\sin}^5$, then the error after one step of (4.83) in H_0^1 norm is given by

$$\|\psi^{[1]}(x) - \psi(x, \tau)\|_{L^2} + \|\nabla(\psi^{[1]}(x) - \psi(x, \tau))\|_{L^2} \leq C\tau^3, \quad (4.92)$$

where C only depends on $\|\psi_0\|_{H_{\sin}^5}$, $V(x)$ and β .

We use formal Lie derivative calculus to study the local error in Lemma 4.8. For a general differential equation $\phi_t = F(\phi)$ ($\phi \in H_0^1$), denote the evolution operator $\varphi_F^t(v)$ as the solution at time t with initial value $\phi(0) = v$. The Lie derivative D_F is given by [139]

$$(D_F G)(v) = \frac{d}{dt} G(\varphi_F^t(v))|_{t=0} = G'(v)F(v), \quad v \in H_0^1(U), \quad (4.93)$$

where G is a vector field on H_0^1 . Let $\hat{T}(\psi) = \frac{i}{2}\Delta\psi$, $\hat{V}(\psi) = -i(V(x) + \beta|\psi|^2)\psi$ and $\hat{H} = \hat{T} + \hat{V}$, and denote D_T , D_V and D_H as the corresponding Lie derivatives (cf. [139]) for \hat{T} , \hat{V} and \hat{H} , respectively. Similar to [139], one can compute the commutator

$$\begin{aligned} [\hat{T}, \hat{V}](\psi) &= \hat{T}'(\psi)\hat{V}(\psi) - \hat{V}'(\psi)\hat{T}(\psi) \\ &= \frac{i}{2}(-i)\Delta(V(x)\psi + \beta|\psi|^2\psi) - \left[-iV\Delta\psi\frac{i}{2} - i\beta \left(2|\psi|^2\Delta\psi\frac{i}{2} - \psi^2\Delta\bar{\psi}\frac{i}{2} \right) \right] \\ &= \frac{1}{2}\psi\Delta V + \nabla V \cdot \nabla\psi + \beta\psi^2\Delta\bar{\psi} + \frac{3}{2}\beta|\nabla\psi|^2\psi + \frac{\beta}{2}\bar{\psi}\nabla\psi \cdot \nabla\psi. \end{aligned}$$

Under assumption (4.84) on potential $V(x)$ with $m \geq 5$, following analogous arguments in [139], we have

$$\|[\hat{T}, \hat{V}](\psi)\|_{H_0^1} \leq C\|\psi\|_{H_{\sin}^3} (1 + \|\psi\|_{H_{\sin}^3}^2), \quad (4.94)$$

$$\|[\hat{T}, [\hat{T}, \hat{V}]](\psi)\|_{H_0^1} \leq C\|\psi\|_{H_{\sin}^5} (1 + \|\psi\|_{H_{\sin}^5}^2). \quad (4.95)$$

Now, we can prove the local error.

Proof of Lemma 4.8. The proof is analogous to that in section 5 of [139]. Here, we outline the main part. First of all, by using variation of constant formula (or Duhamel's principle), one can write the error as

$$\psi^{[1]}(x) - \psi(x, \tau) = \tau f\left(\frac{\tau}{2}\right) - \int_0^\tau f(s)ds + r_2 - r_1, \quad (4.96)$$

where $f(s) = \exp((\tau - s)D_T)D_V \exp(sD_T)\text{Id}(\psi_0)$ (Id the identity operator), and the remainder terms,

$$\begin{aligned} r_1 &= \int_0^\tau \int_0^{\tau-s} \exp((\tau - s - \sigma)D_H)D_V \exp(\sigma D_T)D_V \exp(sD_T)\text{Id}(\psi_0) d\sigma ds, \\ r_2 &= \tau^2 \int_0^1 (1 - \theta) \exp\left(\frac{\tau}{2}D_T\right) \exp(\theta\tau D_T)D_V^2 \exp\left(\frac{\tau}{2}D_T\right)\text{Id}(\psi_0) d\theta. \end{aligned}$$

For the principal part, we notice that the midpoint rule quadrature leads to

$$\tau f\left(\frac{\tau}{2}\right) - \int_0^\tau f(s)ds = \tau^3 \int_0^1 \ker(\theta) f''(\theta\tau) d\theta, \quad (4.97)$$

where $\ker(\theta)$ is the Peano kernel for midpoint rule and [139]

$$f''(s) = e^{i\frac{\tau}{2}\Delta} [\hat{T}, [\hat{T}, \hat{V}]] (e^{i\frac{\tau-s}{2}\Delta} \psi_0). \quad (4.98)$$

Hence the principal part is of order $O(\tau^3)$. For $r_2 - r_1$, denote

$$g(s, \sigma) = \exp((\tau - s - \sigma)D_T)D_V \exp(\sigma D_T)D_V \exp(sD_T)\text{Id}(\psi_0), \quad (4.99)$$

then we have

$$r_2 - r_1 = \frac{\tau^2}{2} g\left(\frac{\tau}{2}, 0\right) - \int_0^\tau \int_0^{\tau-s} g(s, \sigma) d\sigma ds + \tilde{r}_2 - \tilde{r}_1, \quad (4.100)$$

with

$$\tilde{r}_2 = r_2 - \frac{\tau^2}{2} g\left(\frac{\tau}{2}, 0\right), \quad \tilde{r}_1 = r_1 - \int_0^\tau \int_0^{\tau-s} g(s, \sigma) d\sigma ds. \quad (4.101)$$

For \tilde{r}_1 , noticing that

$$\exp(\tau D_H)\text{Id}(\psi_0) = \exp(\tau D_T)\text{Id}(\psi_0) + \int_0^\tau \exp((\tau - s)D_H)D_V \exp(sD_T)\text{Id}(\psi_0),$$

we can derive from the definition of $g(s, \sigma)$ and the form of r_1 that

$$\|\tilde{r}_1\|_{H_0^1} \leq \tilde{C}_1 \tau^3. \quad (4.102)$$

Similarly, we get $\|\tilde{r}_2\|_{H_0^1} \leq \tilde{C}_2 \tau^3$. Here, \tilde{C}_1 and \tilde{C}_2 only depend on $\|\psi_0\|_{H_{\sin}^3}$, V and β . The remainder term is also a quadrature rule and it follows that

$$\left\| \frac{\tau^2}{2} g\left(\frac{\tau}{2}, 0\right) - \int_0^\tau \int_0^{\tau-s} g(s, \sigma) d\sigma ds \right\|_{H_0^1} \leq C_r \tau^3, \quad (4.103)$$

where C_r depends on $\|\psi_0\|_{H_{\sin}^3}$, V and β . Combining the above results together, we can get Lemma 4.8. \square

Theorem 4.4 can be proved by a combination of Lemmas 4.7 and 4.8, using induction [139], and we omit this part here.

Proof of Theorem 4.3. Having Theorem 4.4, we only need to compare the full discretization solution $I_M(\psi^n)(x)$ and the semi-discretization solution $\psi^{[n]}(x)$ ($0 \leq n \leq \frac{T}{\tau}$),

$$I_M(\psi^n)(x) - \psi^{[n]}(x) = I_M(\psi^n)(x) - P_M(\psi^{[n]}(x)) + P_M(\psi^{[n]}(x)) - \psi^{[n]}(x). \quad (4.104)$$

From Theorem 4.4, there exists some $M_2 > 0$ such that $\|\psi^{[n]}\|_{H_{\sin}^m} \leq M_2$. Hence

$$\|P_M(\psi^{[n]}(x)) - \psi^{[n]}(x)\|_{L^2} \lesssim h^m, \quad \|\nabla[P_M(\psi^{[n]}(x)) - \psi^{[n]}(x)]\|_{L^2} \lesssim h^{m-1}. \quad (4.105)$$

Denote $e_I^n(x) = I_M(\psi^n)(x) - P_M(\psi^{[n]}(x))$, then $e_I^0 = I_M(\psi^0)(x) - P_M(\psi^{[0]})(x)$ and

$$\|e_I^0(x)\|_{L^2} \lesssim h^m, \quad \|\nabla e_I^0(x)\|_{L^2} \lesssim h^{m-1}, \quad \|e_I^0(x)\|_{H^2} \lesssim h^{m-2}. \quad (4.106)$$

From the semi-discretization (4.83), there holds

$$\begin{aligned} P_M(\psi^{\{1\}})(x) &= e^{i\tau\Delta/4} P_M(\psi^{[n]}), & P_M(\psi^{\{2\}})(x) &= P_M(e^{-i(V(x)+\beta|\psi^{\{1\}}|^2)\tau} \psi^{\{1\}})(x), \\ P_M(\psi^{[n+1]})(x) &= P_M(e^{i\tau\Delta/4}\psi^{\{2\}})(x), & x &\in U. \end{aligned}$$

Similarly, for the TSSP (4.16), there holds

$$\begin{aligned} I_M(\psi^{(1)})(x) &= e^{i\tau\Delta/4} I_M(\psi^n)(x), & I_M(\psi^{(2)})(x) &= I_M(e^{-i(V(x)+\beta|\psi^{(1)}(x)|^2)\tau} \psi^{(1)})(x), \\ I_M(\psi^{n+1})(x) &= e^{i\tau\Delta/4} I_M(\psi^{(2)})(x), & x &\in U. \end{aligned}$$

Noticing that $e^{i\tau\Delta}$ preserves H_{\sin}^m norm, we find that

$$\begin{aligned} \|e_I^n(x)\|_{H_{\sin}^m} &= \|I_M(\psi^{(1)})(x) - P_M(\psi^{\{1\}})(x)\|_{H_{\sin}^m}, \\ \|e_I^{n+1}(x)\|_{H_{\sin}^m} &= \|I_M(\psi^{(2)})(x) - P_M(\psi^{\{2\}})(x)\|_{H_{\sin}^m}. \end{aligned}$$

Following the analogous mathematical induction for SIFD (Theorem 4.1), we can assume that error estimates (4.86) holds for $n \leq \frac{T}{\tau} - 1$. For $n + 1$, using the techniques and results in [22], we have

$$\begin{aligned} \|I_M(\psi^{(2)})(x) - P_M(\psi^{\{2\}})(x)\|_{L^2} &\lesssim \tau \|I_M(\psi^{(1)})(x) - P_M(\psi^{\{1\}})(x)\|_{L^2} + \tau h^m, \\ \|I_M(\psi^{(2)})(x) - P_M(\psi^{\{2\}})(x)\|_{H_0^1} &\lesssim \tau \|I_M(\psi^{(1)})(x) - P_M(\psi^{\{1\}})(x)\|_{H_0^1} + \tau h^{m-1}. \end{aligned}$$

Hence for $n \leq \frac{T}{\tau} - 1$,

$$\|e_I^{n+1}(x)\|_{L^2} \lesssim \tau \|e_I^n(x)\|_{L^2} + \tau h^m, \quad \|e_I^{n+1}(x)\|_{H_0^1} \lesssim \tau \|e_I^n(x)\|_{H_0^1} + \tau h^{m-1}. \quad (4.107)$$

Then, mathematical induction and discrete Gronwall inequality would imply that for all $n \leq \frac{T}{\tau} - 1$ and small τ ,

$$\|e_I^{n+1}(x)\|_{L^2} \lesssim h^m + \tau^2, \quad \|e_I^{n+1}(x)\|_{H_0^1} \lesssim h^{m-1} + \tau^2. \quad (4.108)$$

Hence $\|I_M(\psi^n)(x) - \psi^{[n]}(x)\|_{H_0^1} \lesssim h^{m-1} + \tau^2$, and discrete Sobolev inequality gives that $\|\psi^n\|_{\infty} \leq M_1 + 1$ ($n \leq \frac{T}{\tau}$) (cf. proof of Theorem 4.1). This would complete the proof of Theorem 4.3. \square

Remark 4.4. Similar as Remark 4.2, results in Theorem 4.3 can be extended to higher dimensions (2D and 3D) and the proof presented in this section is still valid with small modification of Lemma 4.7, by using the fact that $H^2(\mathbb{R}^d) \subset L^\infty(\mathbb{R}^d)$ ($d = 2, 3$).

For time splitting Fourier pseudospectral method and time splitting finite difference method (4.17), similar error estimates to Theorem 4.3 can be established.

4.6. Numerical results. In this section, we report numerical results of the proposed numerical methods.

Example 4.1. 1D defocusing condensate, i.e. we choose $d = 1$ and consider GPE

$$i\partial_t \psi = -\frac{1}{2}\partial_{xx}\psi + \frac{x^2}{2}\psi + \beta|\psi|^2\psi, \quad (4.109)$$

with positive $\beta = 50$. The initial condition is taken as

$$\psi(x, 0) = \frac{1}{\pi^{1/4}} e^{-x^2/2}, \quad x \in \mathbb{R}. \quad (4.110)$$

We solve this problem on $[-16, 16]$, i.e. $a = -16$ and $b = 16$ with homogenous Dirichlet boundary conditions. Let ψ be the ‘exact’ solution which is obtained numerically by using TSSP4 (fourth order time-splitting sine pseudospectral method (4.10)) with a very fine mesh and time step, e.g., $h = \frac{1}{1024}$ and $\tau = 0.0001$, and $\psi_{h,\tau}$ be the numerical solution obtained by using a method with mesh size h and time step τ .

First we compare the discretization error in space. We choose a very small time step, e.g., $\tau = 0.0001$ for CNFD, TSSP4 and TSFD, $\tau = 0.00001$ for TSSP2 such that the error from the time discretization is negligible compared to the spatial discretization error, and solve the GPE using different methods and various spatial mesh sizes h . Tab. 4.1 lists the numerical errors $\|\psi(t) - \psi_{h,\tau}(t)\|_{l^2}$ at $t = 1$ for various spatial mesh sizes h .

Mesh	$h = \frac{1}{4}$	$h = \frac{1}{8}$	$h = \frac{1}{16}$	$h = \frac{1}{32}$	$h = 1/64$
TSSP2	9.318E-2	4.512E-7	<5.0E-10	<5.0E-10	<5.0E-10
TSSP4	9.318E-2	4.512E-7	<5.0E-10	<5.0E-10	<5.0E-10
TSFD	7.943E-1	3.147E-1	9.025E-2	2.239E-2	5.574E-3
CNFD	7.943E-1	3.147E-1	9.026E-2	2.240E-2	5.583E-3

TABLE 4.1. Spatial discretization error analysis: $\|\psi(t) - \psi_{h,\tau}(t)\|_{l^2}$ at time $t = 1$ under $\tau = 0.0001$ for different numerical methods including TSSP2 (4.16), TSFD (4.17), CNFD (4.18), and TSSP4 (fourth order time integrator (4.10) with sine pseudospectral method).

Secondly, we test the discretization error in time. Tab. 4.2 shows the numerical errors $\|\psi(t) - \psi_{h,\tau}(t)\|_{l^2}$ at $t = 1$ with a very small mesh size $h = \frac{1}{1024}$ for different time steps τ and different numerical methods.

Time step	$\tau = 0.01$	$\tau = 0.005$	$\tau = 0.0025$	$\tau = 0.00125$
TSSP2	4.522E-4	1.129E-4	2.821E-5	7.051E-6
TSSP4	1.091E-5	6.756E-7	4.213E-8	2.630E-9
TSFD	3.332E-2	8.261E-3	2.071E-3	5.323E-4
CNFD	1.099E-1	2.884E-2	7.268E-3	1.835E-3

TABLE 4.2. Time discretization error analysis: $\|\psi(t) - \psi_{h,\tau}(t)\|_{l^2}$ at time $t = 1$ under $h = \frac{1}{1024}$.

From Tabs. 4.1-4.2, one can make the following observations: (i) Both TSSP2 and TSSP4 are spectral accurate in space and they share the same accuracy for fixed mesh size h , and resp., TSFD and CNFD are second-order in space and they share the same accuracy for fixed mesh size h . (ii) TSSP2, TSFD and CNFD are second-order in time and TSSP4 is fourth-order in time. In general, for fixed time step τ , the error from time discretization of TSSP2 is much smaller than that of TSFD and CNFD, and the error from time discretization of TSFD is much smaller than that of CNFD. From our computations, the error bounds for SIFD are similar

to CNFD and we omit it here (cf. [20, 21]). For more comparisons, we refer to [42] and references therein.

Among the above numerical methods: (i) TSSP is explicit with computational cost per time step at $O(M \ln M)$ with M the total number of unknowns in 1D, 2D and 3D, TSFD and SIFD are implicit with computational cost per time step $O(M)$ and $O(M \ln M)$ in 1D and 2D/3D, respectively, CNFD is implicit which is the most expensive one since it needs to solve a fully coupled nonlinear system per time step. (ii) The storage requirement of TSSP is little less than those of TSFD, CNFD and SIFD. (iii) TSSP, TSFD and CNFD are unconditionally stable and SIFD is conditionally stable. (iv) TSSP and TSFD are time transverse invariant, where CNFD and SIFD are not. (v) TSSP, TSFD and CNFD conserve the mass in the discretized level, where SIFD doesn't. (vi) CNFD conserves the energy in the discretized level, where TSSP, TSFD and SIFD don't. However, when the time step is small, TSSP, TSFD and SIFD conserve the energy very well in practical computation. (vii) Extension of all the numerical methods to 2D and 3D cases is straightforward without additional numerical difficulty. Based on these comparisons, in order to solve the GPE numerically for computing the dynamics of BEC, when the solution is smooth, we recommend to use TSSP method, and resp., when the solution is not very smooth, e.g. with random potential, we recommend to use TSFD.

4.7. Extension to damped Gross-Pitaevskii equations. In section 2.2.3, a damping term is introduced in GPE to describe the collapse of focusing BEC. Our numerical methods can be generalized to this damped GPE easily. For simplicity, we will only consider 1D case and extensions to 2D and 3D are straightforward. For $d = 1$, the general damped NLSE becomes [30, 32]

$$i\psi_t = -\frac{1}{2}\psi_{xx} + V(x)\psi + \beta|\psi|^{2\sigma}\psi - if(|\psi|^2)\psi, \quad a < x < b, \quad t > 0, \quad (4.111)$$

$$\psi(x, t = 0) = \psi_0(x), \quad a \leq x \leq b, \quad \psi(a, t) = \psi(b, t) = 0, \quad t \geq 0. \quad (4.112)$$

Due to the high performance of TSSP (4.16), we will extend it to solve damped GPE and adopt the same notations and mesh strategy. From time $t = t_n$ to time $t = t_{n+1}$, the damped GPE (4.111) is solved in two steps. One solves

$$i\psi_t = -\frac{1}{2}\psi_{xx}, \quad (4.113)$$

for one time step, followed by solving

$$i\psi_t(x, t) = V(x)\psi(x, t) + \beta|\psi(x, t)|^{2\sigma}\psi(x, t) - if(|\psi(x, t)|^2)\psi(x, t), \quad (4.114)$$

again for the same time step. Equation (4.113) is discretized in space by the sine-spectral method and integrated in time *exactly*. For $t \in [t_n, t_{n+1}]$, multiplying the ODE (4.114) by $\overline{\psi(x, t)}$, the conjugate of $\psi(x, t)$, one obtains

$$i\psi_t(x, t)\overline{\psi(x, t)} = V(x)|\psi(x, t)|^2 + \beta|\psi(x, t)|^{2\sigma+2} - if(|\psi(x, t)|^2)|\psi(x, t)|^2. \quad (4.115)$$

Subtracting the conjugate of Eq. (4.115) from Eq. (4.115) and multiplying by $-i$ one obtains

$$\frac{d}{dt}|\psi(x, t)|^2 = \overline{\psi_t(x, t)}\psi(x, t) + \psi_t(x, t)\overline{\psi(x, t)} = -2f(|\psi(x, t)|^2)|\psi(x, t)|^2. \quad (4.116)$$

Let

$$g(s) = \int \frac{1}{s f(s)} ds, \quad h(s, s') = \begin{cases} g^{-1}(g(s) - 2s'), & s > 0, \quad s' \geq 0, \\ 0, & s = 0, \quad s' \geq 0. \end{cases} \quad (4.117)$$

Then, if $f(s) \geq 0$ for $s \geq 0$, we find

$$0 \leq h(s, s') \leq s, \quad \text{for } s \geq 0, \quad s' \geq 0, \quad (4.118)$$

and the solution of the ODE (4.116) can be expressed as (with $s' = t - t_n$)

$$\begin{aligned} 0 \leq \rho(t) &= \rho(t_n + s') := |\psi(x, t)|^2 = h(|\psi(x, t_n)|^2, t - t_n) := h(\rho(t_n), s') \\ &\leq \rho(t_n) = |\psi(x, t_n)|^2, \quad t_n \leq t \leq t_{n+1}. \end{aligned} \quad (4.119)$$

Combining Eq. (4.119) and Eq. (4.13) we obtain

$$\begin{aligned} i \psi_t(x, t) &= V(x)\psi(x, t) + \beta [h(|\psi(x, t_n)|^2, t - t_n)]^\sigma \psi(x, t) \\ &\quad - i f(h(|\psi(x, t_n)|^2, t - t_n)) \psi(x, t), \quad t_n \leq t \leq t_{n+1}. \end{aligned} \quad (4.120)$$

Integrating (4.120) from t_n to t , we find

$$\begin{aligned} \psi(x, t) &= \exp \{ i [-V(x)(t - t_n) - G(|\psi(x, t_n)|^2, t - t_n)] - F(|\psi(x, t_n)|^2, t - t_n) \} \\ &\quad \times \psi(x, t_n), \quad t_n \leq t \leq t_{n+1}, \end{aligned} \quad (4.121)$$

where we have defined

$$F(s, \eta) = \int_0^\eta f(h(s, s')) ds' \geq 0, \quad G(s, \eta) = \int_0^\eta \beta [h(s, s')]^\sigma ds'. \quad (4.122)$$

To find the time evolution between $t = t_n$ and $t = t_{n+1}$, we combine the splitting steps via the standard second-order Strang splitting (TSSP) for solving the damped GPE (4.111). In detail, the steps for obtaining ψ_j^{n+1} from ψ_j^n are given by

$$\begin{aligned} \psi_j^{(1)} &= \exp \left\{ -F \left(|\psi_j^n|^2, \frac{\tau}{2} \right) + i \left[-V(x_j) \frac{\tau}{2} - G \left(|\psi_j^n|^2, \frac{\tau}{2} \right) \right] \right\} \psi_j^n, \\ \psi_j^{(2)} &= \frac{2}{M} \sum_{l=1}^{M-1} e^{-i\tau\mu_l^2/2} \widetilde{(\psi^{(1)})}_l \sin(\mu_l(x_j - a)), \quad j \in \mathcal{T}_M, \\ \psi_j^{n+1} &= \exp \left\{ -F \left(|\psi_j^{(2)}|^2, \frac{\tau}{2} \right) + i \left[-V(x_j) \frac{\tau}{2} - G \left(|\psi_j^{(2)}|^2, \frac{\tau}{2} \right) \right] \right\} \psi_j^{(2)}, \end{aligned} \quad (4.123)$$

where \widetilde{u}_l are the sine-transform coefficients of a complex vector $u = (u_0, \dots, u_M)^T$ with $u_0 = u_M = 0$ defined in (3.31), and

$$\psi_j^0 = \psi(x_j, 0) = \psi_0(x_j), \quad j = 0, 1, 2, \dots, M. \quad (4.124)$$

For some frequently used damping terms, the integrals in (4.117) and (4.122) can be evaluated analytically (cf. [30]).

5. Theory for rotational BEC. In view of potential applications, the study of quantized vortices, which are related to superfluid properties, is one of the key issues. In fact, bulk superfluids are distinguished from normal fluids by their ability to support dissipationless flow. Such persistent currents are intimately related to the existence of quantized vortices, which are localized phase singularities with integer topological charge [97]. The superfluid vortex is an example of a topological defect that is well known in superconductors and in liquid helium. Currently, one of the most popular ways to generate quantized vortices from BEC ground state is the following: impose a laser beam rotating with an angular velocity on the magnetic trap holding the atoms to create a harmonic anisotropic potential. Various experiments have confirmed the observation of quantized vortices in BEC under a rotational frame [1, 68, 140].

5.1. GPE with an angular momentum rotation term. At temperatures T much smaller than the critical temperature T_c , following the mean field theory (cf. section 1.2), BEC in a rotational frame is well described by the macroscopic wave function $\psi(\mathbf{x}, t)$, whose evolution is governed by the Gross-Pitaevskii equation (GPE) with an angular momentum rotation term [5, 40, 41, 44, 97], (w.l.o.g.) assuming the rotation being around the z -axis:

$$i\hbar \frac{\partial \psi(\mathbf{x}, t)}{\partial t} = \left(-\frac{\hbar^2}{2m} \nabla^2 + V(\mathbf{x}) + Ng|\psi(\mathbf{x}, t)|^2 - \Omega L_z \right) \psi(\mathbf{x}, t), \quad (5.1)$$

where $\mathbf{x} = (x, y, z)^T \in \mathbb{R}^3$ is the spatial coordinate vector, and

$$L_z = -i\hbar(x\partial_y - y\partial_x) \quad (5.2)$$

is the z -component of the angular momentum operator $L = (L_x, L_y, L_z)^T$ given by $L = -i\hbar(\mathbf{x} \wedge \nabla)$. The appearance of the angular momentum term means that we are using a reference frame where the trap is at rest. The energy functional per particle $E(\psi)$ is defined as

$$E(\psi) = \int_{\mathbb{R}^3} \left[\frac{\hbar^2}{2m} |\nabla \psi|^2 + V(\mathbf{x})|\psi|^2 + \frac{Ng}{2} |\psi|^4 - \Omega \bar{\psi} L_z \psi \right] d\mathbf{x}, \quad (5.3)$$

and wave function is normalized as

$$\int_{\mathbb{R}^3} |\psi(\mathbf{x}, t)|^2 d\mathbf{x} = 1. \quad (5.4)$$

5.1.1. Dimensionless form. For the conventional harmonic potential case, by introducing the dimensionless variables: $t \rightarrow t/\omega_0$ with $\omega_0 = \min\{\omega_x, \omega_y, \omega_z\}$, $\mathbf{x} \rightarrow \mathbf{x}x_s$ with $x_s = \sqrt{\hbar/m\omega_0}$, $\psi \rightarrow \psi/x_s^{3/2}$, $\Omega \rightarrow \Omega\omega_0$ and $E(\cdot) \rightarrow \hbar\omega_0 E_{\beta, \Omega}(\cdot)$, we get the dimensionless GPE

$$i \frac{\partial \psi(\mathbf{x}, t)}{\partial t} = \left(-\frac{1}{2} \nabla^2 + V(\mathbf{x}) + \kappa |\psi(\mathbf{x}, t)|^2 - \Omega L_z \right) \psi(\mathbf{x}, t), \quad (5.5)$$

where $\kappa = \frac{gN}{x_s^3 \hbar \omega_0} = \frac{4\pi a_s N}{x_s}$, $L_z = -i(x\partial_y - y\partial_x)$ ($L = -i(\mathbf{x} \wedge \nabla)$), $V(\mathbf{x}) = \frac{1}{2}(\gamma_x^2 x^2 + \gamma_y^2 y^2 + \gamma_z^2 z^2)$ with $\gamma_x = \frac{\omega_x}{\omega_0}$, $\gamma_y = \frac{\omega_y}{\omega_0}$ and $\gamma_z = \frac{\omega_z}{\omega_0}$.

In a disk-shaped condensate with parameters $\omega_x \approx \omega_y$ and $\omega_z \gg \omega_x$ ($\iff \gamma_x = 1$, $\gamma_y \approx 1$ and $\gamma_z \gg 1$ with choosing $\omega_0 = \omega_x$), the 3D GPE (5.5) can be reduced to a 2D GPE with $\mathbf{x} = (x, y)^T$ (cf. section 1.3.3):

$$i \frac{\partial \psi(\mathbf{x}, t)}{\partial t} = -\frac{1}{2} \nabla^2 \psi + V_2(x, y) \psi + c_2 \kappa |\psi|^2 \psi - \Omega L_z \psi, \quad (5.6)$$

where $c_2 = \sqrt{\gamma_z/2\pi}$ and $V_2(x, y) = \frac{1}{2}(\gamma_x^2 x^2 + \gamma_y^2 y^2)$ [20, 44, 46, 97].

Thus here we consider the dimensionless GPE under a rotational frame in d -dimensions ($d = 2, 3$):

$$i \frac{\partial \psi(\mathbf{x}, t)}{\partial t} = -\frac{1}{2} \nabla^2 \psi + V(\mathbf{x}) \psi + \beta |\psi|^2 \psi - \Omega L_z \psi, \quad \mathbf{x} \in \mathbb{R}^d, \quad t > 0, \quad (5.7)$$

where

$$\beta = \kappa \begin{cases} \sqrt{\gamma_z/2\pi}, & d = 2, \\ 1, & d = 3. \end{cases} \quad V(\mathbf{x}) = \begin{cases} \frac{1}{2}(\gamma_x^2 x^2 + \gamma_y^2 y^2), & d = 2, \\ \frac{1}{2}(\gamma_x^2 x^2 + \gamma_y^2 y^2 + \gamma_z^2 z^2), & d = 3. \end{cases} \quad (5.8)$$

Then the dimensionless energy functional per particle $E_{\beta, \Omega}(\psi)$ is defined as

$$E_{\beta, \Omega}(\psi) = \int_{\mathbb{R}^d} \left[\frac{1}{2} |\nabla \psi(\mathbf{x}, t)|^2 + V(\mathbf{x})|\psi|^2 + \frac{\beta}{2} |\psi|^4 - \Omega \bar{\psi} L_z \psi \right] d\mathbf{x}, \quad (5.9)$$

and the normalization is given by

$$\|\psi(\cdot, t)\|_{L^2(\mathbb{R}^d)}^2 = \|\psi(\cdot, 0)\|_{L^2(\mathbb{R}^d)}^2 = 1. \quad (5.10)$$

The vortex structure of rotating BEC in 3D is very complicated [4, 97] due to the presence of vortex lines, while in 2D, the structure is relatively simple as the vortex center is only a point. As a result, most investigations start from the 2D case.

5.2. Theory for ground states. Similar to section 2, the ground state wave function $\phi_g := \phi_g(\mathbf{x})$ of a rotating BEC satisfies the nonlinear eigenvalue problem (Euler-Lagrange equation)

$$\mu \phi(\mathbf{x}) = \left[-\frac{1}{2} \nabla^2 + V(\mathbf{x}) + \beta |\phi|^2 - \Omega L_z \right] \phi(\mathbf{x}), \quad \mathbf{x} \in \mathbb{R}^d, \quad d = 2, 3, \quad (5.11)$$

under the normalization condition

$$\|\phi\|_2^2 = \int_{\mathbb{R}^d} |\phi(\mathbf{x})|^2 d\mathbf{x} = 1, \quad (5.12)$$

with eigenvalue (or chemical potential) μ given by

$$\mu = E_{\beta, \Omega}(\phi) + \frac{\beta}{2} \int_{\mathbb{R}^d} |\phi(\mathbf{x})|^4 d\mathbf{x}. \quad (5.13)$$

The eigenfunction $\phi(\mathbf{x})$ of (5.11) under the constraint (5.12) with least energy is called ground state. The ground state can be found by minimizing the energy functional $E_{\beta, \Omega}(\phi)$ (5.9) over the unit sphere $S = \{\phi \mid \|\phi\|_2 = 1, E_{\beta, \Omega}(\phi) < \infty\}$:

(I) Find $(\mu_{\beta, \Omega}^g, \phi_g \in S)$ such that

$$E_{\beta, \Omega}^g := E_{\beta, \Omega}(\phi_g) = \min_{\phi \in S} E_{\beta, \Omega}(\phi), \quad \mu_{\beta, \Omega}^g := \mu_{\beta, \Omega}^g(\phi_g). \quad (5.14)$$

Any eigenfunction $\phi(\mathbf{x})$ of (5.11) under constraint (5.12) whose energy $E_{\beta, \Omega}(\phi) > E_{\beta, \Omega}(\phi_g)$ is usually called as an excited state in the physics literature.

Existence/nonexistence results of ground state depend on the magnitude $|\Omega|$ of the angular velocity relative to the trapping frequencies [46, 64, 162].

For the existence and simple properties of ground state for rotating BEC, we have the following [46, 162].

Theorem 5.1. *Suppose that $V(\mathbf{x})$ is given in (5.8), then we have the conclusions below.*

i) In 2D, if $\phi_{\beta, \Omega}(x, y) \in S$ is a ground state of the energy functional $E_{\beta, \Omega}(\phi)$, then $\phi_{\beta, \Omega}(x, -y) \in S$ and $\phi_{\beta, \Omega}(-x, y) \in S$ are ground states of the energy functional $E_{\beta, -\Omega}(\phi)$. Furthermore

$$E_{\beta, \Omega}^g = E_{\beta, -\Omega}^g, \quad \mu_{\beta, \Omega}^g = \mu_{\beta, -\Omega}^g. \quad (5.15)$$

ii) In 3D, if $\phi_{\beta, \Omega}(x, y, z) \in S$ is a ground state of the energy functional $E_{\beta, \Omega}(\phi)$, then $\phi_{\beta, \Omega}(x, -y, z) \in S$ and $\phi_{\beta, \Omega}(-x, y, z) \in S$ are ground states of the energy functional $E_{\beta, -\Omega}(\phi)$, and (5.15) is also valid.

iii) When $|\Omega| < \min\{\gamma_x, \gamma_y\}$ and $\beta \geq 0$ in 3D or $\beta > -C_b$ in 2D (C_b given in (2.12)), there exists a minimizer for the minimization problem (5.14), i.e. there exist ground state.

Theorem 5.1 is a direct consequence of the below observation and the theory for non-rotating BEC (cf. section 2).

Lemma 5.1. *Under the conditions of Theorem 5.1, the following results hold.*

i) In 2D, we have

$$E_{\beta,-\Omega}(\phi(x,-y)) = E_{\beta,\Omega}(\phi(x,y)), \quad E_{\beta,-\Omega}(\phi(-x,y)) = E_{\beta,\Omega}(\phi(x,y)), \quad \phi \in S.$$

ii) In 3D, we have

$$E_{\beta,-\Omega}(\phi(x,-y,z)) = E_{\beta,\Omega}(\phi(x,y,z)), \quad E_{\beta,-\Omega}(\phi(-x,y,z)) = E_{\beta,\Omega}(\phi(x,y,z)), \quad \phi \in S.$$

iii) In 2D and 3D, we have

$$\begin{aligned} & \int_{\mathbb{R}^d} \left[\frac{1-|\Omega|}{2} |\nabla\phi(\mathbf{x})|^2 + \left(V(\mathbf{x}) - \frac{|\Omega|}{2}(x^2+y^2) \right) |\phi|^2 + \frac{\beta}{2} |\phi|^4 \right] d\mathbf{x} \leq E_{\beta,\Omega}(\phi) \\ & \leq \int_{\mathbb{R}^d} \left[\frac{1+|\Omega|}{2} |\nabla\phi(\mathbf{x})|^2 + \left(V(\mathbf{x}) + \frac{|\Omega|}{2}(x^2+y^2) \right) |\phi|^2 + \frac{\beta}{2} |\phi|^4 \right] d\mathbf{x}. \end{aligned} \quad (5.16)$$

For understanding the uniqueness question, note that $E_{\beta,\Omega}(\alpha\phi_{\beta,\Omega}^g) = E_{\beta,\Omega}(\phi_{\beta,\Omega}^g)$ for all $\alpha \in \mathbb{C}$ with $|\alpha| = 1$. Thus an additional constraint has to be introduced to show uniqueness. For non-rotating BEC, i.e. $\Omega = 0$, the unique positive minimizer is usually taken as the ground state. In fact, the ground state is unique up to a constant α with $|\alpha| = 1$, i.e. density of the ground state is unique, when $\Omega = 0$. For rotating BEC under $|\Omega| < \min\{\gamma_x, \gamma_y\}$, the density of the ground state may be no longer unique when $|\Omega| > \Omega^c$ with Ω^c a critical angular rotation speed.

When rotational speed exceeds the trap frequency in x - or y - direction, i.e. $\Omega > \min\{\gamma_x, \gamma_y\}$, there will be no ground state [46, 64].

Theorem 5.2. (nonexistence) *Suppose that $V(\mathbf{x})$ is given in (5.8), then there exists no minimizer for problem (5.14) if one of the following holds:*

- (i) $\beta < 0$ in 3D or $\beta < -C_b$ (C_b given in (2.12)) in 2D;*
- (ii) $|\Omega| > \min\{\gamma_x, \gamma_y\}$.*

5.3. Critical speeds for quantized vortices. From Theorems 5.1 and 5.2, only the case of $0 \leq \Omega < \min\{\gamma_x, \gamma_y\}$ is interesting for considering the ground state of a rotating BEC and we will assume $\Omega \geq 0$ in the subsequent discussions. In particular, the vortex appears in the ground state only if the rotational speed exceeds certain critical value. Various experiments and mathematical studies confirm the existence of such critical speeds.

In [162], for a radially symmetric potential in 2D, Seiringer proved that there exists critical velocity $\Omega_0 > 0$ that a state containing vortices is energetically favorable for $\Omega > \Omega_0$. The point is that, as Ω increases from 0 to $\min\{\gamma_x, \gamma_y\}$, the first ground state with vortex should be the *central vortex* state, i.e., a state containing central vortex (vortex line) in the rotational center (axis).

In 2D with radially symmetric potential $V(r)$ ($r = |\mathbf{x}|$, $\mathbf{x} \in \mathbb{R}^2$), the symmetric state ($m = 0$) and central vortex state with index (or winding number or circulation) $0 \neq m \in \mathbb{Z}$ is the solution of the nonlinear eigenvalue problem (5.11)-(5.13) with the form

$$\phi(\mathbf{x}) = \phi_m(r)e^{im\theta}, \quad \text{where } (r, \theta) \text{ is the polar coordinate.} \quad (5.17)$$

In polar coordinate, the angular momentum term (5.2) becomes $L_z = -i\frac{\partial}{\partial\theta}$. In order to find the above central vortex states with index m ($m \neq 0$), $\phi(\mathbf{x}) = \phi_m(r)e^{im\theta}$, we need to find a real nonnegative function $\phi_m(r) := \phi_{\beta,\Omega}^m(r)$ which minimizes the

energy functional

$$\begin{aligned}
 E_{\beta,\Omega}^m(\phi(r)) &= E_{\beta,\Omega}(\phi(r)e^{im\theta}) \\
 &= \pi \int_0^\infty \left[|\phi'(r)|^2 + \left(2V(r) + \frac{m^2}{r^2} \right) |\phi(r)|^2 + \beta |\phi(r)|^4 - 2m\Omega |\phi(r)|^2 \right] r dr \\
 &= E_{\beta,0}^m(\phi(r)) - m\Omega, \quad \Omega \geq 0, \quad m \geq 0,
 \end{aligned} \tag{5.18}$$

over the set $S_r = \{\phi(r) \in \mathbb{R} \mid 2\pi \int_0^\infty |\phi(r)|^2 r dr = 1, E_{\beta,0}^m(\phi) < \infty, \phi'(0) = 0 (m = 0), \text{ and resp. } \phi(0) = 0 (m \neq 0)\}$. The existence and uniqueness of nonnegative minimizer for this minimization problem can be obtained similarly as for the ground state when $\Omega = 0$ [133, 162]. It is clear from (5.18) that contribution of rotation in the energy (5.18) is fixed with index m and the central vortex state with index m is independent of Ω . In fact, let us denote

$$E^m(\phi(r)) = E_{\beta,\Omega}^m(\phi(r)) + m\Omega, \tag{5.19}$$

and the central vortex state can be found as the minimizer of energy $E^m(\phi)$ which is independent of Ω .

Similarly, in order to find the cylindrically symmetric state ($m = 0$), and resp. central vortex line states ($m \neq 0$), in 3D with cylindrical symmetry, i.e. $d = 3$ and $V(\mathbf{x}) = V(r, z)$ in (5.7), we solve the nonlinear eigenvalue problem (5.11)-(5.13) with the special form of wave function as

$$\phi(\mathbf{x}) = \phi_m(x, y, z) = \phi_m(r, z)e^{im\theta}, \tag{5.20}$$

where (r, θ, z) is the cylindrical coordinate, m is an integer and called as index when $m \neq 0$. $\phi_m(r, z)$ is a real function independent of angle. It is equivalent to computing a real nonnegative function $\phi_m(r, z) := \phi_{\beta,\Omega}^m(r, z)$ which minimizes the energy functional

$$\begin{aligned}
 E_{\beta,\Omega}^m(\phi(r, z)) &= E_{\beta,\Omega}(\phi(r, z)e^{im\theta}) \\
 &= \pi \int_0^\infty \int_{-\infty}^\infty \left[|\partial_r \phi|^2 + |\partial_z \phi|^2 + \left(2V(r, z) + \frac{m^2}{r^2} - 2m\Omega \right) |\phi|^2 + \beta |\phi|^4 \right] r dz dr,
 \end{aligned} \tag{5.21}$$

over the set $S_c = \{\phi \in \mathbb{R} \mid 2\pi \int_0^\infty \int_{-\infty}^\infty |\phi(r, z)|^2 r dz dr = 1, E_{\beta,0}^m(\phi) < \infty, \partial_r \phi(0, r) = 0 (m = 0), \text{ and resp. } \phi(0, z) = 0 (m \neq 0), -\infty < z < \infty\}$.

For 2D case, by carefully studying the energy functional (5.18), Seiringer [162] established the estimates of critical velocity Ω_m ($m \geq 0$) when a central vortex $\phi(r)$ with index $m + 1$ is energetically favorable to a central vortex state with index m for $\Omega > \Omega_m$, i.e., $E_{\beta,\Omega}^{m+1}(\phi(r)) < E_{\beta,\Omega}^m(\phi(r))$. The critical speed is given by

$$\Omega_m = \min_{\phi \in S_r} E^{m+1}(\phi(r)) - \min_{\phi \in S_r} E^m(\phi(r)) > 0. \tag{5.22}$$

The estimates for Ω_m is the following.

Theorem 5.3. (cf. [162]) *In 2D, assume potential $V(r) = \frac{1}{2}r^2$ ($r = |\mathbf{x}|$, $\mathbf{x} \in \mathbb{R}^d$), for positive $\beta > 0$ and $m \geq 0$, then the following bounds on Ω_m hold,*

$$\Omega_m \leq (2m + 1) \frac{2\pi e}{\beta} \left(1 + \sqrt{\frac{2\beta}{\pi}} \right) (3 + \lceil \ln(\beta/(2\pi e^2)) \rceil), \tag{5.23}$$

$$\Omega_m \geq \frac{2m + 1}{(m + 2) \sqrt{1 + \frac{\beta}{b_{m+1}(m+2)}}}, \tag{5.24}$$

where $b_m = \frac{2 \times 4^m \pi (m!)^2}{(2m)!}$. In addition, there is a relation between the critical velocities as $\Omega_{m+1} \leq \frac{2m+3}{2m+1} \Omega_m$.

In particular, we notice that Ω_0 is the critical velocity for the appearance of vortex in the ground state. For large Ω , the central vortex state (5.17) will no longer be the right ansatz for ground state due to the symmetry breaking [162].

Theorem 5.4. (cf. [162]) *In 2D, assume potential $V(r) = \frac{1}{2} \gamma_r^2 r^2$ ($r = |\mathbf{x}|$, $\mathbf{x} \in \mathbb{R}^d$), for fixed rotational speed $0 < \Omega < \gamma_r$, there exists a constant β_Ω , such that if $\beta \geq \beta_\Omega$, no ground state of problem (5.14) is an eigenfunction of the angular momentum operator L_z (5.2). Let ϕ_g be the ground state of (5.14) when $\beta \geq \beta_\Omega$, then $|\phi_g|$ is not radially symmetric.*

For small rotational speed Ω with radial potential $V(r)$, the minimizer of problem (5.14) remains the same as the ground state of the non-rotating case, i.e., the ground state of small Ω is the same as that of $\Omega = 0$. This observation is recently proved rigorously by Aftalion et al. [7].

Theorem 5.5. (cf. [7]) *In 2D, assuming potential $V(r) = \frac{1}{2} \gamma_r^2 r^2$ ($r = |\mathbf{x}|$, $\mathbf{x} \in \mathbb{R}^d$), let $\phi_{\beta, \Omega}^g(\mathbf{x})$ be the solution of the minimization problem (5.14) with rotational speed Ω and $\phi_{\beta, 0}^g(r)$ be the unique positive minimizer for (5.14) with $\Omega = 0$ (see section 2). There exists $\beta_0 \geq 0$, such that when $\beta \geq \beta_0$, for $0 \leq \Omega \leq \Omega_\beta$ (constant Ω_β depends on β), $\phi_{\beta, \Omega}^g = e^{i\theta} \phi_{\beta, 0}^g$ for some constant $\theta \in \mathbb{R}$.*

All these results are valid for general potential $V(r)$ [7, 162].

When Ω increases, the number of vortices in the ground state will also increase and the vortices interact. At high rotational speed, vortices will form a lattice, known as an Abrikosov lattice [4, 5, 97]. For the fast rotational speeds, Correggi [83] studied the expansion of energy (5.9) and proved that the vortices will be asymptotically equidistributed, which means that the vortices will form a triangle lattice. For general harmonic potentials in 2D, i.e., $\gamma_x \neq \gamma_y$, Ignat et al. estimated the critical angular velocity for the existence of n vortices in the ground state as well as the location of the vortex centers [119, 120].

If an anharmonic potential, i.e. $V(\mathbf{x}) = V(r) = O(r^4)$ when $r \rightarrow \infty$, is considered instead of harmonic potentials, there exists another phase transition [81, 82]. When Ω increases, the ground state of a rotating BEC with anharmonic potential will first undergo a phase transition to the vortex state, and then become a vortex lattice. If the velocity Ω keeps increasing, the vortex lattice will disappear, and the density will be depleted near the trap center. Then all the vortices will be pushed away from the center and form a giant vortex (or vortex ring) [156]. Thus, there are three typical critical speeds that can be identified with these kinds of phase transitions in rotating BEC [81]. In the study of the critical speeds, a more widely used scaling is different from the one adopted here [5] (cf. section 7).

5.4. Well-posedness of Cauchy problem. This section is devoted to the well-posedness of Cauchy problem for the rotating GPE (5.7). We use the same notations for function spaces as those in section 2.

Like the non-rotating case ($\Omega = 0$) (cf. section 2), the key part is to establish the dispersive estimates like Lemma 2.4 for the evolutionary operator e^{itL_R} generated by the linear operator

$$L_R = -\frac{1}{2} \nabla^2 + V(\mathbf{x}) - \Omega L_z, \quad \mathbf{x} \in \mathbb{R}^d, \quad d = 2, 3. \quad (5.25)$$

For the special case $V(\mathbf{x}) = \frac{\omega^2}{2}|\mathbf{x}|^2$ and $\Omega = \omega$, Hao et al. obtained the dispersive estimates for e^{itL_R} using a generalization of Mehler's formula for the kernel of e^{itL_R} [73,111,112]. Later, Antonelli et al. found another approach to establish the dispersive estimates for e^{itL_R} without those assumptions on Ω and V in [111,112]. It turns out that the rotational term L_z does not affect the dispersive behavior (in short time), and the dispersive estimates for e^{itL_R} are then analogous to those in Lemma 2.4 for harmonic potentials. Then the well-posedness of the rotational GPE (5.7) follows from the classical arguments [73,173].

Theorem 5.6. (cf. [13]) *Assume that $V(\mathbf{x})$ is given by (5.8) and denote $\gamma_{\min} = \min\{\gamma_\alpha\}$ ($\gamma_\alpha > 0$; $\alpha = x, y$ for $d = 2$, and $\alpha = x, y, z$ for $d = 3$), then we have the following results.*

(i) *For any initial data $\psi(\mathbf{x}, t = 0) = \psi_0(\mathbf{x}) \in X(\mathbb{R}^d)$ ($d = 2, 3$), there exists a $T_{\max} \in (0, +\infty]$ such that the Cauchy problem of (5.7) has a unique maximal solution $\psi \in C([0, T_{\max}), X)$. It is maximal in the sense that if $T_{\max} < \infty$, then $\|\psi(\cdot, t)\|_X \rightarrow \infty$ when $t \rightarrow T_{\max}^-$.*

(ii) *As long as the solution $\psi(\mathbf{x}, t)$ remains in the energy space X , the L^2 -norm $\|\psi(\cdot, t)\|_2$ and energy $E_{\beta, \Omega}(\psi(\cdot, t))$ in (5.9) are conserved for $t \in [0, T_{\max})$.*

(iii) *The solution of the Cauchy problem for (5.7) is global in time, i.e., $T_{\max} = \infty$, if $\beta \geq 0$.*

(iv) *If $\beta < 0$ in 2D and 3D, and if either:*

(1) *$V(\mathbf{x})$ is axially symmetric, i.e., $\Omega L_z V(\mathbf{x}) = 0$;*

(2) *$\Omega L_z V(\mathbf{x}) \neq 0$ and $d\sqrt{(1 - (\Omega/\gamma_{\min})^2)} \geq 1$ with $|\Omega| \leq \gamma_{\min}$ ($d = 2, 3$).*

Then there exists $\psi_0 \in X(\mathbb{R}^d)$ such that finite time blow-up happens for the solution of the corresponding Cauchy problem (5.7).

5.5. Dynamical laws. In this section, we present results on the dynamical properties of rotating BEC governed by GPE with an angular momentum term (5.7).

For the dynamics of angular momentum expectation in rotating BEC, we have the following lemmas [28]:

Lemma 5.2. *Suppose $\psi(\mathbf{x}, t)$ is the solution to the Cauchy problem of (5.7), then we have*

$$\frac{d\langle L_z \rangle(t)}{dt} = (\gamma_x^2 - \gamma_y^2) \delta_{xy}(t), \quad \text{where } \delta_{xy}(t) = \int_{\mathbb{R}^d} xy |\psi(\mathbf{x}, t)|^2 d\mathbf{x}, \quad t \geq 0. \quad (5.26)$$

Consequently, the angular momentum expectation and energy for non-rotating part are conserved, that is, for any given initial data $\psi(\mathbf{x}, 0) = \psi_0(\mathbf{x})$,

$$\langle L_z \rangle(t) \equiv \langle L_z \rangle(0), \quad E_{\beta, 0}(\psi) \equiv E_{\beta, 0}(\psi_0), \quad t \geq 0, \quad (5.27)$$

at least for radially symmetric trap in 2D or cylindrically symmetric trap in 3D, i.e. $\gamma_x = \gamma_y$.

For the condensate width defined by $\delta_\alpha(\cdot)$ in (2.54), we can obtain similar results to that in Lemma 2.6 [28].

Lemma 5.3. *Suppose $\psi(\mathbf{x}, t)$ is the solution of the problem (5.7), then we have*

$$\begin{aligned} \ddot{\delta}_\alpha(t) = \int_{\mathbb{R}^d} & \left[(\partial_y \alpha - \partial_x \alpha) (4i\Omega \bar{\psi} (x\partial_y + y\partial_x) \psi + 2\Omega^2 (x^2 - y^2) |\psi|^2) \right. \\ & \left. + 2|\partial_\alpha \psi|^2 + \beta |\psi|^4 - 2\alpha |\psi|^2 \partial_\alpha V(\mathbf{x}) \right] d\mathbf{x}, \quad t \geq 0, \end{aligned} \quad (5.28)$$

$$\delta_\alpha(0) = \delta_\alpha^{(0)} = \int_{\mathbb{R}^d} \alpha^2 |\psi_0(\mathbf{x})|^2 d\mathbf{x}, \quad \alpha = x, y, z, \quad (5.29)$$

$$\dot{\delta}_\alpha(0) = \delta_\alpha^{(1)} = 2 \int_{\mathbb{R}^d} \alpha [-\Omega |\psi_0|^2 (x\partial_y - y\partial_x) \alpha + \text{Im}(\bar{\psi}_0 \partial_\alpha \psi_0)] d\mathbf{x}. \quad (5.30)$$

Lemma 5.4. (i) *In 2D with a radially symmetric trap, i.e. $d = 2$ and $\gamma_x = \gamma_y := \gamma_r$ in (5.7), for any initial data $\psi(x, y, 0) = \psi_0 = \psi_0(x, y)$, we have for any $t \geq 0$,*

$$\delta_r(t) = \frac{E_{\beta, \Omega}(\psi_0) + \Omega \langle L_z \rangle(0)}{\gamma_r^2} [1 - \cos(2\gamma_r t)] + \delta_r^{(0)} \cos(2\gamma_r t) + \frac{\delta_r^{(1)}}{2\gamma_r} \sin(2\gamma_r t), \quad (5.31)$$

where $\delta_r(t) = \delta_x(t) + \delta_y(t)$, $\delta_r^{(0)} := \delta_x(0) + \delta_y(0)$, and $\delta_r^{(1)} := \dot{\delta}_x(0) + \dot{\delta}_y(0)$. Furthermore, when the initial condition $\psi_0(x, y)$ satisfies

$$\psi_0(x, y) = f(r) e^{im\theta} \quad \text{with } m \in \mathbb{Z} \quad \text{and } f(0) = 0 \quad \text{when } m \neq 0, \quad (5.32)$$

we have, for any $t \geq 0$,

$$\begin{aligned} \delta_x(t) = \delta_y(t) &= \frac{1}{2} \delta_r(t) \\ &= \frac{E_{\beta, \Omega}(\psi_0) + m\Omega}{2\gamma_x^2} [1 - \cos(2\gamma_x t)] + \delta_x^{(0)} \cos(2\gamma_x t) + \frac{\delta_x^{(1)}}{2\gamma_x} \sin(2\gamma_x t). \end{aligned} \quad (5.33)$$

This and (2.54) imply that

$$\sigma_x = \sigma_y = \sqrt{\frac{E_{\beta, \Omega}(\psi_0) + m\Omega}{2\gamma_x^2} [1 - \cos(2\gamma_x t)] + \delta_x^{(0)} \cos(2\gamma_x t) + \frac{\delta_x^{(1)}}{2\gamma_x} \sin(2\gamma_x t)}.$$

Thus in this case, the condensate widths $\sigma_x(t)$ and $\sigma_y(t)$ are periodic functions with frequency doubling the trapping frequency.

(ii) For all other cases, we have, for any $t \geq 0$

$$\delta_\alpha(t) = \frac{E_{\beta, \Omega}(\psi_0)}{\gamma_\alpha^2} + \left(\delta_\alpha^{(0)} - \frac{E_{\beta, \Omega}(\psi_0)}{\gamma_\alpha^2} \right) \cos(2\gamma_\alpha t) + \frac{\delta_\alpha^{(1)}}{2\gamma_\alpha} \sin(2\gamma_\alpha t) + f_\alpha(t), \quad (5.34)$$

where $f_\alpha(t)$ is the solution of the following second-order ODE:

$$\ddot{f}_\alpha(t) + 4\gamma_\alpha^2 f_\alpha(t) = F_\alpha(t), \quad f_\alpha(0) = \dot{f}_\alpha(0) = 0, \quad (5.35)$$

with

$$\begin{aligned} F_\alpha(t) = \int_{\mathbb{R}^d} & \left[2|\partial_\alpha \psi|^2 - 2|\nabla \psi|^2 - \beta |\psi|^4 + (2\gamma_\alpha^2 \alpha^2 - 4V(\mathbf{x})) |\psi|^2 + 4\Omega \bar{\psi} L_z \psi \right. \\ & \left. + (\partial_y \alpha - \partial_x \alpha) (4i\Omega \bar{\psi} (x\partial_y + y\partial_x) \psi + 2\Omega^2 (x^2 - y^2) |\psi|^2) \right] d\mathbf{x}. \end{aligned}$$

Let $\phi_e(\mathbf{x})$ be a stationary state of the GPE (5.7) with a chemical potential μ_e , i.e., (μ_e, ϕ_e) satisfies the nonlinear eigenvalue problem (5.11)-(5.12). If the initial data $\psi_0(\mathbf{x})$ for the Cauchy problem of (5.7) is chosen as a stationary state with a

shift in its center, one can construct an exact solution of the GPE with an angular momentum term (5.7), which is similar to Lemma 2.9 [28].

Lemma 5.5. *Suppose $V(\mathbf{x})$ is given by (5.8), if the initial data $\psi_0(\mathbf{x})$ for the Cauchy problem of (5.7) is chosen as*

$$\psi_0(\mathbf{x}) = \phi_e(\mathbf{x} - \mathbf{x}_0), \quad \mathbf{x} \in \mathbb{R}^d, \quad (5.36)$$

where \mathbf{x}_0 is a given point in \mathbb{R}^d , then the exact solution of (5.7) satisfies:

$$\psi(\mathbf{x}, t) = \phi_e(\mathbf{x} - \mathbf{x}_c(t)) e^{-i\mu_e t} e^{iw(\mathbf{x}, t)}, \quad \mathbf{x} \in \mathbb{R}^d, \quad t \geq 0, \quad (5.37)$$

where for any time $t \geq 0$, $w(\mathbf{x}, t)$ is linear for \mathbf{x} , i.e.

$$w(\mathbf{x}, t) = \mathbf{c}(t) \cdot \mathbf{x} + g(t), \quad \mathbf{c}(t) = (c_1(t), \dots, c_d(t))^T, \quad \mathbf{x} \in \mathbb{R}^d, \quad t \geq 0, \quad (5.38)$$

and $\mathbf{x}_c(t) = (x_c(t), y_c(t))^T$ in 2D, and resp., $\mathbf{x}_c(t) = (x_c(t), y_c(t), z_c(t))^T$ in 3D, satisfies the following second-order ODE system:

$$\ddot{x}_c(t) - 2\Omega\dot{y}_c(t) + (\gamma_x^2 - \Omega^2)x_c(t) = 0, \quad (5.39)$$

$$\ddot{y}_c(t) + 2\Omega\dot{x}_c(t) + (\gamma_y^2 - \Omega^2)y_c(t) = 0, \quad t \geq 0, \quad (5.40)$$

$$x_c(0) = x_0, \quad y_c(0) = y_0, \quad \dot{x}_c(0) = \Omega y_0, \quad \dot{y}_c(0) = -\Omega x_0. \quad (5.41)$$

Moreover, if in 3D, another ODE needs to be added:

$$\ddot{z}_c(t) + \gamma_z^2 z_c(t) = 0, \quad z_c(0) = z_0, \quad \dot{z}_c(0) = 0. \quad (5.42)$$

We note that the above ODE system (5.39)-(5.41) can be solved analytically [28].

6. Numerical methods for rotational BEC. In this section, we first present efficient and accurate numerical methods for computing ground states, as well as the central vortex states (5.17) of rotating BEC modeled by the GPE with an angular momentum term (5.7). To compute the dynamics of rotating BEC based on GPE (5.7), there are new difficulties due to the angular momentum term L_z in (5.7). We will show how to design efficient numerical methods for simulating the dynamics of the rotational GPE (5.7). In most cases, we consider the potential $V(\mathbf{x})$ given as (5.8) if no further clarification.

6.1. Computing ground states. In order to find the ground state for rotational GPE (5.7), we need to solve the minimization problem (5.14). Analogous to the non-rotating case (cf. section 3), we adopt the gradient flow with discrete normalization (GFDN) method (or imaginary time method) [45].

$$\phi_t = -\frac{\delta E_{\beta, \Omega}(\phi)}{\delta \bar{\phi}} = \frac{1}{2} \nabla^2 \phi - V(\mathbf{x})\phi - \beta |\phi|^2 \phi + \Omega L_z \phi, \quad t_n < t < t_{n+1}, \quad (6.1)$$

$$\phi(\mathbf{x}, t_{n+1}) \triangleq \phi(\mathbf{x}, t_{n+1}^\pm) = \frac{\phi(\mathbf{x}, t_{n+1}^-)}{\|\phi(\cdot, t_{n+1}^-)\|_2}, \quad \mathbf{x} \in \mathbb{R}^d, \quad d = 2, 3, \quad n \geq 0, \quad (6.2)$$

$$\phi(\mathbf{x}, 0) = \phi_0(\mathbf{x}), \quad \mathbf{x} \in \mathbb{R}^d \quad \text{with} \quad \|\phi_0\|_2 = 1; \quad (6.3)$$

where $0 = t_0 < t_1 < t_2 < \dots < t_n < \dots$ with $\tau_n = t_{n+1} - t_n > 0$ and $\tau = \max_{n \geq 0} \tau_n$, and $\phi(\mathbf{x}, t_n^\pm) = \lim_{t \rightarrow t_n^\pm} \phi(\mathbf{x}, t)$. As stated in section 3, the gradient flow (6.1) can be viewed as applying the steepest descent method to the energy functional $E_{\beta, \Omega}(\phi)$ (5.9) without constraint and (6.2) then projects the solution back to the unit sphere in order to satisfy the constraint (5.12).

In non-rotating BEC, i.e. $\Omega = 0$, the unique real valued nonnegative ground state solution $\phi_g(\mathbf{x}) \geq 0$ for all $\mathbf{x} \in \mathbb{R}^d$ is obtained by choosing a positive initial

datum $\phi_0(\mathbf{x}) \geq 0$ for $\mathbf{x} \in \mathbb{R}^d$, e.g., the ground state solution of linear Schrödinger equation with a harmonic oscillator potential [15, 27]. For rotating BEC, e.g., $|\Omega| < \min\{\gamma_x, \gamma_y\}$, our numerical experiences suggest that the initial data can be chosen as a linear combination of the ground state and central vortex ground state with index $m = 1$ of (5.7) when $\beta = 0$ and $\Omega = 0$, which are given explicitly in section 6.5.

6.1.1. *Backward Euler finite difference method.* In order to derive a full discretization of the GFDN (6.1)-(6.3), we first truncate the physical domain of the problem to a rectangle in 2D or a box in 3D with homogeneous Dirichlet boundary condition, and then apply backward Euler for time discretization and second-order centered finite difference for spatial derivatives. The backward Euler finite difference method is similar to the BEFD discretization for non-rotating BEC in section 3.2 and we omit the details here for brevity [45].

6.1.2. *Backward Euler Fourier pseudospectral method.* Computing the ground state of rotating BEC is a very challenging problem, especially for fast rotational speed Ω close to $\min\{\gamma_x, \gamma_y\}$, where many vortices exist in the ground state. In order to achieve high resolution for the vortex structure, a very fine mesh must be used if BEFD is used for discretizing the GFDN (6.1)-(6.3), when Ω is large. Here, we propose a Fourier pseudospectral discretization in space for the GFDN (6.1)-(6.3) to maintain the accuracy for high rotational speed Ω with less computational cost.

We first truncate the problem (6.1)-(6.3) in 2D on a rectangle $U = [a, b] \times [c, d]$, and resp. in 3D on a box $U = [a, b] \times [c, d] \times [e, f]$ with homogeneous Dirichlet boundary condition:

$$\phi_t = \left[\frac{1}{2} \nabla^2 - V(\mathbf{x}) - \beta |\phi|^2 + \Omega L_z \right] \phi, \quad t_n < t < t_{n+1}, \quad \mathbf{x} \in U, \quad (6.4)$$

$$\phi(\mathbf{x}, t_{n+1}) \stackrel{\Delta}{=} \phi(\mathbf{x}, t_{n+1}^+) = \frac{\phi(\mathbf{x}, t_{n+1}^-)}{\|\phi(\cdot, t_{n+1}^-)\|_{L^2(U)}}, \quad \mathbf{x} \in U, \quad n \geq 0, \quad (6.5)$$

$$\phi(\mathbf{x}, \cdot)|_{\partial U} = 0, \quad \phi(\mathbf{x}, 0) = \phi_0(\mathbf{x}), \quad \mathbf{x} \in U \quad \text{with} \quad \|\phi_0\|_{L^2(U)} = 1; \quad (6.6)$$

where $\phi(\mathbf{x}, t_n^\pm) = \lim_{t \rightarrow t_n^\pm} \phi(\mathbf{x}, t)$.

For the simplicity of notation, we only present the methods in 2D. Generalizations to $d = 3$ are straightforward for tensor product grids and the results remain valid without modifications. Choose mesh sizes $\Delta x := \frac{b-a}{M}$ and $\Delta y := \frac{d-c}{N}$ with M and N two even positive integers and denote the grid points as

$$x_j := a + j \Delta x, \quad j = 0, 1, \dots, M; \quad y_k := c + k \Delta y, \quad k = 0, 1, \dots, N. \quad (6.7)$$

Define the index sets

$$\begin{aligned} \mathcal{T}_{MN} &= \{(j, k) \mid j = 1, 2, \dots, M-1, k = 1, 2, \dots, N-1\}, \\ \mathcal{T}_{MN}^0 &= \{(j, k) \mid j = 0, 1, 2, \dots, M, k = 0, 1, 2, \dots, N\}. \end{aligned}$$

Let ϕ_{jk}^n be the numerical approximation of the solution $\phi(x_j, y_k, t_n)$ of the GFDN (6.4)-(6.6) for $(j, k) \in \mathcal{T}_{MN}^0$ and $n \geq 0$, and denote $\phi^n \in \mathbb{C}^{(M+1) \times (N+1)}$ to be the numerical approximate solution at time $t = t_n$. Define

$$\lambda_p^x = \frac{2p\pi}{b-a}, \quad \lambda_q^y = \frac{2q\pi}{d-c}, \quad p = -\frac{M}{2}, \dots, \frac{M}{2} - 1, \quad q = -\frac{N}{2}, \dots, \frac{N}{2} - 1. \quad (6.8)$$

Then the backward Euler Fourier pseudospectral (BEFP) discretization for solving GFDN (6.4)-(6.6) reads as [26, 45, 191]

$$\frac{\phi_{jk}^{(1)} - \phi_{jk}^n}{\tau} = \frac{1}{2} \nabla_s^2 \phi^{(1)} \Big|_{jk} + i\Omega \left(y \partial_x^s \phi^{(1)} - x \partial_y^s \phi^{(1)} \right) \Big|_{jk} - [\beta |\phi_{jk}^n|^2 + V_{jk}] \phi_{jk}^{(1)}, \quad (6.9)$$

$$\phi_{jk}^{n+1} = \frac{\phi_{jk}^{(1)}}{\|\phi_{jk}^{(1)}\|_2}, \quad \phi_{jk}^0 = \phi_0(x_j, y_k), \quad (j, k) \in \mathcal{T}_{MN}^0, \quad (6.10)$$

where $V_{jk} = V(x_j, y_k)$ for $(j, k) \in \mathcal{T}_{MN}^0$, $\|\phi^{(1)}\|_2$ denotes the discrete l^2 norm given by $\|\phi^{(1)}\|_2^2 = \Delta x \Delta y \sum_{j=0}^{M-1} \sum_{k=0}^{N-1} |\phi_{jk}^{(1)}|^2$, and ∇_s^2 , ∂_x^s and ∂_y^s are the Fourier pseudospectral approximations of ∇^2 , ∂_x and ∂_y , respectively, which can be written as

$$(\nabla_s^2 \phi)_{jk} = \frac{-1}{MN} \sum_{p=-M/2}^{M/2-1} \sum_{q=-N/2}^{N/2-1} [(\lambda_p^x)^2 + (\lambda_q^y)^2] \widehat{\phi}_{pq} e^{i\lambda_p^x(x_j-a)} e^{i\lambda_q^y(y_k-c)}, \quad (6.11)$$

$$(\partial_x^s \phi)_{jk} = \frac{i}{MN} \sum_{p=-M/2}^{M/2-1} \sum_{q=-N/2}^{N/2-1} \lambda_p^x \widehat{\phi}_{pq} e^{i\lambda_p^x(x_j-a)} e^{i\lambda_q^y(y_k-c)}, \quad (6.12)$$

$$(\partial_y^s \phi)_{jk} = \frac{i}{MN} \sum_{p=-M/2}^{M/2-1} \sum_{q=-N/2}^{N/2-1} \lambda_q^y \widehat{\phi}_{pq} e^{i\lambda_p^x(x_j-a)} e^{i\lambda_q^y(y_k-c)}, \quad (6.13)$$

for $-M/2 \leq p \leq M/2 - 1$, $-N/2 \leq q \leq N/2 - 1$. Here $\widehat{\phi}_{pq}$ denotes the Fourier coefficients of mesh function ϕ_{jk} as

$$\widehat{\phi}_{pq} = \sum_{j=0}^{M-1} \sum_{k=0}^{N-1} \phi_{jk} e^{-i\frac{2jp\pi}{M}} e^{-i\frac{2kq\pi}{N}} = \sum_{j=0}^{M-1} \sum_{k=0}^{N-1} \phi_{jk} e^{-i\lambda_p^x(x_j-a)} e^{-i\lambda_q^y(y_k-c)}. \quad (6.14)$$

Similar to those in section 3.3, at every time step, we can design an iterative method to solve the linear system (6.9) for $\phi^{(1)}$ via discrete Fourier transform with a stabilization term. We omit the details here for brevity.

Remark 6.1. For large Ω , there exists many local minimums for the energy (5.9). To calculate the energy accurately, when the pseudospectral discretization BEFP (6.9) is used, the terms involving derivatives in energy (5.9) should use the pseudospectral approximations like (6.11)-(6.13). For a numerical approximation ϕ_{jk}^n given by the BEFP (6.9), the discretized energy $E_{\beta, \Omega}^h(\phi^n)$ can be computed as

$$\begin{aligned} E_{\beta, \Omega}^h(\phi^n) = & \Delta x \Delta y \sum_{j=0}^{M-1} \sum_{k=0}^{N-1} \left[\frac{1}{2} |(\partial_x^s \phi^n)_{jk}|^2 + \frac{1}{2} |(\partial_y^s \phi^n)_{jk}|^2 + V(x_j, y_k) |\phi_{jk}^n|^2 \right. \\ & \left. + i\Omega (x_j (\partial_y^s \phi^n)_{jk} - y_k (\partial_x^s \phi^n)_{jk}) \overline{\phi}_{jk}^n + \frac{\beta}{2} |\phi_{jk}^n|^2 \right]. \end{aligned} \quad (6.15)$$

6.2. Central vortex states with polar/cylindrical symmetry. As shown in Theorem 5.4, if the potential is radially symmetric, the ground state density of a rotating BEC may be no longer radially symmetric. Thus, those simplified finite difference methods for computing ground states of non-rotating BEC with radially

symmetric or cylindrically symmetric potentials in section 3.4 can not be directly used for computing ground states of rotational GPE (5.7).

For central vortex state (5.17) and central vortex line state (5.20), when potential V is radially symmetric in 2D or cylindrically symmetric in 3D, finding the central vortex state (5.17) in 2D or the central line vortex state (5.20) in 3D, is almost the same as computing the radially symmetric (2D) or cylindrically symmetric (3D) ground states in section 3.4. Simplified backward Euler finite difference method can be directly used here.

6.2.1. *Formulation of the problem with cylindrical symmetry.* When we consider the harmonic potential $V(\mathbf{x})$ (5.8), the polar and cylindrical symmetries lead to new efficient and accurate numerical methods. Since angular momentum rotation does not affect the central vortex states, here we will only consider the GPE (5.7) with $\Omega = 0$. In particular, for 3D, we consider GPE

$$i \frac{\partial}{\partial t} \psi = \left[-\frac{1}{2} \left(\frac{\partial^2}{\partial x^2} + \frac{\partial^2}{\partial y^2} + \frac{\partial^2}{\partial z^2} \right) + V(x, y, z) + \beta |\psi|^2 \right] \psi, \quad (6.16)$$

where $V(\mathbf{x}) = \frac{1}{2}(\gamma_r^2(x^2 + y^2) + \gamma_z^2 z^2) + W(z)$, and $\psi := \psi(x, y, z, t)$ is the normalized wave function of the condensate with

$$\|\psi(x, y, z, t)\|_2^2 = \int_{\mathbb{R}^3} |\psi(x, y, z, t)|^2 dx dy dz = 1. \quad (6.17)$$

To find cylindrically symmetric states ($m = 0$) and central vortex line states with index or winding number m ($m \neq 0$) for the BEC, we write [46]

$$\psi(x, y, z, t) = e^{-i\mu_m t} \phi_m(x, y, z) = e^{-i\mu_m t} \phi_m(r, z) e^{im\theta}, \quad (6.18)$$

where (r, θ, z) is the cylindrical coordinates, μ_m is the chemical potential, $\phi_m = \phi_m(r, z)$ is a function independent of time t and angle θ . Denote

$$B_m^r \phi := \frac{1}{2} \left[-\frac{1}{r} \frac{\partial}{\partial r} \left(r \frac{\partial}{\partial r} \right) + \gamma_r^2 r^2 + \frac{m^2}{r^2} \right] \phi, \quad B^z \phi := \frac{1}{2} \left[-\frac{\partial^2}{\partial z^2} + \gamma_z^2 z^2 \right] \phi, \quad (6.19)$$

$$B_m := B_m^r + B^z.$$

Plugging (6.18) into the GPE (6.16) and the normalization condition (6.17), we obtain (see [41, 46–48] for more details)

$$\mu_m \phi_m = [B_m + W(z) + \beta |\phi_m|^2] \phi_m, \quad (r, z) \in (0, +\infty) \times (-\infty, +\infty), \quad (6.20)$$

$$\phi_m(0, z) = 0 \quad (\text{for } m \neq 0), \quad -\infty < z < \infty, \quad (6.21)$$

$$\lim_{r \rightarrow \infty} \phi_m(r, z) = 0, \quad -\infty < z < \infty, \quad \lim_{|z| \rightarrow \infty} \phi_m(r, z) = 0, \quad 0 \leq r < \infty, \quad (6.22)$$

under the normalization condition

$$\|\phi_m\|_c^2 = 2\pi \int_0^\infty \int_{-\infty}^\infty |\phi_m(r, z)|^2 r dz dr = 1. \quad (6.23)$$

From a mathematical point of view, the symmetric states ($m = 0$) and central vortex line states with index m ($m \neq 0$) of the BEC are defined as the minimizer of the nonconvex minimization problem (5.21).

To compute the symmetric states and central vortex line states of BEC, we use the gradient flow with discrete normalization (GFDN) method [41]:

$$\frac{\partial}{\partial t} \phi(r, z, t) = -B_m \phi - [W(z) + \beta |\phi|^2] \phi, \quad t_n \leq t < t_{n+1}, \quad n \geq 0, \quad (6.24)$$

$$\phi(0, z, t) = 0 \quad (\text{for } m \neq 0), \quad z \in \mathbb{R}, \quad t \geq 0, \quad (6.25)$$

$$\lim_{r \rightarrow \infty} \phi(r, z, t) = 0, \quad z \in \mathbb{R}, \quad \lim_{|z| \rightarrow \infty} \phi(r, z, t) = 0, \quad r \in \mathbb{R}^+ = (0, \infty), \quad (6.26)$$

$$\phi(r, z, t_{n+1}) := \phi(r, z, t_{n+1}^+) = \frac{\phi(r, z, t_{n+1}^-)}{\|\phi(\cdot, t_{n+1}^-)\|_c}, \quad (6.27)$$

$$\phi(r, z, 0) = \phi_0(r, z), \quad \text{with} \quad \|\phi_0(\cdot)\|_c = 1; \quad (6.28)$$

where $0 = t_0 < t_1 < \dots$, $\|\phi(\cdot)\|_c^2 = 2\pi \int_0^\infty \int_{-\infty}^\infty |\phi(r, z)|^2 r \, dz dr$, and $\phi(r, z, t_n^\pm) = \lim_{t \rightarrow t_n^\pm} \phi(r, z, t)$.

For the time discretization of (6.24)-(6.28), we adopt the following backward Euler scheme with projection:

Given ϕ^0 , find $\tilde{\phi}^{n+1}$ and ϕ_{MN}^{n+1} such that

$$\frac{\tilde{\phi}^{n+1}(r, z) - \phi^n(r, z)}{\tau} = -B_m \tilde{\phi}^{n+1} - (W(z) + \beta |\phi^n|^2) \tilde{\phi}^{n+1}, \quad (6.29)$$

$$\phi^{n+1}(r, z) = \frac{\tilde{\phi}^{n+1}(r, z)}{\|\tilde{\phi}^{n+1}\|_c}. \quad (6.30)$$

For $\beta = 0$, it is shown in section 3 (cf. [27]) that the scheme (6.29) is energy diminishing. However, (6.29) involves non-constant coefficients so it can not be solved by a direct fast spectral solver. Therefore, we propose to solve (6.29) iteratively (for $p = 0, 1, 2, \dots$) by introducing a stabilization term with constant coefficient (cf. section 3.3)

$$\frac{\tilde{\phi}^{n+1,p+1} - \phi^n}{\tau} = -(B_m + \alpha_n) \tilde{\phi}^{n+1,p+1} + (\alpha_n - W(z) - \beta |\phi^n|^2) \tilde{\phi}^{n+1,p}, \quad (6.31)$$

$$\tilde{\phi}^{n+1,0} = \phi^n, \quad \tilde{\phi}^{n+1} = \lim_{p \rightarrow \infty} \tilde{\phi}^{n+1,p}, \quad \phi^{n+1} = \frac{\tilde{\phi}^{n+1}}{\|\tilde{\phi}^{n+1}\|_c}. \quad (6.32)$$

The stabilization factor α_n is chosen such that the convergence of the iteration is ‘optimal’ and α_n should be chosen as (cf. section 3.3 and [25]) $\alpha_n = \frac{1}{2} (b_{\min}^n + b_{\max}^n)$ with

$$b_{\min}^n = \min_{(r,z) \in \mathbb{R}^+ \times \mathbb{R}} [W(z) + \beta |\phi^n(r, z)|^2], \quad b_{\max}^n = \max_{(r,z) \in \mathbb{R}^+ \times \mathbb{R}} [W(z) + \beta |\phi^n(r, z)|^2].$$

6.2.2. Eigenfunctions of B_m . The numerical scheme for (6.24)-(6.28) requires solving, repeatedly, (6.31). Therefore, it is most convenient to use eigenfunctions of B_m as basis functions. Thanks to (6.19), we only need to find eigenfunctions of B_m^r and B^z . We shall construct these eigenfunctions by properly scaling the Hermite polynomials and generalized Laguerre polynomials.

We start with B^z . Let $H_l(z)$ ($l = 0, 1, 2, \dots$) be the standard Hermite polynomials of degree l satisfying [35, 40, 41]

$$H_l''(z) - 2z H_l'(z) + 2l H_l(z) = 0, \quad z \in \mathbb{R}, \quad l = 0, 1, 2, \dots, \quad (6.33)$$

$$\int_{-\infty}^{\infty} H_l(z) H_{l'}(z) e^{-z^2} dz = \sqrt{\pi} 2^l l! \delta_{ll'}, \quad l, l' = 0, 1, 2, \dots, \quad (6.34)$$

where $\delta_{ll'}$ is the Kronecker delta.

Define the scaled Hermite functions

$$h_l(z) = e^{-\gamma_z z^2/2} H_l(\sqrt{\gamma_z} z) / \sqrt{2^l l! (\gamma_z/\pi)^{1/4}}, \quad z \in \mathbb{R}. \quad (6.35)$$

It is clear that $\lim_{|z| \rightarrow \infty} h_l(z) = 0$.

Plugging (6.35) into (6.33) and (6.34), a simple computation shows

$$B^z h_l(z) = -\frac{1}{2} h_l''(z) + \frac{1}{2} \gamma_z^2 z^2 h_l(z) = \left(l + \frac{1}{2}\right) \gamma_z h_l(z), \quad z \in \mathbb{R}, \quad l \geq 0, \quad (6.36)$$

$$\int_{-\infty}^{\infty} h_l(z) h_{l'}(z) dz = \delta_{ll'}, \quad l, l' = 0, 1, 2, \dots \quad (6.37)$$

Hence $\{h_l\}_{l=0}^{\infty}$ are eigenfunctions of the linear operator B^z in (6.19).

We now consider B_m^r . To this end, we recall the definition for the generalized Laguerre polynomials.

For any fixed m ($m = 0, 1, 2, \dots$), let $\hat{L}_k^m(r)$ ($k = 0, 1, 2, \dots$) be the the generalized-Laguerre polynomials of degree k satisfying [174]

$$\left(r \frac{d^2}{dr^2} + (m+1-r) \frac{d}{dr}\right) \hat{L}_k^m(r) + k \hat{L}_k^m(r) = 0, \quad k = 0, 1, 2, \dots, \quad (6.38)$$

$$\int_0^{\infty} r^m e^{-r} \hat{L}_k^m(r) \hat{L}_{k'}^m(r) dr = C_k^m \delta_{kk'}, \quad k, k' = 0, 1, 2, \dots, \quad (6.39)$$

where

$$C_k^m = \Gamma(m+1) \binom{k+m}{k} = \prod_{j=1}^m (k+j), \quad k = 0, 1, 2, \dots$$

We define the scaled generalized-Laguerre functions L_k^m by

$$L_k^m(r) = \frac{\gamma_r^{(m+1)/2}}{\sqrt{\pi C_k^m}} r^m e^{-\gamma_r r^2/2} \hat{L}_k^m(\gamma_r r^2). \quad (6.40)$$

Plugging (6.40) into (6.38) and (6.39), direct computation leads to

$$B_m^r L_k^m(r) = \gamma_r (2k + m + 1) L_k^m(r), \quad (6.41)$$

$$2\pi \int_0^{\infty} L_k^m(r) L_{k'}^m(r) r dr = \delta_{kk'}. \quad (6.42)$$

Hence $\{L_k^m\}_{k=0}^{\infty}$ are eigenfunctions of B_m^r .

Finally we derive from the above that [35, 40, 41]

$$B_m(L_k^m(r) h_l(z)) = h_l(z) B_m^r L_k^m(r) + L_k^m(r) B^z h_l(z) \quad (6.43)$$

$$\begin{aligned} &= \gamma_r (2k + m + 1) L_k^m(r) h_l(z) + \gamma_z \left(l + \frac{1}{2}\right) L_k^m(r) h_l(z) \\ &= \left[\gamma_r (2k + m + 1) + \gamma_z \left(l + \frac{1}{2}\right)\right] L_k^m(r) h_l(z). \end{aligned} \quad (6.44)$$

Hence, $\{L_k^m(r) h_l(z)\}_{k,l=0}^{\infty}$ are eigenfunctions of the operator B_m defined in (6.19).

6.2.3. *Interpolation operators.* In order to efficiently deal with the term $|\phi^n|^2 \tilde{\phi}^{n+1,p}$ in (6.31), a proper interpolation operator should be used. We shall define below scaled interpolation operators in both r, z directions and in the (r, z) space.

Let $\{\hat{z}_s\}_{s=0}^N$ be the Hermite-Gauss points, i.e., they are the $N+1$ roots of the Hermite polynomial $H_{N+1}(z)$, and let $\{\hat{\omega}_s^z\}_{s=0}^N$ be the associated Hermite-Gauss quadrature weights [174]. We have

$$\sum_{s=0}^N \hat{\omega}_s^z \frac{H_l(\hat{z}_s)}{\pi^{1/4} \sqrt{2^l l!}} \frac{H_{l'}(\hat{z}_s)}{\pi^{1/4} \sqrt{2^{l'} l'!}} = \delta_{ll'}, \quad l, l' = 0, 1, \dots, N. \quad (6.45)$$

We then define the scaled Hermite-Gauss points and weights by

$$z_s = \frac{\hat{z}_s}{\sqrt{\gamma_z}}, \quad \omega_s^z = \frac{\hat{\omega}_s^z e^{\hat{z}_s^2}}{\sqrt{\gamma_z}}, \quad s = 0, 1, 2, \dots, N. \quad (6.46)$$

We derive from (6.35) and (6.45) that

$$\sum_{s=0}^N \omega_s^z h_l(z_s) h_{l'}(z_s) = \delta_{ll'}, \quad l, l' = 0, 1, \dots, N. \quad (6.47)$$

Let us denote

$$Y_N^h = \text{span}\{h_k : k = 0, 1, \dots, N\}. \quad (6.48)$$

We define

$$I_N^z : C(\mathbb{R}) \rightarrow Y_N^h \text{ such that } (I_N^z f)(z_s) = f(z_s), 0 \leq s \leq N, \forall f \in C(\mathbb{R}). \quad (6.49)$$

Now, let $\{\hat{r}_j^m\}_{j=0}^M$ be the generalized-Laguerre-Gauss points [41, 163, 174]; i.e. they are the $M+1$ roots of the polynomial $\hat{L}_{M+1}^m(r)$, and let $\{\hat{\omega}_j^m\}_{j=0}^M$ be the weights associated with the generalized-Laguerre-Gauss quadrature [41, 163, 174]. Then, we have

$$\sum_{j=0}^M \hat{\omega}_j^m \frac{\hat{L}_k^m(\hat{r}_j^m)}{\sqrt{C_k^m}} \frac{\hat{L}_{k'}^m(\hat{r}_j^m)}{\sqrt{C_{k'}^m}} = \delta_{kk'}, \quad k, k' = 0, 1, \dots, M. \quad (6.50)$$

We then define the scaled generalized-Laguerre-Gauss points and weights by

$$r_j^m = \sqrt{\frac{\hat{r}_j^m}{\gamma_r}}, \quad \omega_j^m = \frac{\pi \hat{\omega}_j^m e^{\hat{r}_j^m}}{\gamma_r (\hat{r}_j^m)^m}, \quad j = 0, 1, \dots, M. \quad (6.51)$$

We derive from (6.40) and (6.50) that

$$\begin{aligned} \sum_{j=0}^M \omega_j^m L_k^m(r_j^m) L_{k'}^m(r_j^m) &= \sum_{j=0}^M \frac{\pi \hat{\omega}_j^m e^{\hat{r}_j^m}}{\gamma_r (\hat{r}_j^m)^m} L_k^m\left(\sqrt{\hat{r}_j^m/\gamma_r}\right) L_{k'}^m\left(\sqrt{\hat{r}_j^m/\gamma_r}\right) \\ &= \sum_{j=0}^M \hat{\omega}_j^m \frac{\hat{L}_k^m(\hat{r}_j^m)}{\sqrt{C_k^m}} \frac{\hat{L}_{k'}^m(\hat{r}_j^m)}{\sqrt{C_{k'}^m}} \\ &= \delta_{kk'}, \quad k, k' = 0, 1, \dots, M. \end{aligned} \quad (6.52)$$

Let us denote

$$X_M^m = \text{span}\{L_k^m : k = 0, 1, \dots, M\}. \quad (6.53)$$

We define

$$I_M^m : C(\overline{\mathbb{R}}_+) \rightarrow X_M^m \text{ such that } (I_M^m f)(r_j^m) = f(r_j^m), 0 \leq j \leq M, \forall f \in C(\overline{\mathbb{R}}_+). \quad (6.54)$$

Finally, let

$$X_{MN}^m = \text{span}\{L_k^m(r)h_l(z) : k = 0, 1, 2, \dots, M, l = 0, 1, 2, \dots, N\}. \quad (6.55)$$

we define $I_{MN}^m : C(\overline{\mathbb{R}}_+ \times \mathbb{R}) \rightarrow X_{MN}^m$ such that

$$(I_{MN}^m f)(r_j^m, z_s) = f(r_j^m, z_s), \quad j = 0, 1, \dots, M, \quad s = 0, 1, \dots, N, \quad \forall f \in C(\overline{\mathbb{R}}_+ \times \mathbb{R}). \quad (6.56)$$

It is clear that $I_{MN}^m = I_M^m \circ I_N^z$.

Note that the computation of the weights $\{\omega_j^m, \omega_s^z\}$ from (6.51) and (6.46) is not a stable process for large m, M and N . However, they can be computed in a stable way as suggested in the Appendix of [163].

6.2.4. A Hermite pseudospectral method in 1D. In this section, we introduce a Hermite pseudospectral method for computing ground states of 1D BEC. In fact, when $\gamma_r \gg \gamma_z$ in (6.16), the 3D GPE (6.16) can be approximated by a 1D GPE (cf. section 1.3.3). In this case, the stationary states satisfy

$$\mu \phi = \left[-\frac{1}{2} \frac{\partial^2}{\partial z^2} + \frac{1}{2} \gamma_z^2 z^2 + W(z) + \beta |\phi|^2 \right] \phi, \quad (6.57)$$

under the normalization condition

$$\|\phi\|_2^2 = \int_{-\infty}^{\infty} |\phi(z)|^2 dz = 1, \quad (6.58)$$

where $\phi = \phi(z)$. The stationary states can be viewed as the Euler-Lagrange equations of the energy functional $E(\phi)$, defined as

$$E(\phi) = \int_{-\infty}^{\infty} \left[\frac{1}{2} |\partial_z \phi|^2 + \left(\frac{1}{2} \gamma_z^2 z^2 + W(z) \right) |\phi|^2 + \frac{\beta}{2} |\phi|^4 \right] dz, \quad (6.59)$$

under the constraint (6.58). Similarly, in this case, the normalized gradient flow (6.24)-(6.28) collapses to [35, 40, 41]

$$\frac{\partial}{\partial t} \phi(z, t) = -B^z \phi - W(z) \phi - \beta |\phi|^2 \phi, \quad (6.60)$$

$$\lim_{|z| \rightarrow \infty} \phi(z, t) = 0, \quad t \geq 0, \quad (6.61)$$

$$\phi(z, t_{n+1}) := \phi(z, t_{n+1}^+) = \frac{\phi(z, t_{n+1}^-)}{\|\phi(\cdot, t_{n+1}^-)\|_2}, \quad (6.62)$$

$$\phi(z, 0) = \phi_0(z), \quad z \in \mathbb{R} \quad \text{with} \quad \|\phi_0(\cdot)\|_2 = 1, \quad (6.63)$$

where $\phi(z, t_n^\pm) = \lim_{t \rightarrow t_n^\pm} \phi(z, t)$, $\|\phi(\cdot)\|_2^2 = \int_{-\infty}^{\infty} |\phi(z)|^2 dz$.

Similarly, the scheme (6.31) in this case becomes:

$$\frac{\tilde{\phi}^{n+1,p+1}(z) - \phi^n(z)}{\tau} = -(B^z + \alpha_n) \tilde{\phi}^{n+1,p+1} + (\alpha_n - W(z) - \beta |\phi^n|^2) \tilde{\phi}^{n+1,p}. \quad (6.64)$$

We now describe a pseudo-spectral method based on the scaled Hermite functions $\{h_l(z)\}$ for (6.64)-(6.32).

Let $(u, v)_{\mathbb{R}} = \int_{\mathbb{R}} u v dz$ and $\phi_N^0 \in Y_N^h$. For $n = 0, 1, \dots$, set $\tilde{\phi}_N^{n+1,0} = \phi_N^n$ and $\alpha_n = \frac{1}{2} (b_{\min}^n + b_{\max}^n)$ with

$$b_{\min}^n = \min_{-\infty < z < \infty} [W(z) + \beta |\phi_N^n(z)|^2], \quad b_{\max}^n = \max_{-\infty < z < \infty} [W(z) + \beta |\phi_N^n(z)|^2].$$

Then, the Hermite pseudospectral method for (6.64)-(6.32) is:

Find $\tilde{\phi}_N^{n+1,p+1} \in Y_N^h$ such that

$$\begin{aligned} & \left(\frac{\tilde{\phi}_N^{n+1,p+1} - \phi_N^n}{\tau} + (B^z + \alpha_n) \tilde{\phi}_N^{n+1,p+1}, h_l \right)_{\mathbb{R}} \\ & = \left(I_N^z [(\alpha_n - W - \beta|\phi_N^n|^2) \tilde{\phi}_N^{n+1,p}], h_l \right)_{\mathbb{R}}, \quad 0 \leq l \leq N, \quad p = 0, 1, \dots, \end{aligned} \quad (6.65)$$

$$\tilde{\phi}_N^{n+1} = \lim_{p \rightarrow \infty} \tilde{\phi}_N^{n+1,p}, \quad \phi_N^{n+1} = \frac{\tilde{\phi}_N^{n+1}}{\|\tilde{\phi}_N^{n+1}\|_2}.$$

We note that $\tilde{\phi}_N^{n+1,p+1}$ can be easily determined from (6.65) as follows:

We write the expansion

$$\tilde{\phi}_N^{n+1,p+1}(z) = \sum_{l=0}^N \hat{\phi}_l^{n+1,p+1} h_l(z), \quad \phi_N^n(z) = \sum_{l=0}^N \hat{\phi}_l^n h_l(z), \quad (6.66)$$

and

$$g^{n,p}(z) = I_N^z \left[(\alpha_n - W(z) - \beta|\phi_N^n(z)|^2) \tilde{\phi}_N^{n+1,p}(z) \right] = \sum_{l=0}^N \hat{g}_l^{n,p} h_l(z),$$

where the coefficients $\{\hat{g}_l^{n,p}\}_{l=0}^N$ can be computed from the known function values $\{g^{n,p}(z_s)\}_{s=0}^N$ through the discrete Hermite transform using (6.47), i.e.,

$$\hat{g}_l^{n,p} = \sum_{s=0}^N g^{n,p}(z_s) h_l(z_s) \omega_s^z. \quad (6.67)$$

Thanks to (6.36)-(6.37), we find from (6.65) that

$$\frac{\hat{\phi}_l^{n+1,p+1} - \hat{\phi}_l^n}{\tau} = - \left[\gamma_z \left(l + \frac{1}{2} \right) + \alpha_n \right] \hat{\phi}_l^{n+1,p+1} + \hat{g}_l^{n,p}, \quad l = 0, 1, \dots, N, \quad (6.68)$$

from which we derive

$$\hat{\phi}_l^{n+1,p+1} = \frac{\hat{\phi}_l^n + \tau \hat{g}_l^{n,p}}{1 + \tau \left[\alpha_n + \gamma_z \left(l + \frac{1}{2} \right) \right]}, \quad l = 0, 1, \dots, N. \quad (6.69)$$

Then, $\tilde{\phi}_N^{n+1}$ and ϕ_N^{n+1} can be determined from the second equation in (6.65).

6.2.5. *A generalized-Laguerre pseudospectral method in 2D.* We now consider the 2D BEC with radial symmetry. The physical motivation is that when $\gamma_z \gg \gamma_r$ in (6.16), the 3D GPE (6.16) can be approximated by a 2D GPE (cf. section 1.3.3). In this case, the radial symmetric state ($m = 0$) and central vortex state with index m ($m \neq 0$) satisfy

$$\mu_m \phi_m = \frac{1}{2} \left[-\frac{1}{r} \frac{\partial}{\partial r} \left(r \frac{\partial}{\partial r} \right) + \gamma_r^2 r^2 + \frac{m^2}{r^2} + 2\beta|\phi_m|^2 \right] \phi_m, \quad (6.70)$$

$$\phi_m(0) = 0 \quad (\text{for } m \neq 0), \quad \lim_{r \rightarrow \infty} \phi_m(r) = 0, \quad (6.71)$$

under the normalization condition

$$\|\phi_m\|_r^2 = 2\pi \int_0^\infty |\phi_m(r)|^2 r \, dr = 1, \quad (6.72)$$

where $\phi_m = \phi_m(r)$. Again, this nonlinear eigenvalue problem (6.70)-(6.72) can also be viewed as the Euler-Lagrange equations of the energy functional $E(\phi_m)$, defined by

$$E(\phi_m) = \pi \int_0^\infty \left[|\partial_r \phi_m|^2 + \left(\gamma_r^2 r^2 + \frac{m^2}{r^2} \right) |\phi_m|^2 + \beta |\phi_m|^4 \right] r dr, \quad (6.73)$$

under the constraint (6.72). Accordingly, the normalized gradient flow (6.24)-(6.28) collapses to [35, 40, 41]

$$\frac{\partial}{\partial t} \phi(r, t) = -B_m^r \phi - \beta |\phi|^2 \phi, \quad (6.74)$$

$$\phi(0, t) = 0 \quad (\text{for } m \neq 0), \quad \lim_{r \rightarrow \infty} \phi(r, t) = 0, \quad t \geq 0, \quad (6.75)$$

$$\phi(r, t_{n+1}) := \phi(r, t_{n+1}^+) = \frac{\phi(r, t_{n+1}^-)}{\|\phi(\cdot, t_{n+1}^-)\|_r}, \quad (6.76)$$

$$\phi(r, 0) = \phi_0(r), \quad 0 \leq r < \infty, \quad \text{with } \|\phi_0(\cdot)\|_r = 1, \quad (6.77)$$

where $\phi(r, t_n^\pm) = \lim_{t \rightarrow t_n^\pm} \phi(r, t)$, $\|\phi(\cdot)\|_r^2 = 2\pi \int_0^\infty |\phi(r)|^2 r dr$. The scheme (6.31) in this case becomes:

$$\frac{\tilde{\phi}^{n+1,p+1} - \phi^n(r)}{\tau} = -(B_m^r + \alpha_n) \tilde{\phi}^{n+1,p+1} + (\alpha_n - \beta |\phi^n|^2) \tilde{\phi}^{n+1,p}. \quad (6.78)$$

We now describe a pseudo-spectral method based on the scaled generalized-Laguerre functions $\{L_k^m(r)\}$ for (6.78)-(6.32).

Let $(u, v)_{r, \mathbb{R}^+} = \int_{\mathbb{R}^+} u v r dr$ and $\phi_M^0 \in X_M^m$. For $n = 0, 1, \dots$, set $\tilde{\phi}_M^{n+1,0} = \phi_M^n$ and $\alpha_n = \frac{1}{2} (b_{\min}^n + b_{\max}^n)$ with

$$b_{\min}^n = \min_{0 \leq r < \infty} [\beta |\phi_M^n(r)|^2], \quad b_{\max}^n = \max_{0 \leq r < \infty} [\beta |\phi_M^n(r)|^2].$$

Then, the generalized-Laguerre pseudospectral method for (6.78)-(6.32) is:

Find $\tilde{\phi}_M^{n+1,p+1} \in X_M^m$ such that

$$\begin{aligned} & \left(\frac{\tilde{\phi}_M^{n+1,p+1} - \phi_M^n}{\tau} + (B_m^r + \alpha_n) \tilde{\phi}_M^{n+1,p+1}, L_k^m \right)_{r, \mathbb{R}^+} \\ & = \left(I_M^m [(\alpha_n - \beta |\phi_M^n|^2) \tilde{\phi}_M^{n+1,p}], L_k^m \right)_{r, \mathbb{R}^+}, \quad 0 \leq k \leq M, \quad p = 0, 1, \dots, \end{aligned} \quad (6.79)$$

$$\tilde{\phi}_M^{n+1} = \lim_{p \rightarrow \infty} \tilde{\phi}_M^{n+1,p}, \quad \phi_M^{n+1} = \frac{\tilde{\phi}_M^{n+1}}{\|\tilde{\phi}_M^{n+1}\|_r}.$$

The function $\tilde{\phi}_M^{n+1,p+1}$ can be easily determined from (6.79) as follows:

We write the expansion

$$\begin{aligned} \tilde{\phi}_M^{n+1,p+1}(r) &= \sum_{k=0}^M \hat{\phi}_k^{n+1,p+1} L_k^m(r), \quad \phi_M^n(r) = \sum_{k=0}^M \hat{\phi}_k^n L_k^m(r), \\ g^{n,p}(z) &= I_M^m \left[(\alpha_n - \beta |\phi_M^n(r)|^2) \tilde{\phi}_M^{n+1,p}(r) \right] = \sum_{k=0}^M \hat{g}_k^{n,p} L_k^m(r), \end{aligned} \quad (6.80)$$

where the coefficients $\{\hat{g}_k^{n,p}\}_{k=0}^M$ can be computed from the known function values $\{g^{n,p}(r_j^m)\}_{j=0}^M$ through the discrete generalized-Laguerre transform using (6.52),

i.e.,

$$\hat{g}_k^{n,p} = \sum_{j=0}^M g^{n,p}(r_j^m) L_k^m(r_j^m) \omega_j^r. \quad (6.81)$$

Thanks to (6.41)-(6.42), we find from (6.79) that

$$\frac{\hat{\phi}_k^{n+1,p+1} - \hat{\phi}_k^n}{\tau} = -[\gamma_r(2k+m+1) + \alpha_n] \hat{\phi}_k^{n+1,p+1} + \hat{g}_k^{n,p}, \quad k = 0, \dots, N, \quad (6.82)$$

from which we derive

$$\hat{\phi}_k^{n+1,p+1} = \frac{\hat{\phi}_k^n + \tau \hat{g}_k^{n,p}}{1 + \tau[\alpha_n + \gamma_r(2k+m+1)]}, \quad k = 0, 1, \dots, N. \quad (6.83)$$

Then, $\tilde{\phi}_M^{n+1}$ and ϕ_M^{n+1} can be determined from the second equation in (6.79).

6.2.6. A generalized-Laguerre-Hermite pseudospectral method in 3D. We are now in position to describe the generalized-Laguerre-Hermite pseudo-spectral method for computing symmetric and central vortex line states of 3D BEC with cylindrical symmetry [35, 40, 41].

Let $(u, v)_{r, \mathbb{R}^+ \times \mathbb{R}} = \int_{\mathbb{R}} \int_{\mathbb{R}^+} u v r dr dz$ and $\phi_{MN}^0 \in X_{MN}^m$. For $n = 0, 1, \dots$, set $\tilde{\phi}_{MN}^{n+1,0} = \phi_{MN}^n$ and $\alpha_n = \frac{1}{2}(b_{\min}^n + b_{\max}^n)$ with $U = \mathbb{R}^+ \times \mathbb{R}$,

$$b_{\min}^n = \min_{(r,z) \in U} [W(z) + \beta |\phi_{MN}^n(r, z)|^2], \quad b_{\max}^n = \max_{(r,z) \in U} [W(z) + \beta |\phi_{MN}^n(r, z)|^2].$$

Then, the generalized-Laguerre-Hermite pseudo-spectral method for (6.31)-(6.32) is: find $\tilde{\phi}_{MN}^{n+1,p+1} \in X_{MN}^m$ such that for $0 \leq k \leq M$, $0 \leq l \leq N$, $p = 0, 1, \dots$,

$$\begin{aligned} & \left(\frac{\tilde{\phi}_{MN}^{n+1,p+1} - \phi_{MN}^n}{\tau} + (B_m + \alpha_n) \tilde{\phi}_{MN}^{n+1,p+1}, L_k^m(r) h_l(z) \right)_{r, \mathbb{R}^+ \times \mathbb{R}} \\ &= \left(I_{MN}^m [(\alpha_n - W(z) - \beta |\phi_{MN}^n|^2) \tilde{\phi}_{MN}^{n+1,p}], L_k^m(r) h_l(z) \right)_{r, \mathbb{R}^+ \times \mathbb{R}}, \end{aligned} \quad (6.84)$$

$$\tilde{\phi}_{MN}^{n+1} = \lim_{p \rightarrow \infty} \tilde{\phi}_{MN}^{n+1,p}, \quad \phi_{MN}^{n+1} = \frac{\tilde{\phi}_{MN}^{n+1}}{\|\tilde{\phi}_{MN}^{n+1}\|_c}.$$

The function $\tilde{\phi}_{MN}^{n+1,p+1}$ can be easily determined from (6.84) as follows:

We write the expansion

$$\tilde{\phi}_{MN}^{n+1,p+1} = \sum_{k=0}^M \sum_{l=0}^N \hat{\phi}_{kl}^{n+1,p+1} L_k^m(r) h_l(z), \quad \phi_{MN}^n = \sum_{k=0}^M \sum_{l=0}^N \hat{\phi}_{kl}^n L_k^m(r) h_l(z), \quad (6.85)$$

and

$$g^{n,p}(r, z) = I_{MN}^m [(\alpha_n - W(z) - \beta |\phi_{MN}^n|^2) \tilde{\phi}_{MN}^{n+1,p}] = \sum_{k=0}^M \sum_{l=0}^N \hat{g}_{kl}^{n,p} L_k^m(r) h_l(z),$$

where the coefficients $\{\hat{g}_{kl}^{n,p}\}$ can be computed from the known function values $\{g^{n,p}(r_j^m, z_s)\}$ through the discrete generalized-Laguerre transform and discrete Hermite transform using (6.52) and (6.47), i.e.,

$$\hat{g}_{kl}^{n,p} = \sum_{s=0}^N \sum_{j=0}^M g^{n,p}(r_j^m, z_s) L_k^m(r_j^m) h_l(z_s) \omega_j^r \omega_s^z. \quad (6.86)$$

Thanks to (6.41)-(6.42) and (6.36)-(6.37), we find from (6.84) that

$$\frac{\hat{\phi}_{kl}^{n+1,p+1} - \hat{\phi}_{kl}^n}{\tau} = - \left[\gamma_r(2k+m+1)\gamma_z \left(l + \frac{1}{2} \right) + \alpha_n \right] \hat{\phi}_{kl}^{n+1,p+1} + \hat{g}_{kl}^{n,p}, \quad (6.87)$$

from which we derive

$$\hat{\phi}_{kl}^{n+1,p+1} = \frac{\hat{\phi}_{kl}^n + \tau \hat{g}_{kl}^{n,p}}{1 + \tau \left[\alpha_n + \gamma_r(2k+m+1) + \gamma_z \left(l + \frac{1}{2} \right) \right]}. \quad (6.88)$$

Then, $\tilde{\phi}_{MN}^{n+1}$ and ϕ_{MN}^{n+1} can be determined from the second equation in (6.84).

6.3. Numerical methods for dynamics. In this section, we consider different numerical methods for solving the GPE (5.5) with an angular momentum rotation term in d -dimensions ($d = 2, 3$) for the dynamics of rotating BEC:

$$i \frac{\partial \psi(\mathbf{x}, t)}{\partial t} = -\frac{1}{2} \nabla^2 \psi + V(\mathbf{x})\psi + \beta |\psi|^2 \psi - \Omega L_z \psi, \quad \mathbf{x} \in \mathbb{R}^d, \quad t > 0, \quad (6.89)$$

$$\psi(\mathbf{x}, 0) = \psi_0(\mathbf{x}), \quad \mathbf{x} \in \mathbb{R}^d, \quad \|\psi_0\|_2 = 1, \quad (6.90)$$

where $L_z = -i(x\partial_y - y\partial_x)$ and $V(\mathbf{x})$ in d dimensions is given in (5.8).

In fact, many efficient and accurate numerical methods have been proposed for discretizing the above GPE, such as the time-splitting Fourier pseudospectral method via the alternating direction implicit (ADI) to decouple the angular momentum rotation term [44], time-splitting finite element method based on polar and cylindrical coordinates in 2D and 3D, respectively, such that the angular momentum rotation term becomes constant coefficient [28], time-splitting generalized Laguerre-Hermite pseudospectral method via eigen-expansion of the linear operator [35], finite difference time domain methods [21], etc. Each method has its own advantages and disadvantages. Here we present the detailed algorithms for some of these methods.

6.3.1. Time splitting Fourier pseudospectral method via an ADI technique. Due to the external trapping potential $V(\mathbf{x})$, the solution $\psi(\mathbf{x}, t)$ of (6.89)-(6.90) decays to zero exponentially fast when $|\mathbf{x}| \rightarrow \infty$. Thus in practical computation, we can truncate the problem (6.89)-(6.90) into a bounded computational domain:

$$i \partial_t \psi(\mathbf{x}, t) = -\frac{1}{2} \nabla^2 \psi + [V(\mathbf{x}) + \beta |\psi|^2 - \Omega L_z] \psi, \quad \mathbf{x} \in U, \quad t > 0, \quad (6.91)$$

$$\psi(\mathbf{x}, 0) = \psi_0(\mathbf{x}), \quad \mathbf{x} \in U; \quad (6.92)$$

with periodic boundary condition. Here we choose $U = [a, b] \times [c, d]$ in 2D, and resp., $U = [a, b] \times [c, d] \times [e, f]$ in 3D, with $|a|$, $|b|$, $|c|$, $|d|$, $|e|$ and $|f|$ sufficiently large.

We choose a time step size $\tau > 0$. For $n = 0, 1, 2, \dots$, similar to the case of non-rotating GPE in section 4.1.1, from time $t = t_n = n\tau$ to $t = t_{n+1} = t_n + \tau$, the GPE (6.91) is solved in two splitting steps. One solves first [44]

$$i \partial_t \psi(\mathbf{x}, t) = -\frac{1}{2} \nabla^2 \psi(\mathbf{x}, t) - \Omega L_z \psi(\mathbf{x}, t) \quad (6.93)$$

for the time step of length τ , followed by solving

$$i \partial_t \psi(\mathbf{x}, t) = V(\mathbf{x})\psi(\mathbf{x}, t) + \beta |\psi(\mathbf{x}, t)|^2 \psi(\mathbf{x}, t), \quad (6.94)$$

for the same time step. (6.94) can be integrated exactly [28, 44], and we find for $\mathbf{x} \in U$ and $t_n \leq t \leq t_{n+1}$:

$$\psi(\mathbf{x}, t) = e^{-i[V(\mathbf{x}) + \beta|\psi(\mathbf{x}, t_n)|^2](t-t_n)} \psi(\mathbf{x}, t_n). \quad (6.95)$$

To discretize (6.93) in space, compared with non-rotating BEC (cf. section 4), i.e. $\Omega = 0$ in (6.89), the main difficulty is that the coefficients in L_z are *not* constants which causes big trouble in applying sine or Fourier pseudospectral discretization. Due to the special structure in the angular momentum rotation term L_z , we will apply the alternating direction implicit (ADI) technique and decouple the operator $-\frac{1}{2}\nabla^2 - \Omega L_z$ into two one dimensional operators such that each operator becomes a summation of terms with constant coefficients in that dimension. Therefore, they can be discretized in space by Fourier pseudospectral method and the ODEs in phase space can be integrated analytically.

Discretization in 2D. When $d = 2$ in (6.93), we choose mesh sizes $\Delta x > 0$ and $\Delta y > 0$ with $\Delta x = (b - a)/M$ and $\Delta y = (d - c)/N$ for M and N even positive integers, and let the grid points be

$$x_j = a + j\Delta x, \quad j = 0, 1, 2, \dots, M; \quad y_k = c + k\Delta y, \quad k = 0, 1, 2, \dots, N. \quad (6.96)$$

Let ψ_{jk}^n be the approximation of $\psi(x_j, y_k, t_n)$ and ψ^n be the solution vector with component ψ_{jk}^n .

From time $t = t_n$ to $t = t_{n+1}$, we solve (6.93) first

$$i \partial_t \psi(\mathbf{x}, t) = -\frac{1}{2} \partial_{xx} \psi(\mathbf{x}, t) - i\Omega y \partial_x \psi(\mathbf{x}, t), \quad (6.97)$$

for the time step of length τ , followed by solving

$$i \partial_t \psi(\mathbf{x}, t) = -\frac{1}{2} \partial_{yy} \psi(\mathbf{x}, t) + i\Omega x \partial_y \psi(\mathbf{x}, t), \quad (6.98)$$

for the same time step. Using the standard second order Strang splitting, a time splitting Fourier pseudospectral (TSSP) method for solving (6.91)-(6.92) can be written as [44]:

$$\begin{aligned} \psi_{jk}^{(1)} &= \sum_{p=-M/2}^{M/2-1} e^{-i\tau(\mu_p^2 + 2\Omega y_k \mu_p)/4} \widehat{(\psi_{jk}^n)}_p e^{i\mu_p(x_j - a)}, \quad (j, k) \in \mathcal{T}_{MN}^0, \\ \psi_{jk}^{(2)} &= \sum_{q=-N/2}^{N/2-1} e^{-i\tau(\lambda_q^2 - 2\Omega x_j \lambda_q)/4} \widehat{(\psi_j^{(1)})}_q e^{i\lambda_q(y_k - c)}, \quad (j, k) \in \mathcal{T}_{MN}^0, \\ \psi_{jk}^{(3)} &= e^{-i\tau[V(x_j, y_k) + \beta|\psi_{jk}^{(2)}|^2]} \psi_{jk}^{(2)}, \quad (j, k) \in \mathcal{T}_{MN}^0, \\ \psi_{jk}^{(4)} &= \sum_{q=-N/2}^{N/2-1} e^{-i\tau(\lambda_q^2 - 2\Omega x_j \lambda_q)/4} \widehat{(\psi_j^{(3)})}_q e^{i\lambda_q(y_k - c)}, \quad (j, k) \in \mathcal{T}_{MN}^0, \\ \psi_{jk}^{n+1} &= \sum_{p=-M/2}^{M/2-1} e^{-i\tau(\mu_p^2 + 2\Omega y_k \mu_p)/4} \widehat{(\psi_k^{(4)})}_p e^{i\mu_p(x_j - a)}, \quad (j, k) \in \mathcal{T}_{MN}^0, \end{aligned} \quad (6.99)$$

where for each fixed k , $(\widehat{\psi_k^\alpha})_p$ ($p = -\frac{M}{2}, \dots, \frac{M}{2} - 1$) with an index α , the Fourier coefficients of the vector $\psi_k^\alpha = (\psi_{0k}^\alpha, \psi_{1k}^\alpha, \dots, \psi_{(M-1)k}^\alpha)^T$, are defined as

$$(\widehat{\psi_k^\alpha})_p = \frac{1}{M} \sum_{j=0}^{M-1} \psi_{jk}^\alpha e^{-i\mu_p(x_j - a)}, \quad \mu_p = \frac{2p\pi}{b-a}, \quad p = -\frac{M}{2}, \dots, \frac{M}{2} - 1; \quad (6.100)$$

similarly, for each fixed j , $(\widehat{\psi_j^\alpha})_q$ ($q = -\frac{N}{2}, \dots, \frac{N}{2} - 1$), the Fourier coefficients of the vector $\psi_j^\alpha = (\psi_{j0}^\alpha, \psi_{j1}^\alpha, \dots, \psi_{j(N-1)}^\alpha)^T$, are defined as

$$(\widehat{\psi_j^\alpha})_q = \frac{1}{N} \sum_{k=0}^{N-1} \psi_{jk}^\alpha e^{-i\lambda_q(y_k - c)}, \quad \lambda_q = \frac{2q\pi}{d-c}, \quad q = -\frac{N}{2}, \dots, \frac{N}{2} - 1. \quad (6.101)$$

For the TSSP (6.99), the total memory requirement is $O(MN)$ and the total computational cost per time step is $O(MN \ln(MN))$. The scheme is time reversible just as it holds for the GPE (6.91), i.e. the scheme is unchanged if we interchange $n \leftrightarrow n+1$ and $\tau \leftrightarrow -\tau$ in (6.99). Also, a main advantage of the numerical method is its time-transverse invariance, just as it holds for the GPE (6.91) itself. If a constant α is added to the external potential V , then the discrete wave functions ψ_{jk}^{n+1} obtained from (6.99) get multiplied by the phase factor $e^{-i\alpha(n+1)\tau}$, which leaves the discrete quadratic observable $|\psi_{jk}^{n+1}|^2$ unchanged.

Discretization in 3D. When $d = 3$ in (6.93), we choose mesh sizes $\Delta x > 0$, $\Delta y > 0$ and $\Delta z > 0$ with $\Delta x = (b-a)/M$, $\Delta y = (d-c)/N$ and $\Delta z = (f-e)/L$ for even positive integers M , N and L , and let the grid points be

$$x_j = a + j\Delta x, \quad y_k = c + k\Delta y, \quad (j, k) \in \mathcal{T}_{MN}^0; \quad z_l = e + l\Delta z, \quad 0 \leq l \leq L. \quad (6.102)$$

Let ψ_{jkl}^n be the approximation of $\psi(x_j, y_k, z_l, t_n)$ and ψ^n be the solution vector with component ψ_{jkl}^n .

Similar as those for 2D case, from time $t = t_n$ to $t = t_{n+1}$, we solve (6.93) first

$$i \partial_t \psi(\mathbf{x}, t) = \left(-\frac{1}{2} \partial_{xx} - \frac{1}{4} \partial_{zz} - i\Omega y \partial_x \right) \psi(\mathbf{x}, t), \quad (6.103)$$

for the time step of length τ , followed by solving

$$i \partial_t \psi(\mathbf{x}, t) = \left(-\frac{1}{2} \partial_{yy} - \frac{1}{4} \partial_{zz} + i\Omega x \partial_y \right) \psi(\mathbf{x}, t), \quad (6.104)$$

for the same time step. A second order time splitting Fourier pseudospectral (TSSP) method for solving (6.91)-(6.92) can be written as [44]:

$$\begin{aligned}
 \psi_{jkl}^{(1)} &= \sum_{p=-M/2}^{M/2-1} \sum_{s=-L/2}^{L/2-1} e^{-i\tau(2\mu_p^2+\gamma_s^2+4\Omega y_k \mu_p)/8} \widehat{(\psi_k^n)}_{ps} e^{i\mu_p(x_j-a)} e^{i\gamma_s(z_l-e)}, \\
 \psi_{jkl}^{(2)} &= \sum_{q=-N/2}^{N/2-1} \sum_{s=-L/2}^{L/2-1} e^{-i\tau(2\lambda_q^2+\gamma_s^2-4\Omega x_j \lambda_q)/8} \widehat{(\psi_j^{(1)})}_{qs} e^{i\lambda_q(y_k-c)} e^{i\gamma_s(z_l-e)}, \\
 \psi_{jkl}^{(3)} &= e^{-i\tau[V(x_j, y_k, z_l) + \beta|\psi_{jkl}^{(2)}|^2]} \psi_{jkl}^{(2)}, \quad (j, k, l) \in \mathcal{T}_{MNL}^0, \\
 \psi_{jkl}^{(4)} &= \sum_{q=-N/2}^{N/2-1} \sum_{s=-L/2}^{L/2-1} e^{-i\tau(2\lambda_q^2+\gamma_s^2-4\Omega x_j \lambda_q)/8} \widehat{(\psi_j^{(3)})}_{qs} e^{i\lambda_q(y_k-c)} e^{i\gamma_s(z_l-e)}, \\
 \psi_{jkl}^{n+1} &= \sum_{p=-M/2}^{M/2-1} \sum_{s=-L/2}^{L/2-1} e^{-i\tau(2\mu_p^2+\gamma_s^2+4\Omega y_k \mu_p)/8} \widehat{(\psi_k^{(4)})}_{ps} e^{i\mu_p(x_j-a)} e^{i\gamma_s(z_l-e)},
 \end{aligned} \tag{6.105}$$

where

$$\mathcal{T}_{MNL}^0 = \{(j, k, l) \mid j = 0, 1, \dots, M, k = 0, 1, \dots, N, l = 0, 1, \dots, L\},$$

and for each fixed k , $\widehat{(\psi_k^\alpha)}_{ps}$ ($-M/2 \leq p \leq M/2 - 1$, $-L/2 \leq s \leq L/2 - 1$) with an index α , the Fourier coefficients of the vector ψ_{jkl}^α ($0 \leq j < M$, $0 \leq l < L$), are defined as

$$\widehat{(\psi_k^\alpha)}_{ps} = \frac{1}{ML} \sum_{j=0}^{M-1} \sum_{l=0}^{L-1} \psi_{jkl}^\alpha e^{-i\mu_p(x_j-a)} e^{-i\gamma_s(z_l-e)}, \quad -\frac{M}{2} \leq p < \frac{M}{2}, \quad -\frac{L}{2} \leq s < \frac{L}{2};$$

similarly, for each fixed j , $\widehat{(\psi_j^\alpha)}_{qs}$ ($-N/2 \leq q \leq N/2 - 1$, $-L/2 \leq s \leq L/2 - 1$) with an index α , the Fourier coefficients of the vector ψ_{jkl}^α ($k = 0, \dots, N$, $l = 0, \dots, L$), are defined as

$$\widehat{(\psi_j^\alpha)}_{qs} = \frac{1}{NL} \sum_{m=0}^{N-1} \sum_{l=0}^{L-1} \psi_{jml}^\alpha e^{-i\lambda_q(y_m-c)} e^{-i\gamma_s(z_l-e)}, \quad -\frac{N}{2} \leq q < \frac{N}{2}, \quad -\frac{L}{2} \leq s < \frac{L}{2},$$

with $\gamma_s = \frac{2\pi s}{f-e}$ for $s = -L/2, \dots, L/2 - 1$. For the scheme (6.105), the total memory requirement is $O(MNL)$ and the total computational cost per time step is $O(MNL \ln(MNL))$. Furthermore, the discretization is time reversible and time transverse invariant in the discretized level.

6.3.2. Time-splitting finite element method based on polar/cylindrical coordinates.

As noticed in [21, 28], the angular momentum rotation is a constant coefficient in 2D with polar coordinates and 3D with cylindrical coordinates. Thus the original problem of GPE with an angular momentum rotation term defined in \mathbb{R}^d ($d = 2, 3$) for rotating BEC can also be truncated on a disk in 2D and a cylinder in 3D as bounded computational domain with homogeneous Dirichlet boundary condition:

$$i\partial_t \psi(\mathbf{x}, t) = -\frac{1}{2} \nabla^2 \psi + [V(\mathbf{x}) + \beta|\psi|^2 - \Omega L_z] \psi, \quad \mathbf{x} \in U, \quad t > 0, \tag{6.106}$$

$$\psi(\mathbf{x}, t) = 0, \quad \mathbf{x} \in \Gamma = \partial U, \quad t \geq 0, \quad \psi(\mathbf{x}, 0) = \psi_0(\mathbf{x}), \quad \mathbf{x} \in U; \tag{6.107}$$

where we choose $U = \{\mathbf{x} = (x, y) \mid r = \sqrt{x^2 + y^2} < R\}$ in 2D, and resp., $U = \{\mathbf{x} = (x, y, z) \mid r = \sqrt{x^2 + y^2} < R, Z_1 < z < Z_2\}$ in 3D with $R, |Z_1|, |Z_2|$ sufficiently large.

We choose a time step size $\tau > 0$. For $n = 0, 1, 2, \dots$, from time $t = t_n = n\tau$ to $t = t_{n+1} = t_n + \tau$, the GPE (6.106) is solved in two splitting steps. One solves first

$$i \partial_t \psi(\mathbf{x}, t) = -\frac{1}{2} \nabla^2 \psi(\mathbf{x}, t) - \Omega L_z \psi(\mathbf{x}, t) \quad (6.108)$$

for the time step of length τ , followed by solving

$$i \partial_t \psi(\mathbf{x}, t) = V(\mathbf{x}) \psi(\mathbf{x}, t) + \beta |\psi(\mathbf{x}, t)|^2 \psi(\mathbf{x}, t), \quad (6.109)$$

for the same time step. (6.109) can be integrated exactly [44], and we find for $\mathbf{x} \in U$ and $t_n \leq t \leq t_{n+1}$:

$$\psi(\mathbf{x}, t) = e^{-i[V(\mathbf{x}) + \beta |\psi(\mathbf{x}, t_n)|^2](t - t_n)} \psi(\mathbf{x}, t_n). \quad (6.110)$$

Discretization in 2D. To solve (6.108), we try to formulate the equation in a variable separable form. When $d = 2$, we use the polar coordinate (r, θ) , and discretize in the θ -direction by a Fourier pseudo-spectral method, in the r -direction by a finite element method (FEM) and in time by a Crank-Nicolson (C-N) scheme. Assume [28]

$$\psi(r, \theta, t) = \sum_{l=-L/2}^{L/2-1} \widehat{\psi}_l(r, t) e^{il\theta}, \quad (6.111)$$

where L is an even positive integer and $\widehat{\psi}_l(r, t)$ is the Fourier coefficient for the l -th mode. Plugging (6.111) into (6.108), noticing the orthogonality of the Fourier functions, we obtain for $-\frac{L}{2} \leq l \leq \frac{L}{2} - 1$ and $0 < r < R$:

$$i \partial_t \widehat{\psi}_l(r, t) = -\frac{1}{2r} \frac{\partial}{\partial r} \left(r \frac{\partial \widehat{\psi}_l(r, t)}{\partial r} \right) + \left(\frac{l^2}{2r^2} - l\Omega \right) \widehat{\psi}_l(r, t), \quad (6.112)$$

$$\widehat{\psi}_l(R, t) = 0 \quad (\text{for all } l), \quad \widehat{\psi}_l(0, t) = 0 \quad (\text{for } l \neq 0). \quad (6.113)$$

Let P^k denote all polynomials with degree at most k , $M > 0$ be a chosen integer, $0 = r_0 < r_1 < r_2 < \dots < r_M = R$ be a partition for the interval $[0, R]$ with a mesh size $h = \max_{0 \leq m < M} \{r_{m+1} - r_m\}$. Define a FEM subspace by

$$U^h = \left\{ u^h \in C[0, R] \mid u^h|_{[r_m, r_{m+1}]} \in P^k, 0 \leq m < M, u^h(R) = 0 \right\}$$

for $l = 0$, and for $l \neq 0$,

$$U^h = \left\{ u^h \in C[0, R] \mid u^h|_{[r_m, r_{m+1}]} \in P^k, 0 \leq m < M, u^h(0) = u^h(R) = 0 \right\},$$

then we obtain the FEM approximation for (6.112)-(6.113): Find $\widehat{\psi}_l^h = \widehat{\psi}_l^h(\cdot, t) \in U^h$ such that for all $\phi^h \in U^h$ and $t_n \leq t \leq t_{n+1}$,

$$i \frac{d}{dt} A(\widehat{\psi}_l^h(\cdot, t), \phi^h) = B(\widehat{\psi}_l^h(\cdot, t), \phi^h) + l^2 C(\widehat{\psi}_l^h, \phi^h) - l\Omega A(\widehat{\psi}_l^h, \phi^h), \quad (6.114)$$

where

$$\begin{aligned} A(u^h, v^h) &= \int_0^R r u^h(r) v^h(r) dr, & B(u^h, v^h) &= \int_0^R \frac{r}{2} \frac{du^h(r)}{dr} \frac{dv^h(r)}{dr} dr, \\ C(u^h, v^h) &= \int_0^R \frac{1}{2r} u^h(r) v^h(r) dr, & u^h, v^h &\in U^h. \end{aligned}$$

The ODE system (6.114) is then discretized by the standard Crank-Nicolson scheme in time. Although an implicit time discretization is applied for (6.114), the 1D nature of the problem makes the coefficient matrix for the linear system band-limited. For example, if the piecewise linear polynomial is used, i.e. $k = 1$ in U^h , the matrix is tridiagonal. Fast algorithms can be applied to solve the resulting linear systems.

In practice, we always use the second-order Strang splitting [171], i.e. from time $t = t_n$ to $t = t_{n+1}$: i) first evolve (6.109) for half time step $\tau/2$ with initial data given at $t = t_n$; ii) then evolve (6.108) for one time step τ starting with the new data; iii) and evolve (6.109) for half time step $\tau/2$ with the newer data. For the discretization considered here, the total memory requirement is $O(ML)$ and the total computational cost per time step is $O(ML \ln L)$. Furthermore, it conserves the total density in the discretized level.

Discretization in 3D. When $d = 3$ in (6.108), we use the cylindrical coordinate (r, θ, z) , and discretize in the θ -direction by the Fourier pseudo-spectral method, in the z -direction by the sine pseudo-spectral method, and in the r -direction by finite element or finite difference method and in time by the C-N scheme. Assume that,

$$\psi(r, \theta, z, t) = \sum_{l=-L/2}^{L/2-1} \sum_{k=1}^{K-1} \widehat{\psi}_{l,k}(r, t) e^{il\theta} \sin(\mu_k(z - a)), \quad (6.115)$$

where L and K are two even positive integers, $\mu_k = \frac{\pi k}{b-a}$ ($k = 1, \dots, K - 1$) and $\widehat{\psi}_{l,k}(r, t)$ is the Fourier-sine coefficient for the (l, k) th mode. Plugging (6.115) into (6.108) with $d = 3$, noticing the orthogonality of the Fourier-sine modes, we obtain, for $-\frac{L}{2} \leq l \leq \frac{L}{2} - 1$, $1 \leq k \leq K - 1$ and $0 < r < R$, that [28]:

$$i\partial_t \widehat{\psi}_{l,k}(r, t) = -\frac{1}{2r} \frac{\partial}{\partial r} \left(r \frac{\partial \widehat{\psi}_{l,k}(r, t)}{\partial r} \right) + \left(\frac{l^2}{2r^2} + \frac{\mu_k^2}{2} - l\Omega \right) \widehat{\psi}_{l,k}(r, t), \quad (6.116)$$

with essential boundary conditions

$$\widehat{\psi}_{l,k}(R, t) = 0 \text{ (for all } l), \quad \widehat{\psi}_{l,k}(0, t) = 0 \text{ (for } l \neq 0). \quad (6.117)$$

The discretization of (6.116)-(6.117) is similar as that for (6.112)-(6.113) and it is omitted here.

For the algorithm in 3D, the total memory requirement is $O(MLK)$ and the total computational cost per time step is $O(MLK \ln(LK))$.

6.4. A generalized Laguerre-Fourier-Hermite pseudospectral method. Like section 6.2, for polar coordinate in 2D and cylindrical coordinate in 3D, a similar Laguerre-Hermite pseudospectral method can be designed for computing dynamics for rotating BEC (6.89)-(6.90). Here, we assume that the potential $V(\mathbf{x})$ in (6.89)-(6.90) is given as [35]

$$V(\mathbf{x}) = V_h(\mathbf{x}) + W(\mathbf{x}), \quad V_h(\mathbf{x}) = \begin{cases} \frac{1}{2}(\gamma_r^2(x^2 + y^2) + \gamma_z^2 z^2), & d = 3, \\ \frac{1}{2}\gamma_r^2(x^2 + y^2), & d = 2, \end{cases} \quad (6.118)$$

where $W(\mathbf{x})$ is a real potential.

Denoting

$$B_{\perp}\phi = \left[-\frac{1}{2} \left(\frac{\partial^2}{\partial x^2} + \frac{\partial^2}{\partial y^2} \right) + \frac{1}{2} \gamma_r^2 (x^2 + y^2) - \Omega L_z \right] \phi, \quad (6.119)$$

$$B_z\phi = \left[-\frac{1}{2} \frac{\partial^2}{\partial z^2} + \frac{1}{2} \gamma_z^2 z^2 \right] \phi, \quad (6.120)$$

$$A\phi = [W(\mathbf{x}) + \beta|\phi|^2] \phi, \quad B\phi = \begin{cases} B_{\perp}\phi, & d=2, \\ (B_{\perp} + B_z)\phi, & d=3, \end{cases} \quad (6.121)$$

then the GPE (6.89) becomes

$$i\partial_t \psi(\mathbf{x}, t) = A\psi + B\psi, \quad \mathbf{x} \in \mathbb{R}^d, \quad t > 0. \quad (6.122)$$

For $n = 0, 1, 2, \dots$, let $\psi^n := \psi^n(\mathbf{x})$ be the approximation of $\psi(\mathbf{x}, t_n)$. A standard Strang splitting second-order symplectic time integrator for (6.122) is as follows

$$\psi^{(1)} = e^{-i\tau A/2} \psi^n, \quad \psi^{(2)} = e^{-i\tau B} \psi^{(1)}, \quad \psi^{n+1} = e^{-i\tau A/2} \psi^{(2)}. \quad (6.123)$$

Thus the key for an efficient implementation of (6.123) is to solve efficiently the following two subproblems:

$$i\partial_t \psi(\mathbf{x}, t) = A\psi(\mathbf{x}, t) = [W(\mathbf{x}) + \beta|\psi(\mathbf{x}, t)|^2] \psi(\mathbf{x}, t), \quad \mathbf{x} \in \mathbb{R}^d, \quad (6.124)$$

and

$$i\partial_t \psi(\mathbf{x}, t) = B\psi(\mathbf{x}, t) = \left[-\frac{1}{2} \nabla^2 + V_h(\mathbf{x}) - \Omega L_z \right] \psi(\mathbf{x}, t), \quad \mathbf{x} \in \mathbb{R}^d, \quad (6.125)$$

$$\lim_{|\mathbf{x}| \rightarrow +\infty} \psi(\mathbf{x}, t) = 0.$$

The decaying condition in (6.125) is necessary for satisfying the mass conservation.

6.4.1. *Discretization in 2D.* In the 2D case, we use the polar coordinates (r, θ) , and write the solutions of (6.125) as $\psi(r, \theta, t)$. Therefore, for $t \geq t_s$ (t_s is any given time), (6.125) collapses to [35]

$$i\partial_t \psi(r, \theta, t) = \left[-\frac{1}{2r} \frac{\partial}{\partial r} \left(r \frac{\partial}{\partial r} \right) - \frac{1}{2r^2} \frac{\partial^2}{\partial \theta^2} + \frac{1}{2} \gamma_r^2 r^2 + i\Omega \partial_{\theta} \right] \psi(r, \theta, t) \\ := B_{\perp} \psi(r, \theta, t), \quad (6.126)$$

$$\psi(r, \theta + 2\pi, t) = \psi(r, \theta, t), \quad r \in (0, \infty), \quad \theta \in (0, 2\pi), \quad \lim_{r \rightarrow \infty} \psi(r, \theta, t) = 0.$$

For any fixed m ($m = 0, \pm 1, \pm 2, \dots$), recalling the scaled generalized-Laguerre functions L_k^n (6.40) ($n \geq 0$), a simple calculation shows that

$$B_{\perp} \left(L_k^{|m|}(r) e^{im\theta} \right) = \mu_{km} L_k^{|m|}(r) e^{im\theta}, \quad k = 0, 1, 2, \dots \quad (6.127)$$

where

$$\mu_{km} = \gamma_r(2k + |m| + 1) - m\Omega, \quad k = 0, 1, 2, \dots \quad (6.128)$$

This immediately implies that $\{L_k^{|m|}(r) e^{im\theta}, k = 0, 1, \dots, m = 0, \pm 1, \pm 2, \dots\}$ are eigenfunctions of the linear operator B_{\perp} .

For fixed even integer $M > 0$ and integer $K > 0$, let $X_{KM} = \text{span}\{L_k^{|m|}(r) e^{im\theta} : k = 0, 1, \dots, K, m = -M/2, -M/2+1, \dots, -1, 0, 1, \dots, M/2-1\}$. The generalized-Laguerre-Fourier spectral method for (6.126) is to find $\psi_{KM}(r, \theta, t) \in X_{KM}$, i.e.

$$\psi_{KM}(r, \theta, t) = \sum_{m=-M/2}^{M/2-1} \left[e^{im\theta} \sum_{k=0}^K \hat{\psi}_{km}(t) L_k^{|m|}(r) \right], \quad 0 \leq r < \infty, \quad 0 \leq \theta \leq 2\pi, \quad (6.129)$$

such that

$$\begin{aligned} i \frac{\partial \psi_{KM}(r, \theta, t)}{\partial t} &= \left[-\frac{1}{2r} \frac{\partial}{\partial r} \left(r \frac{\partial}{\partial r} \right) - \frac{1}{2r^2} \frac{\partial^2}{\partial \theta^2} + \frac{1}{2} \gamma_r^2 r^2 + i\Omega \partial_\theta \right] \psi(r, \theta, t) \\ &= B_\perp \psi_{KM}(r, \theta, t), \quad 0 < r < \infty, \quad 0 < \theta < 2\pi. \end{aligned} \quad (6.130)$$

Noting that $\lim_{r \rightarrow \infty} L_k^{|m|}(r) = 0$ for $k = 0, 1, 2, \dots$ and $m = 0, \pm 1, \pm 2, \dots$ [174]; hence, $\lim_{r \rightarrow \infty} \psi_{KM}(r, \theta, t) = 0$ is automatically satisfied. In addition, the expansions in r - and θ -directions for (6.129) do not commute. Plugging (6.129) into (6.130), thanks to (6.127), noticing the orthogonality of the Fourier series, for $k = 0, 1, \dots, K$ and $m = -M/2, -M/2-1, \dots, -1, 0, 1, \dots, M/2-1$, we find

$$i \frac{d\hat{\psi}_{km}(t)}{dt} = \mu_{km} \hat{\psi}_{km}(t) = [\gamma_r(2k + |m| + 1) - m\Omega] \hat{\psi}_{km}(t). \quad (6.131)$$

The above linear ODE can be integrated exactly and the solution is given by

$$\hat{\psi}_{km}(t) = e^{-i\mu_{km}(t-t_s)} \hat{\psi}_{km}(t_s), \quad t \geq t_s. \quad (6.132)$$

Plugging (6.132) into (6.129), we obtain the solution of (6.130) as

$$\begin{aligned} \psi_{KM}(r, \theta, t) &= e^{-iB_\perp(t-t_s)} \psi_{KM}(r, \theta, t_s) \\ &= \sum_{m=-M/2}^{M/2-1} \left[e^{im\theta} \sum_{k=0}^K e^{-i\mu_{km}(t-t_s)} \hat{\psi}_{km}(t_s) L_k^{|m|}(r) \right], \quad t \geq t_s, \end{aligned} \quad (6.133)$$

with

$$\hat{\psi}_{km}(t_s) = \frac{1}{2\pi} \int_0^{2\pi} \left[e^{-im\theta} \int_0^\infty \psi_{KM}(r, \theta, t_s) L_k^{|m|}(r) r dr \right] d\theta. \quad (6.134)$$

To summarize, a second-order time-splitting generalized-Laguerre-Fourier spectral method for the GPE (6.89) with $d = 2$ is as follows:

Let $\psi^0 = \Pi_{KM} \psi_0$ where Π_{KM} is the L^2 projection operator from $L^2((0, \infty) \times (0, 2\pi))$ onto X_{KM} , we determine ψ^{n+1} ($n = 0, 1, \dots$) by [35]

$$\begin{aligned} \psi^{(1)}(r, \theta) &= e^{-i\tau[W(r, \theta) + \beta|\psi^n(r, \theta)|^2]/2} \psi^n(r, \theta), \\ \psi^{(2)}(r, \theta) &= \sum_{m=-M/2}^{M/2-1} \left[e^{im\theta} \sum_{k=0}^K e^{-i\tau\mu_{km}} \widehat{\psi^{(1)}}_{km} L_k^{|m|}(r) \right], \\ \psi^{n+1}(r, \theta) &= e^{-i\tau[W(r, \theta) + \beta|\psi^{(2)}(r, \theta)|^2]/2} \psi^{(2)}(r, \theta), \end{aligned} \quad (6.135)$$

with

$$\widehat{\psi^{(1)}}_{km} = \frac{1}{2\pi} \int_0^{2\pi} \left[e^{-im\theta} \int_0^\infty \psi^{(1)}(r, \theta) L_k^{|m|}(r) r dr \right] d\theta. \quad (6.136)$$

The scheme (6.135) is not suitable in practice due to the difficulty to compute the initial data $\psi_{KM}^0 = \Pi_{KM} \psi_0$ and the integrals in (6.136). We now present an efficient implementation by choosing $\psi_{KM}^0(r, \theta)$ as the interpolation of $\psi(r, \theta, 0)$ on

a suitable grid, and approximating (6.136) (for all m) by a quadrature rule on this grid.

It is clear that the optimal quadrature rule, hence the collocation points, for the r -integral in (6.136) depends on m [40, 41]. However, we have to use the same set of collocation points for all m to form a tensorial grid in the (r, θ) domain. Therefore, let $\{\hat{r}_j\}_{j=0}^{K+M/2}$ be the Laguerre-Gauss points [163, 174]; i.e. they are the $K+M/2+1$ roots of the standard Laguerre polynomial $\hat{L}_{K+M/2+1}^0(r) := \hat{L}_{K+M/2+1}(r)$. Let $\{\hat{\omega}_j\}_{j=0}^{K+M/2}$ be the corresponding weights associated with the generalized-Laguerre-Gauss quadrature (6.50). We then define the scaled generalized-Laguerre-Gauss points and weights r_j and ω_j ($j = 0, 1, \dots, K+M/2$) as in (6.51) and the appendix of [163].

Let $\theta_s = \frac{2s\pi}{M}$ ($s = 0, 1, \dots, M-1$). For any given set of values $\{\psi_{js}, 0 \leq j \leq K+M/2; 0 \leq s \leq M-1\}$, we can define a unique function ψ in X_{KM} interpolating this set, i.e.,

$$\begin{aligned} \psi(r, \theta) &= \sum_{m=-M/2}^{M/2-1} \sum_{k=0}^K \hat{\psi}_{km} L_k^{|m|}(r) e^{im\theta} \quad \text{such that} \\ \psi(r_j, \theta_s) &= \psi_{js}, \quad 0 \leq j \leq K+M/2; 0 \leq s \leq M-1. \end{aligned} \quad (6.137)$$

By using the discrete orthogonality relation (6.52) for the scaled generalized Laguerre functions and the discrete Fourier orthogonality relation

$$\frac{1}{M} \sum_{s=0}^{M-1} e^{ik\theta_s} e^{-ik'\theta_s} = \delta_{kk'}, \quad |k|, |k'| \leq M/2, \quad (6.138)$$

we find that

$$\hat{\psi}_{km} = \frac{1}{M} \sum_{s=0}^{M-1} \left[e^{-im\theta_s} \sum_{j=0}^{K+M/2} \omega_j \psi_{js} L_k^{|m|}(r_j) \right], \quad (6.139)$$

and that

$$\|\psi\|_2^2 := \int_0^{2\pi} \int_0^\infty |\psi|^2 r dr d\theta = 2\pi \sum_{m=-M/2}^{M/2-1} \sum_{k=0}^K |\hat{\psi}_{km}|^2 = \frac{2\pi}{M} \sum_{j=0}^{K+M/2} \sum_{s=0}^{M-1} |\psi_{js}|^2 \omega_j.$$

We can now describe the second-order time-splitting generalized-Laguerre-Fourier pseudospectral (TSGLFP2) method for the GPE (6.89) with $d = 2$ as follows:

Let $\psi_{js}^0 = \psi_0(r_j, \theta_s)$ for $0 \leq j \leq K+M/2$ and $0 \leq s \leq M-1$. For $n = 0, 1, 2, \dots$, we compute ψ_{js}^{n+1} ($0 \leq j \leq K+M/2$, $0 \leq s \leq M-1$) by [35]

$$\begin{aligned} \psi_{js}^{(1)} &= e^{-i\tau[W(r_j, \theta_s) + \beta|\psi_{js}^n|^2]/2} \psi_{js}^n, \\ \psi_{js}^{(2)} &= \sum_{m=-M/2}^{M/2-1} \left[e^{im\theta_s} \sum_{k=0}^K e^{-i\tau\mu_{km}} \widehat{(\psi^{(1)})}_{km} L_k^{|m|}(r_j) \right], \\ \psi_{js}^{n+1} &= e^{-i\tau[W(r_j, \theta_s) + \beta|\psi_{js}^{(2)}|^2]/2} \psi_{js}^{(2)}, \end{aligned} \quad (6.140)$$

where $\{\widehat{(\psi^{(1)})}_{km}\}$ are the expansion coefficients of $\psi^{(1)}$ given by (6.139).

6.4.2. *Discretization in 3D.* In the 3D case, by using the cylindrical coordinates (r, θ, z) , we can write the solutions of (6.125) as $\psi(r, \theta, z, t)$. Therefore, for $t \geq t_s$ (t_s is any given time), (6.125) collapses to [35]

$$\begin{aligned} i\partial_t \psi(r, \theta, z, t) &= \frac{1}{2} \left[-\frac{1}{r} \frac{\partial}{\partial r} \left(r \frac{\partial}{\partial r} \right) - \frac{1}{r^2} \frac{\partial^2}{\partial \theta^2} - \frac{\partial^2}{\partial z^2} + \gamma_r^2 r^2 + \gamma_z z^2 + 2i\Omega \partial_\theta \right] \psi, \\ &= (B_\perp + B_z) \psi(r, \theta, z, t) = B \psi(r, \theta, z, t), \\ \psi(r, \theta + 2\pi, z, t) &= \psi(r, \theta, z, t), \quad 0 < r < \infty, \quad 0 < \theta < 2\pi, \quad z \in \mathbb{R}, \\ \lim_{r \rightarrow \infty} \psi(r, \theta, z, t) &= 0, \quad -\infty < z < \infty, \quad t \geq t_s. \end{aligned}$$

Let the scaled Hermite functions $h_l(z)$ ($l = 0, 1, \dots$) be given in (6.35). For any fixed m ($m = 0, \pm 1, \pm 2, \dots$), we find that [35]

$$B \left(L_k^{|m|}(r) e^{im\theta} h_l(z) \right) = (\mu_{km} + \lambda_l) L_k^{|m|}(r) e^{im\theta} h_l(z), \quad \lambda_l = (l + \frac{1}{2})\gamma_z. \quad (6.141)$$

Hence, $\{L_k^{|m|}(r) e^{im\theta} h_l(z), k, l = 0, 1, \dots, m = 0, \pm 1, \pm 2, \dots\}$ are eigenfunctions of the linear operator $B = B_\perp + B_z$ defined in (6.121) for $d = 3$.

Then a second-order time-splitting generalized-Laguerre-Fourier-Hermite spectral method for the GPE (6.89) with $d = 3$ can be constructed analogously to (6.135). Here, we only present pseudospectral method generalizing TSGLFP2 (6.140).

Define the scaled Hermite-Gauss points z_p and weights ω_p^z ($0 \leq p \leq L$) by (6.46). For any given set of values $\{\psi_{jsp}, 0 \leq j \leq K + M/2; 0 \leq s \leq M - 1; 0 \leq p \leq L\}$, we can define a unique function ψ in $Y_{KML} = \text{span}\{L_k^{|m|}(r) e^{im\theta} h_l(z) : 0 \leq k \leq K, -M/2 \leq m \leq M/2 - 1, 0 \leq l \leq L\}$ interpolating this set, i.e.,

$$\begin{aligned} \psi(r, \theta, z) &= \sum_{m=-M/2}^{M/2-1} \sum_{k=0}^K \sum_{l=0}^L \widehat{\psi}_{kml} L_k^{|m|}(r) e^{im\theta} h_l(z) \quad \text{such that} \\ \psi(r_j, \theta_s, z_p) &= \psi_{jsp}, \quad 0 \leq j \leq K + M/2; 0 \leq s \leq M - 1; 0 \leq p \leq L. \end{aligned} \quad (6.142)$$

By using the discrete orthogonality relations (6.52), (6.138) and (6.47), we find that

$$\widehat{\psi}_{kml} = \frac{1}{M} \sum_{p=0}^L \left[h_l(z_p) \omega_p^z \sum_{s=0}^{M-1} \left(e^{-im\theta_s} \sum_{j=0}^{K+M/2} \omega_j \psi_{jsp} L_k^{|m|}(r_j) \right) \right], \quad (6.143)$$

and that

$$\begin{aligned} \|\psi\|_2^2 &:= \int_{-\infty}^{\infty} \int_0^{\infty} \int_0^{2\pi} |\psi(r, \theta, z)|^2 r \, d\theta dr dz \\ &= 2\pi \sum_{m=-M/2}^{M/2-1} \sum_{k=0}^K \sum_{l=0}^L |\widehat{\psi}_{kml}|^2 = \frac{2\pi}{M} \sum_{j=0}^{K+M/2} \sum_{s=0}^{M-1} \sum_{p=0}^L |\psi_{jsp}|^2 \omega_j \omega_p^z. \end{aligned} \quad (6.144)$$

Then the second-order time-splitting generalized-Laguerre-Fourier-Hermite pseudospectral (TSGLFHP2) method for the GPE (6.89) with $d = 3$ is as follows:

Let $\psi_{jsp}^0 = \psi_0(r_j, \theta_s, z_p)$ for $0 \leq j \leq K + M/2$, $0 \leq s \leq M - 1$ and $0 \leq p \leq L$. For $n = 0, 1, \dots$, we compute ψ_{jsp}^{n+1} by [35]

$$\begin{aligned} \psi_{jsp}^{(1)} &= e^{-i\tau[W(r_j, \theta_s, z_p) + \beta|\psi_{jsp}^n|^2]/2} \psi_{jsp}^n, \\ \psi_{jsp}^{(2)} &= \sum_{l=0}^L \left[h_l(z_p) \sum_{m=-M/2}^{M/2-1} \left(e^{im\theta_s} \sum_{k=0}^K e^{-i\tau(\mu_{km} + \lambda_l)} \widehat{(\psi^{(1)})}_{kml} L_k^{|m|}(r_j) \right) \right], \quad (6.145) \\ \psi_{jsp}^{n+1} &= e^{-i\tau[W(r_j, \theta_s, z_p) + \beta|\psi_{jsp}^{(2)}|^2]/2} \psi_{jsp}^{(2)}, \end{aligned}$$

where $\{\widehat{(\psi^{(1)})}_{kml}\}$ are the expansion coefficients of $\psi^{(1)}$ given by (6.143).

6.5. Numerical results. In this section, we report numerical examples for ground states and central vortex states as well as dynamics for rotating BEC.

Example 6.1. Ground, symmetric and central vortex states, as well as their energy configurations, in 2D, i.e. we take $d = 2$ and $\gamma_x = \gamma_y = 1$ in (5.7). Fig. 6.1 plots surface of the ground state $\phi^g(x, y) := \phi_\Omega^g(x, y)$ with $\beta = 100$ for different Ω . Fig. 6.2 plots the symmetric state $\phi^0(r) := \phi_0^0(r)$ and first three central vortex states $\phi_m(r) := \phi_0^m(r)$ ($m = 1, 2, 3$) for different interaction rate β . Backward Euler finite difference method is used here with a bounded computational domain $U = [-6, 6] \times [-6, 6]$ and initial data for GFDN (6.1)-(6.3) is chosen as $\phi_0(x, y) = \frac{(1-\Omega)\phi_{\text{ho}}(x, y) + \Omega\phi_{\text{ho}}^v(x, y)}{\|(1-\Omega)\phi_{\text{ho}}(x, y) + \Omega\phi_{\text{ho}}^v(x, y)\|_2}$, $(x, y) \in U$, where $\phi_{\text{ho}}^v(x, y) = \frac{x+iy}{\sqrt{\pi}} e^{-(x^2+y^2)/2}$ and $\phi_{\text{ho}}(x, y) = \frac{1}{\sqrt{\pi}} e^{-(x^2+y^2)/2}$. The steady state solution is obtained numerically when $\|\phi^{n+1} - \phi^n\|_\infty := \max_{(j,l)} |\phi_{jl}^{n+1} - \phi_{jl}^n| < \epsilon = 10^{-7}$.

Example 6.2. Dynamics of a rotating BEC in 2D, i.e. we take $d = 2$, $\beta = 100$, $\Omega = 0.5$ and $W(\mathbf{x}) \equiv 0$ in (6.89). The initial data in (6.89) is chosen as

$$\psi_0(x, y) = \frac{x + iy}{\sqrt{\pi}} e^{-(x^2+y^2)/2}, \quad (x, y) \in \mathbb{R}^2. \quad (6.146)$$

We solve the problem by the scheme (6.140) with $\tau = 0.0005$, $M = 128$ and $K = 200$. Fig. 6.3 depicts time evolution of the normalization $N(\psi)$, energy $E_{\beta, \Omega}(\psi)$, condensate width $\delta_r(t)$ and angular momentum expectation $\langle L_z \rangle(t)$ for three sets of parameters in (6.89): (i) $\gamma_x = \gamma_y = 2$, (ii) $\gamma_x = \gamma_y = 0.8$, and (iii) $\gamma_x = 0.8$, $\gamma_y = 1.2$.

From Fig. 6.3, we can draw the following conclusions: (i) the normalization $N(\psi)$ and energy $E_{\beta, \Omega}(\psi)$ are conserved well in the computation (cf. Fig. 6.3a&b); (ii) the angular momentum expectation $\langle L_z \rangle(t)$ is conserved when $\gamma_x = \gamma_y$ (cf. Fig. 6.3d), i.e. the trapping is radially symmetric, which again confirms the analytical results in section 5.5; (iii) the condensate width $\delta_r(t)$ is a periodic function when $\gamma_x = \gamma_y$ (cf. Fig. 6.3c), which again confirms the analytical results in section 5.5.

7. Semiclassical scaling and limit. In section 1.3, we have introduced the scaling in the GPE (1.11) to obtain the dimensionless form which has been widely adopted in physics literatures. For BEC with or without the rotational frame (cf. section 5), the dimensionless GPE in d -dimensions ($d = 1, 2, 3$) (lower dimensions

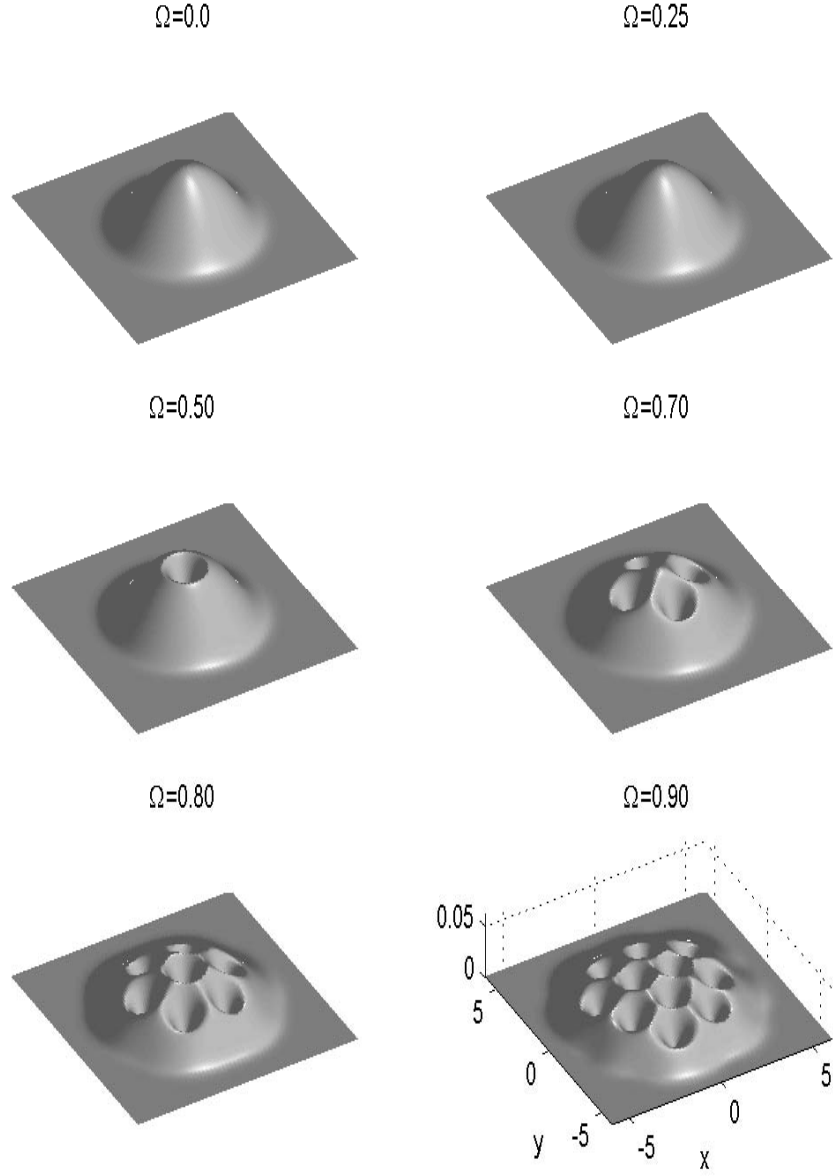


FIGURE 6.1. Surface plots of ground state density function $|\phi_{\Omega}^g(x, y)|^2$ in 2D with $\gamma_x = \gamma_y = 1$ and $\beta = 100$ for different Ω in Example 6.1.

with $d = 1, 2$ are treated as from 3D GPE by dimension reduction) can be written as

$$i\partial_t\psi(\mathbf{x}, t) = \left[-\frac{1}{2}\nabla^2 + V(\mathbf{x}) - \Omega L_z + \beta|\psi|^2 \right] \psi, \quad \mathbf{x} \in U \subseteq \mathbb{R}^d, \quad t > 0, \quad (7.1)$$

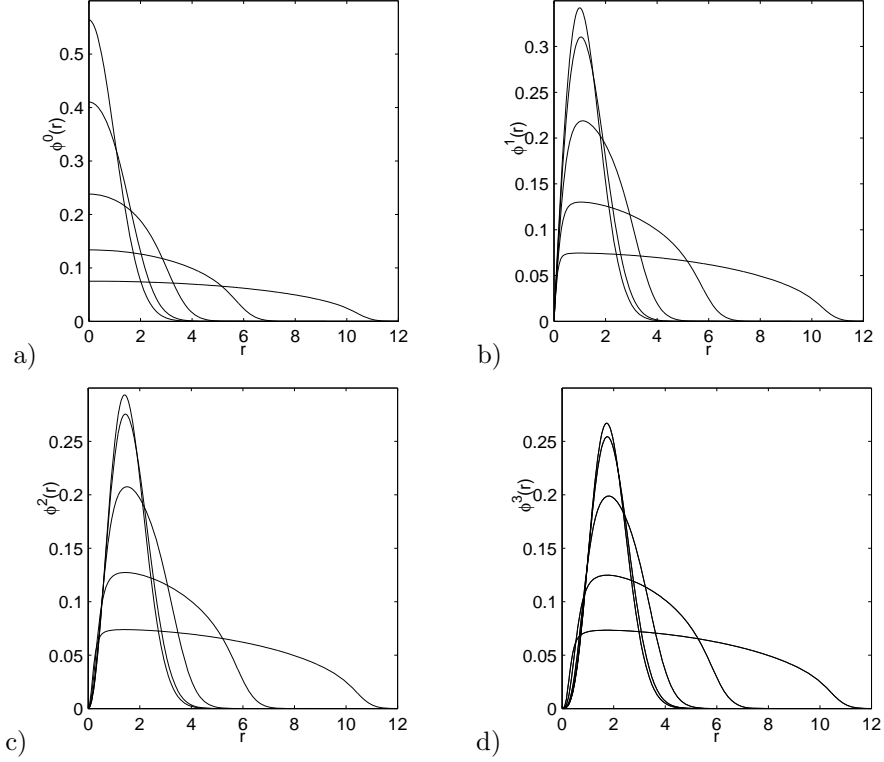


FIGURE 6.2. Symmetric and central vortex states in 2D with $\gamma_x = \gamma_y = 1$ for $\beta = 0, 10, 100, 1000, 10000$ (in the order of decreasing of peak) in Example 6.1. Symmetric state $\phi^0(r)$: a); and central vortex states $\phi^m(r)$: b). $m = 1$, c). $m = 2$ and d). $m = 3$.

with normalization condition

$$\|\psi(\cdot, t)\|_2^2 = \int_{\mathbb{R}^d} |\psi(\mathbf{x}, t)|^2 d\mathbf{x} = 1, \quad (7.2)$$

where $\psi := \psi(\mathbf{x}, t)$ is the macroscopic wave function, $U = [0, 1]^d$ for box potentials, $U = \mathbb{R}^d$ for harmonic potential and other confining potentials (cf. section 1.3), $L_z = -i(y\partial_x - x\partial_y)$ for $d = 2, 3$, and $\Omega = 0$ for $d = 1$. The energy $E(\psi)$ for (7.1) is given by

$$E(\psi(\cdot, t)) = \int_U \left[\frac{1}{2} |\nabla\psi(\mathbf{x}, t)|^2 + V(\mathbf{x})|\psi|^2 + \frac{\beta}{2} |\psi|^4 - \Omega\bar{\psi}L_z\psi \right] d\mathbf{x}. \quad (7.3)$$

The ground state ϕ_g of the GPE (7.1) is the minimizer of the energy $E(\phi)$ (7.3) over the unit sphere $S = \{\phi \mid \|\phi\|_2 = 1, E(\phi) < \infty\}$. It can also be characterized by the nonlinear eigenvalue problem:

$$\begin{aligned} \mu \phi(\mathbf{x}) &= -\frac{1}{2}\Delta\phi(\mathbf{x}) + V(\mathbf{x})\phi(\mathbf{x}) - \Omega L_z\phi + \beta|\phi(\mathbf{x})|^2\phi(\mathbf{x}), \quad \mathbf{x} \in U, \\ \phi(\mathbf{x})|_{\partial U} &= 0, \end{aligned} \quad (7.4)$$

under the normalization condition (7.2) with $\psi = \phi$. Here, the nonlinear eigenvalue (or chemical potential) μ can be computed from its corresponding eigenfunction

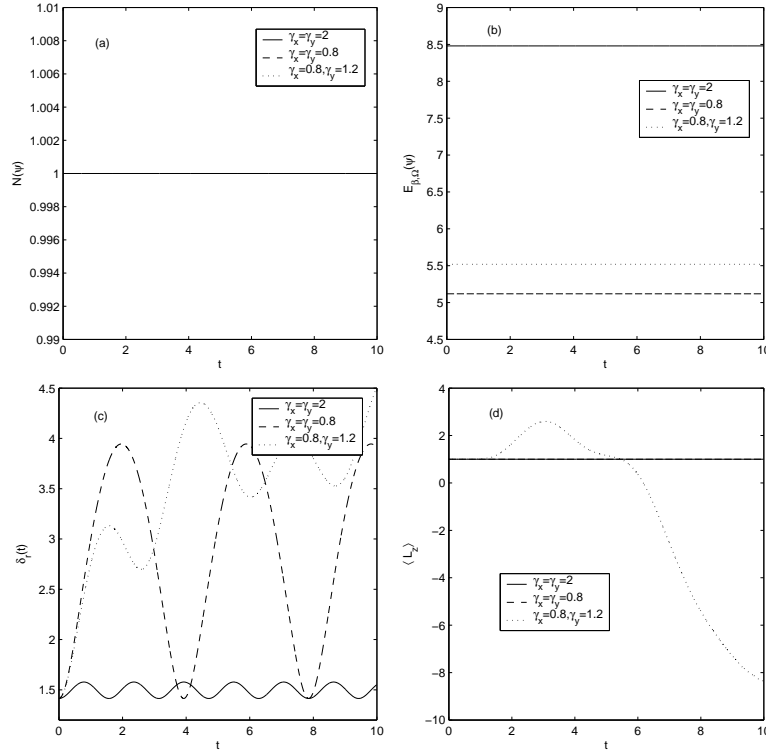


FIGURE 6.3. Time evolution of a few quantities for the dynamics of rotating BEC in 2D with three sets of parameters: (a) normalization $N(\psi)$, (b) energy $E_{\beta, \Omega}(\psi)$, (c) condensate width $\delta_r(t)$, and (d) angular momentum expectation $\langle L_z \rangle(t)$.

$\phi(\mathbf{x})$ by

$$\begin{aligned} \mu &= \mu(\phi) = \int_U \left[\frac{1}{2} |\nabla \phi(\mathbf{x})|^2 + V(\mathbf{x}) |\phi(\mathbf{x})|^2 + \beta |\phi(\mathbf{x})|^4 - \Omega \bar{\phi} L_z \phi \right] dx \\ &= E(\phi) + \int_U \frac{\beta}{2} |\phi(\mathbf{x})|^4 dx. \end{aligned} \quad (7.5)$$

7.1. Semiclassical scaling in the whole space. When $U = \mathbb{R}^d$, $\beta \gg 1$ and $V(\mathbf{x}) = V_0(\mathbf{x}) + W(\mathbf{x})$ satisfies

$$V_0(\lambda \mathbf{x}) = |\lambda|^\alpha V_0(\mathbf{x}), \quad \forall \lambda \in \mathbb{R}, \quad \lim_{|\mathbf{x}| \rightarrow \infty} V_0(\mathbf{x}) = \infty, \quad \lim_{|\mathbf{x}| \rightarrow \infty} \frac{W(\mathbf{x})}{V_0(\mathbf{x})} = 0, \quad (7.6)$$

where $\mathbf{x} \in \mathbb{R}^d$ and $\alpha > 0$, another scaling (under the normalization (7.2) with ψ being replaced by ψ^ε) – semiclassical scaling – for (7.1) is also very useful in practice by choosing, $t \rightarrow t\varepsilon^{(\alpha-2)/(\alpha+2)}$, $\mathbf{x} \rightarrow \mathbf{x}\varepsilon^{-2/(2+\alpha)}$, and $\psi = \psi^\varepsilon \varepsilon^{d/(2+\alpha)}$ with $\varepsilon = 1/\beta^{(\alpha+2)/2(d+\alpha)}$ [24, 28, 47]:

$$i\varepsilon \frac{\partial \psi^\varepsilon(\mathbf{x}, t)}{\partial t} = \left[-\frac{\varepsilon^2}{2} \nabla^2 - \varepsilon^{\frac{2\alpha}{2+\alpha}} \Omega L_z \right] \psi^\varepsilon + (V_0(\mathbf{x}) + W^\varepsilon(\mathbf{x})) \psi^\varepsilon + |\psi^\varepsilon|^2 \psi^\varepsilon, \quad \mathbf{x} \in \mathbb{R}^d, \quad (7.7)$$

where $W^\varepsilon(\mathbf{x}) = \varepsilon^{2\alpha/(2+\alpha)}W(\mathbf{x}/\varepsilon^{2/(2+\alpha)})$ and the energy functional $E^\varepsilon(\psi^\varepsilon)$ is defined as

$$E^\varepsilon(\psi^\varepsilon) = \int_{\mathbb{R}^d} \left[\frac{\varepsilon^2}{2} |\nabla \psi^\varepsilon|^2 - \varepsilon^{\frac{2\alpha}{2+\alpha}} \Omega \overline{\psi^\varepsilon} L_z \psi^\varepsilon + (V_0 + W^\varepsilon) |\psi^\varepsilon|^2 + \frac{|\psi^\varepsilon|^4}{2} \right] d\mathbf{x} = O(1). \quad (7.8)$$

Similarly, the nonlinear eigenvalue problem (7.4) (under the normalization (7.2) with $\psi = \phi^\varepsilon$) reads

$$\mu^\varepsilon \phi^\varepsilon(\mathbf{x}) = -\frac{\varepsilon^2}{2} \Delta \phi^\varepsilon + (V_0(\mathbf{x}) + W^\varepsilon(\mathbf{x})) \phi^\varepsilon - \varepsilon^{\frac{2\alpha}{2+\alpha}} \Omega L_z \phi^\varepsilon + |\phi^\varepsilon|^2 \phi^\varepsilon, \quad \mathbf{x} \in \mathbb{R}^d, \quad (7.9)$$

where eigenvalue μ^ε can be computed from its corresponding eigenfunction ϕ^ε by

$$\mu^\varepsilon = \mu^\varepsilon(\phi^\varepsilon) = E^\varepsilon(\phi^\varepsilon) + \frac{1}{2} \int_{\mathbb{R}^d} |\phi^\varepsilon|^4 d\mathbf{x} = O(1). \quad (7.10)$$

Based on this re-scaling, it is easy to get the leading asymptotics of the energy functional $E(\psi)$ in (7.3) and the chemical potential (7.5) when $\beta \gg 1$ from this scaling [24, 28, 47]:

$$E(\psi) = \varepsilon^{-2\alpha/(2+\alpha)} E^\varepsilon(\psi^\varepsilon) = O\left(\varepsilon^{-2\alpha/(2+\alpha)}\right) = O\left(\beta^{\alpha/(d+\alpha)}\right), \quad (7.11)$$

$$\mu(\phi) = \varepsilon^{-2\alpha/(2+\alpha)} \mu^\varepsilon(\phi^\varepsilon) = O\left(\varepsilon^{-2\alpha/(2+\alpha)}\right) = O\left(\beta^{\alpha/(d+\alpha)}\right). \quad (7.12)$$

In [70, 169], a different rescaling for the nonlinear Schrödinger equation subject to smooth, lattice-periodic potentials was used in the semiclassical regime. There they studied Bloch waves dynamics in BEC on optical lattices.

7.2. Semiclassical scaling in bounded domain. When $U = (0, 1)^d \subset \mathbb{R}^d$ is a bounded domain, $\beta \gg 1$, we use the following scaling (under the normalization (7.2)) with ψ being replaced by ψ^ε – semiclassical scaling – for (7.1) by choosing $t \rightarrow t\varepsilon^{-1}$, and $\psi = \psi^\varepsilon$ with $\varepsilon = 1/\sqrt{\beta}$ [24]:

$$i\varepsilon \frac{\partial \psi^\varepsilon(\mathbf{x}, t)}{\partial t} = \left[-\frac{\varepsilon^2}{2} \nabla^2 - \varepsilon^2 \Omega L_z \right] \psi^\varepsilon + V^\varepsilon(\mathbf{x}) \psi^\varepsilon + |\psi^\varepsilon|^2 \psi^\varepsilon, \quad \mathbf{x} \in U, \quad (7.13)$$

where $V^\varepsilon(\mathbf{x}) = \varepsilon^2 V(\mathbf{x})$ and the energy functional $E^\varepsilon(\psi^\varepsilon)$ is defined as

$$E^\varepsilon(\psi^\varepsilon) = \int_U \left[\frac{\varepsilon^2}{2} |\nabla \psi^\varepsilon|^2 - \varepsilon^2 \Omega \overline{\psi^\varepsilon} L_z \psi^\varepsilon + V^\varepsilon |\psi^\varepsilon|^2 + \frac{|\psi^\varepsilon|^4}{2} \right] d\mathbf{x} = O(1). \quad (7.14)$$

We can derive the leading asymptotics of the energy functional $E(\psi)$ in (7.3) and the chemical potential (7.5) when $\beta \gg 1$ from this scaling in the bounded domain case [24]:

$$E(\psi) = \varepsilon^{-2} E^\varepsilon(\psi^\varepsilon) = O(\varepsilon^{-2}) = O(\beta), \quad (7.15)$$

$$\mu(\phi) = \varepsilon^{-2} \mu^\varepsilon(\phi^\varepsilon) = O(\varepsilon^{-2}) = O(\beta). \quad (7.16)$$

For comparison, Tabs. 7.1 and 7.1 display dimensionless units and several important quantities to obtain the GPE (7.1) under the standard physical scaling and (7.7) or (7.13) under the semiclassical scaling for a BEC in the whole space with harmonic potential (1.13) ($\omega_x = \min\{\omega_x, \omega_y, \omega_z\}$) and in a bounded domain with box potential (1.17), respectively. Again, the dimensionless GPE in lower dimensions with $d = 1, 2$ are treated as from 3D GPE by dimension reduction.

Quantities	Physical scaling	Semiclassical scaling
time unit t_s	$\frac{1}{\omega_x}$	$\frac{1}{\omega_x}$
length unit x_s	$\sqrt{\frac{\hbar}{m\omega_x}} := a_0$	$\frac{a_0}{\varepsilon^{1/2}}$
energy unit E_s	$\hbar\omega_x$	$\frac{\hbar\omega_x}{\varepsilon}$
wave amplitude unit ψ_s	$a_0^{-3/2}$	$a_0^{-3/2} \varepsilon^{d/4}$
healing length ξ_h	$O(\beta^{-1/(2+d)})$	$O(\varepsilon)$
energy E_g	$O(\beta^{2/(d+2)})$	$O(1)$
chemical potential μ_g	$O(\beta^{2/(d+2)})$	$O(1)$
Thomas-Fermi radius R_g^{TF}	$O(\beta^{1/(d+2)})$	$O(1)$
wave amplitude ϕ_g^{max}	$O(\beta^{-d/2(d+2)})$	$O(1)$

TABLE 7.1. Comparison of dimensionless units and several important quantities under the standard physical scaling and semiclassical scaling. Here t_s is time unit, x_s is length unit, E_s is energy unit, ψ_s is wave function unit, where m , \hbar , a_s and N are the mass, Planck constant, s -wave scattering length and total particle number, respectively (cf. 1.3). ξ_h is the healing length [148], E_g is the energy of ground state, μ_g is the chemical potential of ground state, R_g^{TF} is the Thomas-Fermi radius of the ground state, ϕ_g^{max} is the maximum value of ground state. (a) For a BEC in the whole space with a harmonic potential (1.13) ($\omega_x = \min\{\omega_x, \omega_y, \omega_z\}$), β is given in (1.40) and $\varepsilon = 1/\beta^{2/(2+d)}$.

Quantities	Physical scaling	Semiclassical scaling
time unit t_s	$\frac{mL^2}{\hbar}$	$\frac{mL^2}{\hbar\varepsilon^2}$
length unit x_s	L	L
energy unit E_s	$\frac{\hbar^2}{mL^2}$	$\frac{\hbar^2}{m\varepsilon^2 L^2}$
wave amplitude unit ψ_s	$L^{-3/2}$	$L^{-3/2}$
healing length ξ_h	$O(\beta^{-1/2})$	$O(\varepsilon)$
energy E_g	$O(\beta)$	$O(1)$
Chemical potential μ_g	$O(\beta)$	$O(1)$
Thomas-Fermi radius R_g^{TF}	$O(1)$	$O(1)$
wave amplitude ϕ_g^{max}	$O(1)$	$O(1)$

TABLE 7.1. (Con't) (b) For a BEC in the box potential (1.17) with L the size of box potential. $\beta = 4\pi a_s N/L$ and $\varepsilon = \beta^{-1/2}$.

7.3. Semiclassical limits and geometric optics. Suppose $V^\varepsilon(\mathbf{x}) = V_0(\mathbf{x}) + W^\varepsilon(\mathbf{x})$ in (7.7), and we set

$$\psi^\varepsilon(\mathbf{x}, t) = \sqrt{\rho^\varepsilon(\mathbf{x}, t)} \exp\left(\frac{i}{\varepsilon} S^\varepsilon(\mathbf{x}, t)\right), \quad (7.17)$$

where $\rho^\varepsilon = |\psi^\varepsilon|^2$ and S^ε are the density and phase of the wave function, respectively. Inserting (7.17) into the GPE (7.7) and separating real and imaginary parts give [28, 69, 103, 104, 192]

$$\rho_t^\varepsilon + \operatorname{div}(\rho^\varepsilon \nabla S^\varepsilon) + \Omega \hat{L}_z \rho^\varepsilon = 0, \quad (7.18)$$

$$S_t^\varepsilon + \frac{1}{2} |\nabla S^\varepsilon|^2 + \rho^\varepsilon + V^\varepsilon(\mathbf{x}) + \Omega \hat{L}_z S^\varepsilon = \frac{\varepsilon^2}{2} \frac{1}{\sqrt{\rho^\varepsilon}} \Delta \sqrt{\rho^\varepsilon}, \quad (7.19)$$

where $\hat{L}_z = (x\partial_y - y\partial_x)$. The equation (7.18) is the transport equation for the atom density and (7.19) the Hamilton-Jacobi equation for the phase.

By formally passing to the limit $\varepsilon \rightarrow 0$ (cf. [102]), we obtain the system

$$\rho_t^0 + \operatorname{div}(\rho^0 \nabla S^0) + \Omega \hat{L}_z \rho^0 = 0, \quad (7.20)$$

$$S_t^0 + \frac{1}{2} |\nabla S^0|^2 + \rho^0 + V_0(\mathbf{x}) + \Omega \hat{L}_z S^0 = 0. \quad (7.21)$$

It is well known that this limit process is only correct in the defocusing case $\beta > 0$ before caustic onset, i.e. in time-intervals where the solution of the Hamilton-Jacobian equation (7.19) coupled with the atom-number conservation equation (7.18) is smooth. After the breakdown of regularity, oscillations occur, which make the term $\frac{\varepsilon^2}{2} \frac{1}{\sqrt{\rho^\varepsilon}} \Delta \sqrt{\rho^\varepsilon}$ at least $O(1)$ such that the validity of the formal limit process is destroyed. The limiting behavior after caustics onset is not understood yet except in 1D case without confinement, see [122]. Also, the focusing case $\beta < 0$ is not fully understood yet.

Furthermore, by defining the current densities

$$\mathbf{J}^\varepsilon(\mathbf{x}, t) = \rho^\varepsilon \nabla S^\varepsilon = \varepsilon \operatorname{Im} [\overline{\psi^\varepsilon} \nabla \psi^\varepsilon], \quad (7.22)$$

we can rewrite (7.18)-(7.19) as a coupled Euler system with third-order dispersion terms [28, 69, 103, 104, 192]

$$\partial_t \rho^\varepsilon + \operatorname{div} \mathbf{J}^\varepsilon + \Omega \hat{L}_z \rho^\varepsilon = 0, \quad (7.23)$$

$$\partial_t \mathbf{J}^\varepsilon + \operatorname{div} \left(\frac{\mathbf{J}^\varepsilon \otimes \mathbf{J}^\varepsilon}{\rho^\varepsilon} \right) + \rho^\varepsilon \nabla V^\varepsilon(\mathbf{x}) + \frac{1}{2} \nabla (\rho^\varepsilon)^2 + \Omega \hat{L}_z \mathbf{J}^\varepsilon = \frac{\varepsilon^2}{4} \nabla (\rho^\varepsilon \nabla^2 \ln \rho^\varepsilon). \quad (7.24)$$

Letting $\varepsilon \rightarrow 0^+$ in (7.23)-(7.24), formally we get an Euler system coupling through the pressures [28, 69, 103, 104, 192]

$$\partial_t \rho^0 + \operatorname{div} \mathbf{J}^0 + \Omega \hat{L}_z \rho^0 = 0, \quad (7.25)$$

$$\partial_t \mathbf{J}^0 + \operatorname{div} \left(\frac{\mathbf{J}^0 \otimes \mathbf{J}^0}{\rho^0} \right) + \rho^0 \nabla V_0(\mathbf{x}) + \frac{1}{2} \nabla (\rho^0)^2 + \Omega \hat{L}_z \mathbf{J}^0 = 0, \quad (7.26)$$

where $\mathbf{J}^0(\mathbf{x}, t) = \rho^0 \nabla S^0$. The system (7.25)-(7.26) is a coupled isotropic Euler system with quadratic pressure-density constitutive relations in the rotational frame. The formal asymptotics is supposed to hold up to caustic onset time [103, 104].

8. Mathematical theory and numerical methods for dipolar BEC. In the last several years, there has been a quest for realizing a novel kind of quantum gases with the dipolar interaction, acting between particles having a permanent magnetic or electric dipole moment. In 2005, the first dipolar BEC with ^{52}Cr atoms was successfully realized in experiments at the Stuttgart University [107]. Later in 2011, a dipolar BEC with ^{164}Dy atoms, whose dipole-dipole interaction is much stronger than that of ^{52}Cr , was achieved in experiments at the Stanford University [138]. Very recently in 2012, a dipolar BEC of ^{168}Er atoms has been

produced in Innsbruck University [8]. These successes of experiments have renewed interests in theoretically studying dipolar BECs.

8.1. GPE with dipole-dipole interaction. At temperature T much smaller than the critical temperature T_c , a dipolar BEC is well described by the macroscopic wave function $\psi = \psi(\mathbf{x}, t)$ whose evolution is governed by the 3D Gross-Pitaevskii equation (GPE) [49, 161, 187]

$$i\hbar\partial_t\psi(\mathbf{x}, t) = \left[-\frac{\hbar^2}{2m}\nabla^2 + V(\mathbf{x}) + g|\psi|^2 + (V_{\text{dip}} * |\psi|^2) \right] \psi, \quad \mathbf{x} \in \mathbb{R}^3, \quad t > 0, \quad (8.1)$$

where $\mathbf{x} = (x, y, z)^T \in \mathbb{R}^3$ is the Cartesian coordinate and a harmonic trap potential $V(\mathbf{x})$ is considered here. $g = \frac{4\pi\hbar^2 a_s}{m}$ describes local (or short-range) interaction between dipoles in the condensate with a_s the s -wave scattering length. The long-range dipolar interaction potential between two dipoles is given by

$$V_{\text{dip}}(\mathbf{x}) = \frac{\mu_0\mu_{\text{dip}}^2}{4\pi} \frac{1 - 3(\mathbf{x} \cdot \mathbf{n})^2/|\mathbf{x}|^2}{|\mathbf{x}|^3} = \frac{\mu_0\mu_{\text{dip}}^2}{4\pi} \frac{1 - 3\cos^2(\theta)}{|\mathbf{x}|^3}, \quad \mathbf{x} \in \mathbb{R}^3, \quad (8.2)$$

where μ_0 is the vacuum magnetic permeability, μ_{dip} is permanent magnetic dipole moment (e.g. $\mu_{\text{dip}} = 6\mu_B$ for ^{52}Cr with μ_B being the Bohr magneton), $\mathbf{n} = (n_1, n_2, n_3)^T \in \mathbb{R}^3$ is the dipole axis (or dipole moment) which is a given unit vector, i.e. $|\mathbf{n}| = \sqrt{n_1^2 + n_2^2 + n_3^2} = 1$, and θ is the angle between the dipole axis \mathbf{n} and the vector \mathbf{x} . The wave function is normalized according to

$$\|\psi\|_2^2 := \int_{\mathbb{R}^3} |\psi(\mathbf{x}, t)|^2 d\mathbf{x} = N, \quad (8.3)$$

where N is the total number of dipolar particles in the dipolar BEC.

By introducing the dimensionless variables, $t \rightarrow \frac{t}{\omega_0}$ with $\omega_0 = \min\{\omega_x, \omega_y, \omega_z\}$, $\mathbf{x} \rightarrow x_s\mathbf{x}$ with $x_s = \sqrt{\frac{\hbar}{m\omega_0}}$, $\psi \rightarrow \frac{\sqrt{N}\psi}{x_s^{3/2}}$, we obtain the dimensionless GPE in 3D from (8.1) as :

$$i\partial_t\psi(\mathbf{x}, t) = \left[-\frac{1}{2}\nabla^2 + V(\mathbf{x}) + \beta|\psi|^2 + \lambda(U_{\text{dip}} * |\psi|^2) \right] \psi, \quad \mathbf{x} \in \mathbb{R}^3, \quad t > 0, \quad (8.4)$$

where $\beta = \frac{Ng}{\hbar\omega_0 x_s^3} = \frac{4\pi a_s N}{x_s}$, $\lambda = \frac{mN\mu_0\mu_{\text{dip}}^2}{3\hbar^2 x_s}$, $V(\mathbf{x}) = \frac{1}{2}(\gamma_x^2 x^2 + \gamma_y^2 y^2 + \gamma_z^2 z^2)$ is the dimensionless harmonic trapping potential with $\gamma_x = \frac{\omega_x}{\omega_0}$, $\gamma_y = \frac{\omega_y}{\omega_0}$ and $\gamma_z = \frac{\omega_z}{\omega_0}$, and the dimensionless long-range dipolar interaction potential $U_{\text{dip}}(\mathbf{x})$ is given as

$$U_{\text{dip}}(\mathbf{x}) = \frac{3}{4\pi} \frac{1 - 3(\mathbf{x} \cdot \mathbf{n})^2/|\mathbf{x}|^2}{|\mathbf{x}|^3} = \frac{3}{4\pi} \frac{1 - 3\cos^2(\theta)}{|\mathbf{x}|^3}, \quad \mathbf{x} \in \mathbb{R}^3. \quad (8.5)$$

Although the kernel U_{dip} is highly singular near the origin, the convolution is well-defined for $\rho \in L^p(\mathbb{R}^3)$ with $U_{\text{dip}} * \rho \in L^p(\mathbb{R}^3)$ for $p \in (1, \infty)$ [70].

Denote the differential operators $\partial_{\mathbf{n}} = \mathbf{n} \cdot \nabla$ and $\partial_{\mathbf{nn}} = \partial_{\mathbf{n}}\partial_{\mathbf{n}}$, and notice the identity [23]

$$U_{\text{dip}}(\mathbf{x}) = \frac{3}{4\pi|\mathbf{x}|^3} \left(1 - \frac{3(\mathbf{x} \cdot \mathbf{n})^2}{|\mathbf{x}|^2} \right) = -\delta(\mathbf{r}) - 3\partial_{\mathbf{nn}} \left(\frac{1}{4\pi|\mathbf{x}|} \right), \quad \mathbf{x} \in \mathbb{R}^3, \quad (8.6)$$

we can re-formulate the GPE (8.4) as the following Gross-Pitaevskii-Poisson system (GPPS) [18, 23, 65]

$$i\partial_t\psi(\mathbf{x}, t) = \left[-\frac{1}{2}\nabla^2 + V(\mathbf{x}) + (\beta - \lambda)|\psi|^2 - 3\lambda\partial_{\mathbf{nn}}\varphi \right] \psi, \quad \mathbf{x} \in \mathbb{R}^3, \quad t > 0, \quad (8.7)$$

$$\nabla^2\varphi(\mathbf{x}, t) = -|\psi(\mathbf{x}, t)|^2, \quad \mathbf{x} \in \mathbb{R}^3, \quad \lim_{|\mathbf{x}| \rightarrow \infty} \varphi(\mathbf{x}, t) = 0, \quad t \geq 0. \quad (8.8)$$

The above GPPS in 3D conserves the *mass*, or the *normalization* condition,

$$N(\psi(\cdot, t)) := \|\psi(\cdot, t)\|_2^2 = \int_{\mathbb{R}^3} |\psi(\mathbf{x}, t)|^2 d\mathbf{x} \equiv \int_{\mathbb{R}^3} |\psi(\mathbf{x}, 0)|^2 d\mathbf{x} = 1, \quad t \geq 0, \quad (8.9)$$

and *energy* per particle with $\varphi = \frac{1}{4\pi|\mathbf{x}|} * |\psi|^2$,

$$E_{3D}(\psi) = \int_{\mathbb{R}^3} \left[\frac{1}{2}|\nabla\psi|^2 + V(\mathbf{x})|\psi|^2 + \frac{\beta - \lambda}{2}|\psi|^4 + \frac{3\lambda}{2}|\partial_{\mathbf{n}}\nabla\varphi|^2 \right] d\mathbf{x}. \quad (8.10)$$

From (8.6), it is straightforward to get the Fourier transform of $U_{\text{dip}}(\mathbf{x})$ as

$$\widehat{(U_{\text{dip}})}(\xi) = -1 + \frac{3(\mathbf{n} \cdot \xi)^2}{|\xi|^2}, \quad \xi \in \mathbb{R}^3. \quad (8.11)$$

8.2. Dimension reduction. In many physical experiments of dipolar BECs, the condensates are confined with strong harmonic trap in one or two axis directions, resulting in a disk- or cigar-shaped dipolar BEC, respectively. Mathematically speaking, this corresponds to the anisotropic potentials $V(\mathbf{x})$ of the form:

Case I (disk-shaped), potential is strongly confined in vertical z direction with

$$V(\mathbf{x}) = V_2(x, y) + \frac{z^2}{2\varepsilon^4}, \quad \mathbf{x} \in \mathbb{R}^3, \quad (8.12)$$

Case II (cigar-shaped), potential is strongly confined in horizontal $\mathbf{x}_\perp = (x, y)^T \in \mathbb{R}^2$ plane with

$$V(\mathbf{x}) = V_1(z) + \frac{x^2 + y^2}{2\varepsilon^4}, \quad \mathbf{x} \in \mathbb{R}^3, \quad (8.13)$$

where $0 < \varepsilon \ll 1$ ($\varepsilon = 1/\gamma_z$ in Case I and $\varepsilon = 1/\gamma_r$ with $\gamma_x = \gamma_y = \gamma_r$ in Case II) is a small parameter describing the strength of confinement. In such cases, the above GPPS in 3D can be formally reduced to 2D and 1D, respectively [65].

In *Case I*, when $\varepsilon \rightarrow 0^+$, evolution of the solution $\psi(\mathbf{x}, t)$ of GPPS (8.7)-(8.8) in z -direction would essentially occur in the ground state mode of $-\frac{1}{2}\partial_{zz} + \frac{z^2}{2\varepsilon^4}$, which is spanned by $w_\varepsilon(z) = \varepsilon^{-1/2}\pi^{-1/4}e^{-\frac{z^2}{2\varepsilon^2}}$ [18, 65]. By taking the ansatz

$$\psi(\mathbf{x}_\perp, z, t) = e^{-it/2\varepsilon^2} \phi(\mathbf{x}_\perp, t) w_\varepsilon(z), \quad (\mathbf{x}_\perp, z)^T = (x, y, z)^T \in \mathbb{R}^3, \quad t \geq 0, \quad (8.14)$$

the 3D GPPS (8.7)-(8.8) can be formally reduced to a *quasi-2D equation I* [18, 65]:

$$i\partial_t\phi = \left[-\frac{1}{2}\nabla^2 + V_2 + \beta_{2D}|\phi|^2 - \frac{3\lambda}{2}(\partial_{\mathbf{n}_\perp\mathbf{n}_\perp} - n_3^2\nabla^2)\varphi^{2D} \right] \phi, \quad (8.15)$$

where $\beta_{2D} = \frac{\beta - \lambda + 3\lambda n_3^2}{\sqrt{2\pi}\varepsilon}$, $\mathbf{n}_\perp = (n_1, n_2)^T$, $\partial_{\mathbf{n}_\perp} = \mathbf{n}_\perp \cdot \nabla = \mathbf{n}_\perp \cdot (\partial_x, \partial_y)^T$, $\partial_{\mathbf{n}_\perp\mathbf{n}_\perp} = \partial_{\mathbf{n}_\perp}(\partial_{\mathbf{n}_\perp})$, $\nabla^2 = \partial_{xx} + \partial_{yy}$ and

$$\varphi^{2D}(x, y, t) = U_\varepsilon^{2D} * |\phi|^2, \quad U_\varepsilon^{2D}(x, y) = \frac{1}{2\sqrt{2\pi}^{3/2}} \int_{\mathbb{R}} \frac{e^{-s^2/2}}{\sqrt{x^2 + y^2 + \varepsilon^2 s^2}} ds. \quad (8.16)$$

In addition, as $\varepsilon \rightarrow 0^+$, φ^{2D} can be approximated by φ_∞^{2D} [65] as :

$$\varphi_\infty^{2D}(\mathbf{x}_\perp, t) = U_{\text{dip}}^{2D} * |\phi|^2, \quad \text{with} \quad U_{\text{dip}}^{2D}(\mathbf{x}_\perp) = \frac{1}{2\pi|\mathbf{x}_\perp|}, \quad (8.17)$$

which can be re-written as a fractional Poisson equation

$$(-\nabla^2)^{1/2} \varphi_\infty^{2D}(\mathbf{x}_\perp, t) = |\phi(\mathbf{x}_\perp, t)|^2, \quad \lim_{|\mathbf{x}_\perp| \rightarrow \infty} \varphi_\infty^{2D}(\mathbf{x}_\perp, t) = 0, \quad t \geq 0. \quad (8.18)$$

Thus an alternative *quasi-2D equation II* can be obtained as:

$$i\partial_t \phi = \left(-\frac{1}{2} \nabla^2 + V_2 + \beta_{2D} |\phi|^2 - \frac{3\lambda}{2} (\partial_{\mathbf{n}_\perp \mathbf{n}_\perp} - n_3^2 \nabla^2) (-\nabla^2)^{-\frac{1}{2}} (|\phi|^2) \right) \phi. \quad (8.19)$$

Similarly, in *Case II*, evolution of the solution $\psi(x, y, z, t)$ of GPPS (8.7)-(8.8) in (x, y) plane would essentially occur in the ground state mode of $-\frac{1}{2}(\partial_{xx} + \partial_{yy}) + \frac{x^2+y^2}{2\varepsilon^4}$, which is spanned by $w_\varepsilon(x, y) = \varepsilon^{-1} \pi^{-1/2} e^{-\frac{x^2+y^2}{2\varepsilon^2}}$ [18, 65]. Again, by taking the ansatz

$$\psi(x, y, z, t) = e^{-it/\varepsilon^2} \phi(z, t) w_\varepsilon(x, y), \quad t \geq 0, \quad (8.20)$$

the 3D GPPS (8.7)-(8.8) can be formally reduced to a *quasi-1D equation*:

$$i\partial_t \phi = \left[-\frac{1}{2} \partial_{zz} + V_1 + \beta_{1D} |\phi|^2 - \frac{3\lambda(3n_3^2 - 1)}{8\sqrt{2\pi}\varepsilon} \partial_{zz} \varphi^{1D} \right] \phi, \quad z \in \mathbb{R}, \quad t > 0, \quad (8.21)$$

where $\beta_{1D} = \frac{\beta + \frac{1}{2}\lambda(1-3n_3^2)}{2\pi\varepsilon^2}$ and

$$\varphi^{1D}(z, t) = U_\varepsilon^{1D} * |\phi|^2, \quad U_\varepsilon^{1D}(z) = \frac{\sqrt{2}e^{z^2/2\varepsilon^2}}{\sqrt{\pi}\varepsilon} \int_{|z|}^\infty e^{-s^2/2\varepsilon^2} ds. \quad (8.22)$$

Remark 8.1. To describe a rotating dipolar BEC, we only need to include the angular momentum term (5.2) in the dipolar GPE (8.1). Therefore, dimensionless rotating dipolar GPEs in 3D and quasi-2D regime are straightforward.

8.3. Theory for ground states. In this section, we report results for ground state of dipolar BECs. Denote unit sphere

$$S = X \cap \{u \in L^2(\mathbb{R}^d) \mid \|u\|_{L^2(\mathbb{R}^d)} = 1\}, \quad (8.23)$$

where X is the energy space associated with corresponding potential (2.6).

8.3.1. 3D case. In 3D, the ground state of GPPS (8.7)-(8.8) is the minimizer of energy E_{3D} (8.10) over the nonconvex set S [23].

Theorem 8.1. *Assume $V(\mathbf{x}) \geq 0$ for $\mathbf{x} \in \mathbb{R}^3$ and $\lim_{|\mathbf{x}| \rightarrow \infty} V(\mathbf{x}) = \infty$ (i.e., confining potential) in GPPS (8.7)-(8.8), then we have:*

(i) *If $\beta \geq 0$ and $-\frac{1}{2}\beta \leq \lambda \leq \beta$, there exists a ground state $\phi_g \in S$, and the positive ground state $|\phi_g|$ is unique. Moreover, $\phi_g = e^{i\theta_0} |\phi_g|$ for some constant $\theta_0 \in \mathbb{R}$.*

(ii) *If $\beta < 0$, or $\beta \geq 0$ and $\lambda < -\frac{1}{2}\beta$ or $\lambda > \beta$, there exists no ground state, i.e., $\inf_{\phi \in S} E_{3D}(\phi) = -\infty$.*

By splitting the total energy $E_{3D}(\cdot)$ in (8.10) into kinetic, potential, interaction and dipolar energies, i.e.

$$E_{3D}(\phi) = E_{\text{kin}}(\phi) + E_{\text{pot}}(\phi) + E_{\text{int}}(\phi) + E_{\text{dip}}(\phi), \quad (8.24)$$

where

$$\begin{aligned} E_{\text{kin}}(\phi) &= \frac{1}{2} \int_{\mathbb{R}^3} |\nabla \phi(\mathbf{x})|^2 d\mathbf{x}, \quad E_{\text{pot}}(\phi) = \int_{\mathbb{R}^3} V(\mathbf{x}) |\phi(\mathbf{x})|^2 d\mathbf{x}, \quad E_{\text{int}}(\phi) = \frac{\beta}{2} \int_{\mathbb{R}^3} |\phi(\mathbf{x})|^4 d\mathbf{x}, \\ E_{\text{dip}}(\phi) &= \frac{\lambda}{2} \int_{\mathbb{R}^3} (U_{\text{dip}} * |\phi|^2) |\phi(\mathbf{x})|^2 d\mathbf{x} = \frac{\lambda}{2} \int_{\mathbb{R}^3} |\phi(\mathbf{x})|^2 [-|\phi(\mathbf{x})|^2 - 3\partial_{\mathbf{nn}}\varphi] d\mathbf{x} \quad (8.25) \\ &= \frac{\lambda}{2} \int_{\mathbb{R}^3} [-|\phi(\mathbf{x})|^4 + 3(\nabla^2\varphi)(\partial_{\mathbf{nn}}\varphi)] d\mathbf{x} = \frac{\lambda}{2} \int_{\mathbb{R}^3} [-|\phi(\mathbf{x})|^4 + 3|\partial_{\mathbf{n}}\nabla\varphi|^2] d\mathbf{x}, \end{aligned}$$

with $\varphi = \frac{1}{4\pi|\mathbf{x}|} * |\phi|^2$, we have the following Viral identity [23]:

Proposition 8.1. *Suppose $V(\lambda\mathbf{x}) = \lambda^2 V(\mathbf{x})$ for all $\lambda \in \mathbb{R}$ and ϕ_g is the ground state of a dipolar BEC, i.e., the minimizer of energy (8.10) under the normalization constraint (8.9), then we have*

$$2E_{\text{kin}}(\phi_e) - 2E_{\text{pot}}(\phi_e) + 3E_{\text{int}}(\phi_e) + 3E_{\text{dip}}(\phi_e) = 0. \quad (8.26)$$

8.3.2. *Quasi-2D case I.* Associated to the quasi-2D equation I (8.15)-(8.16), the energy is

$$E_{2\text{D}}(\phi) = \int_{\mathbb{R}^2} \left[\frac{1}{2} |\nabla \phi|^2 + V_2(\mathbf{x}_{\perp}) |\phi|^2 + \beta_{2\text{D}} |\phi|^4 - \frac{3\lambda}{4} |\phi|^2 \widetilde{\varphi}^{2\text{D}} \right] d\mathbf{x}_{\perp}, \quad \phi \in X, \quad (8.27)$$

where $\beta_{2\text{D}} = \frac{\beta - \lambda + 3\lambda n_3^2}{\sqrt{2\pi}\varepsilon}$ and

$$\widetilde{\varphi}^{2\text{D}} = (\partial_{\mathbf{n}_{\perp}\mathbf{n}_{\perp}} - n_3^2 \nabla^2) \varphi^{2\text{D}}, \quad \varphi^{2\text{D}} = U_{\varepsilon}^{2\text{D}} * |\phi|^2. \quad (8.28)$$

The ground state $\phi_g \in S$ of (8.15) is the minimizer of the nonconvex minimization problem [18]:

$$\text{Find } \phi_g \in S, \quad \text{such that } E_{2\text{D}}(\phi_g) = \min_{\phi \in S} E_{2\text{D}}(\phi). \quad (8.29)$$

Theorem 8.2. *Assume $0 \leq V_2(\mathbf{x}_{\perp})$ and $\lim_{|\mathbf{x}_{\perp}| \rightarrow \infty} V_2(\mathbf{x}_{\perp}) = \infty$, then we have*

(i) *There exists a ground state $\phi_g \in S$ of the system (8.15)-(8.16) if one of the following conditions holds*

- (A1) $\lambda \geq 0$ and $\beta - \lambda > -\sqrt{2\pi} C_b \varepsilon$;
- (A2) $\lambda < 0$ and $\beta + \frac{1}{2}(1 + 3|2n_3^2 - 1|)\lambda > -\sqrt{2\pi} C_b \varepsilon$,

where C_b is given in (2.12).

(ii) *The positive ground state $|\phi_g|$ is unique under one of the following conditions:*

- (A1') $\lambda \geq 0$ and $\beta - \lambda \geq 0$;
- (A2') $\lambda < 0$ and $\beta + \frac{1}{2}(1 + 3|2n_3^2 - 1|)\lambda \geq 0$.

Moreover, any ground state is of the form $\phi_g = e^{i\theta_0} |\phi_g|$ for some constant $\theta_0 \in \mathbb{R}$.

(iii) *If $\beta + \frac{1}{2}\lambda(1 - 3n_3^2) < -\sqrt{2\pi} C_b \varepsilon$, there exists no ground state of Eq. (8.15).*

8.3.3. *Quasi-2D case II.* Associated to the quasi-2D equation II (8.19), the energy is

$$\tilde{E}_{2\text{D}}(\phi) = \int_{\mathbb{R}^2} \left[\frac{1}{2} |\nabla \phi|^2 + V_2(\mathbf{x}_{\perp}) |\phi|^2 + \beta_{2\text{D}} |\phi|^4 - \frac{3\lambda}{4} |\phi|^2 \varphi \right] d\mathbf{x}, \quad \phi \in X, \quad (8.30)$$

where

$$\varphi(\mathbf{x}_{\perp}) = (\partial_{\mathbf{n}_{\perp}\mathbf{n}_{\perp}} - n_3^2 \nabla^2) ((-\nabla^2)^{-1/2} |\phi|^2). \quad (8.31)$$

The ground state $\phi_g \in S$ of the equation (8.19) is defined as the minimizer of the nonconvex minimization problem:

$$\text{Find } \phi_g \in S, \quad \text{such that } \tilde{E}_{2\text{D}}(\phi_g) = \min_{\phi \in S} \tilde{E}_{2\text{D}}(\phi). \quad (8.32)$$

For the above ground state, we have the following results [18].

Theorem 8.3. *Assume $0 \leq V_2(\mathbf{x}_\perp)$ and $\lim_{|\mathbf{x}_\perp| \rightarrow \infty} V_2(\mathbf{x}_\perp) = \infty$, then we have*

(i) *There exists a ground state $\phi_g \in S$ of the equation (8.19) if one of the following conditions holds*

- (B1) $\lambda = 0$ and $\beta > -\sqrt{2\pi}C_b \varepsilon$;
- (B2) $\lambda > 0$, $n_3 = 0$ and $\beta - \lambda > -\sqrt{2\pi}C_b \varepsilon$;
- (B3) $\lambda < 0$, $n_3^2 \geq \frac{1}{2}$ and $\beta - (1 - 3n_3^2)\lambda > -\sqrt{2\pi}C_b \varepsilon$.

(ii) *The positive ground state $|\phi_g|$ is unique under one of the following conditions*

- (B1') $\lambda = 0$ and $\beta \geq 0$;
- (B2') $\lambda > 0$, $n_3 = 0$ and $\beta \geq \lambda$;
- (B3') $\lambda < 0$, $n_3^2 \geq \frac{1}{2}$ and $\beta - (1 - 3n_3^2)\lambda \geq 0$.

Moreover, any ground state $\phi_g = e^{i\theta_0}|\phi_g|$ for some constant $\theta_0 \in \mathbb{R}$.

(iii) *There exists no ground state of the equation (8.19) if one of the following conditions holds*

- (B1'') $\lambda > 0$ and $n_3 \neq 0$;
- (B2'') $\lambda < 0$ and $n_3^2 < \frac{1}{2}$;
- (B3'') $\lambda = 0$ and $\beta < -\sqrt{2\pi}C_b \varepsilon$.

8.3.4. *Quasi-1D case.* Associated to the quasi-1D equation (8.21), the energy is

$$E_{1D}(\phi) = \int_{\mathbb{R}} \left[\frac{1}{2} |\partial_z \phi|^2 + V_1(z) |\phi|^2 + \frac{1}{2} \beta_{1D} |\phi|^4 + \frac{3\lambda(1 - 3n_3^2)}{16\sqrt{2\pi}\varepsilon} |\phi|^2 \varphi \right] dz, \quad (8.33)$$

where $\beta_{1D} = \frac{\beta + \frac{1}{2}\lambda(1 - 3n_3^2)}{2\pi\varepsilon^2}$ and

$$\varphi(z) = \partial_{zz}(U_\varepsilon^{1D} * |\phi|^2), \quad U_\varepsilon^{1D}(z) = \frac{2e^{-\frac{z^2}{2\varepsilon^2}}}{\sqrt{\pi}} \int_{|z|}^{\infty} e^{-\frac{s^2}{2\varepsilon^2}} ds. \quad (8.34)$$

Again, the ground state $\phi_g \in S$ of the equation (8.21) is defined as the minimizer of the nonconvex minimization problem:

$$\text{Find } \phi_g \in S, \quad \text{such that } E_{1D}(\phi_g) = \min_{\phi \in S} E_{1D}(\phi). \quad (8.35)$$

For the above ground state, we have the following results [18].

Theorem 8.4. *(Existence and uniqueness of ground state) Assume $0 \leq V_1(z)$ and $\lim_{|z| \rightarrow \infty} V_1(z) = \infty$, for any parameter β , λ and ε , there exists a ground state $\phi_g \in S$ of the quasi-1D equation (8.21)-(8.22), and the positive ground state $|\phi_g|$ is unique under one of the following conditions:*

- (C1) $\lambda(1 - 3n_3^2) \geq 0$ and $\beta - (1 - 3n_3^2)\lambda \geq 0$;
- (C2) $\lambda(1 - 3n_3^2) < 0$ and $\beta + \frac{\lambda}{2}(1 - 3n_3^2) \geq 0$.

Moreover, $\phi_g = e^{i\theta_0}|\phi_g|$ for some constant $\theta_0 \in \mathbb{R}$.

8.4. **Well-posedness for dynamics.** In this section, we study the well-posedness for dynamics of dipolar BECs.

8.4.1. *3D case.* In 3D, we have the following results for GPPS (8.7)-(8.8) [23].

Theorem 8.5. *(Well-posedness) Suppose the real-valued trap potential $V(\mathbf{x}) \in C^\infty(\mathbb{R}^3)$ such that $V(\mathbf{x}) \geq 0$ for $\mathbf{x} \in \mathbb{R}^3$ and $D^\alpha V(\mathbf{x}) \in L^\infty(\mathbb{R}^3)$ for all $\alpha \in \mathbb{N}_0^3$ with $|\alpha| \geq 2$. For any initial data $\psi(\mathbf{x}, t = 0) = \psi_0(\mathbf{x}) \in X$, there exists*

$T_{\max} \in (0, +\infty]$ such that the problem (8.7)-(8.8) has a unique maximal solution $\psi \in C([0, T_{\max}), X)$. It is maximal in the sense that if $T_{\max} < \infty$, then $\|\psi(\cdot, t)\|_X \rightarrow \infty$ when $t \rightarrow T_{\max}^-$. Moreover, the mass $N(\psi(\cdot, t))$ and energy $E_{3D}(\psi(\cdot, t))$ defined in (8.9) and (8.10), respectively, are conserved for $t \in [0, T_{\max})$. Specifically, if $\beta \geq 0$ and $-\frac{1}{2}\beta \leq \lambda \leq \beta$, the solution to (8.7)-(8.8) is global in time, i.e., $T_{\max} = \infty$.

Theorem 8.6. (Finite time blow-up) If $\beta < 0$, or $\beta \geq 0$ and $\lambda < -\frac{1}{2}\beta$ or $\lambda > \beta$, and assume $V(\mathbf{x})$ satisfies $3V(\mathbf{x}) + \mathbf{x} \cdot \nabla V(\mathbf{x}) \geq 0$ for $\mathbf{x} \in \mathbb{R}^3$. For any initial data $\psi(\mathbf{x}, t = 0) = \psi_0(\mathbf{x}) \in X$ to the problem (8.7)-(8.8), there exists finite time blow-up, i.e., $T_{\max} < \infty$, if one of the following holds:

- (i) $E_{3D}(\psi_0) < 0$;
- (ii) $E_{3D}(\psi_0) = 0$ and $\text{Im} \left(\int_{\mathbb{R}^3} \bar{\psi}_0(\mathbf{x}) (\mathbf{x} \cdot \nabla \psi_0(\mathbf{x})) d\mathbf{x} \right) < 0$;
- (iii) $E_{3D}(\psi_0) > 0$ and $\text{Im} \left(\int_{\mathbb{R}^3} \bar{\psi}_0(\mathbf{x}) (\mathbf{x} \cdot \nabla \psi_0(\mathbf{x})) d\mathbf{x} \right) < -\sqrt{3E_{3D}(\psi_0)} \|\mathbf{x}\psi_0\|_{L^2}$.

8.4.2. *Quasi-2D case I.* For quasi-2D equation I (8.15)-(8.16), we have the following results [18].

Theorem 8.7. (Well-posedness of Cauchy problem) Suppose the real-valued trap potential satisfies $V_2(\mathbf{x}_\perp) \geq 0$ for $\mathbf{x}_\perp \in \mathbb{R}^2$ and

$$V_2(\mathbf{x}_\perp) \in C^\infty(\mathbb{R}^2) \text{ and } D^{\mathbf{k}}V_2(\mathbf{x}_\perp) \in L^\infty(\mathbb{R}^2), \quad \text{for all } \mathbf{k} \in \mathbb{N}_0^2 \text{ with } |\mathbf{k}| \geq 2, \quad (8.36)$$

then we have

(i) For any initial data $\phi(\mathbf{x}_\perp, t = 0) = \phi_0(\mathbf{x}_\perp) \in X$, there exists a $T_{\max} \in (0, +\infty]$ such that the problem (8.15)-(8.16) has a unique maximal solution $\phi \in C([0, T_{\max}), X)$. It is maximal in the sense that if $T_{\max} < \infty$, then $\|\phi(\cdot, t)\|_X \rightarrow \infty$ when $t \rightarrow T_{\max}^-$.

(ii) As long as the solution $\phi(\mathbf{x}_\perp, t)$ remains in the energy space X , the L^2 -norm $\|\phi(\cdot, t)\|_2$ and energy $E_{2D}(\phi(\cdot, t))$ in (8.27) are conserved for $t \in [0, T_{\max})$.

(iii) Under either condition (A1) or (A2) in Theorem 8.2 with constant C_b being replaced by $C_b/\|\phi_0\|_2^2$, the solution of (8.15)-(8.16) is global in time, i.e., $T_{\max} = \infty$.

Theorem 8.8. (Finite time blow-up) For any initial data $\phi(\mathbf{x}_\perp, t = 0) = \phi_0(\mathbf{x}_\perp) \in X$ with $\int_{\mathbb{R}^2} |\mathbf{x}_\perp|^2 |\phi_0(\mathbf{x}_\perp)|^2 d\mathbf{x}_\perp < \infty$, if conditions (A1) and (A2) with constant C_b being replaced by $C_b/\|\phi_0\|_2^2$ are not satisfied and assume $V_2(\mathbf{x}_\perp)$ satisfies $2V_2(\mathbf{x}_\perp) + \mathbf{x}_\perp \cdot \nabla V_2(\mathbf{x}_\perp) \geq 0$, and let $\phi := \phi(\mathbf{x}_\perp, t)$ be the solution of the problem (8.15), there exists finite time blow-up, i.e., $T_{\max} < \infty$, if $\lambda = 0$, or $\lambda > 0$ and $n_3^2 \geq \frac{1}{2}$, and one of the following holds:

- (i) $E_{2D}(\phi_0) < 0$;
- (ii) $E_{2D}(\phi_0) = 0$ and $\text{Im} \left(\int_{\mathbb{R}^2} \bar{\phi}_0(\mathbf{x}_\perp) (\mathbf{x}_\perp \cdot \nabla \phi_0(\mathbf{x}_\perp)) d\mathbf{x}_\perp \right) < 0$;
- (iii) $E_{2D}(\phi_0) > 0$ and $\text{Im} \left(\int_{\mathbb{R}^2} \bar{\phi}_0(\mathbf{x}_\perp) (\mathbf{x}_\perp \cdot \nabla \phi_0(\mathbf{x}_\perp)) d\mathbf{x}_\perp \right) < -\sqrt{2E_{2D}(\phi_0)} \|\mathbf{x}_\perp \phi_0\|_2$.

8.4.3. *Quasi-2D case II.* For quasi-2D equation II (8.19), noticing the nonlinearity $\phi(\partial_{\mathbf{n}_\perp \mathbf{n}_\perp} - n_3^2 \nabla^2)((-\nabla^2)^{-1/2} |\phi|^2)$ is actually a derivative nonlinearity, it would bring significant difficulty in analyzing the dynamic behavior. The Cauchy problem of the Schrödinger equation with derivative nonlinearity has been investigated extensively in the literatures [115, 125]. We are able to prove the existence results in the energy space with the special structure of our nonlinearity [18].

Theorem 8.9. (Existence for Cauchy problem) Suppose the real potential $V_2(\mathbf{x}_\perp)$ satisfies (8.36) and $\lim_{|\mathbf{x}_\perp| \rightarrow \infty} V_2(\mathbf{x}_\perp) = \infty$, and initial value $\phi_0(\mathbf{x}_\perp) \in X$, either condition (B2) or (B3) in Theorem 8.3 holds with constant C_b being replaced by

$C_b/\|\phi_0\|_2^2$, then there exists a solution $\phi \in L^\infty([0, \infty); X) \cap W^{1,\infty}([0, \infty); X^*)$ for the Cauchy problem of (8.19). Here X^* denotes the dual space of X . Moreover, there holds for L^2 norm and energy \tilde{E}_{2D} (8.30) conservation, i.e.

$$\|\phi(\cdot, t)\|_{L^2(\mathbb{R}^2)} = \|\phi_0\|_{L^2(\mathbb{R}^2)}, \quad \tilde{E}_{2D}(\phi(\cdot, t)) \leq \tilde{E}_{2D}(\phi_0), \quad \forall t \geq 0. \quad (8.37)$$

Next, we discuss possible finite time blow-up for the continuous solutions of the quasi-2D equation II (8.19). To this purpose, the following assumptions are introduced:

(A) Assumption on the trap and coefficient of the cubic term, i.e. $V_2(\mathbf{x}_\perp)$ satisfies $3V_2(\mathbf{x}_\perp) + \mathbf{x}_\perp \cdot \nabla V_2(\mathbf{x}_\perp) \geq 0$, $\frac{\beta - \lambda + 3\lambda n_3^2}{\sqrt{2\pi}\varepsilon} \geq -\frac{C_b}{\|\phi_0\|_2^2}$, with ϕ_0 being the initial data of equation (8.19);

(B) Assumption on the trap and coefficient of the nonlocal term, i.e. $V_2(\mathbf{x}_\perp)$ satisfies $2V_2(\mathbf{x}_\perp) + \mathbf{x}_\perp \cdot \nabla V_2(\mathbf{x}_\perp) \geq 0$, $\lambda = 0$ or $\lambda > 0$ and $n_3^2 \geq \frac{1}{2}$.

Theorem 8.10. (*Finite time blow-up*) For any initial data $\phi(\mathbf{x}_\perp, t = 0) = \phi_0(\mathbf{x}_\perp) \in X$ with finite variance $\delta_V^0 = \int_{\mathbb{R}^2} |\mathbf{x}_\perp|^2 |\phi_0(\mathbf{x}_\perp)|^2 d\mathbf{x}_\perp < \infty$, if conditions (B1), (B2) and (B3) with constant C_b being replaced by $C_b/\|\phi_0\|_2^2$ are not satisfied, let $\phi := \phi(\mathbf{x}_\perp, t) \in C([0, T_{\max}), X)$ solution of the problem (8.19) with L^2 norm and energy conservation, then there exists finite time blow-up, i.e., $T_{\max} < \infty$, if one of the following condition holds:

- (i) $\tilde{E}_{2D}(\phi_0) < 0$, and either Assumption (A) or (B) holds;
- (ii) $\tilde{E}_{2D}(\phi_0) = 0$ and $\text{Im} \left(\int_{\mathbb{R}^2} \bar{\phi}_0(\mathbf{x}_\perp) (\mathbf{x}_\perp \cdot \nabla \phi_0(\mathbf{x}_\perp)) d\mathbf{x}_\perp \right) < 0$, and either Assumption (A) or (B) holds;
- (iii) $\tilde{E}_{2D}(\phi_0) > 0$, and $\text{Im} \left(\int_{\mathbb{R}^2} \bar{\phi}_0(\mathbf{x}_\perp) (\mathbf{x}_\perp \cdot \nabla \phi_0(\mathbf{x}_\perp)) d\mathbf{x}_\perp \right) < -(3\tilde{E}_{2D}^0)^{1/2} \delta_V^0$ if Assumption (A) holds, or $\text{Im} \left(\int_{\mathbb{R}^2} \bar{\phi}_0(\mathbf{x}_\perp) (\mathbf{x}_\perp \cdot \nabla \phi_0(\mathbf{x}_\perp)) d\mathbf{x}_\perp \right) < -(2\tilde{E}_{2D}^0)^{1/2} \delta_V^0$ if Assumption (B) holds. Here $\tilde{E}_{2D}^0 = \tilde{E}_{2D}(\phi_0)$.

8.4.4. *Quasi-1D case.* Concerning the Cauchy problem, similar results as Theorem 8.7 can be obtained for the equation (8.21) [18].

Theorem 8.11. (*Well-posedness for Cauchy problem*) Suppose the real-valued trap potential satisfies $V_1(z) \geq 0$ for $z \in \mathbb{R}$ and $V_1(z) \in C^\infty(\mathbb{R})$, $D^k V_1(z) \in L^\infty(\mathbb{R})$ for all integers $k \geq 2$, for any initial data $\phi(z, t = 0) = \phi_0(z) \in X$, there exists a unique solution $\phi \in C([0, \infty), X) \cap C^1([0, \infty), X^*)$ to the Cauchy problem of equation (8.21).

8.5. Convergence rate of dimension reduction. In this section, we discuss the dimension reduction of 3D GPPS to lower dimensions. In lower dimensions, we require that in the quasi-2D case, $\beta = O(\varepsilon)$, $\lambda = O(\varepsilon)$, and in the quasi-1D case, $\beta = O(\varepsilon^2)$, $\lambda = O(\varepsilon^2)$, i.e. we are considering the weak interaction regime, then we would get an ε -independent limiting equation. In this regime, we will see that GPPS will reduce to a regular GPE in lower dimensions [18].

8.5.1. *Reduction to 2D.* We consider the weak interaction regime, i.e., $\beta \rightarrow \varepsilon\beta$, $\lambda \rightarrow \varepsilon\lambda$. In Case I (8.12), for full 3D GPPS (8.7)-(8.8), introduce the re-scaling $z \rightarrow \varepsilon z$, $\psi \rightarrow \varepsilon^{-1/2} \psi^\varepsilon$ which preserves the normalization, then

$$i\partial_t \psi^\varepsilon(\mathbf{x}_\perp, z, t) = \left[\mathbf{H}_{\mathbf{x}_\perp}^V + \frac{1}{\varepsilon^2} \mathbf{H}_z + (\beta - \lambda) |\psi^\varepsilon|^2 - 3\varepsilon\lambda \partial_{\mathbf{n}_\varepsilon \mathbf{n}_\varepsilon} \varphi^\varepsilon \right] \psi^\varepsilon, \quad (8.38)$$

where $\mathbf{x}_\perp = (x, y) \in \mathbb{R}^2$ and

$$\mathbf{H}_{\mathbf{x}_\perp}^V = -\frac{1}{2}(\partial_{xx} + \partial_{yy}) + V_2(x, y), \quad \mathbf{H}_z = -\frac{1}{2}\partial_{zz} + \frac{z^2}{2}, \quad (8.39)$$

$$\mathbf{n}_\varepsilon = (n_1, n_2, n_3/\varepsilon), \quad \partial_{\mathbf{n}_\varepsilon} = \mathbf{n}_\varepsilon \cdot \nabla, \quad \partial_{\mathbf{n}_\varepsilon \mathbf{n}_\varepsilon} = \partial_{\mathbf{n}_\varepsilon}(\partial_{\mathbf{n}_\varepsilon}), \quad (8.40)$$

$$(-\partial_{xx} - \partial_{yy} - \frac{1}{\varepsilon^2}\partial_{zz})\varphi^\varepsilon = \frac{1}{\varepsilon}|\psi^\varepsilon|^2, \quad \lim_{|\mathbf{x}| \rightarrow \infty} \varphi^\varepsilon(\mathbf{x}_\perp, z, t) = 0. \quad (8.41)$$

It is well-known that \mathbf{H}_z has eigenvalues $\mu_k = k + 1/2$ with corresponding eigenfunction $w_k(z)$ ($k = 0, 1, \dots$), where $\{w_k\}_{k=0}^\infty$ forms an orthonormal basis of $L^2(\mathbb{R})$ [174], specifically, $w_0(z) = \frac{1}{\pi^{1/4}}e^{-z^2/2}$. It is convenient to consider the initial data concentrated on the ground mode of \mathbf{H}_z , i.e.,

$$\psi^\varepsilon(\mathbf{x}_\perp, z, 0) = \phi_0(\mathbf{x}_\perp)w_0(z), \quad \phi_0 \in X(\mathbb{R}^2) \text{ and } \|\phi_0\|_{L^2(\mathbb{R}^2)} = 1. \quad (8.42)$$

In Case I (8.12), when $\varepsilon \rightarrow 0^+$, quasi-2D equation I (8.15), II (8.19) will yield an ε -independent equation in the weak interaction regime,

$$i\partial_t \phi(\mathbf{x}_\perp, t) = \mathbf{H}_{\mathbf{x}_\perp}^V \phi + \frac{\beta - (1 - 3n_3^2)\lambda}{\sqrt{2\pi}} |\phi|^2 \phi, \quad \mathbf{x}_\perp = (x, y) \in \mathbb{R}^2, \quad (8.43)$$

with initial condition $\phi(\mathbf{x}_\perp, 0) = \phi_0(\mathbf{x}_\perp)$.

Theorem 8.12. (*Dimension reduction to 2D*) Suppose V_2 satisfies condition (8.36), $-\frac{\beta}{2} \leq \lambda \leq \beta$ and $\beta \geq 0$, let $\psi^\varepsilon \in C([0, \infty); X(\mathbb{R}^3))$ and $\phi \in C([0, \infty); X(\mathbb{R}^2))$ be the unique solutions of equations (8.38)-(8.42) and (8.43), respectively, then for any $T > 0$, there exists $C_T > 0$ such that

$$\left\| \psi^\varepsilon(\mathbf{x}_\perp, z, t) - e^{-i\frac{\mu_0 t}{\varepsilon^2}} \phi(\mathbf{x}_\perp, t)w_0(z) \right\|_{L^2(\mathbb{R}^3)} \leq C_T \varepsilon, \quad \forall t \in [0, T]. \quad (8.44)$$

8.5.2. *Reduction to 1D.* In this case, we again consider the weak interaction regime $\beta \rightarrow \varepsilon^2\beta$, $\lambda \rightarrow \varepsilon^2\lambda$. In Case II (8.13), for the full 3D GPPS (8.7)-(8.8), introducing the re-scaling $x \rightarrow \varepsilon x$, $y \rightarrow \varepsilon y$, $\psi \rightarrow \varepsilon^{-1}\psi^\varepsilon$ which preserves the normalization, then

$$i\partial_t \psi^\varepsilon(\mathbf{x}_\perp, z, t) = \left[\mathbf{H}_z^V + \frac{1}{\varepsilon^2} \mathbf{H}_{\mathbf{x}_\perp} + (\beta - \lambda)|\psi^\varepsilon|^2 - 3\varepsilon\lambda \partial_{\tilde{\mathbf{n}}_\varepsilon} \varphi^\varepsilon \right] \psi^\varepsilon, \quad (8.45)$$

where $\mathbf{x}_\perp = (x, y) \in \mathbb{R}^2$, $z \in \mathbb{R}$ and

$$\mathbf{H}_z^V = -\frac{1}{2}\partial_{zz} + V_1(z), \quad \mathbf{H}_{\mathbf{x}_\perp} = -\frac{1}{2}(\partial_{xx} + \partial_{yy} + x^2 + y^2), \quad (8.46)$$

$$\tilde{\mathbf{n}}_\varepsilon = (n_1/\varepsilon, n_2/\varepsilon, n_3), \quad \partial_{\tilde{\mathbf{n}}_\varepsilon} = \tilde{\mathbf{n}}_\varepsilon \cdot \nabla, \quad \partial_{\tilde{\mathbf{n}}_\varepsilon \tilde{\mathbf{n}}_\varepsilon} = \partial_{\tilde{\mathbf{n}}_\varepsilon}(\partial_{\tilde{\mathbf{n}}_\varepsilon}), \quad (8.47)$$

$$\left(-\frac{1}{\varepsilon^2}\partial_{xx} - \frac{1}{\varepsilon^2}\partial_{yy} - \partial_{zz}\right)\varphi^\varepsilon = \frac{1}{\varepsilon^2}|\psi^\varepsilon|^2, \quad \lim_{|\mathbf{x}| \rightarrow \infty} \varphi^\varepsilon(\mathbf{x}_\perp, z, t) = 0. \quad (8.48)$$

Note that the ground state mode of $\mathbf{H}_{\mathbf{x}_\perp}$ is given by $w_0(x)w_0(y)$ with eigenvalue 1, and the initial data is then assumed to be

$$\psi^\varepsilon(\mathbf{x}_\perp, z, 0) = \phi_0(z)w_0(x)w_0(y), \quad \phi_0 \in X(\mathbb{R}) \text{ and } \|\phi_0\|_{L^2(\mathbb{R})} = 1. \quad (8.49)$$

In Case II (8.13), when $\varepsilon \rightarrow 0^+$, the quasi-1D equation (8.21) will lead to an ε -independent equation in the weak interaction regime,

$$i\partial_t \phi(z, t) = \mathbf{H}_z^V \phi + \frac{\beta + \frac{1}{2}\lambda(1 - 3n_3^2)}{2\pi} |\phi|^2 \phi, \quad z \in \mathbb{R}, \quad t > 0, \quad (8.50)$$

with the initial condition $\phi(z, 0) = \phi_0(z)$.

We can prove the following results [18].

Theorem 8.13. (*Dimension reduction to 1D*) Suppose the real-valued trap potential satisfies $V_1(z) \geq 0$ for $z \in \mathbb{R}$ and $V_1(z) \in C^\infty(\mathbb{R})$, $D^k V_1(z) \in L^\infty(\mathbb{R})$ for all $k \geq 2$. Assume $-\frac{\beta}{2} \leq \lambda \leq \beta$ and $\beta \geq 0$, and let $\psi^\varepsilon \in C([0, \infty); X(\mathbb{R}^3))$ and $\phi \in C([0, \infty); X(\mathbb{R}))$ be the unique solutions of the equations (8.45)-(8.49) and (8.50), respectively, then for any $T > 0$, there exists $C_T > 0$ such that

$$\left\| \psi^\varepsilon(\mathbf{x}_\perp, z, t) - e^{-it/\varepsilon^2} \phi(z, t) w_0(x) w_0(y) \right\|_{L^2(\mathbb{R}^3)} \leq C_T \varepsilon, \quad \forall t \in [0, T]. \quad (8.51)$$

8.6. Numerical methods for computing ground states. In this section, we present efficient and accurate numerical methods for computing ground states of dipolar BECs, based on the new formulation GPPS (8.7)-(8.8) of dipolar GPE (8.4) in 3D.

The difficulty of computing dipolar GPE mainly comes from the dipolar term. In most of the numerical methods used in the literatures for theoretically and/or numerically studying the ground states of dipolar BECs, the way to deal with the convolution in (8.4) is usually to use the Fourier transform [154, 186]. However, due to the high singularity in the dipolar interaction potential (8.5), there are two drawbacks in these numerical methods: (i) the Fourier transforms of the dipolar interaction potential (8.5) and the density function $|\psi|^2$ are usually carried out in the continuous level on the whole space \mathbb{R}^3 and in the discrete level on a bounded computational domain U , respectively, and due to this mismatch, there is a locking phenomena in practical computation as observed in [154]; (ii) the second term in the Fourier transform of the dipolar interaction potential is $\frac{0}{0}$ -type for 0-mode, i.e when $\xi = 0$ (see (8.11) for details), and it is artificially omitted when $\xi = 0$ in practical computation [154, 186, 188] thus this may cause some numerical problems too. With formulation (8.7)-(8.8), new numerical methods for computing ground states and dynamics of dipolar BECs can be constructed, which can avoid the above two drawbacks and thus they are more accurate than those currently used in the literatures.

Based on the new mathematical formulation for the energy associated with GPPS (8.7)-(8.8) in (8.10), we will present an efficient and accurate backward Euler sine pseudospectral (BESP) method for computing the ground states of a dipolar BEC.

In practice, the whole space problem is usually truncated into a bounded computational domain $U = [a, b] \times [c, d] \times [e, f]$ with homogeneous Dirichlet boundary condition. We adopt the method of gradient flow with discrete normalization (GFDN) as in section 3: choose a time step $\tau > 0$ and set $t_n = n \tau$ for $n = 0, 1, \dots$. Applying the steepest decent method to the energy functional $E_{3D}(\phi)$ in (8.10) without the normalization constraint (8.9), and then projecting the solution back to the unit sphere S at the end of each time interval $[t_n, t_{n+1}]$ in order to satisfy the constraint (8.9). Then GFDN for computing ground state of the GPPS (8.7)-(8.8) is [23]:

$$\partial_t \phi(\mathbf{x}, t) = \left[\frac{1}{2} \nabla^2 - V(\mathbf{x}) - (\beta - \lambda) |\phi(\mathbf{x}, t)|^2 + 3\lambda \partial_{\mathbf{nn}} \varphi(\mathbf{x}, t) \right] \phi(\mathbf{x}, t), \quad (8.52)$$

$$\nabla^2 \varphi(\mathbf{x}, t) = -|\phi(\mathbf{x}, t)|^2, \quad \mathbf{x} \in U, \quad t_n \leq t < t_{n+1}, \quad (8.53)$$

$$\phi(\mathbf{x}, t_{n+1}) := \phi(\mathbf{x}, t_{n+1}^+) = \frac{\phi(\mathbf{x}, t_{n+1}^-)}{\|\phi(\cdot, t_{n+1}^-)\|_2}, \quad \mathbf{x} \in U, \quad n \geq 0, \quad (8.54)$$

$$\phi(\mathbf{x}, t)|_{\mathbf{x} \in \partial U} = \varphi(\mathbf{x}, t)|_{\mathbf{x} \in \partial U} = 0, \quad t \geq 0, \quad (8.55)$$

$$\phi(\mathbf{x}, 0) = \phi_0(\mathbf{x}), \quad \text{with } \|\phi_0\|_2 = 1; \quad (8.56)$$

where $\phi(\mathbf{x}, t_n^\pm) = \lim_{t \rightarrow t_n^\pm} \phi(\mathbf{x}, t)$.

Let M , K and L be even positive integers and define the index sets

$$\begin{aligned} \mathcal{T}_{MKL} &= \{(j, k, l) \mid j = 1, 2, \dots, M-1, k = 1, 2, \dots, K-1, l = 1, 2, \dots, L-1\}, \\ \mathcal{T}_{MKL}^0 &= \{(j, k, l) \mid j = 0, 1, \dots, M, k = 0, 1, \dots, K, l = 0, 1, \dots, L\}. \end{aligned}$$

Choose the spatial mesh sizes as $h_x = \frac{b-a}{M}$, $h_y = \frac{d-c}{K}$ and $h_z = \frac{f-e}{L}$ and define

$$x_j := a + j h_x, \quad y_k = c + k h_y, \quad z_l = e + l h_z, \quad (j, k, l) \in \mathcal{T}_{MKL}^0.$$

Denote the space

$$Y_{MKL} = \text{span}\{\Phi_{jkl}(\mathbf{x}), \quad (j, k, l) \in \mathcal{T}_{MKL}\},$$

with

$$\Phi_{jkl}(\mathbf{x}) = \sin(\mu_j^x(x-a)) \sin(\mu_k^y(y-c)) \sin(\mu_l^z(z-e)), \quad \mathbf{x} \in U, \quad (8.57)$$

$$\mu_j^x = \frac{\pi j}{b-a}, \quad \mu_k^y = \frac{\pi k}{d-c}, \quad \mu_l^z = \frac{\pi l}{f-e}, \quad (j, k, l) \in \mathcal{T}_{MKL};$$

and $P_{MKL} : Y = \{\varphi \in C(U) \mid \varphi(\mathbf{x})|_{\mathbf{x} \in \partial U} = 0\} \rightarrow Y_{MKL}$ be the standard project operator, i.e.

$$(P_{MKL}v)(\mathbf{x}) = \sum_{p=1}^{M-1} \sum_{q=1}^{K-1} \sum_{s=1}^{L-1} \hat{v}_{pqs} \Phi_{pqs}(\mathbf{x}), \quad \mathbf{x} \in U, \quad \forall v \in Y,$$

with

$$\hat{v}_{pqs} = \int_U v(\mathbf{x}) \Phi_{pqs}(\mathbf{x}) d\mathbf{x}, \quad (p, q, s) \in \mathcal{T}_{MKL}. \quad (8.58)$$

Then a backward Euler sine spectral discretization for (8.52)-(8.56) reads: Find $\phi^{n+1}(\mathbf{x}) \in Y_{MKL}$ (i.e. $\phi^+(\mathbf{x}) \in Y_{MKL}$) and $\varphi^n(\mathbf{x}) \in Y_{MKL}$ such that

$$\begin{aligned} \frac{\phi^+(\mathbf{x}) - \phi^n(\mathbf{x})}{\tau} &= -P_{MKL} \{ [V(\mathbf{x}) + (\beta - \lambda)|\phi^n(\mathbf{x})|^2 - 3\lambda \partial_{\mathbf{nn}} \varphi^n(\mathbf{x})] \phi^+(\mathbf{x}) \} \\ &\quad + \frac{1}{2} \nabla^2 \phi^+(\mathbf{x}), \end{aligned} \quad (8.59)$$

$$\nabla^2 \varphi^n(\mathbf{x}) = -P_{MKL} (|\phi^n(\mathbf{x})|^2), \quad \phi^{n+1}(\mathbf{x}) = \frac{\phi^+(\mathbf{x})}{\|\phi^+(\mathbf{x})\|_2}, \quad \mathbf{x} \in U, \quad (8.60)$$

where $n \geq 0$ and $\phi^0(\mathbf{x}) = P_{MKL}(\phi_0(\mathbf{x}))$ is given.

The above discretization can be solved in phase space and it is not suitable in practice due to the difficulty of computing the integrals in (8.58). We now present an efficient implementation by choosing $\phi^0(\mathbf{x})$ as the interpolation of $\phi_0(\mathbf{x})$ on the grid points $\{(x_j, y_k, z_l), (j, k, l) \in \mathcal{T}_{MKL}^0\}$, i.e. $\phi^0(x_j, y_k, z_l) = \phi_0(x_j, y_k, z_l)$ for $(j, k, l) \in \mathcal{T}_{MKL}^0$, and approximating the integrals in (8.58) by a quadrature rule on the grid points. Let ϕ_{jkl}^n and φ_{jkl}^n be the approximations of $\phi(x_j, y_k, z_l, t_n)$ and $\varphi(x_j, y_k, z_l, t_n)$, respectively, which are the solutions of (8.52)-(8.56); denote $V_{jkl} = V(x_j, y_k, z_l)$, $\rho_{jkl}^n = |\phi_{jkl}^n|^2$ and choose $\phi_{jkl}^0 = \phi_0(x_j, y_k, z_l)$ for $(j, k, l) \in \mathcal{T}_{MKL}^0$. For $n = 0, 1, \dots$, a backward Euler sine pseudospectral (BESP) discretization for

(8.52)-(8.56) reads [23]:

$$\begin{aligned} \frac{\phi_{jkl}^+ - \phi_{jkl}^n}{\tau} = & - \left[V_{jkl} + (\beta - \lambda) |\phi_{jkl}^n|^2 - 3\lambda (\partial_{\mathbf{nn}}^s \varphi^n)|_{jkl} \right] \phi_{jkl}^+ \\ & + \frac{1}{2} (\nabla_s^2 \phi^+)|_{jkl}, \quad (j, k, l) \in \mathcal{T}_{MKL}, \end{aligned} \quad (8.61)$$

$$- (\nabla_s^2 \varphi^n)|_{jkl} = |\phi_{j,k,l}^n|^2 = \rho_{jkl}^n, \quad \phi_{jkl}^{n+1} = \frac{\phi_{jkl}^+}{\|\phi^+\|_2}, \quad (j, k, l) \in \mathcal{T}_{MKL}, \quad (8.62)$$

$$\phi_{0kl}^{n+1} = \phi_{Mkl}^{n+1} = \phi_{j0l}^{n+1} = \phi_{jKl}^{n+1} = \phi_{jk0}^{n+1} = \phi_{jkL}^{n+1} = 0, \quad (j, k, l) \in \mathcal{T}_{MKL}^0, \quad (8.63)$$

$$\varphi_{0kl}^n = \varphi_{Mkl}^n = \varphi_{j0l}^n = \varphi_{jKl}^n = \varphi_{jk0}^n = \varphi_{jkL}^n = 0, \quad (j, k, l) \in \mathcal{T}_{MKL}^0; \quad (8.64)$$

where ∇_s^2 and $\partial_{\mathbf{nn}}^s$ are sine pseudospectral approximations of ∇^2 and $\partial_{\mathbf{nn}}$, respectively, defined for $(j, k, l) \in \mathcal{T}_{MKL}$ as

$$\begin{aligned} (\nabla_s^2 \phi^n)|_{jkl} = & - \sum_{p=1}^{M-1} \sum_{q=1}^{K-1} \sum_{s=1}^{L-1} \lambda_{pqs} (\widetilde{\phi^n})_{pqs} \sin\left(\frac{jp\pi}{M}\right) \sin\left(\frac{kq\pi}{K}\right) \sin\left(\frac{ls\pi}{L}\right), \\ (\partial_{\mathbf{nn}}^s \varphi^n)|_{jkl} = & \sum_{p=1}^{M-1} \sum_{q=1}^{K-1} \sum_{s=1}^{L-1} \frac{(\widetilde{\rho^n})_{pqs}}{(\mu_p^x)^2 + (\mu_q^y)^2 + (\mu_s^z)^2} (\partial_{\mathbf{nn}} \Phi_{pqs}(\mathbf{x}))|_{(x_j, y_k, z_l)}, \end{aligned} \quad (8.65)$$

with $\lambda_{pqs} = (\mu_p^x)^2 + (\mu_q^y)^2 + (\mu_s^z)^2$, $(\widetilde{\phi^n})_{pqs}$ ($(p, q, s) \in \mathcal{T}_{MKL}$) the discrete sine transform coefficients of the vector ϕ^n for $(p, q, s) \in \mathcal{T}_{MKL}$ as

$$(\widetilde{\phi^n})_{pqs} = \frac{8}{MKL} \sum_{j=1}^{M-1} \sum_{k=1}^{K-1} \sum_{l=1}^{L-1} \phi_{jkl}^n \sin\left(\frac{jp\pi}{M}\right) \sin\left(\frac{kq\pi}{K}\right) \sin\left(\frac{ls\pi}{L}\right), \quad (8.66)$$

and the discrete norm is defined as

$$\|\phi^+\|_2^2 = h_x h_y h_z \sum_{j=1}^{M-1} \sum_{k=1}^{K-1} \sum_{l=1}^{L-1} |\phi_{jkl}^+|^2.$$

Similar as those in section 3.3 (cf. [25]), the linear system (8.61)-(8.64) can be iteratively solved in phase space very efficiently via discrete sine transform and we omit the details here for brevity.

8.7. Time splitting scheme for dynamics. Similarly, based on the new Gross-Pitaevskii-Poisson type system (8.7)-(8.8), we will present an efficient and accurate time-splitting sine pseudospectral (TSSP) method for computing the dynamics of a dipolar BEC.

Again, in practice, the whole space problem is truncated into a bounded computational domain $U = [a, b] \times [c, d] \times [e, f]$ with homogeneous Dirichlet boundary condition. From time $t = t_n$ to time $t = t_{n+1}$, the Gross-Pitaevskii-Poisson type system (8.7)-(8.8) is solved in two steps. One solves first

$$i\partial_t \psi(\mathbf{x}, t) = -\frac{1}{2} \nabla^2 \psi(\mathbf{x}, t), \quad \mathbf{x} \in U, \quad \psi(\mathbf{x}, t)|_{\mathbf{x} \in \partial U} = 0, \quad t_n \leq t \leq t_{n+1}, \quad (8.67)$$

for the time step of length τ , followed by solving

$$i\partial_t \psi(\mathbf{x}, t) = [V(\mathbf{x}) + (\beta - \lambda) |\psi(\mathbf{x}, t)|^2 - 3\lambda \partial_{\mathbf{nn}} \varphi(\mathbf{x}, t)] \psi(\mathbf{x}, t), \quad (8.68)$$

$$\nabla^2 \varphi(\mathbf{x}, t) = -|\psi(\mathbf{x}, t)|^2, \quad \mathbf{x} \in U, \quad t_n \leq t \leq t_{n+1}; \quad (8.69)$$

$$\varphi(\mathbf{x}, t)|_{\mathbf{x} \in \partial U} = 0, \quad \psi(\mathbf{x}, t)|_{\mathbf{x} \in \partial U} = 0, \quad t_n \leq t \leq t_{n+1}; \quad (8.70)$$

for the same time step. Eq. (8.67) will be discretized in space by sine pseudospectral method and integrated in time *exactly*. For $t \in [t_n, t_{n+1}]$, the equations (8.68)-(8.70) leave $|\psi|$ and φ invariant in t and therefore they collapse to

$$i\partial_t \psi(\mathbf{x}, t) = [V(\mathbf{x}) + (\beta - \lambda)|\psi(\mathbf{x}, t_n)|^2 - 3\lambda\partial_{\mathbf{nn}}\varphi(\mathbf{x}, t_n)] \psi(\mathbf{x}, t), \quad t_n \leq t \leq t_{n+1}, \quad (8.71)$$

$$\nabla^2 \varphi(\mathbf{x}, t_n) = -|\psi(\mathbf{x}, t_n)|^2, \quad \mathbf{x} \in U. \quad (8.72)$$

Again, equation (8.72) will be discretized in space by sine pseudospectral method [23, 47, 164, 165] and the linear ODE (8.71) can be integrated in time *exactly*.

Let ψ_{jkl}^n and φ_{jkl}^n be the approximations of $\psi(x_j, y_k, z_l, t_n)$ and $\varphi(x_j, y_k, z_l, t_n)$, respectively, which are the solutions of (8.7)-(8.8); and choose $\psi_{jkl}^0 = \psi_0(x_j, y_k, z_l)$ for $(j, k, l) \in \mathcal{T}_{MKL}^0$. For $n = 0, 1, \dots$, a second-order TSSP method for solving (8.7)-(8.8) via the standard Strang splitting is [23]

$$\begin{aligned} \psi_{jkl}^{(1)} &= \sum_{p=1}^{M-1} \sum_{q=1}^{K-1} \sum_{s=1}^{L-1} e^{-i\tau \frac{(\mu_p^x)^2 + (\mu_q^y)^2 + (\mu_s^z)^2}{4}} \widetilde{(\psi^n)}_{pqs} \sin\left(\frac{jp\pi}{M}\right) \sin\left(\frac{kq\pi}{K}\right) \sin\left(\frac{ls\pi}{L}\right), \\ \psi_{jkl}^{(2)} &= e^{-i\tau [V(x_j, y_k, z_l) + (\beta - \lambda)|\psi_{jkl}^{(1)}|^2 - 3\lambda(\partial_{\mathbf{nn}}^s \varphi^{(1)})|_{jkl}]} \psi_{jkl}^{(1)}, \quad (j, k, l) \in \mathcal{T}_{MKL}^0, \\ \psi_{jkl}^{n+1} &= \sum_{p=1}^{M-1} \sum_{q=1}^{K-1} \sum_{s=1}^{L-1} e^{-i\tau \frac{(\mu_p^x)^2 + (\mu_q^y)^2 + (\mu_s^z)^2}{4}} \widetilde{(\psi^{(2)})}_{pqs} \sin\left(\frac{jp\pi}{M}\right) \sin\left(\frac{kq\pi}{K}\right) \sin\left(\frac{ls\pi}{L}\right); \end{aligned} \quad (8.73)$$

where $\widetilde{(\psi^n)}_{pqs}$ and $\widetilde{(\psi^{(2)})}_{pqs}$ ($(p, q, s) \in \mathcal{T}_{MKL}$) are the discrete sine transform coefficients of the vectors ψ^n and $\psi^{(2)}$, respectively (defined similarly as those in (8.66)); and $(\partial_{\mathbf{nn}}^s \varphi^{(1)})|_{jkl}$ can be computed as in (8.65) with $\rho_{jkl}^n = \rho_{jkl}^{(1)} := |\psi_{jkl}^{(1)}|^2$ for $(j, k, l) \in \mathcal{T}_{MKL}^0$.

The above method is explicit and unconditionally stable. The memory cost is $O(MKL)$ and the computational cost per time step is $O(MKL \ln(MKL))$.

8.8. Numerical results. In this section, we first compare our new methods and the standard method used in the literatures [186, 188] to evaluate numerically the dipolar energy and then report ground states and dynamics of dipolar BECs by using our new numerical methods.

	Case I		Case II		Case III	
	DST	DFT	DST	DFT	DST	DFT
$h = 1$	2.756E-2	2.756E-2	3.555E-18	1.279E-4	0.1018	0.1020
$h = 0.5$	1.629E-3	1.614E-3	9.154E-18	1.278E-4	9.788E-5	2.269E-4
$h = 0.25$	1.243E-7	1.588E-5	7.454E-17	1.278E-4	6.406E-7	1.284E-4

TABLE 8.1. Comparison for evaluating dipolar energy under different mesh sizes h .

Example 8.1. Comparison of different methods. Let

$$\phi := \phi(\mathbf{x}) = \pi^{-3/4} \gamma_x^{1/2} \gamma_z^{1/4} e^{-\frac{1}{2}(\gamma_x(x^2+y^2) + \gamma_z z^2)}, \quad \mathbf{x} \in \mathbb{R}^3. \quad (8.74)$$

Then the dipolar energy $E_{\text{dip}}(\phi)$ in (8.25) can be evaluated analytically as [178]

$$E_{\text{dip}}(\phi) = -\frac{\lambda\gamma_x\sqrt{\gamma_z}}{4\pi\sqrt{2\pi}} \begin{cases} \frac{1+2\chi^2}{1-\chi^2} - \frac{3\chi^2\arctan(\sqrt{\chi^2-1})}{(1-\chi^2)\sqrt{\chi^2-1}}, & \chi > 1, \\ 0, & \chi = 1, \\ \frac{1+2\chi^2}{1-\chi^2} - \frac{1.5\chi^2}{(1-\chi^2)\sqrt{1-\chi^2}} \ln\left(\frac{1+\sqrt{1-\chi^2}}{1-\sqrt{1-\chi^2}}\right), & \chi < 1, \end{cases} \quad (8.75)$$

with $\chi = \sqrt{\frac{\gamma_z}{\gamma_x}}$. This provides a perfect example to test the efficiency of different numerical methods to deal with the dipolar potential. Based on our new formulation, the dipolar energy can be evaluated via discrete sine transform (DST) as

$$E_{\text{dip}}(\phi) \approx \frac{\lambda h_x h_y h_z}{2} \sum_{j=1}^{M-1} \sum_{k=1}^{K-1} \sum_{l=1}^{L-1} |\phi(x_j, y_k, z_l)|^2 \left[-|\phi(x_j, y_k, z_l)|^2 - 3 (\partial_{\mathbf{nn}}^s \varphi^n)|_{jkl} \right],$$

where $(\partial_{\mathbf{nn}}^s \varphi^n)|_{jkl}$ is computed as in (8.65) with $\rho_{jkl}^n = |\phi(x_j, y_k, z_l)|^2$ for $(j, k, l) \in \mathcal{T}_{MKL}^0$. In the literatures [186, 188], this dipolar energy is usually calculated via discrete Fourier transform (DFT) as

$$E_{\text{dip}}(\phi) \approx \frac{\lambda h_x h_y h_z}{2} \sum_{j=0}^{M-1} \sum_{k=0}^{K-1} \sum_{l=0}^{L-1} |\phi(x_j, y_k, z_l)|^2 \left[\mathcal{F}_{jkl}^{-1} \left(\widehat{(U_{\text{dip}})}(2\mu_p^x, 2\mu_q^y, 2\mu_s^z) \cdot \mathcal{F}_{pq}^s(|\phi|^2) \right) \right],$$

where \mathcal{F} and \mathcal{F}^{-1} are the discrete Fourier and inverse Fourier transforms over the grid points $\{(x_j, y_k, z_l), (j, k, l) \in \mathcal{T}_{MKL}^0\}$, respectively [186]. We take $\lambda = 8\pi/3$, the bounded computational domain $U = [-16, 16]^3$, $M = K = L$ and thus $h = h_x = h_y = h_z = \frac{32}{M}$. Tab. 8.1 lists the errors $e := |E_{\text{dip}}(\phi) - E_{\text{dip}}^h|$ with E_{dip}^h computed numerically via either DST (8.76) or DFT with mesh size h for three cases:

- Case I. $\gamma_x = 0.25$ and $\gamma_z = 1$, $\chi = 2.0$ and $E_{\text{dip}}(\phi) = 0.0386708614$;
- Case II. $\gamma_x = \gamma_z = 1$, $\chi = 1.0$ and $E_{\text{dip}}(\phi) = 0$;
- Case III. $\gamma_x = 2$ and $\gamma_z = 1$, $\chi = \sqrt{0.5}$ and $E_{\text{dip}}(\phi) = -0.1386449741$.

Example 8.2. Ground states of dipolar BEC. Here we report the ground states of a dipolar BEC (e.g., ^{52}Cr [147]) with different parameters and trapping potentials by using the numerical method (8.61)-(8.64). In our computation and results, we always use the dimensionless quantities. We take $M = K = L = 128$, time step $\tau = 0.01$, dipolar direction $\mathbf{n} = (0, 0, 1)^T$ and the bounded computational domain $U = [-8, 8]^3$ for all cases except $U = [-16, 16]^3$ for the cases $\frac{N}{10000} = 1, 5, 10$ and $U = [-20, 20]^3$ for the cases $\frac{N}{10000} = 50, 100$ in Tab. 8.2. The ground state ϕ_g is reached numerically when $\|\phi^{n+1} - \phi^n\|_\infty := \max_{0 \leq j \leq M, 0 \leq k \leq K, 0 \leq l \leq L} |\phi_{jkl}^{n+1} - \phi_{jkl}^n| \leq \epsilon := 10^{-6}$ in (8.61)-(8.64). Tab. 8.2 shows the energy $E^g := E_{3D}(\phi_g)$, chemical potential $\mu^g := \mu(\phi_g)$, kinetic energy $E_{\text{kin}}^g := E_{\text{kin}}(\phi_g)$, potential energy $E_{\text{pot}}^g := E_{\text{pot}}(\phi_g)$, interaction energy $E_{\text{int}}^g := E_{\text{int}}(\phi_g)$, dipolar energy $E_{\text{dip}}^g := E_{\text{dip}}(\phi_g)$, condensate widths $\sigma_x^g := \sigma_x(\phi_g)$ and $\sigma_z^g := \sigma_z(\phi_g)$ in (2.54) and central density $\rho_g(\mathbf{0}) := |\phi_g(0, 0, 0)|^2$ with harmonic potential $V(x, y, z) = \frac{1}{2}(x^2 + y^2 + 0.25z^2)$ for different $\beta = 0.20716N$ and $\lambda = 0.033146N$ with N the total number of particles in the condensate; and Tab. 8.3 lists similar results with $\beta = 207.16$ for different values of $-0.5 \leq \frac{\lambda}{\beta} \leq 1$. In addition, Fig. 8.1 depicts the ground state $\phi_g(\mathbf{x})$, e.g. surface plots of $|\phi_g(x, 0, z)|^2$ and isosurface plots of $|\phi_g(\mathbf{x})| = 0.01$, of a dipolar BEC with $\beta = 401.432$ and $\lambda = 0.16\beta$ for harmonic potential $V(\mathbf{x}) = \frac{1}{2}(x^2 + y^2 + z^2)$,

double-well potential $V(\mathbf{x}) = \frac{1}{2}(x^2 + y^2 + z^2) + 4e^{-z^2/2}$ and optical lattice potential $V(\mathbf{x}) = \frac{1}{2}(x^2 + y^2 + z^2) + 100[\sin^2(\frac{\pi}{2}x) + \sin^2(\frac{\pi}{2}y) + \sin^2(\frac{\pi}{2}z)]$.

$\frac{N}{10000}$	E^g	μ^g	E_{kin}^g	E_{pot}^g	E_{int}^g	E_{dip}^g	σ_x^g	σ_z^g	$\rho_g(\mathbf{0})$
0.1	1.567	1.813	0.477	0.844	0.262	-0.015	0.796	1.299	0.06139
0.5	2.225	2.837	0.349	1.264	0.659	-0.047	0.940	1.745	0.02675
1	2.728	3.583	0.296	1.577	0.925	-0.070	1.035	2.009	0.01779
5	4.745	6.488	0.195	2.806	1.894	-0.151	1.354	2.790	0.00673
10	6.147	8.479	0.161	3.654	2.536	-0.204	1.538	3.212	0.00442
50	11.47	15.98	0.101	6.853	4.909	-0.398	2.095	4.441	0.00168
100	15.07	21.04	0.082	9.017	6.498	-0.526	2.400	5.103	0.00111

TABLE 8.2. Different quantities of the ground states of a dipolar BEC for $\beta = 0.20716N$ and $\lambda = 0.033146N$ with different number of particles N .

$\frac{\lambda}{\beta}$	E^g	μ^g	E_{kin}^g	E_{pot}^g	E_{int}^g	E_{dip}^g	σ_x^g	σ_z^g	$\rho_g(\mathbf{0})$
-0.5	2.957	3.927	0.265	1.721	0.839	0.131	1.153	1.770	0.01575
-0.25	2.883	3.817	0.274	1.675	0.853	0.081	1.111	1.879	0.01605
0	2.794	3.684	0.286	1.618	0.890	0.000	1.066	1.962	0.01693
0.25	2.689	3.525	0.303	1.550	0.950	-0.114	1.017	2.030	0.01842
0.5	2.563	3.332	0.327	1.468	1.047	-0.278	0.960	2.089	0.02087
0.75	2.406	3.084	0.364	1.363	1.212	-0.534	0.889	2.141	0.02536
1.0	2.193	2.726	0.443	1.217	1.575	-1.041	0.786	2.189	0.03630

TABLE 8.3. Different quantities of the ground states of a dipolar BEC with different values of $\frac{\lambda}{\beta}$ with $\beta = 207.16$.

Example 8.3. Dynamics of a dipolar BEC. Here we compute the dynamics of a dipolar BEC (e.g., ^{52}Cr [147]) by using our numerical method (8.73). Again, in the computation and results, we always use the dimensionless quantities. We take the bounded computational domain $U = [-8, 8]^2 \times [-4, 4]$, $M = K = L = 128$, i.e. $h = h_x = h_y = 1/8, h_z = 1/16$, time step $\tau = 0.001$. The initial data $\psi(\mathbf{x}, 0) = \psi_0(\mathbf{x})$ is chosen as the ground state of a dipolar BEC computed numerically by our numerical method with $\mathbf{n} = (0, 0, 1)^T$, $V(\mathbf{x}) = \frac{1}{2}(x^2 + y^2 + 25z^2)$, $\beta = 103.58$ and $\lambda = 0.8\beta = 82.864$.

We study the dynamics of suddenly changing the dipolar direction from $\mathbf{n} = (0, 0, 1)^T$ to $\mathbf{n} = (1, 0, 0)^T$ at $t = 0$ and keeping all other quantities unchanged. Fig. 8.2 depicts the time evolution of the energy $E_{3\text{D}}(t) := E_{3\text{D}}(\psi(\cdot, t))$, chemical potential $\mu(t) = \mu(\psi(\cdot, t))$, kinetic energy $E_{\text{kin}}(t) := E_{\text{kin}}(\psi(\cdot, t))$, potential energy $E_{\text{pot}}(t) := E_{\text{pot}}(\psi(\cdot, t))$, interaction energy $E_{\text{int}}(t) := E_{\text{int}}(\psi(\cdot, t))$, dipolar energy $E_{\text{dip}}(t) := E_{\text{dip}}(\psi(\cdot, t))$, condensate widths $\sigma_x(t) := \sigma_x(\psi(\cdot, t))$, $\sigma_z(t) := \sigma_z(\psi(\cdot, t))$, and central density $\rho(t) := |\psi(\mathbf{0}, t)|^2$, as well as the isosurface of the density function $\rho(\mathbf{x}, t) := |\psi(\mathbf{x}, t)|^2 = 0.01$ for different times.

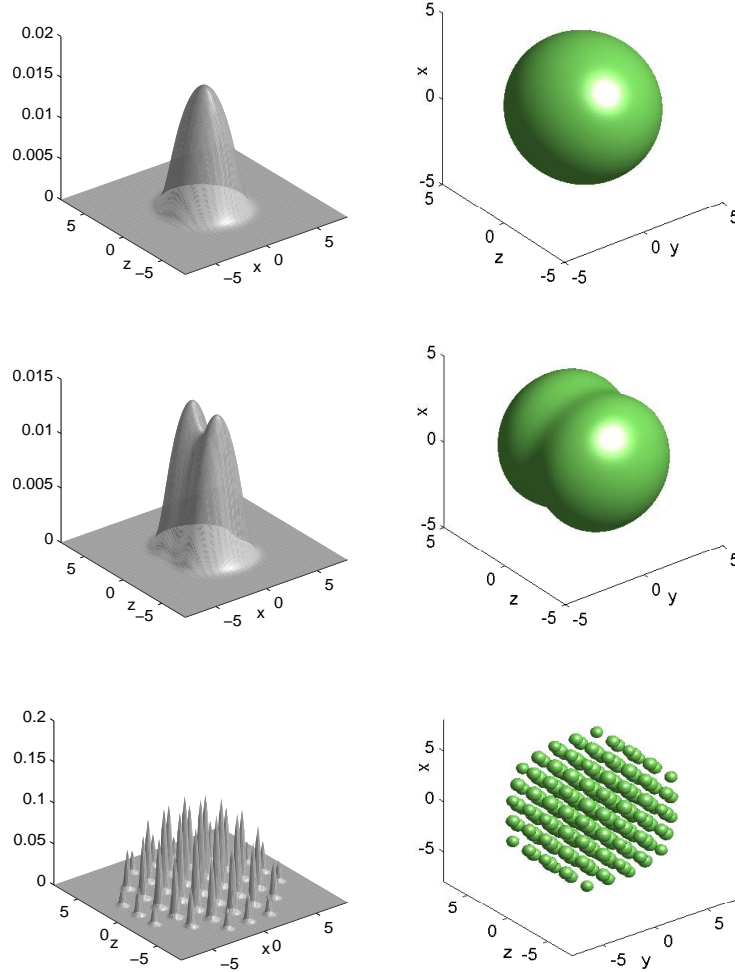


FIGURE 8.1. Surface plots of $|\phi_g(x, 0, z)|^2$ (left column) and iso-surface plots of $|\phi_g(x, y, z)| = 0.01$ (right column) for the ground state of a dipolar BEC with $\beta = 401.432$ and $\lambda = 0.16\beta$ for harmonic potential (top row), double-well potential (middle row) and optical lattice potential (bottom row).

From the above numerical results, we can see that the numerical methods based on the GPPS (8.7)-(8.8) are much more efficient and accurate than those used in the literatures based on (8.1).

8.9. Extensions in lower dimensions. Here, we consider the numerical methods for computing ground states and dynamics for dipolar BECs in 2D and 1D. The difficulties arise from the nonlocal terms, i.e., the dipolar terms in quasi-2D equation I (8.15), quasi-2D equation II (8.19) and quasi-1D equation (8.21). It is obvious that those methods introduced in sections 3 and 4 can be extended here, provided that the nonlocal terms can be computed properly.

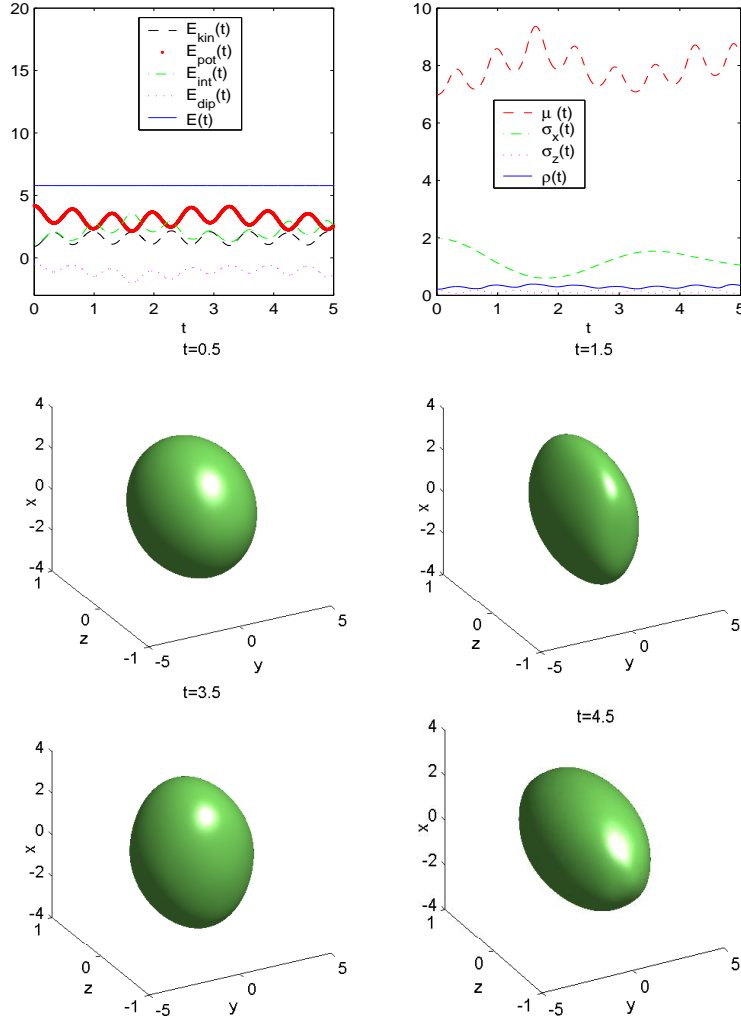


FIGURE 8.2. Time evolution of different quantities and isosurface plots of the density function $\rho(\mathbf{x}, t) := |\psi(\mathbf{x}, t)|^2 = 0.01$ at different times for a dipolar BEC when the dipolar direction is suddenly changed from $\mathbf{n} = (0, 0, 1)^T$ to $(1, 0, 0)^T$ at time $t = 0$.

We propose to compute the convolution terms in (8.15), (8.19) and (8.21) by Fourier transform. Unlike the 3D case, there are no singularities for convolution kernels at origin, thus discrete Fourier transform is accurate in these cases.

Lemma 8.1. (Kernels U_ε^{2D} in (8.16) and U_ε^{1D} (8.22)) For any real function $f(\mathbf{x})$ in the Schwartz space $\mathcal{S}(\mathbb{R}^2)$, we have

$$\widehat{U_\varepsilon^{2D} * f}(\xi) = \hat{f}(\xi) \widehat{U_\varepsilon^{2D}}(\xi) = \frac{\hat{f}(\xi)}{\pi} \int_{\mathbb{R}} \frac{e^{-\varepsilon^2 s^2/2}}{|\xi|^2 + s^2} ds, \quad f \in \mathcal{S}(\mathbb{R}^2). \quad (8.76)$$

For any $g(z)$ in the Schwartz space $\mathcal{S}(\mathbb{R})$, we have

$$\widehat{U_\varepsilon^{1D} * g}(\xi) = \hat{g}(\xi) \widehat{U_\varepsilon^{1D}}(\xi) = \frac{\sqrt{2\varepsilon} \hat{g}(\xi)}{\sqrt{\pi}} \int_0^\infty \frac{e^{-\varepsilon^2 s/2}}{|\xi|^2 + s} ds, \quad \xi \in \mathbb{R}. \quad (8.77)$$

Here \hat{f} and \hat{g} denote the Fourier transforms of f and g , respectively.

The Fourier transforms of U_ε^{2D} and U_ε^{1D} can be written in terms of the second kind Bessel functions [65].

9. Mathematical theory and numerical methods for two component BEC.

In view of potential applications, such as the generation of bright beams of coherent matter waves (atom laser), a central goal in the study of BEC has been the formation of condensate with the number of atoms being as large as possible. It is thus of particular interest to study a scenario where this goal is achieved by uniting two (or more) independently grown condensates to form one large single condensate. The first experiment involving the uniting of multiple-component BEC was performed with atoms evaporatively cooled in the $|F = 2, m_f = 2\rangle$ and $|1, -1\rangle$ spin states of ^{87}Rb [142]. It demonstrated the possibility of producing long-lived multiple condensate systems, and that the condensate wave function is dramatically affected by the presence of inter-component interactions.

9.1. Coupled Gross-Pitaevskii equations. At temperatures T much smaller than the critical temperature T_c [150], a two-component BEC with an internal atomic Josephson junction (or an external driving field) can be well described by the coupled Gross-Pitaevskii equations (CGPEs) [19, 131, 134, 185, 195],

$$\begin{aligned} i\hbar\partial_t\psi_1 &= \left[-\frac{\hbar^2}{2m}\nabla^2 + V(\mathbf{x}) + \hbar\delta + g_{11}|\psi_1|^2 + g_{12}|\psi_2|^2 \right] \psi_1 + \lambda\hbar\psi_2, \\ i\hbar\partial_t\psi_2 &= \left[-\frac{\hbar^2}{2m}\nabla^2 + V(\mathbf{x}) + g_{21}|\psi_1|^2 + g_{22}|\psi_2|^2 \right] \psi_2 + \lambda\hbar\psi_1, \quad \mathbf{x} \in \mathbb{R}^3. \end{aligned} \quad (9.1)$$

Here $\Psi := \Psi(\mathbf{x}, t) = (\psi_1(\mathbf{x}, t), \psi_2(\mathbf{x}, t))^T$ is the complex-valued macroscopic wave function, $V(\mathbf{x})$ is the real-valued external trapping potential, λ is the effective Rabi frequency describing the strength to realize the internal atomic Josephson junction (JJ) by a Raman transition, δ is the Raman transition constant. The interactions of particles are described by $g_{jl} = \frac{4\pi\hbar^2 a_{jl}}{m}$ with $a_{jl} = a_{lj}$ ($j, l = 1, 2$) being the s -wave scattering lengths between the j th and l th component (positive for repulsive interaction and negative for attractive interaction). It is necessary to ensure that the wave function is properly normalized. Especially, we require

$$\int_{\mathbb{R}^3} [|\psi_1(\mathbf{x}, t)|^2 + |\psi_2(\mathbf{x}, t)|^2] d\mathbf{x} = N = N_1^0 + N_2^0, \quad (9.2)$$

where

$$N_j^0 = \int_{\mathbb{R}^3} |\psi_j(\mathbf{x}, 0)|^2 d\mathbf{x},$$

is the particle number of the j th ($j = 1, 2$) component at time $t = 0$ and N the total number of particle in the two-component BEC.

By properly nondimensionalization and dimension reduction, we can obtain the following dimensionless CGPEs in d -dimensions ($d = 1, 2, 3$) for a two-component

BEC [19, 195]

$$\begin{aligned} i\partial_t\psi_1 &= \left[-\frac{1}{2}\nabla^2 + V(\mathbf{x}) + \delta + (\beta_{11}|\psi_1|^2 + \beta_{12}|\psi_2|^2) \right] \psi_1 + \lambda\psi_2, & \mathbf{x} \in \mathbb{R}^d, \\ i\partial_t\psi_2 &= \left[-\frac{1}{2}\nabla^2 + V(\mathbf{x}) + (\beta_{12}|\psi_1|^2 + \beta_{22}|\psi_2|^2) \right] \psi_2 + \lambda\psi_1, & \mathbf{x} \in \mathbb{R}^d. \end{aligned} \quad (9.3)$$

Here $\Psi := \Psi(\mathbf{x}, t) = (\psi_1(\mathbf{x}, t), \psi_2(\mathbf{x}, t))^T$ is the dimensionless complex-valued macroscopic wave function, $V(\mathbf{x})$ is the dimensionless real-valued external trapping potential, $\beta_{11}, \beta_{12} = \beta_{21}, \beta_{22}$ are dimensionless interaction constants, δ and λ are dimensionless constants. In addition, the wave function is normalized as

$$\|\Psi\|_2^2 := \int_{\mathbb{R}^d} [|\psi_1(\mathbf{x}, t)|^2 + |\psi_2(\mathbf{x}, t)|^2] d\mathbf{x} = 1. \quad (9.4)$$

The dimensionless CGPEs (9.3) conserves the total mass or normalization, i.e.

$$N(t) := \|\Psi(\cdot, t)\|^2 = N_1(t) + N_2(t) \equiv \|\Psi(\cdot, 0)\|^2 = 1, \quad t \geq 0, \quad (9.5)$$

with

$$N_j(t) = \|\psi_j(\mathbf{x}, t)\|_2^2 := \|\psi_j(\mathbf{x}, t)\|_2^2 = \int_{\mathbb{R}^d} |\psi_j(\mathbf{x}, t)|^2 d\mathbf{x}, \quad t \geq 0, \quad j = 1, 2, \quad (9.6)$$

and the energy

$$\begin{aligned} E(\Psi) &= \int_{\mathbb{R}^d} \left[\frac{1}{2} (|\nabla\psi_1|^2 + |\nabla\psi_2|^2) + V(\mathbf{x})(|\psi_1|^2 + |\psi_2|^2) + \delta|\psi_1|^2 + \frac{1}{2}\beta_{11}|\psi_1|^4 \right. \\ &\quad \left. + \frac{1}{2}\beta_{22}|\psi_2|^4 + \beta_{12}|\psi_1|^2|\psi_2|^2 + 2\lambda \cdot \text{Re}(\psi_1\bar{\psi}_2) \right] d\mathbf{x}. \end{aligned} \quad (9.7)$$

In addition, if there is no internal Josephson junction in (9.3), i.e. $\lambda = 0$, the mass of each component is also conserved, i.e.

$$N_1(t) \equiv \int_{\mathbb{R}^d} |\psi_1(\mathbf{x}, 0)|^2 d\mathbf{x} := \alpha, \quad N_2(t) \equiv \int_{\mathbb{R}^d} |\psi_2(\mathbf{x}, 0)|^2 d\mathbf{x} := 1 - \alpha, \quad (9.8)$$

with $0 \leq \alpha \leq 1$ a given constant.

9.2. Ground states for the case without Josephson junction. If there is no external driving field in (9.3), i.e. $\lambda = 0$, for any given $\alpha \in [0, 1]$, the ground state $\Phi_g^\alpha(\mathbf{x}) = (\phi_1^\alpha(\mathbf{x}), \phi_2^\alpha(\mathbf{x}))^T$ of the two-component BEC is defined as the minimizer of the following nonconvex minimization problem:

Find $(\Phi_g^\alpha \in S_\alpha)$, such that

$$E_g^\alpha := E_0(\Phi_g^\alpha) = \min_{\Phi \in S_\alpha} E_0(\Phi), \quad (9.9)$$

where S_α is a nonconvex set defined as

$$S_\alpha := \{ \Phi = (\phi_1, \phi_2)^T \mid \|\phi_1\|_2^2 = \alpha, \|\phi_2\|_2^2 = 1 - \alpha, E_0(\Phi) < \infty \}, \quad (9.10)$$

and the energy functional $E_0(\Phi)$ is defined as

$$\begin{aligned} E_0(\Phi) &= \int_{\mathbb{R}^d} \left[\frac{1}{2} (|\nabla\phi_1|^2 + |\nabla\phi_2|^2) + V(\mathbf{x})(|\phi_1|^2 + |\phi_2|^2) + \delta|\phi_1|^2 + \frac{1}{2}\beta_{11}|\phi_1|^4 \right. \\ &\quad \left. + \frac{1}{2}\beta_{22}|\phi_2|^4 + \beta_{12}|\phi_1|^2|\phi_2|^2 \right] d\mathbf{x}. \end{aligned} \quad (9.11)$$

Again, it is easy to see that the ground state Φ_g^α satisfies the following Euler-Lagrange equations,

$$\begin{aligned}\mu_1 \phi_1 &= \left[-\frac{1}{2} \nabla^2 + V(\mathbf{x}) + \delta + (\beta_{11} |\phi_1|^2 + \beta_{12} |\phi_2|^2) \right] \phi_1, & \mathbf{x} \in \mathbb{R}^d, \\ \mu_2 \phi_2 &= \left[-\frac{1}{2} \nabla^2 + V(\mathbf{x}) + (\beta_{12} |\phi_1|^2 + \beta_{22} |\phi_2|^2) \right] \phi_2, & \mathbf{x} \in \mathbb{R}^d,\end{aligned}\quad (9.12)$$

under the two constraints

$$\|\phi_1\|_2^2 := \int_{\mathbb{R}^d} |\phi_1(\mathbf{x})|^2 d\mathbf{x} = \alpha, \quad \|\phi_2\|_2^2 := \int_{\mathbb{R}^d} |\phi_2(\mathbf{x})|^2 d\mathbf{x} = 1 - \alpha, \quad (9.13)$$

with μ_1 and μ_2 being the Lagrange multipliers or chemical potentials corresponding to the two constraints (9.13). Again, the above time-independent CGPEs (9.12) can also be obtained from the CGPEs (9.3) with $\lambda = 0$ by substituting the ansatz

$$\psi_1(\mathbf{x}, t) = e^{-i\mu_1 t} \phi_1(\mathbf{x}), \quad \psi_2(\mathbf{x}, t) = e^{-i\mu_2 t} \phi_2(\mathbf{x}). \quad (9.14)$$

Considering the case $\alpha \in (0, 1)$ in minimization problem (9.9), denote

$$\beta'_{11} := \alpha \beta_{11}, \quad \beta'_{22} := (1 - \alpha) \beta_{22}, \quad \beta'_{12} := \sqrt{\alpha(1 - \alpha)} \beta_{12}, \quad \alpha' := \alpha(1 - \alpha),$$

and

$$B = \begin{pmatrix} \beta_{11} & \beta_{12} \\ \beta_{21} & \beta_{22} \end{pmatrix}, \quad B' = \begin{pmatrix} \beta'_{11} & \beta'_{12} \\ \beta'_{21} & \beta'_{22} \end{pmatrix}.$$

Then the following conclusions can be drawn [19].

Theorem 9.1. (*Existence and uniqueness of (9.9)*) Suppose $V(\mathbf{x}) \geq 0$ satisfying $\lim_{|\mathbf{x}| \rightarrow \infty} V(\mathbf{x}) = \infty$ and at least one of the following condition holds,

- (i) $d = 1$;
- (ii) $d = 2$ and $\beta'_{11} \geq -C_b$, $\beta'_{22} \geq -C_b$, and $\beta'_{12} \geq -\sqrt{(C_b + \beta'_{11})(C_b + \beta'_{22})}$;
- (iii) $d = 3$ and B is either positive semi-definite or nonnegative,

then there exists a ground state $\Phi_g = (\phi_1^g, \phi_2^g)^T$ of (9.9). In addition, $\tilde{\Phi}_g := (e^{i\theta_1} |\phi_1^g|, e^{i\theta_2} |\phi_2^g|)$ is also a ground state of (9.9) with two constants θ_1 and θ_2 . Furthermore, if the matrix B' is positive semi-definite, the ground state $(|\phi_1^g|, |\phi_2^g|)^T$ of (9.9) is unique. In contrast, if one of the following conditions holds,

- (i) $d = 2$ and $\beta'_{11} < -C_b$ or $\beta'_{22} < -C_b$ or $\beta'_{12} < -\frac{1}{2\sqrt{\alpha'}} (\alpha\beta'_{11} + (1 - \alpha)\beta'_{22} + C_b)$;
- (ii) $d = 3$ and $\beta_{11} < 0$ or $\beta_{22} < 0$ or $\beta_{12} < -\frac{1}{2\alpha'} (\alpha^2\beta_{11} + (1 - \alpha)^2\beta_{22})$.

there exists no ground states of (9.9).

9.3. Ground states for the case with Josephson junction. The ground state $\Phi_g(\mathbf{x}) = (\phi_1^g(\mathbf{x}), \phi_2^g(\mathbf{x}))^T$ of the two-component BEC with an internal Josephson junction (9.3) is defined as the minimizer of the following nonconvex minimization problem:

Find $(\Phi_g \in S)$, such that

$$E_g := E(\Phi_g) = \min_{\Phi \in S} E(\Phi), \quad (9.15)$$

where S is a nonconvex set defined as

$$S := \left\{ \Phi = (\phi_1, \phi_2)^T \mid \int_{\mathbb{R}^d} (|\phi_1(\mathbf{x})|^2 + |\phi_2(\mathbf{x})|^2) d\mathbf{x} = 1, E(\Phi) < \infty \right\}. \quad (9.16)$$

It is easy to see that the ground state Φ_g satisfies the following Euler-Lagrange equations,

$$\begin{aligned}\mu \phi_1 &= \left[-\frac{1}{2} \nabla^2 + V(\mathbf{x}) + \delta + (\beta_{11} |\phi_1|^2 + \beta_{12} |\phi_2|^2) \right] \phi_1 + \lambda \phi_2, \quad \mathbf{x} \in \mathbb{R}^d, \\ \mu \phi_2 &= \left[-\frac{1}{2} \nabla^2 + V(\mathbf{x}) + (\beta_{12} |\phi_1|^2 + \beta_{22} |\phi_2|^2) \right] \phi_2 + \lambda \phi_1, \quad \mathbf{x} \in \mathbb{R}^d,\end{aligned}\tag{9.17}$$

under the constraint

$$\|\Phi\|_2^2 := \|\Phi\|_2^2 = \int_{\mathbb{R}^d} [|\phi_1(\mathbf{x})|^2 + |\phi_2(\mathbf{x})|^2] d\mathbf{x} = 1,\tag{9.18}$$

with the eigenvalue μ being the Lagrange multiplier or chemical potential corresponding to the constraint (9.18), which can be computed as

$$\begin{aligned}\mu &= \mu(\Phi) = \int_{\mathbb{R}^d} \left[\frac{1}{2} (|\nabla \phi_1|^2 + |\nabla \phi_2|^2) + V(\mathbf{x})(|\phi_1|^2 + |\phi_2|^2) + \delta |\phi_1|^2 + \beta_{11} |\phi_1|^4 \right. \\ &\quad \left. + \beta_{22} |\phi_2|^4 + 2\beta_{12} |\phi_1|^2 |\phi_2|^2 + 2\lambda \cdot \operatorname{Re}(\phi_1 \bar{\phi}_2) \right] d\mathbf{x}.\end{aligned}\tag{9.19}$$

In fact, the above time-independent CGPEs (9.17) can also be obtained from the CGPEs (9.3) by substituting the ansatz

$$\psi_1(\mathbf{x}, t) = e^{-i\mu t} \phi_1(\mathbf{x}), \quad \psi_2(\mathbf{x}, t) = e^{-i\mu t} \phi_2(\mathbf{x}).\tag{9.20}$$

The eigenfunctions of the nonlinear eigenvalue problem (9.17) under the normalization (9.18) are usually called as stationary states of the two-component BEC (9.3). Among them, the eigenfunction with minimum energy is the ground state and those whose energy are larger than that of the ground state are usually called as excited states.

It is easy to see that the ground state Φ_g defined in (9.15) is equivalent to the following:

Find $(\Phi_g \in S)$, such that

$$E(\Phi_g) = \min_{\Phi \in S} E(\Phi) = \min_{\alpha \in [0,1]} E(\alpha), \quad E(\alpha) = \min_{\Phi \in S_\alpha} E(\Phi).\tag{9.21}$$

Denote

$$\mathcal{D} = \{ \Phi = (\phi_1, \phi_2)^T \mid V |\phi_j|^2 \in L^1(\mathbb{R}^d), \phi_j \in H^1(\mathbb{R}^d) \cap L^4(\mathbb{R}^d), j = 1, 2 \},\tag{9.22}$$

then the ground state Φ_g of (9.15) is also given by the following:

Find $(\Phi_g \in \mathcal{D}_1)$, such that

$$E_g := E(\Phi_g) = \min_{\Phi \in \mathcal{D}_1} E(\Phi),\tag{9.23}$$

where

$$\mathcal{D}_1 = \mathcal{D} \cap \left\{ \Phi = (\phi_1, \phi_2)^T \mid \|\Phi\|^2 = \int_{\mathbb{R}^d} (|\phi_1(\mathbf{x})|^2 + |\phi_2(\mathbf{x})|^2) d\mathbf{x} = 1 \right\}.\tag{9.24}$$

In addition, we introduce the auxiliary energy functional

$$\begin{aligned}\tilde{E}(\Phi) &= \int_{\mathbb{R}^d} \left\{ \frac{1}{2} (|\nabla \phi_1|^2 + |\nabla \phi_2|^2) + [V(\mathbf{x})(|\phi_1|^2 + |\phi_2|^2) + \delta |\phi_1|^2] \right. \\ &\quad \left. + \left(\frac{1}{2} \beta_{11} |\phi_1|^4 + \frac{1}{2} \beta_{22} |\phi_2|^4 + \beta_{12} |\phi_1|^2 |\phi_2|^2 \right) - 2|\lambda| \cdot |\phi_1| \cdot |\phi_2| \right\} d\mathbf{x},\end{aligned}\tag{9.25}$$

and the auxiliary nonconvex minimization problem:
Find $(\Phi_g \in \mathcal{D}_1)$, such that

$$\tilde{E}(\Phi_g) = \min_{\Phi \in \mathcal{D}_1} \tilde{E}(\Phi). \quad (9.26)$$

For $\Phi = (\phi_1, \phi_2)^T$, we write $E(\phi_1, \phi_2) = E(\Phi)$ and $\tilde{E}(\phi_1, \phi_2) = \tilde{E}(\Phi)$. Then we have the following lemmas [19]:

Lemma 9.1. *For the minimizers $\Phi_g(\mathbf{x}) = (\phi_1^g(\mathbf{x}), \phi_2^g(\mathbf{x}))^T$ of the nonconvex minimization problems (9.23) and (9.26), we have*

(i). *If Φ_g is a minimizer of (9.23), then $\phi_1^g(\mathbf{x}) = e^{i\theta_1}|\phi_1^g(\mathbf{x})|$ and $\phi_2^g(\mathbf{x}) = e^{i\theta_2}|\phi_2^g(\mathbf{x})|$ with θ_1 and θ_2 two constants satisfying $\theta_1 = \theta_2$ if $\lambda < 0$; and $\theta_1 = \theta_2 \pm \pi$ if $\lambda > 0$. In addition, $\tilde{\Phi}_g = (e^{i\theta_3}\phi_1^g, e^{i\theta_4}\phi_2^g)^T$ with θ_3 and θ_4 two constants satisfying $\theta_3 = \theta_4$ if $\lambda < 0$; and $\theta_3 = \theta_4 \pm \pi$ if $\lambda > 0$ is also a minimizer of (9.23).*

(ii). *If Φ_g is a minimizer of (9.26), then $\phi_1^g(\mathbf{x}) = e^{i\theta_1}|\phi_1^g(\mathbf{x})|$ and $\phi_2^g(\mathbf{x}) = e^{i\theta_2}|\phi_2^g(\mathbf{x})|$ with θ_1 and θ_2 two constants. In addition, $\tilde{\Phi}_g = (e^{i\theta_3}\phi_1^g, e^{i\theta_4}\phi_2^g)^T$ with θ_3 and θ_4 two constants is also a minimizer of (9.26).*

(iii). *If Φ_g is a minimizer of (9.23), then Φ_g is also a minimizer of (9.26).*

(iv). *If Φ_g is a minimizer of (9.26), then $\tilde{\Phi}_g = (|\phi_1^g|, -\text{sign}(\lambda)|\phi_2^g|)^T$ is a minimizer of (9.23).*

For the auxiliary minimization problem (9.26), we have the following results generalizing the single component BEC case in section 2.

Theorem 9.2. *(Existence and uniqueness of (9.26) [19]) Suppose $V(\mathbf{x}) \geq 0$ satisfying $\lim_{|\mathbf{x}| \rightarrow \infty} V(\mathbf{x}) = \infty$, then there exists a minimizer $\Phi^\infty = (\phi_1^\infty, \phi_2^\infty)^T \in \mathcal{D}_1$ of (9.26) if one of the following conditions holds,*

(i) $d = 1$;

(ii) $d = 2$ and $\beta_{11} \geq -C_b, \beta_{22} \geq -C_b, \beta_{12} \geq -C_b - \sqrt{C_b + \beta_{11}}\sqrt{C_b + \beta_{22}}$;

(iii) $d = 3$ and B is either positive semi-definite or nonnegative,

where C_b is given in (2.12). In addition, if the matrix B is positive semi-definite and at least one of the parameters $\delta, \lambda, \gamma_1$ and γ_2 are nonzero, then the minimizer $(|\phi_1^\infty|, |\phi_2^\infty|)^T$ is unique.

Combining Theorem 9.2 and Lemma 9.1, we draw the conclusions [19]:

Theorem 9.3. *(Existence and uniqueness of (9.15)) Suppose $V(\mathbf{x}) \geq 0$ satisfying $\lim_{|\mathbf{x}| \rightarrow \infty} V(\mathbf{x}) = \infty$ and at least one of the following condition holds,*

(i) $d = 1$;

(ii) $d = 2$ and $\beta_{11} \geq -C_b, \beta_{22} \geq -C_b$, and $\beta_{12} \geq -C_b - \sqrt{C_b + \beta_{11}}\sqrt{C_b + \beta_{22}}$;

(iii) $d = 3$ and B is either positive semi-definite or nonnegative,

there exists a ground state $\Phi_g = (\phi_1^g, \phi_2^g)^T$ of (9.15). In addition, $\tilde{\Phi}_g := (e^{i\theta_1}|\phi_1^g|, e^{i\theta_2}|\phi_2^g|)$ is also a ground state of (9.15) with θ_1 and θ_2 two constants satisfying $\theta_1 - \theta_2 = \pm\pi$ when $\lambda > 0$ and $\theta_1 - \theta_2 = 0$ when $\lambda < 0$, respectively. Furthermore, if the matrix B is positive semi-definite and at least one of the parameters $\delta, \lambda, \gamma_1$ and γ_2 are nonzero, then the ground state $(|\phi_1^g|, -\text{sign}(\lambda)|\phi_2^g|)^T$ is unique. In contrast, if one of the following conditions holds,

(i) $d = 2$ and $\beta_{11} < -C_b$ or $\beta_{22} < -C_b$ or $\beta_{12} < -C_b - \sqrt{C_b + \beta_{11}}\sqrt{C_b + \beta_{22}}$;

(ii) $d = 3$ and $\beta_{11} < 0$ or $\beta_{22} < 0$ or $\beta_{12} < 0$ with $\beta_{12}^2 > \beta_{11}\beta_{22}$;

there exists no ground state of (9.15).

When either $|\delta|$ or $|\lambda|$ goes to infinity, the two component ground state problem (9.15) will collapse to a single component ground state problem in section 2 [19].

For fixed $\beta_{11} \geq 0$ and $\beta_{22} \geq 0$, when $\beta_{12} \rightarrow \infty$, the phase of two components of the ground state $\Phi_g = (\phi_1^g, \phi_2^g)^T$ will be segregated [63, 66, 92], i.e. Φ_g will converge to a state such that $\phi_1^g \cdot \phi_2^g = 0$.

Remark 9.1. If the potential $V(\mathbf{x})$ in the two equations in (9.3) is chosen to be different in different equations, i.e. $V_j(\mathbf{x})$ in the j th ($j = 1, 2$) equation, and they satisfy $V_j(\mathbf{x}) \geq 0$, $\lim_{|\mathbf{x}| \rightarrow \infty} V_j(\mathbf{x}) = \infty$ ($j = 1, 2$), then the conclusions in the above Lemmas and Theorems 9.2-9.3 are still valid under the similar conditions.

9.4. Dynamical properties. Well-posedness of Cauchy problem of the CGPEs (9.3) in energy space is quite similar to that of single GPE (cf. section 2), and we omit the results here. If there is no internal Josephson junction, i.e. $\lambda = 0$, the density of each component is conserved. With an internal Josephson junction, we have the following lemmas for the dynamics of the density of each component [195]:

Lemma 9.2. *Suppose $(\psi_1(\mathbf{x}, t), \psi_2(\mathbf{x}, t))$ is the solution of the CGPEs (9.3) with potential $V(\mathbf{x}) + \delta$ for the first component ψ_1 replaced by $V_1(\mathbf{x})$ and potential $V(\mathbf{x})$ for the second component ψ_2 replaced by $V_2(\mathbf{x})$; then we have, for $j = 1, 2$*

$$\ddot{N}_j(t) = -2\lambda^2 [2N_j(t) - 1] + F_j(t), \quad t \geq 0, \quad (9.27)$$

with initial conditions

$$N_j(0) = N_j^{(0)} = \int_{\mathbb{R}^d} |\psi_j^0(\mathbf{x})|^2 d\mathbf{x} = \frac{N_j^0}{N}, \quad (9.28)$$

$$\dot{N}_j(0) = N_j^{(1)} = 2\lambda \int_{\mathbb{R}^d} \text{Im} \left[\psi_j^0(\mathbf{x}) \left(\overline{\psi_{k_j}^0(\mathbf{x})} \right) \right] d\mathbf{x}; \quad (9.29)$$

where $k_1 = 2, k_2 = 1$ and for $t \geq 0$,

$$F_j(t) = \lambda \int_{\mathbb{R}^d} \left(\overline{\psi_j} \psi_{k_j} + \psi_j \overline{\psi_{k_j}} \right) \left[V_{k_j}(\mathbf{x}) - V_j(\mathbf{x}) - (\beta_{jj} - \beta_{k_j j}) |\psi_j|^2 + (\beta_{k_j k_j} - \beta_{j k_j}) |\psi_{k_j}|^2 \right] d\mathbf{x}, \quad t \geq 0.$$

From this lemma, we have [195]

Lemma 9.3. *If $\delta = 0$ and $\beta_{11} = \beta_{12} = \beta_{21} = \beta_{22}$ in (9.3), for any initial data $\Psi(\mathbf{x}, t = 0) = (\psi_1^0(\mathbf{x}), \psi_2^0(\mathbf{x}))^T$, we have, for $t \geq 0$,*

$$N_j(t) = \|\psi_j(\cdot, t)\|_2^2 = \left(N_j^{(0)} - \frac{1}{2} \right) \cos(2\lambda t) + \frac{N_j^{(1)}}{2\lambda} \sin(2\lambda t) + \frac{1}{2}, \quad j = 1, 2. \quad (9.30)$$

Thus in this case, the density of each component is a periodic function with period $T = \pi/|\lambda|$ depending only on λ .

9.5. Numerical methods for computing ground states. To find the ground state, we first present a continuous normalized gradient flow (CNGF) method discussed in section 3.1 and then propose a GFDN method based on discretization of CNGF.

9.5.1. *Continuous normalized gradient flow and its discretization.* In order to compute the ground state of two-component BEC with an internal Josephson junction (9.15), we construct the following CNGF [19]:

$$\begin{aligned}\frac{\partial \phi_1(\mathbf{x}, t)}{\partial t} &= \left[\frac{1}{2} \nabla^2 - V(\mathbf{x}) - \delta - (\beta_{11} |\phi_1|^2 + \beta_{12} |\phi_2|^2) \right] \phi_1 - \lambda \phi_2 + \mu_\Phi(t) \phi_1, \\ \frac{\partial \phi_2(\mathbf{x}, t)}{\partial t} &= \left[\frac{1}{2} \nabla^2 - V(\mathbf{x}) - (\beta_{12} |\phi_1|^2 + \beta_{22} |\phi_2|^2) \right] \phi_2 - \lambda \phi_1 + \mu_\Phi(t) \phi_2,\end{aligned}\tag{9.31}$$

where $\Phi(\mathbf{x}, t) = (\phi_1(\mathbf{x}, t), \phi_2(\mathbf{x}, t))^T$ and $\mu_\Phi(t)$ is chosen such that the above CNGF is mass or normalization conservative and it is given as

$$\begin{aligned}\mu_\Phi(t) &= \frac{1}{\|\Phi(\cdot, t)\|_2^2} \int_{\mathbb{R}^d} \left[\frac{1}{2} (|\nabla \phi_1|^2 + |\nabla \phi_2|^2) + V(\mathbf{x})(|\phi_1|^2 + |\phi_2|^2) + \delta |\phi_1|^2 \right. \\ &\quad \left. + \beta_{11} |\phi_1|^4 + \beta_{22} |\phi_2|^4 + 2\beta_{12} |\phi_1|^2 |\phi_2|^2 + 2\lambda \operatorname{Re}(\phi_1 \bar{\phi}_2) \right] d\mathbf{x} \\ &= \frac{\mu(\Phi(\cdot, t))}{\|\Phi(\cdot, t)\|_2^2}, \quad t \geq 0.\end{aligned}\tag{9.32}$$

For the above CNGF, we have [19]

Theorem 9.4. *For any given initial data*

$$\Phi(\mathbf{x}, 0) = (\phi_1^0(\mathbf{x}), \phi_2^0(\mathbf{x}))^T := \Phi^{(0)}(\mathbf{x}), \quad \mathbf{x} \in \mathbb{R}^d,\tag{9.33}$$

satisfying $\|\Phi^{(0)}\|_2^2 = 1$, the CNGF (9.31) is mass or normalization conservative and energy diminishing, i.e.

$$\|\Phi(\cdot, t)\|_2^2 \equiv \|\Phi^{(0)}\|_2^2 = 1, \quad E(\Phi(\cdot, t)) \leq E(\Phi(\cdot, s)), \quad 0 \leq s \leq t.\tag{9.34}$$

For practical computation, here we also present a second-order in both space and time full discretization for the above CNGF (9.31). For simplicity of notation, we introduce the method for the case of one spatial dimension (1D) in a bounded domain $U = (a, b)$ with homogeneous Dirichlet boundary condition

$$\Phi(a, t) = \Phi(b, t) = \mathbf{0}, \quad t \geq 0.\tag{9.35}$$

Generalizations to higher dimensions are straightforward for tensor product grids.

Let $\Phi_j^n = (\phi_{1,j}^n, \phi_{2,j}^n)^T$ be the numerical approximation of $\Phi(x_j, t_n)$ and Φ^n be the solution vector with component Φ_j^n . In addition, denote $\Phi_j^{n+1/2} = (\phi_{1,j}^{n+1/2}, \phi_{2,j}^{n+1/2})^T$ with

$$\phi_{l,j}^{n+1/2} = \frac{1}{2} (\phi_{l,j}^{n+1} + \phi_{l,j}^n), \quad j = 0, 1, 2, \dots, M, \quad l = 1, 2.\tag{9.36}$$

Then a second-order full discretization for the CNGF (9.31) is given, for $j = 1, 2, \dots, M-1$ and $n \geq 0$, as

$$\begin{aligned}\frac{\phi_{1,j}^{n+1} - \phi_{1,j}^n}{\tau} &= \frac{\phi_{1,j+1}^{n+1/2} - 2\phi_{1,j}^{n+1/2} + \phi_{1,j-1}^{n+1/2}}{2h^2} - \left[V(x_j) + \delta - \mu_{\Phi,h}^{n+1/2} \right] \phi_{1,j}^{n+1/2} - \lambda \phi_{2,j}^{n+1/2} \\ &\quad - \frac{1}{2} [\beta_{11} (|\phi_{1,j}^{n+1/2}|^2 + |\phi_{1,j}^n|^2) + \beta_{12} (|\phi_{2,j}^{n+1/2}|^2 + |\phi_{2,j}^n|^2)] \phi_{1,j}^{n+1/2}, \\ \frac{\phi_{2,j}^{n+1} - \phi_{2,j}^n}{\tau} &= \frac{\phi_{2,j+1}^{n+1/2} - 2\phi_{2,j}^{n+1/2} + \phi_{2,j-1}^{n+1/2}}{2h^2} - \left[V(x_j) - \mu_{\Phi,h}^{n+1/2} \right] \phi_{2,j}^{n+1/2} - \lambda \phi_{1,j}^{n+1/2} \\ &\quad - \frac{1}{2} [\beta_{12} (|\phi_{1,j}^{n+1/2}|^2 + |\phi_{1,j}^n|^2) + \beta_{22} (|\phi_{2,j}^{n+1/2}|^2 + |\phi_{2,j}^n|^2)] \phi_{2,j}^{n+1/2},\end{aligned}$$

where

$$\mu_{\Phi,h}^{n+1/2} = \frac{D_{\Phi,h}^{n+1/2}}{h \sum_{j=0}^{M-1} \left(|\phi_{1,j}^{n+1/2}|^2 + |\phi_{2,j}^{n+1/2}|^2 \right)}, \quad n \geq 0, \quad (9.37)$$

with

$$\begin{aligned} D_{\Phi,h}^{n+1/2} = & h \sum_{j=0}^{M-1} \left\{ \sum_{l=1}^2 \left(\frac{1}{2h^2} |\phi_{l,j+1}^{n+1/2} - \phi_{l,j}^{n+1/2}|^2 + V(x_j) |\phi_{l,j}^{n+1/2}|^2 \right) + \delta |\phi_{1,j}^{n+1/2}|^2 \right. \\ & + \frac{1}{2} \beta_{11} (|\phi_{1,j}^{n+1}|^2 + |\phi_{1,j}^n|^2) |\phi_{1,j}^{n+1/2}|^2 + \frac{1}{2} \beta_{22} (|\phi_{2,j}^{n+1}|^2 + |\phi_{2,j}^n|^2) |\phi_{2,j}^{n+1/2}|^2 \\ & + \frac{1}{2} \beta_{12} \left[(|\phi_{2,j}^{n+1}|^2 + |\phi_{2,j}^n|^2) |\phi_{1,j}^{n+1/2}|^2 + (|\phi_{1,j}^{n+1}|^2 + |\phi_{1,j}^n|^2) |\phi_{2,j}^{n+1/2}|^2 \right] \\ & \left. + 2\lambda \operatorname{Re} \left(\phi_{1,j}^{n+1/2} \bar{\phi}_{2,j}^{n+1/2} \right) \right\}. \end{aligned} \quad (9.38)$$

The boundary condition (9.35) is discretized as

$$\phi_{1,0}^{n+1} = \phi_{1,M}^{n+1} = \phi_{2,0}^{n+1} = \phi_{2,M}^{n+1} = 0, \quad n = 0, 1, 2, \dots \quad (9.39)$$

The initial data (9.33) is discretized as

$$\phi_{1,j}^0 = \phi_1^0(x_j), \quad \phi_{2,j}^0 = \phi_2^0(x_j), \quad j = 0, 1, \dots, M. \quad (9.40)$$

In the above full discretization, at every time step, we need to solve a fully nonlinear system which is very tedious in practical computation. Below we present a more efficient discretization for the CNGF (9.31) for computing the ground states.

9.5.2. *Gradient flow with discrete normalization.* Another more efficient way to discretize the CNGF (9.31) is through the construction of the following GFDN [19]:

$$\begin{aligned} \frac{\partial \phi_1}{\partial t} &= \left[\frac{1}{2} \nabla^2 - V(\mathbf{x}) - \delta - (\beta_{11} |\phi_1|^2 + \beta_{12} |\phi_2|^2) \right] \phi_1 - \lambda \phi_2, \\ \frac{\partial \phi_2}{\partial t} &= \left[\frac{1}{2} \nabla^2 - V(\mathbf{x}) - (\beta_{12} |\phi_1|^2 + \beta_{22} |\phi_2|^2) \right] \phi_2 - \lambda \phi_1, \quad t \in (t_n, t_{n+1}), \end{aligned} \quad (9.41)$$

followed by a projection step as

$$\phi_l(\mathbf{x}, t_{n+1}) := \phi_l(\mathbf{x}, t_{n+1}^+) = \sigma_l^{n+1} \phi_l(\mathbf{x}, t_{n+1}^-), \quad l = 1, 2, \quad n \geq 0, \quad (9.42)$$

where $\phi_l(\mathbf{x}, t_{n+1}^\pm) = \lim_{t \rightarrow t_{n+1}^\pm} \phi_l(\mathbf{x}, t)$ ($l = 1, 2$) and σ_l^{n+1} ($l = 1, 2$) are chosen such that

$$\|\Phi(\mathbf{x}, t_{n+1})\|^2 = \|\phi_1(\mathbf{x}, t_{n+1})\|_2^2 + \|\phi_2(\mathbf{x}, t_{n+1})\|_2^2 = 1, \quad n \geq 0. \quad (9.43)$$

The above GFDN (9.41)-(9.42) can be viewed as applying the first-order splitting method to the CNGF (9.31) and the projection step (9.42) is equivalent to solving the following ordinary differential equations (ODEs)

$$\frac{\partial \phi_1(\mathbf{x}, t)}{\partial t} = \mu_\Phi(t) \phi_1, \quad \frac{\partial \phi_2(\mathbf{x}, t)}{\partial t} = \mu_\Phi(t) \phi_2, \quad t_n \leq t \leq t_{n+1}, \quad (9.44)$$

which immediately suggests that the projection constants in (9.42) are chosen as

$$\sigma_1^{n+1} = \sigma_2^{n+1}, \quad n \geq 0. \quad (9.45)$$

Plugging (9.45) and (9.42) into (9.43), we obtain

$$\sigma_1^{n+1} = \sigma_2^{n+1} = \frac{1}{\|\Phi(\cdot, t_{n+1}^-)\|_2} = \frac{1}{\sqrt{\|\phi_1(\cdot, t_{n+1}^-)\|_2^2 + \|\phi_2(\cdot, t_{n+1}^-)\|_2^2}}, \quad n \geq 0. \quad (9.46)$$

Then, BEFD in section 3.2 can be used to discretize the GFDN (9.41)-(9.42) and we omit the detailed scheme here, as the generalization is straightforward.

9.6. Numerical methods for computing dynamics. To compute dynamics of a two component BEC, finite difference time domain methods in section 4.2 can be directly extended to solve the CGPEs (9.3). Here we focus on the time splitting methods. For $n = 0, 1, \dots$, from time $t = t_n = n\tau$ to $t = t_{n+1} = t_n + \tau$, the CGPEs (9.3) are solved in three splitting steps [181, 183, 195]. One first solves

$$i \frac{\partial \psi_j}{\partial t} = -\frac{1}{2} \nabla^2 \psi_j, \quad j = 1, 2, \quad (9.47)$$

for the time step of length τ , followed by solving

$$i \frac{\partial \psi_j}{\partial t} = V_j(\mathbf{x}) \psi_j + \sum_{l=1}^2 \beta_{jl} |\psi_l|^2 \psi_j, \quad j = 1, 2, \quad (9.48)$$

for the same time step with $V_1(\mathbf{x}) = V(\mathbf{x}) + \delta$ and $V_2(\mathbf{x}) = V(\mathbf{x})$, and then by solving

$$i \frac{\partial \psi_1}{\partial t} = -\lambda \psi_2, \quad i \frac{\partial \psi_2}{\partial t} = -\lambda \psi_1, \quad (9.49)$$

for the same time step. For time $t \in [t_n, t_{n+1}]$, the ODE system (9.48) leaves $|\psi_1(\mathbf{x}, t)|$ and $|\psi_2(\mathbf{x}, t)|$ invariant in t , and thus it can be integrated *exactly* to obtain [31, 33, 47, 48, 193], for $j = 1, 2$ and $t \in [t_n, t_{n+1}]$

$$\psi_j(\mathbf{x}, t) = \psi_j(\mathbf{x}, t_n) \exp \left[-i \left(V_j(\mathbf{x}) + \sum_{l=1}^2 \beta_{jl} |\psi_l(\mathbf{x}, t_n)|^2 \right) (t - t_n) \right]. \quad (9.50)$$

For the ODE system (9.49), we can rewrite it as

$$i \frac{\partial \Psi}{\partial t} = -\lambda A \Psi, \quad \text{with } A = \begin{pmatrix} 0 & 1 \\ 1 & 0 \end{pmatrix} \quad \text{and } \Psi = \begin{pmatrix} \psi_1 \\ \psi_2 \end{pmatrix}. \quad (9.51)$$

Since A is a real and symmetric matrix, it can be diagonalized and integrated *exactly*, and then we obtain [15, 195], for $t \in [t_n, t_{n+1}]$

$$\Psi(\mathbf{x}, t) = e^{i\lambda A (t-t_n)} \Psi(\mathbf{x}, t_n) = \begin{pmatrix} \cos(\lambda(t-t_n)) & i \sin(\lambda(t-t_n)) \\ i \sin(\lambda(t-t_n)) & \cos(\lambda(t-t_n)) \end{pmatrix} \Psi(\mathbf{x}, t_n).$$

Then, time splitting spectral method introduced in sections 4 and 6 can be applied to compute the dynamics of the CGPEs (9.3), by a suitable composition of the above three steps (cf. section 4.1). The detailed scheme is omitted here for brevity.

9.7. Numerical results. In this section, we will report the ground states of (9.15), computed by our numerical methods.

Example 9.1. Ground states of a two-component BEC with an external driving field when B is positive definite, i.e. we take $d = 1$, $V(x) = \frac{1}{2}x^2$ and $\beta_{11} : \beta_{12} : \beta_{22} = (1 : 0.94 : 0.97)\beta$ in (9.15) [15, 19]. In this case, since $\lambda \leq 0$ and B is positive definite when $\beta > 0$, thus we know that the positive ground state $\Phi_g = (\phi_1, \phi_2)^T$

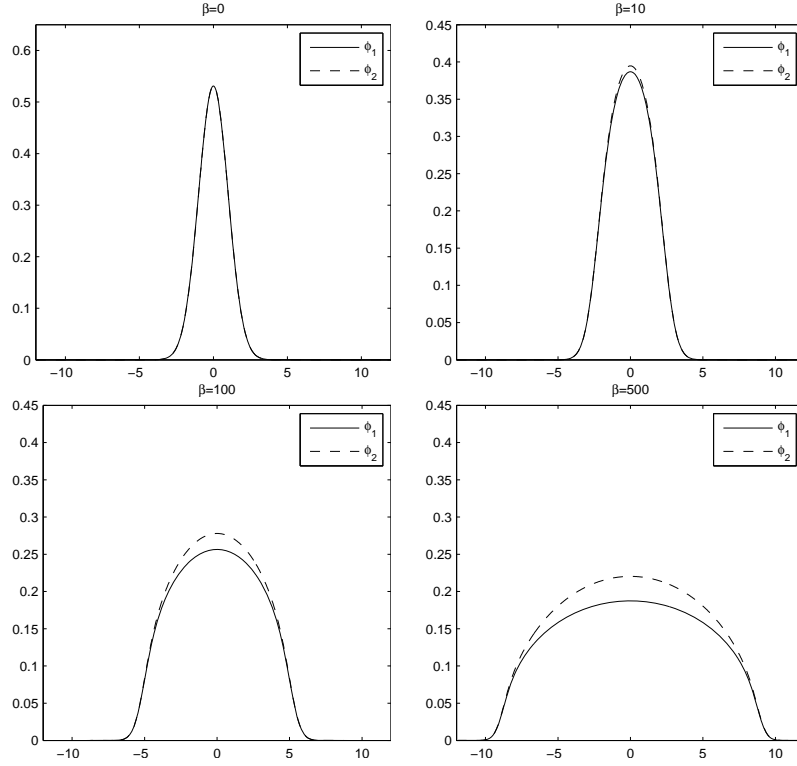


FIGURE 9.1. Ground states $\Phi_g = (\phi_1, \phi_2)^T$ in Example 9.1 when $\delta = 0$ and $\lambda = -1$ for different β .

is unique. In our computations, we take the computational domain $U = [-16, 16]$ with mesh size $h = \frac{1}{32}$ and time step $\tau = 0.1$. The initial data in (9.33) is chosen as

$$\phi_1^0(x) = \phi_2^0(x) = \frac{1}{\pi^{1/4}\sqrt{2}}e^{-x^2/2}, \quad x \in \mathbb{R}. \quad (9.52)$$

Fig. 9.1 plots the ground states Φ_g when $\delta = 0$ and $\lambda = -1$ for different β . Fig. 9.2 shows mass of each component $N(\phi_j) = \|\phi_j\|^2$ ($j = 1, 2$), energy $E := E(\Phi_g)$ and chemical potential $\mu := \mu(\Phi_g)$ of the ground states when $\beta = 100$ and $\delta = 0, 1$ for different λ , and Fig. 9.3 depicts similar results when $\beta = 100$ and $\lambda = 0, -5$ for different δ .

10. Perspectives and challenges. So far, we have introduced mathematical results and numerical methods for ground states and dynamics of a single/two component rotating/nonrotating BEC with/without dipole-dipole interactions described by mean field GPE. Despite these BEC systems, much progress has been made towards realizing other kinds of gaseous BEC, such as spinor condensates, condensates at finite temperature, Bose-Fermi mixtures, etc. These achievements have brought great challenges to atomic physics community and scientific computing community for modeling, simulating and understanding various interesting phenomena.

10.1. Spin-1 BEC. In earlier BEC experiments, the atoms were confined in magnetic trap [12, 59, 86], in which the spin degrees of freedom is frozen. In recent

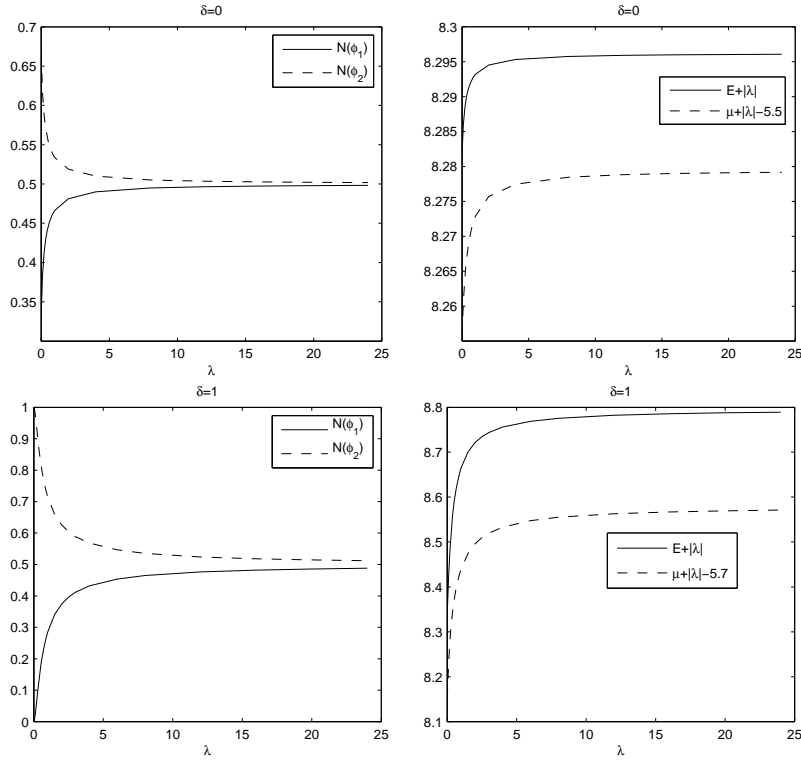


FIGURE 9.2. Mass of each component $N(\phi_j) = \|\phi_j\|^2$ ($j = 1, 2$), energy $E := E(\Phi_g)$ and chemical potential $\mu := \mu(\Phi_g)$ of the ground states in Example 9.1 when $\beta = 100$ and $\delta = 0, 1$ for different λ .

years, experimental achievement of spin-1 and spin-2 condensates [50, 124] offers new regimes to study various quantum phenomena that are generally absent in a single component condensate. The spinor condensate is achieved experimentally when an optical trap, instead of a magnetic trap, is used to provide equal confinement for all hyperfine states.

The theoretical studies of spinor condensate have been carried out in several papers since the achievement of it in experiments [115, 128]. In contrast to single component condensate, a spin- F ($F \in \mathbb{N}$) condensate is described by a generalized coupled GPEs which consists of $2F+1$ equations, each governing one of the $2F+1$ hyperfine states ($m_F = -F, -F+1, \dots, F-1, F$) within the mean-field approximation. For a spin-1 condensate, at temperature much lower than the critical temperature T_c , the three-components wave function $\Psi := \Psi(\mathbf{x}, t) = (\psi_1(\mathbf{x}, t), \psi_0(\mathbf{x}, t), \psi_{-1}(\mathbf{x}, t))^T$

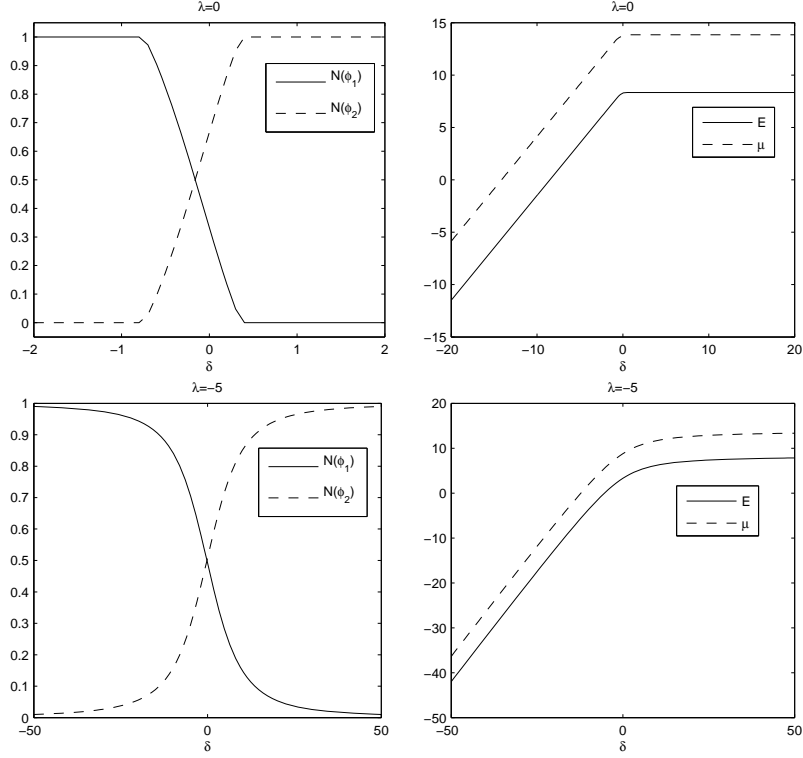


FIGURE 9.3. Mass of each component $N(\phi_j) = \|\phi_j\|^2$ ($j = 1, 2$), energy $E := E(\Phi_g)$ and chemical potential $\mu := \mu(\Phi_g)$ of the ground states in Example 9.1 when $\beta = 100$ and $\lambda = 0, -5$ for different δ .

are well described by the following coupled GPEs [36, 124],

$$i\hbar \partial_t \psi_1(\mathbf{x}, t) = \left[-\frac{\hbar^2}{2m} \nabla^2 + V(\mathbf{x}) + (c_0 + c_2)(|\psi_1|^2 + |\psi_0|^2) + (c_0 - c_2)|\psi_{-1}|^2 \right] \psi_1 + c_2 \bar{\psi}_{-1} \psi_0^2, \quad (10.1)$$

$$i\hbar \partial_t \psi_0(\mathbf{x}, t) = \left[-\frac{\hbar^2}{2m} \nabla^2 + V(\mathbf{x}) + (c_0 + c_2)(|\psi_1|^2 + |\psi_{-1}|^2) + c_0 |\psi_0|^2 \right] \psi_0 + 2c_2 \psi_{-1} \bar{\psi}_0 \psi_1, \quad (10.2)$$

$$i\hbar \partial_t \psi_{-1}(\mathbf{x}, t) = \left[-\frac{\hbar^2}{2m} \nabla^2 + V(\mathbf{x}) + (c_0 + c_2)(|\psi_{-1}|^2 + |\psi_0|^2) + (c_0 - c_2)|\psi_1|^2 \right] \psi_{-1} + c_2 \psi_0^2 \bar{\psi}_1, \quad \mathbf{x} = (x, y, z)^T \in \mathbb{R}^3. \quad (10.3)$$

Here $V(\mathbf{x})$ is an external trapping potential. There are two atomic collision terms, $c_0 = \frac{4\pi\hbar^2}{3m}(a_0 + 2a_2)$ and $c_2 = \frac{4\pi\hbar^2}{3m}(a_2 - a_0)$, expressed in terms of the s -wave scattering lengths, a_0 and a_2 , for scattering channel of total hyperfine spin 0 (anti-parallel spin collision) and spin 2 (parallel spin collision), respectively. The usual mean-field

interaction, c_0 , is positive for repulsive interaction and negative for attractive interaction. The spin-exchange interaction, c_2 , is positive for antiferromagnetic interaction and negative for ferromagnetic interaction. The wave function is normalized according to

$$\|\Psi\|_2^2 := \int_{\mathbb{R}^3} |\Psi(\mathbf{x}, t)|^2 d\mathbf{x} = \int_{\mathbb{R}^3} \sum_{l=-1}^1 |\psi_l(\mathbf{x}, t)|^2 d\mathbf{x} := \sum_{l=-1}^1 \|\psi_l\|_2^2 = N, \quad (10.4)$$

where N is the total number of particles in the condensate. This normalization is conserved by coupled GPEs (10.1)-(10.3), and so are the magnetization

$$M(\Psi(\cdot, t)) := \int_{\mathbb{R}^3} [|\psi_1(\mathbf{x}, t)|^2 - |\psi_{-1}(\mathbf{x}, t)|^2] d\mathbf{x} \equiv M(\Psi(\cdot, 0)) = M \quad (10.5)$$

and the energy per particle

$$\begin{aligned} E(\Psi(\cdot, t)) &= \int_{\mathbb{R}^3} \left\{ \sum_{l=-1}^1 \left(\frac{\hbar^2}{2m} |\nabla \psi_l|^2 + V(\mathbf{x}) |\psi_l|^2 \right) + (c_0 - c_2) |\psi_1|^2 |\psi_{-1}|^2 \right. \\ &\quad \left. + \frac{c_0}{2} |\psi_0|^4 + \frac{c_0 + c_2}{2} [|\psi_1|^4 + |\psi_{-1}|^4 + 2|\psi_0|^2 (|\psi_1|^2 + |\psi_{-1}|^2)] \right. \\ &\quad \left. + c_2 (\overline{\psi}_{-1} \psi_0^2 \overline{\psi}_1 + \psi_{-1} \overline{\psi}_0^2 \psi_1) \right\} d\mathbf{x} \equiv E(\Psi(\cdot, 0)), \quad t \geq 0. \quad (10.6) \end{aligned}$$

Then ground states of spin-1 BEC can be defined as the minimizer of energy E under the normalization and magnetization constraints [26, 36, 45]. In particular, when the external traps for all the components are the same, ground states for ferromagnetic and antiferromagnetic spin-1 BECs can be simplified [26]. Generally speaking, for spin- F BEC, the complicated nonlinear terms in (10.1)-(10.3) lead to new difficulties for mathematical analysis and numerical simulation [182]. Much work needs to be done in future, especially when rotational frame and dipole-dipole interactions are taken into account in spin- F BECs [124].

10.2. Bogoliubov excitation. The theory of interacting Bose gases, developed by Bogoliubov in 1947, is very useful and important to understand BEC in dilute atomic gases. One of the key issue is the Bogoliubov excitation.

To describe the condensate, we have the lowest order approximation, i.e., the Gross-Pitaevskii energy by assuming that all particles are in the ground state. However, due to the interactions between the atoms, there is a small portion occupying the excited states. Thus, if a higher order approximation of the ground state energy is considered, excitations have to be included. Using a perturbation technique, Bogoliubov has investigated this problem and shown that the excited states of a system of interacting Bose particles can be described by a system of noninteracting quasi-particles satisfying the Bogoliubov dispersion relation.

To determine the Bogoliubov excitation spectrum, we consider small perturbations around the ground state of Eq. (1.19). For simplicity we assume a vanishing harmonic potential $V(\mathbf{x}) = 0$ and homogeneous density ν . A stationary state of the GPE (1.19) is given by $\psi(\mathbf{x}, t) = \psi(t) = e^{-i\mu t} \sqrt{\nu}$ with the chemical potential

$$\mu = \beta\nu. \quad (10.7)$$

Now we add a local perturbation $\xi(\mathbf{x}, t)$ to the stationary state $\psi(t)$, that is, $\psi(\mathbf{x}, t) = e^{-i\mu t} [\sqrt{\nu} + \xi(\mathbf{x}, t)]$. We expand the perturbation in a plane wave basis as $\xi(\mathbf{x}, t) = \int_{\mathbb{R}^3} (u_{\mathbf{q}} e^{i(\mathbf{q}\cdot\mathbf{x} - \omega_{\mathbf{q}} t)} + \overline{v_{\mathbf{q}}} e^{-i(\mathbf{q}\cdot\mathbf{x} - \omega_{\mathbf{q}} t)}) d\mathbf{q}$ and insert $\psi(\mathbf{x}, t)$ into Eq.

(1.19). Here, $\omega_{\mathbf{q}}$ are the excitation frequencies of quasimomentum \mathbf{q} and $u_{\mathbf{q}}, v_{\mathbf{q}}$ are the mode functions. Keeping terms linear in the excitations $u_{\mathbf{q}}$ and $v_{\mathbf{q}}$ we find the Bogoliubov-de Gennes equations

$$\begin{aligned}\omega_{\mathbf{q}}u_{\mathbf{q}} &= \frac{\mathbf{q}^2}{2}u_{\mathbf{q}} + \nu\beta(v_{\mathbf{q}} + u_{\mathbf{q}}), \\ -\omega_{\mathbf{q}}v_{\mathbf{q}} &= \frac{\mathbf{q}^2}{2}v_{\mathbf{q}} + \nu\beta(v_{\mathbf{q}} + u_{\mathbf{q}}).\end{aligned}\tag{10.8}$$

Then we can find the eigenenergies of Eq. (10.8) by solving the eigenvalue problem. The resulting Bogoliubov energy $E_B(\mathbf{q}) = \omega_{\mathbf{q}}$ is determined by

$$E_B^2(\mathbf{q}) = \frac{\mathbf{q}^2}{2} \left(\frac{\mathbf{q}^2}{2} + 2\beta\nu \right).\tag{10.9}$$

When an external potential is considered, the Bogoliubov energy would be more complicated. In 1999, the Bogoliubov excitation spectrum was observed for the first time in atomic BEC [170], using light scattering. Later in 2008, observation of Bogoliubov excitations was announced in exciton-polariton condensates [179]. Such elementary excitations are crucial in understanding various phenomenon in BEC.

10.3. BEC at finite temperature. The process of creating a BEC in a trap by means of evaporative cooling starts in a regime covered by the quantum Boltzmann equation (QBE) and finishes in a regime where the GPE is expected to be valid. The GPE is capable to describe the main properties of the condensate at very low temperatures, it treats the condensate as a classical field and neglects quantum and thermal fluctuations. As a consequence, the theory breaks down at higher temperatures where the non-condensed fraction of the gas cloud is significant. An approach which allows the treatment of both condensate and noncondensate parts simultaneously was developed in [39, 190].

The resulting equations of motion reduce to a generalized GPE for the condensate wave function coupled with a semiclassical QBE for the thermal cloud:

$$\begin{aligned}i\hbar\partial_t\psi(\mathbf{x}, t) &= \left[-\frac{\hbar^2}{2m}\nabla^2 + (n_c(\mathbf{x}, t) + 2n(\mathbf{x}, t))g - iR(\mathbf{x}, t) \right] \psi, \\ \frac{\partial F}{\partial t} + \frac{\mathbf{p}}{m} \cdot \nabla_{\mathbf{x}}F - \nabla_{\mathbf{x}}U \cdot \nabla_{\mathbf{p}}F &= Q(F) + Q_c(F),\end{aligned}\tag{10.10}$$

where $n_c(\mathbf{x}, t) = |\psi(\mathbf{x}, t)|^2$ is the condensate density, $F := F(\mathbf{x}, \mathbf{p}, t)$ describes the distribution of thermal atoms in the phase space and it gives the particle number with momentum \mathbf{p} at position \mathbf{x} and time t in the thermal cloud. $n(\mathbf{x}, t) = \int_{\mathbb{R}^3} F(\mathbf{x}, \mathbf{p}, t)/(2\pi\hbar)^3 d\mathbf{p}$, $V(\mathbf{x})$ is the confining potential and $g = 4\pi\hbar^2 a_s/m$. The collision integral $Q(F)$ is given by

$$\begin{aligned}Q(F) &= \frac{2g^2}{(2\pi)^5\hbar^7} \int_{\mathbb{R}^3 \times \mathbb{R}^3 \times \mathbb{R}^3} \delta(\mathbf{p} + \mathbf{p}_* - \mathbf{p}' - \mathbf{p}'_*) \times \delta(\epsilon + \epsilon_* - \epsilon' - \epsilon'_*) \\ &\quad \times [(1+F)(1+F_*)F'F'_* - FF_*(1+F')(1+F'_*)] d\mathbf{p}_* d\mathbf{p}' d\mathbf{p}'_*,\end{aligned}$$

where $\epsilon = U(\mathbf{x}, t) + \mathbf{p}^2/2m$, $U(\mathbf{x}, t) = V(\mathbf{x}) + 2gn_c(\mathbf{x}, t) + 2gn(\mathbf{x}, t)$ and $\delta(\cdot)$ is the Dirac distribution. $Q_c(F)$ which describes collisions between condensate and non

condensate particles is given by

$$\begin{aligned}
 Q_c(F) = & \frac{2g^2 n_c}{(2\pi)^2 \hbar^4} \int_{\mathbb{R}^3 \times \mathbb{R}^3 \times \mathbb{R}^3} \delta(m\mathbf{v}_c + \mathbf{p}_* - \mathbf{p}' - \mathbf{p}'_*) \\
 & \times \delta(\epsilon_c + \epsilon_* - \epsilon' - \epsilon'_*) [\delta(\mathbf{p} - \mathbf{p}_*) - \delta(\mathbf{p} - \mathbf{p}') - \delta(\mathbf{p} - \mathbf{p}'_*)] \\
 & \times [(1 + F_*)F'F'_* - F_*(1 + F')(1 + F'_*)] d\mathbf{p}_* d\mathbf{p}' d\mathbf{p}'_*,
 \end{aligned}$$

where

$$\epsilon_c(\mathbf{x}, t) = \frac{1}{2} m \mathbf{v}_c(\mathbf{x}, t)^2 + \mu_c(\mathbf{x}, t), \tag{10.11}$$

and \mathbf{v}_c is the quantum hydrodynamic velocity, μ_c is the effective potential acting on the condensate [108, 190]. $R(\mathbf{x}, t)$ is then written as

$$R(\mathbf{x}, t) = \frac{\hbar}{2n_c} \int_{\mathbb{R}^3} \frac{Q_c(F)}{(2\pi\hbar)^3} d\mathbf{p}. \tag{10.12}$$

Note that for low temperatures $T \rightarrow 0$ we have $n, R \rightarrow 0$ and we recover the conventional GPE. The system (10.10) is normalized as $N_c(0) = N_c^0$ and $N_t(0) = N_t^0$ with

$$N_c(t) = \int_{\mathbb{R}^3} |\psi(\mathbf{x}, t)|^2 d\mathbf{x}, \quad N_t(t) = \int_{\mathbb{R}^3} |n(\mathbf{x}, t)|^2 d\mathbf{x}, \quad t \geq 0, \tag{10.13}$$

where N_c^0 and N_t^0 are the number of particles in the condensate and thermal cloud at time $t = 0$, respectively. It is easy to see from the equations (10.10) that the total number of particles defined as $N_{\text{total}}(t) = N_c(t) + N_t(t) = N_{\text{total}}^0 = N_c^0 + N_t^0$ is conserved. For this set of equations, the GPE part can be solved efficiently, and the main trouble comes from the Boltzmann equation part. Alternatively, projected GPE model is also used for simulating BEC at finite temperature [85, 87].

Acknowledgments. We would like to thank our collaborators: Naoufel Ben Abdallah, Francois Castella, I-Liang Chern, Qiang Du, Jiangbin Gong, Dieter Jaksch, Shi Jin, Baowen Li, Hai-Liang Li, Fong-Yin Lim, Peter A. Markowich, Florian Méhats, Lorenzo Pareschi, Han Pu, Matthias Rosenkranz, Christian Schmeiser, Jie Shen, Weijun Tang, Hanquan Wang, Rada M. Weishäupl, Yanzhi Zhang, etc. for their significant contributions and fruitful collaborations on the topic over the last decade. We have learned a lot from them during the fruitful collaboration and interaction. This work was supported by the Academic Research Fund of Ministry of Education of Singapore grant R-146-000-120-112.

REFERENCES

[1] J. R. Abo-Shaeer, C. Raman, J. M. Vogels and W. Ketterle, *Observation of vortex lattices in Bose-Einstein condensates*, Science, **292** (2001), 476–479.
 [2] S. K. Adhikari and P. Muruganandam, *Bose-Einstein condensation dynamics from the numerical solution of the Gross-Pitaevskii equation*, J. Phys. B: At. Mol. Opt. Phys., **35** (2002), 2831–2843.
 [3] S. K. Adhikari and P. Muruganandam, *Mean-field model for the interference of matter-waves from a three-dimensional optical trap*, Phys. Lett. A, **310** (2003), 229–235.
 [4] A. Aftalion, “Vortices in Bose-Einstein Condensates,” Progress in Nonlinear Differential Equations and their Applications, 67, Birkhäuser, Boston, 2006.
 [5] A. Aftalion and Q. Du, *Vortices in a rotating Bose-Einstein condensate: Critical angular velocities and energy diagrams in the Thomas-Fermi regime*, Phys. Rev. A, **64** (2001), 063603.
 [6] A. Aftalion, Q. Du and Y. Pomeau, *Dissipative flow and vortex shedding in the Painlevé boundary layer of a Bose Einstein condensate*, Phys. Rev. Lett., **91** (2003), 090407.
 [7] A. Aftalion, R. Jerrard and J. Royo-Letelier, *Non-existence of vortices in the small density region of a condensate*, J. Funct. Anal., **260** (2011), 2387–2406.

- [8] K. Aikawa, A. Frisch, M. Mark, S. Baier, A. Rietzler, R. Grimm and F. Ferlaino, *Bose-Einstein condensation of Erbium*, Phys. Rev. Lett., **108** (2012), 210401.
- [9] G. Akrivis, *Finite difference discretization of the cubic Schrödinger equation*, IMA J. Numer. Anal., **13** (1993), 115–124.
- [10] G. Akrivis, V. Dougalis and O. Karakashian, *On fully discrete Galerkin methods of second-order temporal accuracy for the nonlinear Schrödinger equation*, Numer. Math., **59** (1991), 31–53.
- [11] J. O. Andersen, *Theory of the weakly interacting Bose gas*, Rev. Mod. Phys., **76** (2004), 599–639.
- [12] M. H. Anderson, J. R. Ensher, M. R. Matthews, C. E. Wieman and E. A. Cornell, *Observation of Bose-Einstein condensation in a dilute atomic vapor*, Science, **269** (1995), 198–201.
- [13] P. Antonelli, D. Marahrens and C. Sparber, *On the Cauchy problem for nonlinear Schrödinger equations with rotation*, Discrete Contin. Dyn. Syst., **32** (2012), 703–715.
- [14] W. Bao, *The nonlinear Schrödinger equation and applications in Bose-Einstein condensation and plasma physics*, In “Dynamics in Models of Coarsening, Coagulation, Condensation and Quantization” (IMS Lecture Notes Series, World Scientific), **9** (2007), 141–240.
- [15] W. Bao, *Ground states and dynamics of multicomponent Bose-Einstein condensates*, Multi-scale Model. Simul., **2** (2004), 210–236.
- [16] W. Bao, *Numerical methods for the nonlinear Schrödinger equation with nonzero far-field conditions*, Methods Appl. Anal., **11** (2004), 367–387.
- [17] W. Bao, *Analysis and efficient computation for the dynamics of two-component Bose-Einstein condensates: Stationary and time dependent Gross-Pitaevskii equations*, Contemp. Math., **473** (2008), 1–26.
- [18] W. Bao, N. Ben Abdallah and Y. Cai, *Gross-Pitaevskii-Poisson equations for dipolar Bose-Einstein condensate with anisotropic confinement*, SIAM J. Math. Anal., **44** (2012), 1713–1741.
- [19] W. Bao and Y. Cai, *Ground states of two-component Bose-Einstein condensates with an internal atomic Josephson junction*, East Asia J. Appl. Math., **1** (2010), 49–81.
- [20] W. Bao and Y. Cai, *Uniform error estimates of finite difference methods for the nonlinear Schrödinger equation with wave operator*, SIAM J Numer. Anal., **50** (2012), 492–521.
- [21] W. Bao and Y. Cai, *Optimal error estimates of finite difference methods for the Gross-Pitaevskii equation with angular momentum rotation*, Math. Comp., to appear.
- [22] W. Bao and Y. Cai, *Uniform and optimal error estimates of an exponential wave integrator sine pseudospectral method for the nonlinear Schrödinger equation with wave operator*, preprint.
- [23] W. Bao, Y. Cai and H. Wang, *Efficient numerical methods for computing ground states and dynamics of dipolar Bose-Einstein condensates*, J. Comput. Phys., **229** (2010), 7874–7892.
- [24] W. Bao and M. H. Chai, *A uniformly convergent numerical method for singularly perturbed nonlinear eigenvalue problems*, Commun. Comput. Phys., **4** (2008), 135–160.
- [25] W. Bao, I. Chern and F. Y. Lim, *Efficient and spectrally accurate numerical methods for computing ground and first excited states in Bose-Einstein condensates*, J. Comput. Phys., **219** (2006), 836–854.
- [26] W. Bao, I. Chern and Y. Zhang, *Efficient methods for computing ground states of spin-1 Bose-Einstein condensates based on their characterizations*, preprint.
- [27] W. Bao and Q. Du, *Computing the ground state solution of Bose-Einstein condensates by a normalized gradient flow*, SIAM J. Sci. Comput., **25** (2004), 1674–1697.
- [28] W. Bao, Q. Du and Y. Zhang, *Dynamics of rotating Bose-Einstein condensates and its efficient and accurate numerical computation*, SIAM J. Appl. Math., **66** (2006), 758–786.
- [29] W. Bao, Y. Ge, D. Jaksch, P. A. Markowich and R. M. Weishäupl, *Convergence rate of dimension reduction in Bose-Einstein condensates*, Comput. Phys. Comm., **177** (2007), 832–850.
- [30] W. Bao and D. Jaksch, *An explicit unconditionally stable numerical method for solving damped nonlinear Schrödinger equations with a focusing nonlinearity*, SIAM J. Numer. Anal., **41** (2003), 1406–1426.
- [31] W. Bao, D. Jaksch and P. A. Markowich, *Numerical solution of the Gross-Pitaevskii equation for Bose-Einstein condensation*, J. Comput. Phys., **187** (2003), 318–342.
- [32] W. Bao, D. Jaksch and P. A. Markowich, *Three dimensional simulation of jet formation in collapsing condensates*, J. Phys. B: At. Mol. Opt. Phys., **37** (2004), 329–343.

- [33] W. Bao, S. Jin and P. A. Markowich, *On time-splitting spectral approximation for the Schrödinger equation in the semiclassical regime*, J. Comput. Phys., **175** (2002), 487–524.
- [34] W. Bao, S. Jin and P. A. Markowich, *Numerical study of time-splitting spectral discretizations of nonlinear Schrödinger equations in the semiclassical regimes*, SIAM J. Sci. Comput., **25** (2003), 27–64.
- [35] W. Bao, H.-L. Li and J. Shen, *A generalized Laguerre-Fourier-Hermite pseudospectral method for computing the dynamics of rotating Bose-Einstein condensates*, SIAM J. Sci. Comput., **31** (2009), 3685–3711.
- [36] W. Bao and F. Y. Lim, *Computing ground states of spin-1 Bose-Einstein condensates by the normalized gradient flow*, SIAM J. Sci. Comput., **30** (2008), 1925–1948.
- [37] W. Bao, F. Y. Lim and Y. Zhang, *Energy and chemical potential asymptotics for the ground state of Bose-Einstein condensates in the semiclassical regime*, Bull. Inst. Math. Acad. Sin. (N.S.), **2** (2007), 495–532.
- [38] W. Bao, P. A. Markowich, C. Schmeiser and R. M. Weishäupl, *On the Gross-Pitaevskii equation with strongly anisotropic confinement: formal asymptotics and numerical experiments*, Math. Models Meth. Appl. Sci., **15** (2005), 767–782.
- [39] W. Bao, L. Pareschi and P. A. Markowich, *Quantum kinetic theory: modeling and numerics for Bose-Einstein condensation*, In “Modeling and Computational Methods for Kinetic Equations” (Birkhäuser Series: Modeling and Simulation in Science, Engineering and Technology), 2004, 287–321.
- [40] W. Bao and J. Shen, *A fourth-order time-splitting Laguerre-Hermite pseudospectral method for Bose-Einstein condensates*, SIAM J. Sci. Comput., **26** (2005), 2020–2028.
- [41] W. Bao and J. Shen, *A generalized-Laguerre-Hermite pseudospectral method for computing symmetric and central vortex states in Bose-Einstein condensates*, J. Comput. Phys., **227** (2008), 9778–9793.
- [42] W. Bao and Q. Tang, *Numerical methods and comparison for computing dark and bright solitons in the nonlinear Schrödinger equation*, preprint.
- [43] W. Bao and W. Tang, *Ground-state solution of Bose-Einstein condensate by directly minimizing the energy functional*, J. Comput. Phys., **187** (2003), 230–254.
- [44] W. Bao and H. Wang, *An efficient and spectrally accurate numerical method for computing dynamics of rotating Bose-Einstein condensates*, J. Comput. Phys., **217** (2006), 612–626.
- [45] W. Bao and H. Wang, *A mass and magnetization conservative and energy-diminishing numerical method for computing ground state of spin-1 Bose-Einstein condensates*, SIAM J. Numer. Anal., **45** (2007), 2177–2200.
- [46] W. Bao, H. Wang and P. A. Markowich, *Ground, symmetric and central vortex states in rotating Bose-Einstein condensates*, Commun. Math. Sci., **3** (2005), 57–88.
- [47] W. Bao and Y. Zhang, *Dynamics of the ground state and central vortex states in Bose-Einstein condensation*, Math. Models Methods Appl. Sci., **15** (2005), 1863–1896.
- [48] W. Bao and Y. Zhang, *Dynamical laws of the coupled Gross-Pitaevskii equations for spin-1 Bose-Einstein condensates*, Methods Appl. Anal., **17** (2010), 49–80.
- [49] M. A. Baranov, M. Dalmonte, G. Pupillo and P. Zolle, *Condensed matter theory of dipolar quantum gases*, Chem. Rev., **112** (2012), 5012–5061.
- [50] M. D. Barrett, J. A. Sauer and M. S. Chapman, *All-optical formation of an atomic Bose-Einstein condensate*, Phys. Rev. Lett., **87** (2001), 010404.
- [51] N. Ben Abdallah, Y. Cai, F. Castella and F. Méhats, *Second order averaging for the nonlinear Schrödinger equation with strongly anisotropic potential*, Kinet. Relat. Models, **4** (2011), 831–856.
- [52] N. Ben Abdallah, F. Castella and F. Méhats, *Time averaging for the strongly confined nonlinear Schrödinger equation, using almost periodicity*, J. Diff. Eqn., **245** (2008), 154–200.
- [53] N. Ben Abdallah, F. Méhats, C. Schmeiser and R. M. Weishäupl, *The nonlinear Schrödinger equation with a strongly anisotropic harmonic potential*, SIAM J. Math. Anal., **37** (2005), 189–199.
- [54] C. Besse, B. Bidégaray and S. Descombes, *Order estimates in time of splitting methods for the nonlinear Schrödinger equation*, SIAM J. Numer. Anal., **40** (2002), 26–40.
- [55] I. Bialynicki-Birula and Z. Bialynicki-Birula, *Center-of-mass motion in the many-body theory of Bose-Einstein condensates*, Phys. Rev. A, **65** (2002), 063606.
- [56] I. Bloch, J. Dalibard and W. Zwerger, *Many-body physics with ultracold gases*, Rev. Mod. Phys., **80** (2008), 885–964.
- [57] N. N. Bogoliubov, *On the theory of superfluidity*, J. Phys. USSR, **11** (1947), 23–32.

- [58] S. N. Bose, *Plancks gesetz und lichtquantenhypothese*, Zeitschrift fr Physik, **3** (1924), 178–181.
- [59] C. C. Bradley, C. A. Sackett, J. J. Tollett and R. G. Hulet, *Evidence of Bose-Einstein condensation in an atomic gas with attractive interaction*, Phys. Rev. Lett., **75** (1995), 1687–1690.
- [60] C. C. Bradley, C. A. Sackett and R. G. Hulet, *Bose-Einstein condensation of Lithium: observation of limited condensates*, Phys. Rev. Lett., **78** (1997), 985–989.
- [61] J. C. Bronski, L. D. Carr, B. Deconinck, J. N. Kutz and K. Promislow, *Stability of repulsive Bose-Einstein condensates in a periodic potential*, Phys. Rev. E, **63** (2001), 036612.
- [62] M. Bruderer, W. Bao and D. Jaksch, *Self-trapping of impurities in Bose-Einstein condensates: Strong attractive and repulsive coupling*, EPL, **82** (2008), 30004.
- [63] L. Cafferelli and F. H. Lin, *An optimal partition problem for eigenvalues*, J. Sci. Comput., **31** (2007), 5–18.
- [64] Yongyong Cai, “Mathematical Theory and Numerical Methods for the Gross-Pitaevskii Equations and Applications”, Ph.D Thesis, National Universtiy of Singapore, 2011.
- [65] Y. Cai, M. Rosenkranz, Z. Lei and W. Bao, *Mean-field regime of trapped dipolar Bose-Einstein condensates in one and two dimensions*, Phys. Rev. A, **82** (2010), 043623.
- [66] M. Caliari and M. Squassina, *Location and phase segregation of ground and excited states for 2D Gross-Pitaevskii systems*, Dynamics of PDE, **5** (2008), 117–137.
- [67] P. Capuzzi and S. Hernandez, *Bose-Einstein condensation in harmonic double wells*, Phys. Rev. A, **59** (1999), 1488.
- [68] B. M. Caradoc-Davis, R. J. Ballagh and K. Burnett, *Coherent dynamics of vortex formation in trapped Bose-Einstein condensates*, Phys. Rev. Lett., **83** (1999), 895–898.
- [69] R. Carles, “Semi-Classical Analysis for Nonlinear Schrödinger Equations,” World Scntific, 2008.
- [70] R. Carles, P. A. Markowich and C. Sparber, *Semiclassical asymptotics for weakly nonlinear Bloch waves*, J. Statist. Phys., **117** (2004), 343–375.
- [71] R. Carles, P. A. Markowich and C. Sparber, *On the Gross-Pitaevskii equation for trapped dipolar quantum gases*, Nonlinearity, **21** (2008), 2569–2590.
- [72] L. D. Carr, C. W. Clark and W. P. Reinhardt, *Stationary solutions of the one dimensional nonlinear Schrodinger equation I. case of repulsive nonlinearity*, Phys. Rev. A, **62** (2000), 063610.
- [73] T. Cazenave, “Semilinear Schrödinger Equations,” Courant Lect. Notes Math., 10, Amer. Math. Soc., Providence, R.I., 2003.
- [74] M. M. Cerimele, M. L. Chiofalo, F. Pistella, S. Succi and M. P. Tosi, *Numerical solution of the Gross-Pitaevskii equation using an explicit finite-difference scheme: An application to trapped Bose-Einstein condensates*, Phys. Rev. E, **62** (2000), 1382–1389.
- [75] M. M. Cerimele, F. Pistella and S. Succi, *Particle-inspired scheme for the Gross-Pitaevskii equation: An application to Bose-Einstein condensation*, Comput. Phys. Comm., **129** (2000), 82–90.
- [76] Q. Chang, B. Guo and H. Jiang, *Finite difference method for generalized Zakharov equations*, Math. Comp., **64** (1995), 537–553.
- [77] S. M. Chang, W. W. Lin and S. F. Shieh, *Gauss-Seidel-type methods for energy states of a multi-component Bose-Einstein condensate*, J. Comput. Phys., **202** (2005), 367–390.
- [78] M. L. Chiofalo, S. Succi and M. P. Tosi, *Ground state of trapped interacting Bose-Einstein condensates by an explicit imaginary-time algorithm*, Phys. Rev. E, **62** (2000), 7438–7444.
- [79] D. I. Choi and Q. Niu, *Bose-Einstein condensation in an optical lattice*, Phys. Rev. Lett., **82** (1999), 2022–2025.
- [80] E. A. Cornell and C. E. Wieman, *Nobel Lecture: Bose-Einstein condensation in a dilute gas, the first 70 years and some recent experiments*, Rev. Mod. Phys., **74** (2002), 875–893.
- [81] M. Correggi, P. Florian, N. Rougerie and J. Yngvason, *Rotating superfluids in anharmonic traps: From vortex lattices to giant vortices*, Phys. Rev. A, **84** (2011), 053614.
- [82] M. Correggi, N. Rougerie and J. Yngvason, *The transition to a giant vortex phase in a fast rotating Bose-Einstein condensate*, Comm. Math. Phys., **303** (2011), 451–508.
- [83] M. Correggi and J. Yngvason, *Energy and vorticity in fast rotating Bose-Einstein condensates*, J. Phys. A, **41** (2008), 44.
- [84] F. Dalfovo, S. Giorgini, L. P. Pitaevskii and S. Stringari, *Theory of Bose-Einstein condensation in trapped gases*, Rev. Mod. Phys., **71** (1999), 463–512.
- [85] M. J. Davis and P. B. Blakie, *Critical temperature of a trapped Bose gas: comparison of theory and experiment*, Phys. Rev. Lett., **96** (2006), 060404.

- [86] K. B. Davis, M. O. Mewes, M. R. Andrews, N. J. van Druten, D. S. Durfee, D. M. Kurn and W. Ketterle, *Bose-Einstein condensation in a gas of sodium atoms*, Phys. Rev. Lett., **75** (1995), 3969–3973.
- [87] M. J. Davis, S. A. Morgan and K. Burnett, *Simulations of Bose-fields at finite temperature*, Phys. Rev. Lett., **87** (2001), 160402.
- [88] A. Debussche and E. Faou, *Modified energy for split-step methods applied to the linear Schrödinger equations*, SIAM J. Numer. Anal., **47** (2009), 3705–3719.
- [89] C. M. Dion and E. Cancès, *Spectral method for the time-dependent Gross-Pitaevskii equation with a harmonic trap*, Phys. Rev. E, **67** (2003), 046706.
- [90] R. J. Dodd, *Approximate solutions of the nonlinear Schrödinger equation for ground and excited states for Bose-Einstein condensates*, J. Res. Natl. Inst. Stand. Technol., **101** (1996), 545–552.
- [91] Q. Du, *Numerical computations of quantized vortices in Bose-Einstein condensate*, in “Recent Progress in Computational and Applied PDEs” (eds. T. Chan et. al.), Kluwer Academic Publisher, (2002), 155–168.
- [92] Q. Du and F. H. Lin, *Numerical approximations of a norm preserving gradient flow and applications to an optimal partition problem*, Nonlinearity, **22** (2009), 67–83.
- [93] M. Edwards and K. Burnett, *Numerical solution of the nonlinear Schrödinger equation for small samples of neutral atoms*, Phys. Rev. A, **51** (1995), 101103.
- [94] A. Einstein, *Quantentheorie des einatomigen idealen gases*, Sitzungsberichte der Preussischen Akademie der Wissenschaften, **22** (1924), 261–267.
- [95] A. Einstein, *Quantentheorie des einatomigen idealen gases, zweite abhandlung*, Sitzungsberichte der Preussischen Akademie der Wissenschaften, **1** (1925), 3–14.
- [96] L. Erdős, B. Schlein and H. T. Yau, *Derivation of the Gross-Pitaevskii equation for the dynamics of Bose-Einstein condensate*, Ann. Math., **172** (2010), 291–370.
- [97] A. L. Fetter, *Rotating trapped Bose-Einstein condensates*, Rev. Mod. Phys., **81** (2009), 647–691.
- [98] A. L. Fetter and A. A. Svidzinsky, *Vortices in trapped dilute Bose-Einstein condensate*, J. Phys.: Condens. Matter, **13** (2001), 135–194.
- [99] D. G. Fried, T. C. Killian, L. Willmann, D. Landhuis, S. C. Moss, D. Kleppner and T. J. Greytak, *Bose-Einstein condensation of atomic hydrogen*, Phys. Rev. Lett, **81** (1998), 3811.
- [100] J. J. Garcia-Ripoll and V. M. Perez-Garcia, *Optimizing Schrödinger functional using Sobolev gradients: applications to quantum mechanics and nonlinear optics*, SIAM J. Sci. Comput., **23** (2001), 1315–1333.
- [101] J. J. Garcia-Ripoll, V. M. Perez-Garcia and V. Vekslerchik, *Construction of exact solutions by spatial translations in inhomogeneous nonlinear Schrödinger equations*, Phys. Rev. E, **64** (2001), 056602.
- [102] S. A. Gardiner, D. Jaksch, R. Dum, J. I. Cirac and P. Zoller, *Nonlinear matter wave dynamics with a chaotic potential*, Phys. Rev. A, **62** (2000), 023612.
- [103] I. Gasser and P. A. Markowich, *Quantum hydrodynamics, Wigner transforms and the classical limit*, Asymptot. Anal., **14** (1997), 97–116.
- [104] P. Gerard, P. A. Markowich, N. J. Mauser and F. Poupaud, *Homogenization limits and Wigner transforms*, Comm. Pure Appl. Math., **50** (1997), 321–377.
- [105] S. Giorgini, L. P. Pitaevskii and S. Stringari, *Theory of ultracold atomic Fermi gases*, Rev. Mod. Phys., **80** (2008), 1215–1274.
- [106] R. T. Glassey, *Convergence of an energy-preserving scheme for the Zakharov equations in one space dimension*, Math. Comp., **58** (1992), 83–102.
- [107] A. Griesmaier, J. Werner, S. Hensler, J. Stuhler and T. Pfau, *Bose-Einstein condensation of Chromium*, Phys. Rev. Lett., **94** (2005), 160401.
- [108] A. Griffin, T. Nikuni and E. Zaremba, “Bose-Condensed Gases at Finite Temperatures,” Cambridge University Press, 2009.
- [109] E. P. Gross, *Structure of a quantized vortex in boson systems*, Nuovo. Cimento., **20** (1961), 454–457.
- [110] Paul Lee Halkyard, “Dynamics in Cold Atomic Gases: Resonant Behaviour of the Quantum Delta-Kicked Accelerator and Bose-Einstein Condensates in Ring Traps”, Ph.D Thesis, Durham University, 2010.
- [111] C. Hao, L. Hsiao and H.-L. Li, *Global well-posedness for the Gross-Pitaevskii equation with an angular momentum rotational term*, Math. Methods Appl. Sci., **31** (2008), 655–664.

- [112] C. Hao, L. Hsiao and H.-L. Li, *Global well-posedness for the Gross-Pitaevskii equation with an angular momentum rotational term in three dimensions*, J. Math. Phys., **48** (2007), 102105.
- [113] D. S. Hall, M. R. Matthews, J. R. Ensher, C. E. Wieman and E. A. Cornell, *Dynamics of component separation in a binary mixture of Bose-Einstein condensates*, Phys. Rev. Lett., **81** (1998), 1539-1542.
- [114] R. H. Hardin and F. D. Tappert, *Applications of the split-step Fourier method to the numerical solution of nonlinear and variable coefficient wave equations*, SIAM Rev. Chronicle, **15** (1973), 423.
- [115] N. Hayashi and T. Ozawa, *Remarks on nonlinear Schrödinger equations in one space dimension*, Differ. Integral Equ., **2** (1994), 453-461.
- [116] C. E. Hecht, *The possible superfluid behaviour of hydrogen atom gases and liquids*, Physica, **25** (1959), 1159-1161.
- [117] T. L. Ho, *Spinor Bose condensates in optical traps*, Phys. Rev. Lett., **81** (1998), 742-745.
- [118] M. Holthaus, *Towards coherent control of a Bose-Einstein condensate in a double well*, Phys. Rev. A, **64** (2001), 011601.
- [119] R. Ignat and V. Millot, *The critical velocity for vortex existence in a two-dimensional rotating Bose-Einstein condensate*, J. Funct. Anal. **233** (2006), 260-306.
- [120] R. Ignat and V. Millot, *Energy expansion and vortex location for a two-dimensional rotating Bose-Einstein condensate*, Rev. Math. Phys., **18** (2006), 119-162.
- [121] D. Jaksch, S. A. Gardiner, K. Schulze, J. I. Cirac and P. Zoller, *Uniting Bose-Einstein condensates in optical resonators*, Phys. Rev. Lett., **86** (2001), 4733-4736.
- [122] S. Jin, C. D. Levermore and D. W. McLaughlin, *The semiclassical limit of the defocusing nonlinear Schrödinger hierarchy*, Comm. Pure Appl. Math., **52** (1999), 613-654.
- [123] G. Karrali and C. Sourdis, *The ground state of a Gross-Pitaevskii energy with general potential in the Thomas-Fermi limit*, preprint, [arXiv:1205.5997v2](https://arxiv.org/abs/1205.5997v2).
- [124] Y. Kawaguchi and M. Ueda, *Spinor Bose-Einstein condensates*, Phys. Rep., in press.
- [125] C. E. Kenig, G. Ponce and L. Vega, *The Cauchy problem for quasi-linear Schrödinger equations*, Invent. Math., **158** (2004), 343-388.
- [126] W. Ketterle, *Nobel lecture: When atoms behave as waves: Bose-Einstein condensation and the atom laser*, Rev. Mod. Phys., **74** (2002), 1131-1151.
- [127] I. Kyza, C. Makridakis and M. Plexousakis, *Error control for time-splitting spectral approximations of the semiclassical Schrödinger equation*, IMA J. Numer. Anal., **31** (2011), 416-441.
- [128] C. K. Law, H. Pu and N. P. Bigelow, *Quantum spins mixing in spinor Bose-Einstein condensates*, Phys. Rev. Lett., **81** (1998), 5257-5261.
- [129] A. J. Leggett, *Bose-Einstein condensation in the alkali gases: Some fundamental concepts*, Rev. Mod. Phys., **73** (2001), 307-356.
- [130] E. H. Lieb and M. Loss, "Analysis," Graduate Studies in Mathematics, Amer. Math. Soc., 2nd ed., 2001.
- [131] E. H. Lieb and R. Seiringer, *Derivation of the Gross-Pitaevskii equation for rotating Bose gases*, Comm. Math. Phys., **264** (2006), 505-537.
- [132] E. H. Lieb, R. Seiringer, J. P. Solovej and J. Yngvason, "The Mathematics of the Bose Gas and its Condensation," Oberwolfach Seminars 34, Birkhäuser Verlag, Basel, 2005.
- [133] E. H. Lieb, R. Seiringer and J. Yngvason, *Bosons in a trap: A rigorous derivation of the Gross-Pitaevskii energy functional*, Phys. Rev. A, **61** (2000), 043602.
- [134] E. H. Lieb and J. P. Solovej, *Ground state energy of the two-component charged Bose gas*, Comm. Math. Phys., **252** (2004), 485-534.
- [135] Fong Yin Lim, "Analytical and Numerical Studies of Bose-Einstein Condensates", Ph.D Thesis, National University of Singapore, 2008.
- [136] W. M. Liu, B. Wu and Q. Niu, *Nonlinear effects in interference of Bose-Einstein condensates*, Phys. Rev. Lett., **84** (2000), 2294-2297.
- [137] F. London, *The λ -phenomenon of liquid helium and the Bose-Einstein degeneracy*, Nature, **141** (1938), 643-644.
- [138] M. Lu, N. Q. Burdick, S.-H. Youn and B. L. Lev, *A strongly dipolar Bose-Einstein condensate of Dysprosium*, Phys. Rev. Lett., **107** (2011), 190401.
- [139] C. Lubich, *On splitting methods for Schrödinger-Poisson and cubic nonlinear Schrödinger equations*, Math. Comp., **77** (2008), 2141-2153.

- [140] K. W. Madison, F. Chevy, W. Wohlleben and J. Dalibard, *Vortex formation in a stirred Bose-Einstein condensate*, Phys. Rev. Lett., **84** (2000), 806–809.
- [141] M. R. Matthews, B. P. Anderson, P. C. Haljan, D. S. Hall, C. E. Wieman and E. A. Cornell, *Vortices in a Bose-Einstein condensate*, Phys. Rev. Lett., **83** (1999), 2498–2501.
- [142] C. J. Myatt, E. A. Burt, R. W. Ghrist, E. A. Cornell and C. E. Wieman, *Production of two overlapping Bose-Einstein condensates by sympathetic cooling*, Phys. Rev. Lett., **78** (1997), 586–589.
- [143] G. J. Milburn, J. Corney, E. M. Wright and D. F. Walls, *Quantum dynamics of an atomic Bose-Einstein condensate in a double-well potential*, Phys. Rev. A, **55** (1997), 4318.
- [144] O. Morsch and M. Oberthaler, *Dynamics of Bose-Einstein condensates in optical lattices*, Rev. Mod. Phys., **78** (2006), 179–215.
- [145] C. Neuhauser and M. Thalhammer, *On the convergence of splitting methods for linear evolutionary Schrödinger equations involving an unbounded potential*, BIT, **49** (2009), 199–215.
- [146] R. Ozeri, N. Katz, J. Steinhauer and N. Davidson, *Colloquium: Bulk Bogoliubov excitations in a Bose-Einstein condensate*, Rev. Mod. Phys., **77** (2005), 187–205.
- [147] N. G. Parker, C. Ticknor, A. M. Martin and D. H. J. O’Dell, *Structure formation during the collapse of a dipolar atomic Bose-Einstein condensate*, Phys. Rev. A, **79** (2009), 013617.
- [148] C. J. Pethick and H. Smith, “Bose-Einstein Condensation in Dilute Gases,” Cambridge University Press, 2002.
- [149] L. P. Pitaevskii, *Vortex lines in an imperfect Bose gas*, Soviet Phys. JETP, **13** (1961), 451–454.
- [150] L. P. Pitaevskii and S. Stringari, “Bose-Einstein Condensation,” Clarendon Press, Oxford, 2003.
- [151] A. Posazhennikova, *Colloquium: Weakly interacting, dilute Bose gases in 2D*, Rev. Mod. Phys., **78** (2006), 1111–1134.
- [152] J. L. Roberts, N. R. Claussen, S. L. Cornish and C. E. Wieman, *Magnetic field dependence of ultracold inelastic collisions near a Feshbach resonance*, Phys. Rev. Lett., **85** (2000), 728–731.
- [153] M. P. Robinson, G. Fairweather and B. M. Herbst, *On the numerical solution of the cubic Schrödinger equation in one space variable*, J. Comput. Phys., **104** (1993), 277–284.
- [154] S. Ronen, D. C. E. Bortolotti and J. L. Bohn, *Bogoliubov modes of a dipolar condensate in a cylindrical trap*, Phys. Rev. A, **74** (2006), 013623.
- [155] M. Rosenkranz, D. Jaksch, F. Y. Lim and W. Bao, *Self-trapping of Bose-Einstein condensate expanding into shallow optical lattices*, Phys. Rev. A, **77** (2008), 063607.
- [156] N. Rougerie, *Vortex rings in fast rotating Bose-Einstein condensates*, Arch. Ration. Mech. Anal., **203** (2012), 69–135.
- [157] P. A. Ruprecht, M. J. Holland, K. Burnett and M. Edwards, *Time-dependent solution of the nonlinear Schrödinger equation for Bose-condensed trapped neutral atoms*, Phys. Rev. A, **51** (1995), 4704–4711.
- [158] C. Ryu, M. F. Andersen, P. Cladé, Vasant Natarajan, K. Helmerson and W. D. Phillips, *Observation of persistent flow of a Bose-Einstein condensate in a toroidal trap*, Phys. Rev. Lett., **99** (2007), 260401.
- [159] H. Saito and M. Ueda, *Intermittent implosion and pattern formation of trapped Bose-Einstein condensates with an attractive interaction*, Phys. Rev. Lett., **86** (2001), 1406–1409.
- [160] J. A. Sanders, F. Verhulst and J. Murdock, “Averaging Methods in Nonlinear Dynamical Systems,” 2nd edition, Appl. Math. Sci., 59, Springer, 2007.
- [161] L. Santos, G. Shlyapnikov, P. Zoller and M. Lewenstein, *Bose-Einstein condensation in trapped dipolar gases*, Phys. Rev. Lett., **85** (2000), 1791–1797.
- [162] R. Seiringer, *Gross-Pitaevskii theory of the rotating Bose gas*, Comm. Math. Phys., **229** (2002), 491–509.
- [163] J. Shen, *Stable and efficient spectral methods in unbounded domains using Laguerre functions*, SIAM J. Numer. Anal., **38** (2000), 1113–1133.
- [164] J. Shen and T. Tang, “Spectral and High-Order Methods with Applications,” Science Press, Beijing, 2006.
- [165] J. Shen, T. Tang and L.-L. Wang, “Spectral Methods. Algorithms, Analysis and Applications,” Springer, Heidelberg, 2011.
- [166] J. Shen and Z.-Q. Wang, *Error analysis of the Strang time-splitting Laguerre-Hermite/Hermite collocation methods for the Gross-Pitaevskii equation*, J. Found. Comput. Math., to appear.

- [167] I. F. Silvera and J. T. M. Walraven, *Stabilization of atomic Hydrogen at low temperature*, Phys. Rev. Lett., **44** (1980), 164–168.
- [168] T. P. Simula, A. A. Penckwitt and R. J. Ballagh, *Giant vortex lattice deformation in rapidly rotating Bose-Einstein condensates*, Phys. Rev. Lett., **92** (2004), 060401.
- [169] C. Sparber, *Effective mass theorems for nonlinear Schrödinger equations*, SIAM J. Appl. Math., **66** (2006), 820–842.
- [170] D. M. Stamper-Kurn, A. P. Chikkatur, A. Görlitz, S. Inouye, S. Gupta, D. E. Pritchard and W. Ketterle, *Excitation of phonons in a Bose-Einstein condensate by light scattering*, Phys. Rev. Lett., **83** (1999), 2876–2879.
- [171] G. Strang, *On the construction and comparison of difference schemes*, SIAM J. Numer. Anal., **5** (1968), 506–517.
- [172] R. S. Strichartz, *Restriction of Fourier transform to quadratic surfaces and decay of solutions of wave equations*, Duke Math. J., **44** (1977), 705–714.
- [173] C. Sulem and P. L. Sulem, “The Nonlinear Schrödinger Equation, Self-focusing and Wave Collapse,” Springer-Verlag, New York, 1999.
- [174] G. Szegő, “Orthogonal Polynomials,” 4th edition, Amer. Math. Soc. Colloq. Publ. 23, AMS, Providence, R.I., 1975.
- [175] T. R. Taha and M. J. Ablowitz, *Analytical and numerical aspects of certain nonlinear evolution equations, II. Numerical, nonlinear Schrödinger equation*, J. Comput. Phys., **55** (1984), 203–230.
- [176] M. Thalhammer, *High-order exponential operator splitting methods for time-dependent Schrödinger equations*, SIAM J. Numer. Anal., **46** (2008), 2022–2038.
- [177] V. Thomée, “Galerkin Finite Element Methods for Parabolic Problems,” Springer-Verlag, Berlin, Heidelberg, 1997.
- [178] I. Tikhonenkov, B. A. Malomed and A. Vardi, *Anisotropic solitons in dipolar Bose-Einstein condensates*, Phys. Rev. Lett., **100** (2008), 090406.
- [179] S. Utsunomiya, L. Tian, G. Roumpos, C. W. Lai, N. Kumada, T. Fujisawa, M. Kuwata-Gonokami, A. Löffler, S. Höfling, A. Forchel and Y. Yamamoto, *Observation of Bogoliubov excitations in exciton-polariton condensates*, Nature Phys., **4** (2008), 700–705.
- [180] Hanquan Wang, “Quantized Vortices States and Dynamics in Bose-Einstein condensates”, PhD Thesis, National University of Singapore, 2006.
- [181] H. Wang, *A time-splitting spectral method for coupled Gross-Pitaevskii equations with applications to rotating Bose-Einstein condensates*, J. Comput. Appl. Math., **205** (2007), 88–104.
- [182] H. Wang, *An efficient numerical method for computing dynamics of spin $F = 2$ Bose-Einstein condensates*, J. Comput. Phys., **230** (2011), 6155–6168.
- [183] H. Wang and W. Xu, *An efficient numerical method for simulating the dynamics of coupling Bose-Einstein condensates in optical resonators*, Comput. Phys. Comm., **182** (2011), 706–718.
- [184] M. I. Weinstein, *Nonlinear Schrödinger equations and sharp interpolation estimates*, Comm. Math. Phys., **87** (1983), 567–576.
- [185] J. Williams, R. Walser, J. Cooper, E. Cornell and M. Holland, *Nonlinear Josephson-type oscillations of a driven two-component Bose-Einstein condensate*, Phys. Rev. A, **59** (1999), R31-R34.
- [186] B. Xiong, J. Gong, H. Pu, W. Bao and B. Li, *Symmetry breaking and self-trapping of a dipolar Bose-Einstein condensate in a double-well potential*, Phys. Rev. A, **79** (2009), 013626.
- [187] S. Yi and L. You, *Trapped atomic condensates with anisotropic interactions*, Phys. Rev. A, **61** (2000), 041604(R).
- [188] S. Yi and L. You, *Expansion of a dipolar condensate*, Phys. Rev. A, **67** (2003), 045601.
- [189] H. Yoshida, *Construction of higher order symplectic integrators*, Phys. Lett. A, **150** (1990), 262–268.
- [190] E. Zaremba, T. Nikuni and A. Griffin, *Dynamics of trapped Bose gases at finite temperature*, J. Low Temp. Phys., **116** (1999), 277.
- [191] R. Zeng and Y. Zhang, *Efficiently computing vortex lattices in fast rotating Bose-Einstein condensates*, Comput. Phys. Commun., **180** (2009), 854–860.
- [192] P. Zhang, “Wigner Measure and Semiclassical Limits of Nonlinear Schrödinger Equations,” Courant Lect. Notes Math., 17, Amer. Math. Soc., Providence, R.I., 2008.
- [193] Yanzhi Zhang, “Mathematical Analysis and Numerical Simulation for Bose-Einstein condensation”, PhD Thesis, National University of Singapore, 2006.

- [194] Y. Zhang and W. Bao, *Dynamics of the center of mass in rotating Bose-Einstein condensates*, Appl. Numer. Math., **57** (2007), 697–709.
- [195] Y. Zhang, W. Bao and H. Li, *Dynamics of rotating two-component Bose-Einstein condensates and its efficient computation*, Phys. D, **234** (2007), 49–69.

Received xxxx 20xx; revised xxxx 20xx.

E-mail address: bao@math.nus.edu.sg

E-mail address: yongyong.cai@gmail.com